Indian J. Chem. Vol. 27A No. 6 pp. 469-560
June 1988
CODEN : IJOCAP ISSN : 0019-5103
27A(6) 469-560 (1988)

470
5/8/88

Indian Journal of
CHEMISTRY

SECTION A
(Inorganic, Physical, Theoretical & Analytical)

Published by
PUBLICATIONS & INFORMATION DIRECTORATE, CSIR, NEW DELHI
in association with
THE INDIAN NATIONAL SCIENCE ACADEMY, NEW DELHI

THE WEALTH OF INDIA

An Encyclopaedia of Indian Raw Materials and Industrial Products, published in two series :
(i) Raw Materials, and **(ii) Industrial Products.**

RAW MATERIALS

The articles deal with Animal Products, Dyes & Tans, Essential Oils, Fats & Oils, Fibres & Pulps, Foods & Fodders, Drugs, Minerals, Spices & Flavourings, and Timbers and other Forest products. Names in Indian languages, and trade names are provided.

For important crops, their origin, distribution, evolution of cultivated types and methods of cultivation, harvesting and storage are mentioned in detail. Data regarding area and yield and import and export are provided. Regarding minerals, their occurrence and distribution in the country and modes of exploitation and utilization are given. The articles are well illustrated. Adequate literature references are provided.

Eleven volumes of the series covering letters A–Z have been published.

Vol. I : A (Revised) Rs. 300.00; Vol. I (A-B) Rs. 120.00; Vol. II (C) Rs. 143.00; Vol. III (D-E) with index to Vols. I-III Rs. 158.00; Vol. IV (F-G) Rs. 98.00; Vol. IV Suppl. Fish & Fisheries Rs. 84.00; Vol. V (H-K) Rs. 171.00; Vol. VI (L-M) Rs. 135.00; Vol. VI : Suppl. on Livestock including poultry Rs. 153.00; Vol. VII (N-Pe) Rs. 150.00; Vol. VIII (Ph-Re) Rs. 129.00; Vol. IX (Rh-Sc) Rs. 156.00; Vol. X (Sp-W) Rs. 338.00; Vol. XI (X-Z) with Cumulative Index to Vols. I-XI Rs. 223.00.

INDUSTRIAL PRODUCTS

Includes articles giving a comprehensive account of various large, medium and small scale industries. Some of the major industries included are : Acids, Carriages, Diesel Engines, Fertilizers, Insecticides & Pesticides, Iron & Steel, Paints & Varnishes, Petroleum Refining, Pharmaceuticals, Plastics, Ship & Boatbuilding, Rubber, Silk, etc.

The articles include an account of the raw materials and their availability, manufacturing processes, and uses of products, and industrial potentialities. Specifications of raw materials as well as finished products and statistical data regarding production, demand, exports, imports, prices, etc. are provided. The articles are suitably illustrated. References to the sources of information are provided.

Nine volumes of the series covering letters A–Z have been published.

Part I (A-B) Rs. 87.00; Part II (C) Rs. 111.00; Part III (D-E) with Index to Parts I-III Rs. 150.00; Part IV (F-H) Rs. 189.00; Part V (I-L) Rs. 135.00; Part VI (M-Pi) Rs. 42.00; Part VII (Pl-Sh) Rs. 90.00; Part VIII (Sl-Tl) Rs. 99.00; Part IX (To-Z) with Index to Parts I-IX Rs. 120.00.

HINDI EDITION : BHARAT KI SAMPADA—PRAKRITIK PADARTH

Vols. I to VII and two supplements of Wealth of India—Raw Materials series in Hindi already published.

Published Volumes :

Vol. I (अ-औ) Rs. 57.00; Vol. II (क) Rs. 54.00; Vol. III (ख-न) Rs. 54.00; Vol. IV (प) Rs. 125.00; Vol. V (फ-मेरे) Rs. 90.00; Vol. VI (मेल-रू) Rs. 120.00; Vol. VII (रे-वाटा) Rs. 203.00; Vol. VIII (वाय-सीसे) Rs. 300.00.

Supplements :

Fish & Fisheries (Matsya & Matsyaki) Rs. 74.00;
Livestock (Pashudhan aur Kukkut Palan) Rs. 51.00

Vols. IX to XI under publication.

Please contact :

SENIOR SALES AND DISTRIBUTION OFFICER
PUBLICATIONS & INFORMATION DIRECTORATE, CSIR
Hillside Road, New Delhi 110 012

INDIAN JOURNAL OF CHEMISTRY

Section A: Inorganic, Physical, Theoretical & Analytical Chemistry

Editorial Board

Prof. C.N.R. Rao
Director
Indian Institute of Science
Bangalore 560 012

Prof. R.P. Rastogi
Vice-Chancellor
Banaras Hindu University
Varanasi 221 005

Prof. A.R. Vasudeva Murthy
Department of Inorganic &
Physical Chemistry
Indian Institute of Science
Bangalore 560 012

Prof. J.C. Kuriacose
Department of Chemistry
Indian Institute of Technology
Madras 600 036

Prof. D.V.S. Jain
Department of Chemistry
Panjab University
Chandigarh 160 014

Prof. P. Natarajan
Department of Inorganic Chemistry
University of Madras
Madras 600 025

Prof. N.K. Ray
Department of Chemistry
University of Delhi
Delhi 110 007

Prof. A. Chakravorty
Department of Inorganic Chemistry
Indian Association for the
Cultivation of Science
Calcutta 700 032

Prof. S. Mitra
Tata Institute of Fundamental Research
Bombay 400 005

Dr K.N. Rao
Chemistry Division
Bhabha Atomic Research Centre
Trombay, Bombay 400 085

Prof. S.M. Khopkar
Department of Chemistry
Indian Institute of Technology
Powai, Bombay 400 076

Prof. P.T. Manoharan
Department of Chemistry
Indian Institute of Technology
Madras 600 036

Dr A.C. Dash
Department of Chemistry
Utkal University
Bhubaneswar 751 004

Shri S.P. Ambasta, Editor-in-Chief
(*Ex-officio*)

Editors

S.S. Saksena — B.C. Sharma — S. Sivakamasundari

Assistant Editor

S.K. Bhasin

Published by the Publications & Information Directorate (CSIR), Hillside Road, New Delhi 110 012

Editor-in-Chief: S.P. Ambasta

Copyright, 1988, by the Council of Scientific & Industrial Research, New Delhi 110 012

The Indian Journal of Chemistry is issued monthly in two sections: A and B. Communications regarding contributions for publication in the journal should be addressed to the Editor, Indian Journal of Chemistry, Publications & Information Directorate, Hillside Road, New Delhi 110 012.

Correspondence regarding subscriptions and advertisements should be addressed to the Sales & Distribution Officer, Publications & Information Directorate, hillside Road, New Delhi 110 012.

The Publications & Information Directorate (CSIR) assumes no responsibility for the statements and opinions advanced by contributors. The Editorial Board in its work of examining papers received for publication is assisted, in an honorary capacity by a large number of distinguished scientists, working in various parts of India.

Annual Subscription: Rs. 300.00 £ 70.00 $ 100.00; 50% discount admissible to research workers and students and 25% discount to non-research individuals on annual subscription.

Single Copy: Rs. 30.00 £ 7.00 $ 10.00

Payments in respect of subscriptions and advertisements may be sent by cheque, bank draft, money order or postal order marked payable to Publications & Information Directorate, Hillside Road, New Delhi 110 012.

Claims for missing numbers will be allowed only if received within 3 months of the date of issue of the journal plus the time normally required for postal delivery of the journal and the claim.

Author Index

Abu El-Nader H M 540
Aminabhavi T M 529
Anil Kumar 479, 527
Anjaneyulu Y 555
Anoop Kumar 482

Balundgi R H 529
Banerjee Sati Prasad 532

Chang L F 558
Chaudhuri Mihir K 504
Chodha Arun 519

Das Bimalendu 504
Deshpande S G 552
Devasingh C Newman Paul 498
Dhabhai D N 536

Ganorkar M C 542
Girgis Maher M 474
Gokavi G S 494
Goyal Muni R 487
Goyal R N 482
Gupta Y K 487

Halligudi S B 529

Indrasenan P 545

Jain S C 552
Janardhan R 547
Jayasankar H 545

Kameswara Rao N 555
Kannappan V 538
Kapur Neeta 519
Katyal M 558
Keshavan B 547
Khalil Zarif H 474
Kothiwal A S 507

Lalitha Rajaraman 538
Laxma Reddy K 510
Lingaiah P 510
Lohar J M 536

Malhotra Rajesh 519
Manjeshwar L S 529
Mehrotra R C 507
Mittal Rama K 487
Moussa M N H 540
Mukherjee G N 514

Nalanda Sharada L 542
Nanjan M J 538
Narula Suraj P 519

Prabhakara Rao R 555
Puri B K 558

Rai A K 507
Raju J R 494
Ramachandran M S 498
Ravi Shankar 519

Sangurdekar P R 523
Sarkar S 514
Satake M 558
Seetharama Rao T 510
Siddiqui M A 550
Singh A 507
Singh Prem Paul 469
Singhai Neelu 532
Srivastava S K 550
Srivastava T N 550
Sudersanan M 523

Vivekanandam T S 498

Indian Journal of Chemistry

Sect. A: Inorganic, Physical, Theoretical & Analytical

VOL 27A NUMBER 6 JUNE 1988

CONTENTS

Topological Investigations of the Viscous Behaviour of Binary Mixtures of Non-electrolytes 469
Prem Paul Singh

Charge-Transfer Complexes of Hydroxystyrylcyanine Dyes & Their Analogues with Nicotine: Structure-Activity Relationship Studies 474
Maher M Girgis* & Zarif H Khalil

Solution Densities of Aqueous Potassium Chloride-Barium Chloride Mixtures at 298.15K & Different Ionic Strengths 479
Anil Kumar

Electrochemical Behaviour of Bisazo Dye, Acid Red-150 482
R N Goyal* & Anoop Kumar

Redox Chemistry of Hyponitrous Acid: Part I—Stoichiometry, Kinetics & Mechanism of Its Oxidation by Ethylenediaminetetraacetatothallium (III) in Aqueous Perchloric Acid Medium 487
Muni R Goyal, Rama K Mittal & Y K Gupta*

Chromium(VI) Oxidation of Thallium (I) in Aqueous Acetic Acid & Effect of Added Vanadium (V) on the Reaction 494
G S Gokavi & J R Raju*

Kinetics & Mechanism of Oxidation of Glutamine & Serine by Peroxomonosulphate in the Absence & Presence of Acetaldehyde & Propionaldehyde 498
M S Ramachandran*, T S Vivekanandam & C Newman Paul Devasingh

Synthesis & Characterisation of Potassium, Cesium & Ammonium Oxotetrafluorotitanates (IV) 504
Mihir K Chaudhuri* & Bimalendu Das

Synthesis & Infrared, ^{1}H, ^{13}C, ^{119}Sn NMR & ^{119}Sn Mössbauer Studies of Some New Diorganotin Dichloride Adducts 507
A S Kothiwal, A Singh, A K Rai & R C Mehrotra*

Synthesis & Characterization of Complexes of Ru(II), Pt(II) & Pd(II) with Substituted Chalcones 510
T Seetharama Rao, K Laxma Reddy & P Lingaiah*

Metal Complexes of Some Peptide Derivatives: Part V—Complex Formation of Copper(II) with N-Salicyloyl Derivatives of Some Amino Acids. 514
G N Mukherjee* & (Miss) S Sarkar

Continued overleaf

Coordination Compounds of Organometallic Bases of Group(IV) Elements: Part XI—Reactions of N,N′-(Phenyl/*o*-chlorophenyl/*p*-methylphenyl/benzyl/diethyl)-1,1-di-*n*-propoxy/*n*-butoxy-silanediamines with Tin(IV) & Titanium (IV) Chlorides at −10°C 519
Suraj P Narula*, Neeta Kapur, Ravi Shankar, Arun Chodha & Rajesh Malhotra

Solvent Extraction Studies of Mixed Chelates of Europium. 523
P R Sangurdekar & M Sudersanan*

Notes

Application of Mean Spherical Approximation in Estimating Activity Coefficients of Aqueous Mixed Electrolyte Solutions 527
Anil Kumar

Excess Properties of Binary Liquid Mixtures at 293.15K 529
T M Aminabhavi*, L S Manjeshwar, S B Halligudi & R H Balundgi

Studies of New Zeolite Derivatives of Stilbite. 532
Neelu Singhai & Sati Prasad Banerjee*

Studies of New Mesogens: Part II—*p*-(*p*′-*n*-Alkoxycinnamoyloxy)benzylidene-*p*″-*n*-butoxyanilines 536
J M Lohar & D N Dhabhai*

Charge Density-Activation Energy Correlations in Bromination of Thiophenes by N-Bromosuccinimide in Solution 538
Lalitha Rajaraman, M J Nanjan & V Kannappan*

Mechanism of Ligand Substitution Reaction of Monobipyridyl Complex of Manganese(II) 540
H M Abu El-Nader* & M N H Moussa

Complexes of Oxovanadium(IV), Chromium(III), Manganese(II), Iron(II), Cobalt(II), Nickel(II) & Copper(II) with 6-Chloro-4-hydroxy-3-acetylcoumarin (Cl-HAC). 542
(Miss) L Nalanda Sharada & M C Ganorkar*

Lanthanide Nitrate Complexes of Schiff Base Derived from 1-Isonicotinyl-Hydrazide & 2-Hydroxy-1-naphthaldehyde 545
H Jayasankar & P Indrasenan*

Mixed Valence Paramagnetic Trinuclear Complexes of Rhodium with N-Alkylphenothiazines 547
B Keshavan* & R Janardhan

Molecular Adducts of Tellurocyclopentane Diperchlorate with Neutral Donors . . 550
T N Srivastava*, M A Siddiqui & S K Srivastava

Mixed Ligand Complexes of Uranium 552
S G Deshpande & S C Jain*

Studies on the Formation Equilibria of Binary & Ternary Complexes of Copper(II) with Acetylacetone & Some Amino Acids 555
Y Anjaneyulu*, N Kameswara Rao & R Prabhakara Rao

Atomic Absorption Spectrophotometric Determination of Copper after Adsorption of Its Rubeanate onto Microcrystalline Naphthalene 558
B K Puri, M Katyal, M Satake* & L F Chang

Authors for correspondence are indicated by (*)

Indian Journal of Chemistry
Vol. 27A, June 1988, pp. 469-473

Topological Investigations of the Viscous Behaviour of Binary Mixtures of Non-electrolytes

PREM PAUL SINGH
Department of Chemistry, Maharshi Dayanand University, Rohtak 124 001

Received 9 *June* 1987; *revised* 21 *September* 1987; *accepted* 9 *November* 1987

A graph theoretical approach has been developed to evaluate viscosity change ($\Delta\eta$) data on mixing components of binary mixtures of non-electrolytes. The approach describes well the ($\Delta\eta$) data of those binary mixtures whose components do not undergo complexation reaction. A simple relation has also been developed between ($\Delta\eta$) and molar excess volume (V^E) of an (A+B) mixture. The relationship is quite successful in describing ($\Delta\eta$) data of even those (A+B) mixtures which are characterised by specific interactions between their components or when A is associated in the pure state and the addition of B causes rupture of this association.

A binary (A+B) mixture is formed by the replacement of like contacts in the pure A and B by unlike contacts A−B in the mixture. Consequently, there must be some correlation between the molar excess volume (V^E) and the viscosity change ($\Delta\eta$) data of a binary liquid mixture. The rupture of like contacts in the pure A and B and the formation of new A−B contacts in the (A+B) mixtures may be described mathematically using graph theory[1-6] treating structural formulas of organic compounds as molecular graphs. In the present investigation an approach has been developed to (i) evaluate ($\Delta\eta$) data and (ii) correlate V^E and ($\Delta\eta$) data of an (A+B) mixture.

Method of Calculation & Results

The resistance to flow of a liquid has been attributed to velocity gradient between the liquid layers. Each layer exerts a drag on the next layer, and for Newtonian flow the magnitude[7] of the retarding force has been taken to be proportional to the velocity gradient and to the area of contact between the moving liquid layers. In the case of the organic molecules the effective area of contact between the moving liquid layers depends on the length of the carbon-carbon (C−C) backbone and the degree of branching of the molecules of the liquid. Larger the C−C chain length, larger would be the effective area of contact of the moving liquid layers, and hence larger would be the viscosity. But larger the degree of branching in a molecule, smaller would be the area in effective contact between the moving liquid layers, and so smaller would be the viscosity. This is corroborated by the available viscosity data[8-12] at 288.15K of a number of liquid non-electrolytes where η is found to vary as: isopentane < *n*-pentane; *n*-heptane < 2, 3-dimethyl-pentane; 3,3-dimethylpentane < *n*-nonane; chloroform < carbon tetrachloride, chlorobenzene < bromobenzene; benzene < *m*-xylene < *p*-xylene. It is interesting to point out that the molar volumes of these liquids also vary in the same manner. Kier[13] and Singh *et al.*[14] have shown that the molar volumes of most of the liquid non-electrolytes depend directly on $^1\zeta$ and inversely on $^3\zeta$ parameters of these molecules. It appears, therefore, that the viscosity, η, of these liquids must have a similar type of dependence on $^1\zeta$ and $^3\zeta$ parameters of these molecules. Consequently, following Kier[13] and Singh *et al.*[14], we express η of a liquid by,

$$\eta = \alpha_V {}^3\zeta + \beta_V {}^1\zeta + \gamma_V \qquad \ldots (1)$$

where α_V, β_V and γ_V are constants and $^1\zeta$ and $^3\zeta$ are connectivity parameters of the first and the third degree respectively and are defined[14] by,

$$^1\zeta = \sum_{i<j} (\delta_i \delta_j)^{-0.5} \qquad \ldots (2)$$

$$^3\zeta = \sum_{i<j} \sum_{i<k} \sum_{k<l} (\delta_i \delta_j \delta_k \delta_l)^{-0.5} \qquad \ldots (3)$$

where δ_i denotes the valency[14] of the *i*th vertice in the graph of the molecule.

In order to check as to how well Eq. 1 reproduces the η values of liquid non-electrolytes, we utilized the η values[12] at 288.15K of *n*-pentane, *n*-hexane and *n*-heptane to evaluate α_V, β_V and γ_V parameters of Eq. (1), and these in turn were used to evaluate η of a number of alkanes. These η values are recorded in Table 1 and are also compared with the corresponding literature values[8-12]. It is quite apparent from Table 1 that the predicted η values are mostly within 10 percent (20 percent in a few cases)

Table 1—Comparison of η Values Calculated at 288.15K from Eq. 1 with The Corresponding Literature Values for Some Liquid Non-electrolytes

	η (millipoise)		$^3\zeta$	$^1\zeta$
	Calc.	Lit.		
Isopentane	2.18	2.34[12(b)]	0.817	2.27
2-Methylpentane	3.08	3.24[9]	0.866	2.770
3-Methylpentane	3.20	3.39[9]	1.393	2.807
2,2-Dimethylpentane	3.62	4.01[10]	1.000	3.061
2,3-Dimethylpentane	3.85	4.36[9]	1.213	3.180
2,5-Dimethylhexane	4.63	5.12[12(f)]	1.322	3.614
n-Octane	5.17	5.79[12(e)]	1.457	3.914
n-Nonane	6.88	7.50[12(g)]	1.707	4.414

of the literature values. We next employed η data[15] at 298.15K of benzene *m*-xylene and *p*-xylene to evaluate η of toluene. The calculated η (toluene) value of 6.80 millipoise agrees within 10 percent with the corresponding literature value[15] (6.23 millipoise) even though the molar valume of toluene is more than that of benzene and its viscosity is less than that of benzene. We hope that Eq. 1 would also describe well the η data of other liquid non-electrolytes.

The ideal viscosity, η_{id}, of the mixture $(x_A A + x_B B)$ (where x_A is the mole fraction of A), would then be given by,

$$\eta_{id} = \Sigma x_A \cdot \eta_A = x_A \alpha_{V_A} / {}^3\zeta_A + x_A \beta_{V_A} {}^1\zeta_A + x_A \gamma_{V_A} + x_B \alpha_{V_B} / {}^3\zeta_B + x_B \beta_{V_B} {}^1\zeta_B + x_B \gamma_{V_B} \quad \ldots (4)$$

The viscosity, η_m, of this mixture would also be expressible[14] by an expression analogous to Eq. 1, i.e.,

$$\eta_m = \alpha_{V_m} / {}^3\zeta_m + \beta_{V_m} {}^1\zeta_m + \gamma_{V_m} \quad \ldots (5)$$

we now assume[14] that

$${}^3\zeta_m = \Sigma x_A \cdot {}^3\zeta_A \quad \ldots (6)$$

$$\beta_{V_m}({}^1\zeta_m) = \Sigma x_A . \beta_{V_A} {}^1\zeta_A \quad \ldots (7)$$

$$\gamma_{V_m} = \Sigma x_A \gamma_{V_A} \quad \ldots (8)$$

and

$$\alpha_{V_m} \approx \alpha_{V_A} \approx \alpha_{V_B} \approx \alpha \quad \ldots (9)$$

so that the viscosity change $(\Delta\eta)$ on mixing the components of this binary mixture would be given by,

$$(\Delta\eta) = \eta_m - \eta_{id} = \alpha \left[\frac{1}{\Sigma x_A \cdot {}^3\zeta_A} - \sum \frac{x_A}{{}^3\zeta_A} \right] \quad \ldots (10)$$

Evaluation of $(\Delta\eta)$ of a binary mixture (A+B) would thus require a knowledge of its α parameter; the $^3\zeta$ parameters of A and B can be calculated from Eq. 3 in the manner described elsewhere[16] utilizing δ^v (δ^v = valence δ values[13,16]) of the vertices of their molecular graphs. For the present investigations we evaluated α for an (A+B) mixture by utilizing its $(\Delta\eta)$ value at $x_A = 0.5$. This value of α was next employed to evaluate $(\Delta\eta)$ for the mixture at $x_A = 0.1$, 0.3, 0.7 and 0.9. Such $(\Delta\eta)$ values are recorded in Table 2 and are also compared with the corresponding literature values[17-20]. Examination of Table 2 shows that Eq. 10 is successful in reproducing $(\Delta\eta)$ values of mixtures No. 1-11, and 14. It is interesting to note that even though there is evidence[21] for complex formation between benzene (A) and carbon tetrachloride (B), Eq. 10 reproduces its $(\Delta\eta)$ data. Again although methylene chloride (A) + aromatic hydrocarbons (B) mixtures have been charactgerized[20,22] by weak specific interactions between A and B, yet their $(\Delta\eta)$ data are also well described by Eq. 10. For methylene chloride (A) + *p*-xylene (B) mixture, however, $(\Delta\eta)$ values calculated from Eq. 10 compare resonably well with the corresponding literature[19] values in the range $x_A < 0.3$; in the rest of the composition range, while the calculated $(\Delta\eta)$ values are positive the experimental $(\Delta\eta)$ values are negative. Further, for chloroform (A) + 1,4-dioxane or ether (B) system, while the calculated $(\Delta\eta)$ values have the same sign as the experimental $(\Delta\eta)$ values, the agreement between these values is not good in the range $x_A \geq 0.6$. This is understandable since in the latter mixtures[23] specific interactions exist between their components which form well characterized molecular species in solution. This approach, however, cannot be worked out for methanol (A) + aromatic hydrocarbons (B) since A in these mixtures is known to be associated in the pure state, and as the degree or the extent of association in A is not known with certainty[24-27], the $^3\zeta$ parameter of A cannot be evaluated in the pure state. The addition of B to A in these mixtures would further complicate the matters so far as the evaluation of $^3\zeta$ values in (A+B) mixtures is concerned. In fact in ROH(A) (R = CH_3 or C_2H_5) + CHX_3(B) (X = Cl or Br) or CH_2Br_2(B) mixtures, A has been shown[28] to be self-associated in the pure state, i.e., while methanol has been shown[29] to exist mainly as a cyclic dimer (with open chain dimers and trimers), ethanol exists mainly as an open chain trimer. It has further been shown[28] that in these mixtures $^3\zeta$ values of A are indeed different the pure A and (A+B) mixtures. Again, these mixtures have been shown[28] to be characterized by the presence of AB and or A_2B molecular species in solution. Such (A+B) mixtures where complexation reaction takes place between A and B leading to the formation of molecular species in so-

Table 2—Comparison of ($\Delta\eta$) Values Calculated (for $x_A = 0.1, 0.3, 0.7$ and 0.9 at 298.15K) from Eqs 10 and 14 with the Corresponding Literature Values for Some (A+B) Mixtures

Sl No.	Mixture	$\Delta\eta$ (Millipoise)	x_A			
			0.1	0.3	0.7	0.9
1	Benzene (A) + ethylene chloride (B)	Calc.	−0.240	−0.527	−0.545	−0.239
		Expt.[17]	−0.270	−0.650	−0.600	−0.223
		(Calc.)*	(−0.307)	(−0.657)	(−0.657)	(−0.284)
		$[^3\zeta_A = 0.667, {}^3\zeta_B = 0.714, \alpha = 378.767, K = 3.304]$				
2	Benzene (A) + cyclohexane (B)	Calc.	−0.386	−1.019	−1.390	−0.728
		Expt.[17]	−0.550	−1.300	−1.050	−0.400
		(Calc.)*	(−0.540)	(−1.209)	(−1.167)	(−0.480)
		$[^3\zeta_A = 0.667, {}^3\zeta_B = 1.500, \alpha = 8.7484, K = -2.1212]$				
3	Benzene (A) + chlorobenzene (B)	Calc.	−0.016	−0.040	−0.048	−0.022
		Expt.[18]	−0.030	−0.040	−0.042	−0.016
		(Calc.)*	(−0.020)	(−0.050)	(−0.040)	(−0.020)
		$[^3\zeta_A = 0.667, {}^3\zeta_B = 1.007, \alpha = 0.10115, K = -0.260]$				
4	Benzene (A) + bromobenzene (B)	Calc.	−0.069	−0.179	−0.230	−0.115
		Expt.[18]	−0.080	−0.180	−0.196	−0.070
		(Calc.)*	(−0.077)	(−0.200)	(−0.200)	(−0.078)
		$[^3\zeta_A = 0.667, {}^3\zeta_B = 1.273, \alpha = 0.2153, K = 7.74194]$				
5	Benzene (A) + *n*-pentane (B)	Calc.	−0.320	−0.848	−0.870	−0.30
		Expt.[19]	−0.300	−0.700	−1.000	−0.40
		(Calc.)*	(−0.430)	(−0.880)	(−0.870)	(−0.40)
		$[^3\zeta_A = 0.667, {}^3\zeta_B = 0.707, \alpha = 82.4, K = 1.021]$				
6	Benzene (A) + *n*-hexane (B)	Calc.	−0.330	−0.859	−0.948	−0.440
		Expt.[19]	−0.300	−0.800	−1.000	−0.450
		(Calc.)*	(−0.380)	(−0.881)	(−0.900)	(−0.390)
		$[^3\zeta_A = 0.667, {}^3\zeta_B = 0.957, \alpha = 2.5884, K = -0.2540]$				
7	Benzene (A) + carbon tetrachloride	Calc.	−0.014	−0.036	−0.042	−0.020
		Expt.[17]	−0.014	−0.038	−0.034	−0.012
		(Calc.)*	(−0.044)	(−0.061)	(−0.034)	(−0.021)
		$[^3\zeta_A = 0.667, {}^3\zeta_B = 1.000, \alpha = 0.9224, K = 9.7561]$				
8	Toluene (A) + Chlorobenzene (B)	Calc.	0.032	0.075	0.077	0.033
		Expt.[18]	0.031	0.061	0.100	0.045
		(Calc.)*	(0.032)	(0.075)	(0.076)	(0.033)
		$[^3\zeta_A = 0.94, {}^3\zeta_B = 1.007, \alpha = -7.39, K = -0.08867]$				
9	Toluene (A) + bromobenzene (B)	Calc.	−0.100	−0.250	−0.280	−0.129
		Expt.[18]	−0.120	−0.260	−0.280	−0.120
		(Calc.)*	(−0.110)	(−0.260)	(−0.260)	(−0.110)
		$[^3\zeta_A = 0.94, {}^3\zeta_B = 1.273, \alpha = 1.4806, K = 0.2352]$				
10	Methylenechloride (A) + Benzene (B)	Calc.	−0.170	−0.365	−0.311	−0.124
		Expt.[19]	−0.130	−0.350	−0.330	−0.150
		(Calc.)*	(−0.150)	(−0.340)	(−0.339)	(−0.150)
		$[^3\zeta_A = 1.0, {}^3\zeta_B = 0.667, \alpha = 0.8028, K = -0.1520]$				
11	Methylenechloride (A) + Toluene (B)	Calc.	−0.013	−0.031	−0.036	−0.017
		Expt.[19]	−0.010	−0.030	−0.040	−0.023
		(Calc.)*	(−0.010)	(−0.028)	(−0.038)	(−0.018)

(Cont.)

Table 2—Comparison of $(\Delta\eta)$ Values Calculated (for $x_A = 0.1, 0.3, 0.7$ and 0.9 at 298.15K) from Eqs 10 and 14 with the Corresponding Literature Values for Some (A+B) Mixtures—*Contd.*

Sl No.	Mixture	$\Delta\eta$ (Millipoise)	x_A 0.1	0.3	0.7	0.9
		$[^3\zeta_A = 1.0, {}^3\zeta_B = 0.94, \alpha = 0.1525, K = -0.0181]$				
12	Methylenechloride (A)+ *m*-xylene (B)	Calc.	0.031	0.065	0.070	0.035
		Expt.[19]	0.010	0.070	0.020	0.000
		(Calc.)*	(0.023)	(0.065)	(0.086)	(0.04)
		$[^3\zeta_A = 1.0, {}^3\zeta_B = 1.174, \alpha = -1.5267, K = 0.027]$				
13	Methylenechloride (A)+ *p*-xylene (B)	Calc.	0.018	0.044	0.048	0.021
		Expt.[19]	0.040	0.060	−0.020	−0.020
		(Calc.)*	(0.013)	(0.038)	(0.054)	(0.027)
		$[^3\zeta_A = 1.0, {}^3\zeta_B = 1.217, \alpha = 0.6288, K = 0.0239]$				
14	Acetone (A)+ Benzene (B)	Calc.	−0.154	−0.329	−0.280	−0.112
		Expt.[19]	−0.140	−0.290	−0.230	−0.050
		(Calc.)*	(−0.090)	(−0.251)	(−0.250)	(−0.075)
		$[^3\zeta_A = 1.0, {}^3\zeta_B = 0.667, \alpha = 0.7219, K = 0.4656]$				
15	Chloroform (A)+ 1,4-Dioxane (B)	Calc.	−0.273	−0.598	−0.532	−0.216
		Expt.[19]	−0.040	−0.339	−0.717	−0.420
		(Calc.)*	(−0.040)	(−0.278)	(−0.860)	(−0.440)
		$[^3\zeta_A = 1.0, {}^3\zeta_B = 0.744, \alpha = 2.6531, K = -0.3289]$				
16	Chloroform (A)+ ether (B)	Calc.	—	—	—	—
		Expt.[19]	−0.060	−0.181	−0.460	−0.242
		(Calc.)*	(−0.083)	(−0.236)	(−0.232)	(−0.090)
		$[K = -0.0278]$				
17	Methanol (A)+ benzene (B)	Expt.[20]	−0.162	−0.376	−0.329	−0.131
		(Calc.)*	(−0.124)	(−0.342)	(−0.330)	(−0.135)
		$[K = 0.1515]$				
18	Methanol (A)+ Toluene (B)	Expt.[20]	−0.000	−0.030	−0.070	−0.050
		(Calc.)*	(−0.020)	(−0.040)	(−0.055)	(−0.032)
		$[K = 0.0319]$				
19	Methanol (A)+ *m*-xylene (B)	Expt.[20]	0.025	0.068	0.067	0.000
		(Calc.)*	(0.025)	(0.068)	(0.080)	(0.040)
		$[K = 0.0270]$				

*Values in parenthesis are those calculated by using Eq. 14.

lution, $(\Delta\eta)$ values should be expressed (in view of equations 4, 5, 7-9) by

$$(\Delta\eta) = \alpha\left[\frac{1}{{}^3\zeta_m} - \sum\frac{x_A}{{}^3\zeta_A}\right] \quad \ldots (11)$$

where ${}^3\zeta_m$ is the ${}^3\zeta$ of the (A+B) mixture and is not given by Eq. 6. Since no method is available for the evaluation of α and ${}^3\zeta_m$ for these $(x_A A + x_B B)$ mixtures from the ${}^3\zeta$ values of pure A and B, we devised an alternative approach.

Expressing $(\Delta\eta)$ of these (A+B) mixtures by Eq. (11) would require that the molar excess volume, V^E, of these mixtures be also expressed by,

$$V^E = \alpha_{AB}\left[\frac{1}{{}^3\zeta_m} - \sum\frac{x_A}{{}^3\zeta_A}\right] \quad \ldots (12)$$

In fact, (V^E) data for ROH(A) ($R = CH_3$ or C_2H_5) $+ CHX_3$ (X = Cl or Br) or CH_2Br_2 (B) mixtures have been best reproduced[28] by Eq. 12 and the information[28] that this equation has yielded about the nature of the molecular species in these mixtures has further been substantiated by independent ideal

associated approach study[29] on the thermodynamic excess properties of ROH(A) ($R = CH_3$ or C_2H_5) + CHX_3(B) (X = Cl or Br) mixtures.

Consequently, Eqs 11 and 12 yield,

$$\frac{\Delta\eta}{V^E} = \frac{\alpha}{\alpha_{AB}} = K \qquad \ldots (13)$$

or

$$(\Delta\eta) = K V^E \qquad \ldots (14)$$

Equation 14 thus provides a very simple relationship between $(\Delta\eta)$ and (V^E) values of an (A+B) mixture.

Evaluation of $(\Delta\eta)$ values for a binary mixture from Eq. 14 requires a knowledge of its K parameter provided its V^E data are available. For the present analysis we employed $(\Delta\eta)$ and V^E values for $x_A = 0.5$ to compute its K parameter. This value of K was further coupled with the V^E data at any x_A to evaluate $(\Delta\eta)$ value for the mixture at that x_A. Such $(\Delta\eta)$ values at $x_A = 0.1$, 0.3, 0.7 and 0.9 are recorded (in paranthesis) in Table 2 and are also compared with the corresponding literature values[17-20]; the necessary V^E data were taken from literature[22,29-32].

Examination of Table 2 reveals that Eq. 14 describes reasonably well $(\Delta\eta)$ values of all the present (A+B) mixtures. However, Eq. 14 gives a poorer description of methylene chloride (A) + *o*-xylene (B) mixture than does Eq. 10.

Thus, in those (A+B) mixtures where it is possible to compute ${}^3\zeta$ of A and B, Eq. 10 provides a convenient means to evaluate $(\Delta\eta)$ for the mixture provided its $(\Delta\eta)$ value at $x_A = 0.5$ is available. On the other hand, when V^E data at various x_A and $(\Delta\eta)$ value at any one x_A are available. $(\Delta\eta)$ values for the mixture can be easily evaluated from Eq. 14 for any x_A.

Acknowledgement

The author expresses his thanks to the Head of the Chemistry Department of Maharshi Dayand University, Rohtak for providing necessary facilities.

References

1 Hosoya H, *Bull chem Soc Japan*, **44** (1971) 2332.
2 Rouvary D H, *RIC Rev*, **4** (1971) 173.
3 Graovac A, Gutaman I, Trinajstic N & Tivkovic T, *Theor chim Acta*, **26** (1970) 67.
4 Balaban A T, *Chemical applications of graph theory* (Academic press, London), 1976.
5 Hall L H & Kier L B, *J pharm Sci*, **67** (1978) 1743.
6 Coulson C A, *Proc Cambridge Philos Soc*, **46** (1950) 202.
7 Atkins P W, *Physical chemistry* (W H Freeman, San Fransisco), (1978) 805.
8 Chaoanne G & Risseghem H V, *Bull Soc chim Belg*, **31** (1922) 87.
9 Graef H D, *Bull Soc chim Belg*, **34** (1925) 427.
10 Edgar G, *Ind Eng Chem*, **19** (1927) 145.
11 Smyth C P & Stoops W N, *J Am chem Soc*, **50** (1928) 1883.
12 Timmerman J, *Physico-chemical constants of pure organic compounds* (Elsevier, Amsterdam), 1950, pp, (a) 34; (b) 38; (c) 44; (d) 63; (e) 86; (f) 91; (g) 98.
13 Kier L B, *Physico-chemical properties of drugs*, edited by S H Yolkowsky, A A Sinkula & S C Valvani (Marcel Dekker, New York) Chap. 9, p. 297.
14 Singh P P, Nigam R K, Singh K C & Sharma V K, *Thermochim Acta*, **46** (1981) 175.
15 *CRC handbook of chemistry and physics*, 58th Edn, 1977-78, pp. F-62, F-57.
16 Singh P P, *Thermochim Acta*, **66** (1983) 37.
17 Fort R J & Moore W R, *Trans Faraday Soc*, **62** (1966) 1112.
18 Nigam R K & Singh P P, *Indian J Chem*, **9** (1971) 691.
19 Mahl B S, Ph.D thesis, Kurukshetra University, 1973.
20 Maini N N, Ph.D thesis, Kurukshetra University, 1971.
21 Rowlinson J S, *Liquid and liquid mixtures*, (Butterworths, London), 1959, p. 182.
22 Nigam R K & Mahl B S, *J chem Soc, Faraday Trans-I*, **68** (1972) 1508.
23 McGlashan M L & Rastogi R P, *Trans Faraday Soc*, **54** (1958) 496.
24 Mecke R, Reuter A & Schupp R, *Z Naturforsch*, **49** (1949) 182.
25 Pimental G C & McClellan A L, *The hydrogen bond* (Freeman, San Fransisco) 1960.
26 Whetsel K B & Lady J H, *Spectroscopy of fuels* (Plenum, New York), 1970, pp. 259-279.
27 Woolley E M, Travers J G, Erno B P & Hepler L G, *J phys Chem*, **75** (1971) 3591.
28 Singh P P, Sharma V K & Sharma S P, *Thermochim Acta*, **106** (1986) 293.
29 Singh P P, Sharma B R & Sindhu K S, *Aust J Chem*, **30** (1977) 1241.
30 Nigam R K & Singh P P, *Trans Faraday Soc*, **65** (1969) 950.
31 Mishra R, Ph.D thesis, M.D. University, Rohtak, 1980.
32 Levien B J & Marsh K N, *J chem thermodyn*, **5** (1973) 651.

Indian Journal of Chemistry
Vol. 27A, June 1988, pp. 474-478

Charge-Transfer Complexes of Hydroxystyrylcyanine Dyes & Their Analogues with Nicotine: Structure—Activity Relationship Studies

MAHER M GIRGIS* & ZARIF H KHALIL

Chemistry Department, Faculty of Science, Assiut University Assiut, Egypt.

Received 20 *July* 1987; *revised and accepted* 3 *November* 1987

UV-visible spectrophotometric studies on the interaction of nicotine with hydroxystyrylcyanine dyes and their analogues [dyes (I-IX)] in 10% (v/v) aq ethanol at 29°C demonstrate the formation of charge-transfer complexes of dyes (I, III-VI) only. Addition of increasing amounts of nicotine to a solution containing fixed [dye] causes a decrease in the dye absorptivity with a gradual development of a new band at considerably longer wavelength characteristic of the complex formed. The spectra exhibit a clear unique isosbestic point. The stability constants and the molar absorptivities of the complexes formed have been calculated assuming the formation of 1:1 complexes. The experimental results have been interpreted in terms of molecular structure of the interacting molecules.

Nicotine finds growing interest for its biochemical[1] and pharmacological[2,3] effects. The biological activity of cyanine dyes is attributed to the adsorption of the dye molecules on active sites of the living cells[4]. Structure-activity relationship has been conducted on styryl and aza cyanine dye analogues to study their effect on breaking period of dormancy in garlic[5], essential oil production in sweet marjoram (*Origanum majorana* Linn)[6] and chromosomal behaviour in *Vicia faba* seeds[7]. To shed some light on the cause of bioeffect of aza cyanine dyes, formation of charge-transfer (CT) complexes between one of the nucleic acid bases (adenine) and azacyanine dyes has been investigated[8], and the results obtained were in accord with the biological activity of aza cyanine dyes when applied as bioregulator for *V. faba* seeds in the field.

The interactions between nicotine and drugs have been the subject of many investigations[3,9]. The interactions between nicotine and cyanine dyes have not been investigated. In this work we aim to study the CT interaction of nicotine with hydroxystyrylcyanine dyes and their analogues and the effect of geometry[10] on the complexation with a view to selecting an appropriate configuration for the development of radio immunoassay for tobacco alkaloids[11].

Materials and Methods

Nicotine (BDH) was used as such. Styrylcyanine dyes (I-IX) were prepared by the method described before[12] and recrystallized from ethanol. Their purity was checked by elemental analyses and spectral data.

All experiments were carried out in 10% (v/v) ethanol-water mixture. The calculated volumes of nicotine (0.05 mol dm^{-3}), dye (0.001 mol dm^{-3}) and ethanol were mixed together and the volume made up to 10 ml in a dark-coloured bottle by adding doubly dis-

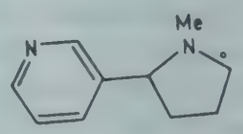

3 [1-Methyl-2-pyrrolidinyl] -pyridine (Nicotine)

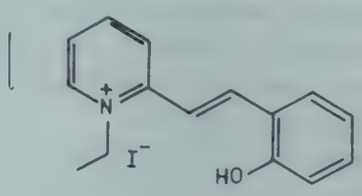

2 [2-Hydroxystyryl] pyridinium-1-ethyl iodide. (Dye I)

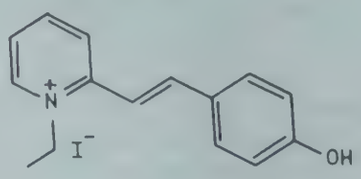

2 [4-Hydroxystyryl] pyridinium-1-ethyl iodide. (Dye II)

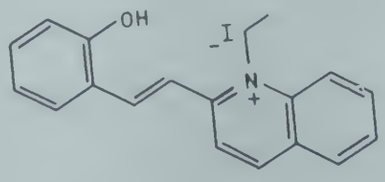

2 [2-Hydroxystyryl] quinolinium-1-ethyl iodide. (Dye III)

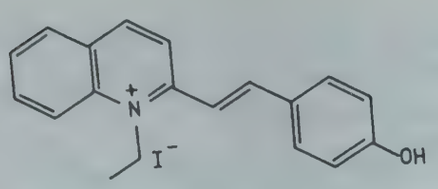

2 [4-Hydroxystyryl] quinolinium-1-ethyl iodide. (Dye IV)

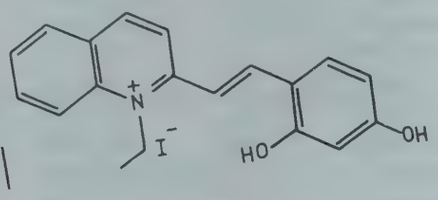

2 [2,4-Dihydroxystyryl] quinolinium-1-ethyl iodide. (Dye V)

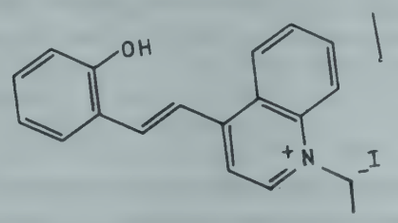

4 [2-Hydroxystyryl] quinolinium-1-ethyl iodide. (Dye VI)

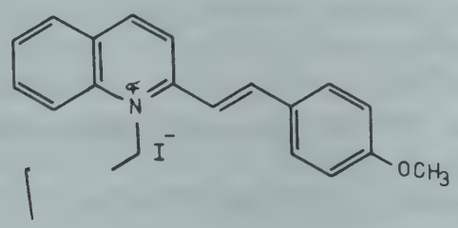

2 [4-Methoxystyryl] quinolinium-1-ethyl iodide. (Dye VII)

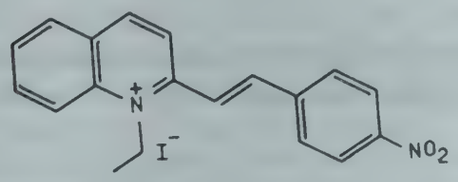

2 [4-Nitrostyryl] quinolinium-1-ethyl iodide. (Dye VIII)

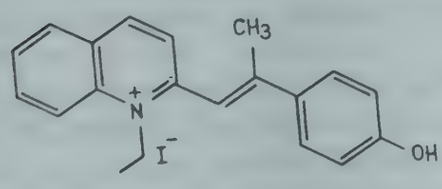

2 [2-Methyl-2(4-hydroxyphenyl)ethenyl] quinolinium-1-ethyliodide. (Dye IX)

tilled water. The solutions were freshly prepared each day, and their aborbances were measured within 5 hr. All the operations were performed at 22°C in subdued light.

Spectrophotometric measurements were made on a Shimadzu UV-200S double beam spectrophotometer, using a rectangular cell of 1 cm pathlength against solvent as the blank. The absorbances were measured at fixed wavelengths to minimize errors arising from the steepness of absorption spectra. The absorption band of the complex formed between nicotine and the dye was detected at wavelength longer than those of the individual components at concentrations identical to that in the mixture. The absorbances were measured within ~ 10 min after mixing the solutions and placing the cell in a thermostated cell holder for equilibrium. The accuracy of the measurement was ± 0.01 absorbance unit.

Results and Discussion

The absorption spectra of the dyes I, III, IV and VI are presented in Fig. 1. For some dye-nicotine mixtures, the visible absorption band of the dye diminishes gradually with increase in nicotine content in the mixture and a new band gradually appears at longer wavelength. The spectra of the mixture show a clear unique isosbestic point (Fig. 2). This behaviour is noticed only for nicotine-dye (I, III-VI) combinations, but not with other nicotine-dye (II, VII-IX) combinations. The appearance of this new longer wavelength band is attributed to the formation of a charge-transfer (CT) complex between nicotine and the dyes I and III-VI.

The stoichiometry of the CT complex ($N_n D_d$) of nicotine (N) and dye (D),

$$nN + dD \rightleftharpoons N_nD_d \qquad \ldots(1)$$

was determined applying Eq. (2)[13]

$$A_\lambda^{CT} = K_c^{CT} \cdot \varepsilon_\lambda^{CT} [N]^n [D]^d \qquad \ldots(2)$$

where A_λ^{CT} and ε_λ^{CT} are the absorbance and the molar absorptivity, respectively, of the complex at wavelength λ, and K_c^{CT} is the thermodynamic equilibrium constant. A plot of A_λ^{CT} versus concentration of one component, that of other being kept constant, on log paper, proved that the complex has 1:1 composition. Thus, for the equilibrium

$$N + D \rightleftharpoons N\,D \qquad \ldots(3)$$

the equilibrium constant (K_c^{ND}) is given by Eq. (4)

$$K_c^{ND} = \frac{[ND]}{[N][D]} = \frac{[ND]}{\{[N]_0 - [ND]\}\{[D]_0 - [ND]\}} \qquad \ldots(4)$$

where ND is the complex formed, and $[N]_0$ and $[D]_0$

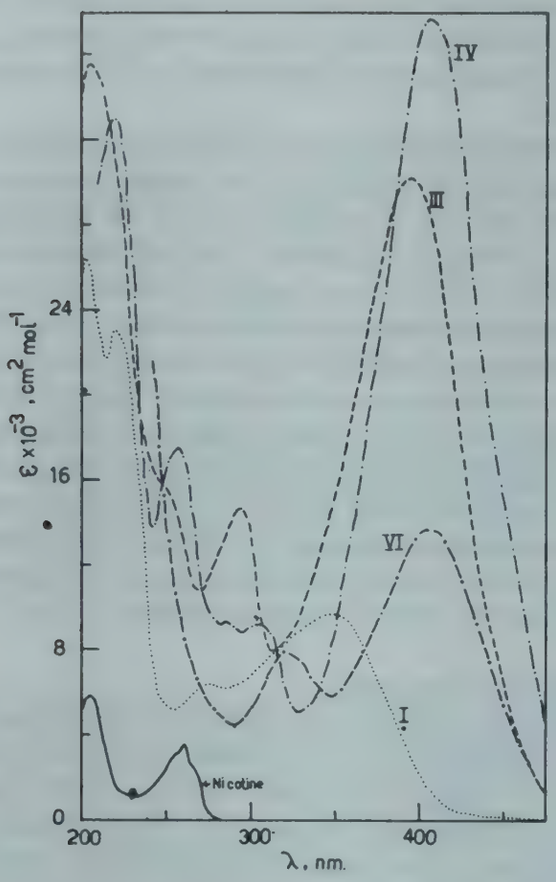

Fig. 1—Electronic absorption spectra of dyes (I, III, IV and VI) and nicotine in 10% (v/v) aq ethanol at 29°C.

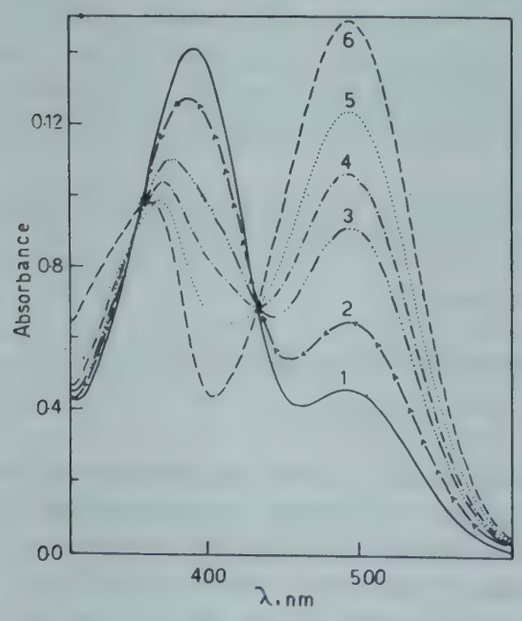

Fig. 2—Absorption spectra of 5.56×10^{-5} mol dm^{-3} dye(III) in 10% (v/v) aq ethanol at 29°C to which the following amounts of nicotine (mol dm$^{-3} \times 10^4$) were added: (1) 0.50; (2) 0.86; (3) 1.72; (4) 2.50; (5) 5.00; (6) 50.00.

are the initial concentrations of nicotine and the dye respectively. Eq. (4) may be rearranged to obtain Eq. (5)

$$\frac{[D]_0}{[ND]} = \frac{1}{K_c^{ND}} \cdot \frac{1}{[N]_0} + \frac{[D]_0}{[N]_0} + 1 - \frac{[ND]}{[N]_0} \quad \ldots(5)$$

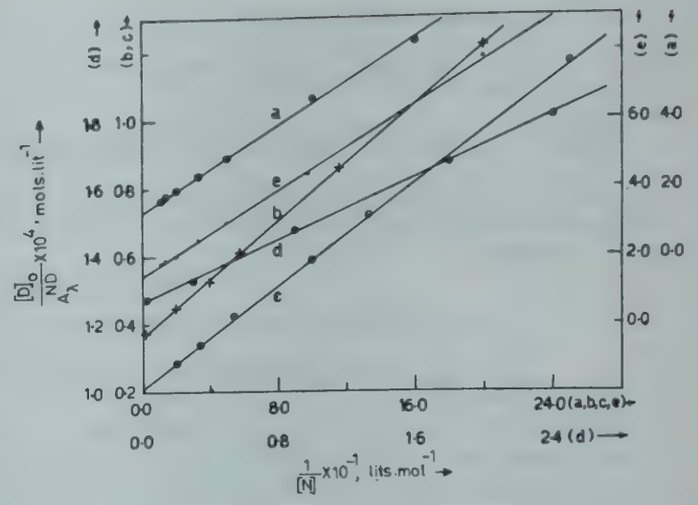

Fig. 3—Plots of $[D]_0/A_\lambda^{ND}$ versus $1/[N]_0$ for 10% (v/v) aq ethanol containing fixed [dye] and different [nicotine] at 29°C. [The combinations are: (a) nicotine-dye(I) ([dye I] = 7.40×10^{-5} mol dm^{-3}); (b) nicotine-dye(III) ([dye III] = 5.58×10^{-5} mol dm^{-3}); (c) nicotine-dye(IV) ([dye IV] = 3.87×10^{-5} mol dm^{-3}); (d) nicotine-dye (V) ([dye V] = 9.27×10^{-5} mol dm^{-3}); (e) nicotine-dye(VI) ([dye VI] = 9.30×10^{-5} mol dm^{-3})].

Since the absorbance in the region of the new band is due to the complex ND (Fig. 2), and the solution is of 1 cm pathlength, for two molecules forming complex in accordance with Eq. (3), the molar absorptivity of the complex at wavelength λ is given by Eq. (6)

$$\varepsilon_\lambda^{ND} = \frac{A_\lambda^{ND}}{[ND]} \quad \ldots(6)$$

where A_λ^{ND} is the absorbance of the complex (ND) at the wavelength λ.
Combining Eqs (5) and (6), we get

$$\frac{[D]_0}{A_\lambda^{ND}} = \frac{1}{K_c^{ND} \cdot \varepsilon_\lambda^{ND}} \cdot \frac{1}{[N]_0} + \frac{[D]_0}{[N]_0 \varepsilon_\lambda^{ND}} + \frac{1}{\varepsilon_\lambda^{ND}} - \frac{[ND]}{[N]_0 \varepsilon_\lambda^{ND}} \quad \ldots(7)$$

Since $[N]_0 \gg [ND]$ it is possible to neglect the last term in the right hand side of Eq. (7)[14a], so that

$$\frac{[D]_0}{A_\lambda^{ND}} = \frac{1}{[N]_0}\left(\frac{1}{K_c^{ND}\ \varepsilon_\lambda^{ND}} + \frac{[D]_0}{\varepsilon_\lambda^{ND}}\right) + \frac{1}{\varepsilon_\lambda^{ND}} \quad \ldots(8)$$

For a series of solutions of constant $[D]_0$ and varying $[N]_0$ a plot of $[D]_0/A_\lambda^{ND}$ against $1/[N]_0$ should be linear. The intercept of the line with ordinate gives $(\varepsilon_\lambda^{ND})^{-1}$ and the gradient is equal to $[(K_c^{ND} \cdot \varepsilon_\lambda^{ND})^{-1} + [D]_0(\varepsilon_\lambda^{ND})^{-1}]$, so that K_c^{ND} and ε_λ^{ND} can be evaluated. Plots of Eq. (8) for nicotine-dye (I, III-VI) mixtures at 29°C are represented in Fig. 3 while K_c^{ND} and ε_λ^{ND} values are given in Table 1.

Various pyridinium salts are utilized as coenzyme models. Pyridine and its derivatives, e.g. nicotinic acid, act as electron donors on mixing with electron acceptors such as riboflavin[15] and iodine[16] forming CT

Table 1—$\lambda_{max}(\varepsilon_{max})$ Values of CT Bands of Styrylcyanine Dyes (I-IX) and Nicotine-Dye (ND) Combinations, Isosbestic Points and Equilibrium Constants $(K_c^{ND})^{a-c}$

Dye	CT-band λ_{max}^{D} ($\varepsilon_{max}^{D} \cdot 10^{-3}$)	Combination	CT-band λ_{max}^{ND} ($\varepsilon_{max}^{ND} \cdot 10^{-3}$)	Isosbestic point (nm)	$K_c^{ND} \cdot 10^{-3}$ ($dm^3 mol^{-1}$)
I	348(9.7)	Nicotine-dye(I)	424(7.7)	375	5.99
II	330*sh*(8.3)	Nicotine-dye(II)	—	—	—
III	394(30.2)	Nicotine-dye(III)	506(27.4)	434	16.40
IV	406(37.7)	Nicotine-dye(IV)	496(47.6)	436	7.08
V	511(4.0)	Nicotine-dye(V)	549(7.9)	473	11.66
VI	404(13.7)	Nicotine-dye(VI)	505(7.1)	444	7.61
VII	400(29.0)	Nicotine-dye(VII)	—	—	—
VIII	364(29.5)	Nicotine-dye(VIII)	—	—	—
IX	585(6.3)	Nicotine-dye(IX)	—	—	—

(a) λ_{max} in nm; ε_{max} in $cm^2 mol^{-1}$.

(b) All measurements were carried out in 10% (v/v) aq ethanol at 29°C.

(c) Nicotine has a characteristic band: $\lambda_{max} = 261$ nm ($\varepsilon_{max} = 3.5 \times 10^3$ cm^2 mol^{-1}).

complexes. Kosower and coworkers[17] have shown that pyridinium ion acts as an electron acceptor during formation of a CT complex with iodide ion as the electron donor. Such complexes are essentially ion-pairs in the ground state[14b]. Absorption of energy within the CT-band causes excitation to a covalent excited state. The coloured nature of the quinolinium iodide[18] as compared to the lack of absorption in the visible region by most of other quinolinium salts has been explained in terms of CT interaction between the two ions. Bispyridinium cation derivatives form 1:1 CT complexes with neutral donor species[19].

Experimental results show that the absorption spectrum of nicotine is not changed by the addition of iodide ions, indicating that there is no CT interaction between nicotine and iodide ions.

The spectra of nicotine-dye (I, III-VI) mixtures exhibit (Fig. 2) isosbestic point which may be taken as an evidence for 1:1 complex formation[20]. Application of Eq. (8) gives linear slopes (Fig. 3) supporting 1:1 complex formation. The results show wavelength-independence of the equilibrium constant indicating the formation of only one type of complex[21].

Exact geometry of the complex cannot be determined from the present absorption measurements, but parallel stacking interactions between nicotine and dye can be invoked as have been for similar systems[22].

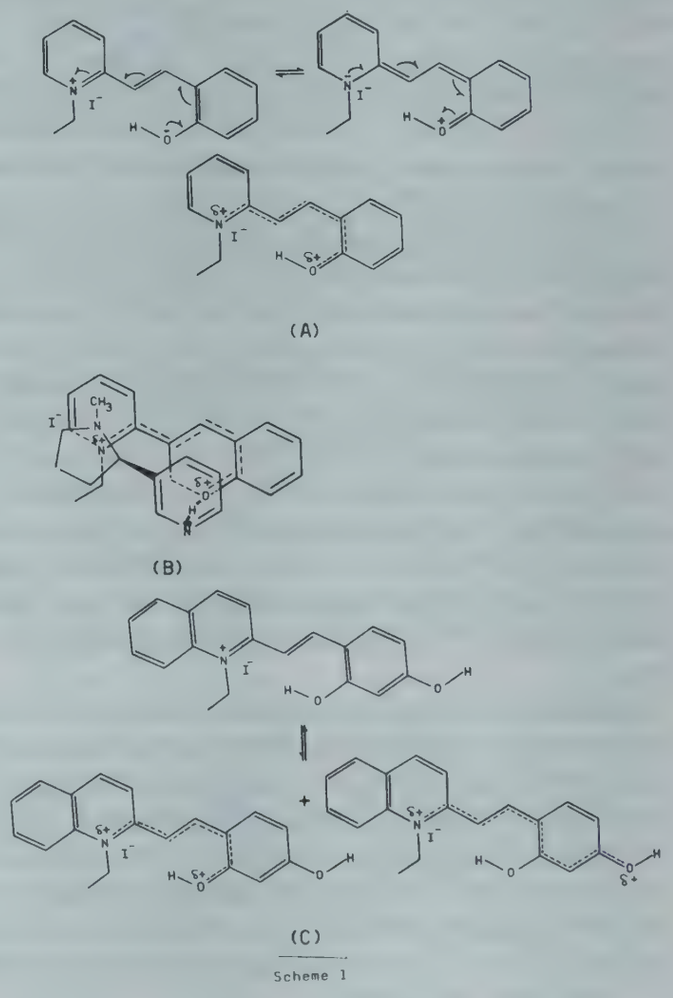

Scheme 1

In the present investigation, it is found that the ability of nicotine to form CT complexes with styrylcyanine dyes depends mainly on their molecular structures. Thus, 2-(2-hydroxystyryl)-pyridinium-1-ethyl iodide (dye I) forms CT complex on mixing with nicotine. This CT complex is assumed to be formed by 1:1 parallel stacking interaction between nicotine as an electron donor and dye(I) as an electron acceptor. The acceptor character of the dye results from the two partially positive centres located at the quaternary nitrogen and the oxygen atom of the hydroxystyryl moiety (Scheme 1A). The hydrogen atom of the hydroxyl group may act as a bridge between the O-phenyl of dye (I) and the unshared electron pair located at

the N-pyridine of nicotine molecule. The two partially positive centres of dye(I) are located at a distance equal to the distance between the two N-atoms of pyridine and pyrrolidinyl moieties of nicotine, since the distance geometry[10] is approximately the same. The suggested 1:1 parallel stacking interaction is presented in Scheme 1 B[23]. In support of this suggestion, 2-(4-hydroxystyryl)-pyridinium-1-ethyl iodide (dye II) does not form CT complex with nicotine as the two positive centres of dye(II) do not fit the distance geometry[10] and the ring-ring[24] size formation with nicotine.

On the other hand 2-(2-hydroxystyryl)-quinolinium-1-ethyl iodide (dye III) and 2-(4-hydroxystyryl) quinolinium-1-ethyl iodide (dye IV) form CT complexes. This behaviour of dye(IV) in contrast to that of dye(II) may be attributed to greater delocalisation of the positive charge at the N-quaternary atom of quinolinium moiety, due to the extra-fused benzene ring which enables the formation of a stable CT complex with nicotine. The stability constant (K_c^{ND}) of nicotine-dye(IV) complex (7.08×10^3 dm^3 mol^{-1}) is much less than that of nicotine-dye (III) complex (16.40×10^3 dm^3 mol^{-1}). The dye 2-(2,4-dihydroxystyryl)-quinolinium-1-ethyl iodide (dye V) forms a CT complex with $K_c^{ND} = 11.66 \times 10^3$ dm^3 mol^{-1}, a value which is half of the sum of stability constants of CT complexes of nicotine with dyes III and IV (Table 1). This may be attributed to the fact that dye(V) has two resonance hybrid structures giving two types of complexes (of Scheme 1C). 4-(2-Hydroxystyryl)-quinolinium-1-ethyl iodide (dye VI) forms a CT-complex with nicotine having $K_c^{ND} = 7.61 \times 10^3$ dm^3 mol^{-1}. This value is much less than that of nicotine-dye(III) complex, but is approximately the same as that of nicotine-dye (IV) complex. This is due to the fact that dyes(IV) and (VI) have approximately the same distance geometry[10] between two partially positive centres.

Substitution of the hydroxyl group in 4-hydroxystyryl moiety by a methoxyl group (electron releasing) as in dye (VII), or a nitro group (electron withdrawing) as in dye(VIII) does not help in the formation of CT complexes. This provides further new evidence for the formation of H-bridge between the hydroxystyryl and the N-pyridine moieties, since this H-bridge is absent in the dyes (VII) and (VIII), and consequently no CT complexes are formed.

Substitution at the ethenyl moiety ($-CH=CH-$) of the 4-hydroxystyryl group (dye IX) also does not lead to CT complex formation with nicotine. This may be due to steric congestion between the interacting molecules and the inability to adopt ring-ring conformations needed[24].

References

1 Aceto M D, Martin B R & May E L, *CRC Handbook stereoisomers: Drugs psychopharmacol*, edited by Donald F Smith (CRC, Boca Raton, Fla) 1984, p. 67-78.

2 Balfour D J K, *Int encycl pharmacol Ther*, edited by D J K Balfour (Pergamon, UK.) 1984, pp. 101-12.

3 Masafumi H & Gerhard L, *J pharm Sci*, **74** (1985) 412.

4 Terada H, Nagamune H, Morikawa N & Ikuno M, *Biochem Biophys Acta*, **807** (1985) 168

5 Abdou R F, Waly E A, Abde[illegible] A & Khalil Z H, *Assiut J Agric Sci, Egypt*, **14** (1983) 15.

6 El-Keltawi N E & Khalil Z H, *Flavour Fragrance J*, **1** (1986) 63.

7 Abdou R F, Omara M K, Hussein M Y & Khalil Z H, *Assiut J Agric Sci, Egypt*, **13** (1982) 117.

8 Girgis M M & Khalil Z H, *Croat Chem Acta*, **2** (1987) 225.

9 Jusko W J, *J Pharmacokinet Biopharm*, **6** (1978) 7.

10 Sheridan R P, Nilakantan R, Dixon J S & Venkataraghavan R, *J mednl Chem*, **29** (1986) 899.

11 (a) Shibagaki M, Matsushita H, Shibata S, Saito A, Ysujino Y & Kaneko H, *Heterocycles*, **19** (1982) 1641.
(b) Castro A, Monji N, Ali H, Yi M, Bowman E R & Mckennis H, *Eur J Biochem*, **104** (1980) 331.

12 Phillips A P, *J org Chem*, **12** (1947) 233.

13 Slifkin M A, *Charge transfer interactions of biomolecules* (Academic Press, London) 1971, p. 17.

14 Foster R, *Organic charge-transfer complexes* (Academic Press, London) 1969, (a) p. 135, (b) p. 340.

15 (a) Draper R D & Ingraham Ll L, *Archs Biochem Biophys Acta*, **139** (1970) 265, (b) Mc Cormick D B, Heng-Chun Li & Mackenzie R E, *Spectrochim Acta*, **23** (1967) 2353.

16 (a) Krishna V G & Bhowmik B B, *J Am chem Soc*, **90** (1968) 1700. (b) Popov A I & Rygg R H, *J Am chem Soc*, **79** (1957) 4622. (c) Srivastava R D & Prasad G, *Spectrochim Acta*, **22** (1966) 825. (d) Bhaskar K R & Singh S, *spectrochim Acta*, **23** (1967) 1155. (e) Mckinney W J, wong M K & Popov A I, *Inorg Chem*, **7** (1968) 1001.

17 (a) Kosower E M & Klinedinst P E, Jr., *J Am chem Soc*, **78** (1956) 3493. (b) Kosower E M, *J Am chem Soc*, **78** (1956) 3497. (c) Kosower E M & Burbach J C, *J Am chem Soc*, **78** (1956) 5838. (d) Kosower E M, *J Am chem Soc*, **80** (1958) 3253. (e) Kosower E M, Skorez J A, Schwarz W M, Jr. & Patton J W, *J Am chem Soc*, **82** (1960) 2188. (f) Kosower E M & Skorez J A, *J Am chem Soc*, **82** (1960) 2195. (g) Kosower E M, *Molecular biochemistry*, (McGraw-Hill, New York) (1962), p. 180.

18 (a) Mason S F, *J chem Soc* (1960) 2437. (b) Briegleb G, Jung W & Herre W, *Z phys Chem Frankf Ausg*, **38** (1963) 253.

19 (a) Nakahara A & Wang J H, *J phys Chem*, **67** (1963) 496. (b) Ledwith A & Iles D H, *Chem Brit*, **4** (1968) 266.

20 Gouterman M & Stevenson P E, *J chem Phys*, **37** (1965) 2266.

21 Johnson G D & Bower R E, *J Am chem Soc*, **87** (1965) 1655.

22 (a) Dimicoli J L & Helene C, *J Am chem Soc*, **95** (1973) 1036. (b) Dimicoli J L, *Biochem Biophys Acta*, **254** (1971) 349.

23 Tsibris J C M, Mc Cormick D B & Wright L D, *Biochemistry*, **4** (1965) 504.

24 Jaffrey I S, Henry V S, Homer H & Roseanne G, *J Am chem Soc*, **102** (1980) 7741.

Indian Journal of Chemistry
Vol. 27A, June 1988, pp. 479-481

Solution Densities of Aqueous Potassium Chloride-Barium Chloride Mixtures at 298.15 K & Different Ionic Strengths

ANIL KUMAR†
Institute of Physical Chemistry, University of Karlsruhe, 7500, Karlsruhe, F.R. Germany

Received 16 *July* 1987; *accepted* 14 *September* 1987

The solution densities of aqueous KCl-$BaCl_2$ mixtures are reported at 298.15K from ionic strength 0.5 to 4.5 mol kg^{-1} of water. The negative excess volumes (ΔV_m) obtained from the experimental mean apparent molal volumes are fitted to the Friedman equation. The reliable estimates of the mixture densities can be made by the Young's rule with the addition of the ΔV_m values. In general, the densities can be predicted to within 14 ppm with the use of ΔV_m term as compared to 211 ppm obtained without the use.

Recently, there has been growing interest in the thermodynamic properties of concentrated electrolyte mixtures. Although, a large number of papers have appeared on osmotic and activity coefficients of these mixtures, only a little[1-3] has been accomplished as regard their PVT properties in concentrated region. A knowledge of PVT properties is essential in obtaining the pressure dependence of activity coefficients in these solutions. Thus, the present investigation reports the densities and mean apparent molal volumes of aqueous KCl-$BaCl_2$ mixtures at 298.15K and at ionic strengths of 0.5, 1, 3 and 4.5 mol kg^{-1} of water. The experimental measurements cover the range from pure KCl to pure $BaCl_2$ solutions.

Materials and Methods

Both KCl and $BaCl_2$ (Baker analysed) were recrystallized twice from water before use. The stock and working solutions were prepared by dissolving a definite weight in degassed ion-exchanged water. The concentrations of these solutions were determined gravimetrically using $AgNO_3$ solution. The mixtures of KCl and $BaCl_2$ were prepared at constant ionic strength as $Y_{BaCl_2} = 3m_{BaCl_2}/(m_{KCl} + 3m_{BaCl_2})$, where m and Y respectively refer to molality and ionic strength fraction of an electrolyte in mixture and $Y_{KCl} + Y_{BaCl_2} = 1$.

The densities were measured using a Paar vibrating tube densimeter[4]. The relative densities (Δd) were evaluated as the difference between density of solution (d) and that of pure water (= 0.997047 gm^{-3} at 298.15K). The densimeter was calibrated with the known densities of water[5] and NaCl solutions[6]. The temperature of the densimeter was controlled within ± 0.005°C and the densities were precise to ± 3 ppm.

† Present address: Department of Sugar Chemistry, Deccan Sugar Institute, Manjari (BK), Pune 412 307

Results and Discussion

In Table 1 are reported the relative densities (Δd) as a function of Y_{BaCl_2} for aqueous KCl-$BaCl_2$ at I = 0.5, 1, 3 and 4.5 mol kg^{-1} of water.

Apparent molal volumes, ϕ_V of pure KCl and $BaCl_2$ solutions were calculated using Eq (1)[7]

$$\phi_V = [10^3(d_0 - d)/mdd_0] + (M/d) \quad \ldots (1)$$

where M refers to the formula weight of an electrolyte.

The mean apparent molal volumes in mixtures, ϕ_V^* were obtained using Eq. (2)

Table 1—Experimental Density Differences (Δd/g cm^{-3}) as a Function of Y_{BaCl_2} for the System aq. KCl-$BaCl_2$ at 298.15K

Y_{BaCl_2}	$\Delta d \times 10^3$ g cm^{-3}	Y_{BaCl_2}	$\Delta d \times 10^3$ g cm^{-3}
I = 0.5 mol kg^{-1}		I = 3 mol kg^{-1}	
0	22.721	0	121.266
0.1253	23.618	0.1259	127.482
0.2317	24.379	0.2483	133.577
0.3518	25.238	0.3596	139.152
0.4006	25.603	0.4929	145.844
0.5001	26.300	0.6103	151.800
0.6198	27.165	0.7185	157.309
0.7251	27.902	0.8399	163.509
0.8098	28.524	0.9385	168.575
0.9321	29.225	1.0000	171.750
1.0000	29.877		
I = 1 mol kg^{-1}		I = 4.5 mol kg^{-1}	
0	44.291	0	171.038
0.1582	46.628	0.1195	180.054
0.3051	48.805	0.2428	189.556
0.4182	50.481	0.3775	199.945
0.4995	51.685	0.4952	209.155
0.6128	53.366	0.6111	218.349
0.7523	55.437	0.7275	227.684
0.8951	57.556	0.8505	237.643
1.0000	59.115	0.9301	244.152
		1.0000	249.950

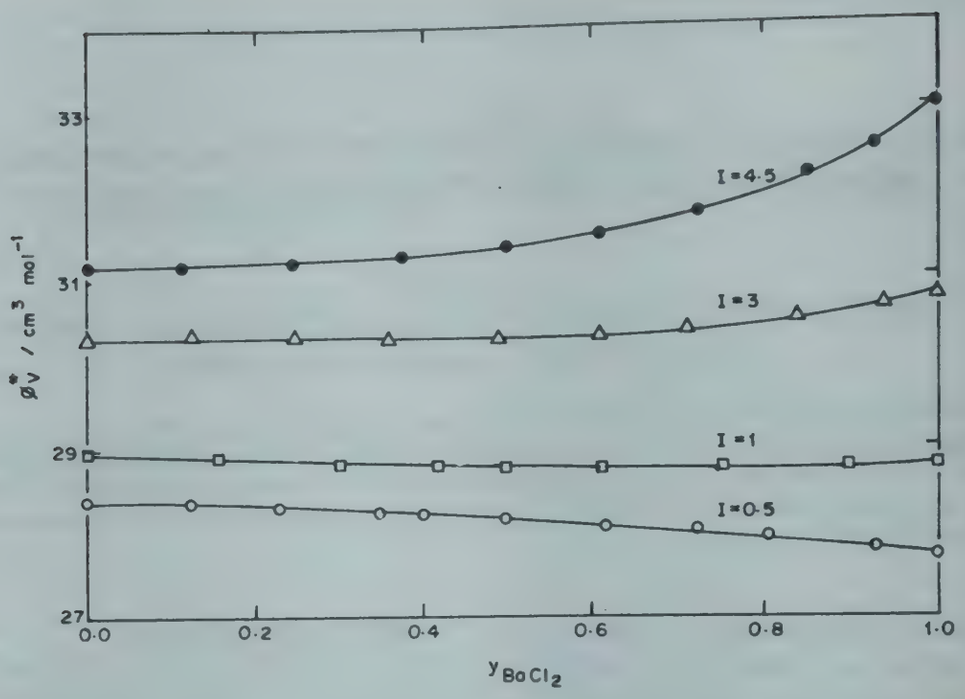

Fig. 1 – Experimental mean apparent molal volumes (ϕ_V^*) as a function of Y_{BaCl_2} at different ionic strengths for aq. KCl-$BaCl_2$

$$\phi_V^* = [10^3(d_0 - d)/m_T d d_0] + (M_T/m_T d) \quad \ldots (2)$$

where $m_T = m_{KCl} + m_{BaCl_2}$;
$M_T = (m_{KCl}M_{KCl} + m_{BaCl_2}.M_{BaCl_2})$.

The values of ϕ_V^* at each ionic strength are plotted as a function of Y_{BaCl_2} in Fig. 1 showing nonlinear variation.

The excess volumes of mixing, ΔV_m were calculated by the expression (3)

$$\Delta V_m = \phi_V^* m_T - \phi'_{V,KCl}.m_{KCl} - \phi'_{V,BaCl2}.m_{BaCl_2} \quad \ldots (3)$$

Where ϕ'_V refers to the apparent molal volume of an individual electrolyte solution at the ionic strength of mixture. The ΔV_m values, thus obtained can be fitted to Friedman's equation[8] (see Eq. 4),

$$\Delta V_m = Y_{BaCl_2}(1 - Y_{BaCl_2})I^2[v_0 + v_1(1 - 2Y_{BaCl_2})] \quad \ldots (4)$$

where v_0 and v_1 indicate the binary (K^+, Ba^{2+}) and ternary (K^+, $Ba^{2+}Cl^-$) interactions respectively. In Fig. 2, the ΔV_m values are plotted against Y_{BaCl_2}, except at $I = 0.5$ mol kg^{-1} because of extremely small ΔV_m values. The ΔV_m values are negative throughout. The plots in Fig. 2 exhibit symmetrical parabola at $Y_{BaCl_2} = 0.5$. Thus, v_1 in Eq. (4) may be neglected. The values of v_0 obtained from Eq (4) are -0.122, -0.178, -0.272 and -0.528 at $I = 4.5$, 3, 1 and 0.5 mol kg^{-1} of water, respectively with an average standard deviation of fit for ΔV_m to be 0.01 cm^{3}kg^{-1} of water.

Wood and Gamkhar[9] have reported the heats of mixing (ΔH_m) data for this system, and fitted these data to an equation analogous to Eq. (4) and obtained h_0 and h_1 values similar to v_0 and v_1. The decrease v_0 with increase in ionic strength is supported by a similar trend in h_0 values reported by Wood and Gamkhar[9]. The magnitude of h_1 is extremely small, thus suggesting negligible triple interactions. A similar situation is found for ΔV_m. In addition, Pitzer and Kim[10] analysed the osmotic and activity coefficient data[11] on aq. KCl-$BaCl_2$ system using their virial coefficient approach. They obtained negative binary mixing and zero ternary terms supporting our ΔV_m results.

The need for considering ΔV_m values in estimating the densities of mixtures can be demonstrated by comparing the experimental densities with those calculated by Eq. (5)

$$d = d_0(1000 + M_T)/(\phi^*_{V,est} m_T d_0 + 1000) \quad \ldots (5)$$

where

$$\phi^*_{V,est} = x_{KCl}\phi'_{V,KCl} + x_{BaCl_2}\phi'_{BaCl_2} + \Delta V_m/m_T \quad \ldots (6)$$

and $x = m/m_T$

The first two terms on the right hand side of Eq. (6) represent the well known Young's rule[12], which states that no volume change occurs on mixing the solutions of equal ionic strength. The last term on right hand side of Eq. (6) gives the correction term or excess property.

In Eq. (6), $\phi^*_{V,est}$ can be calculated with and without ΔV_m and so the values of d can be obtained. Table 2 reports the maximum and minimum differences (δ) between experimental and those obtained with and without the use of ΔV_m. One, for example, can see that

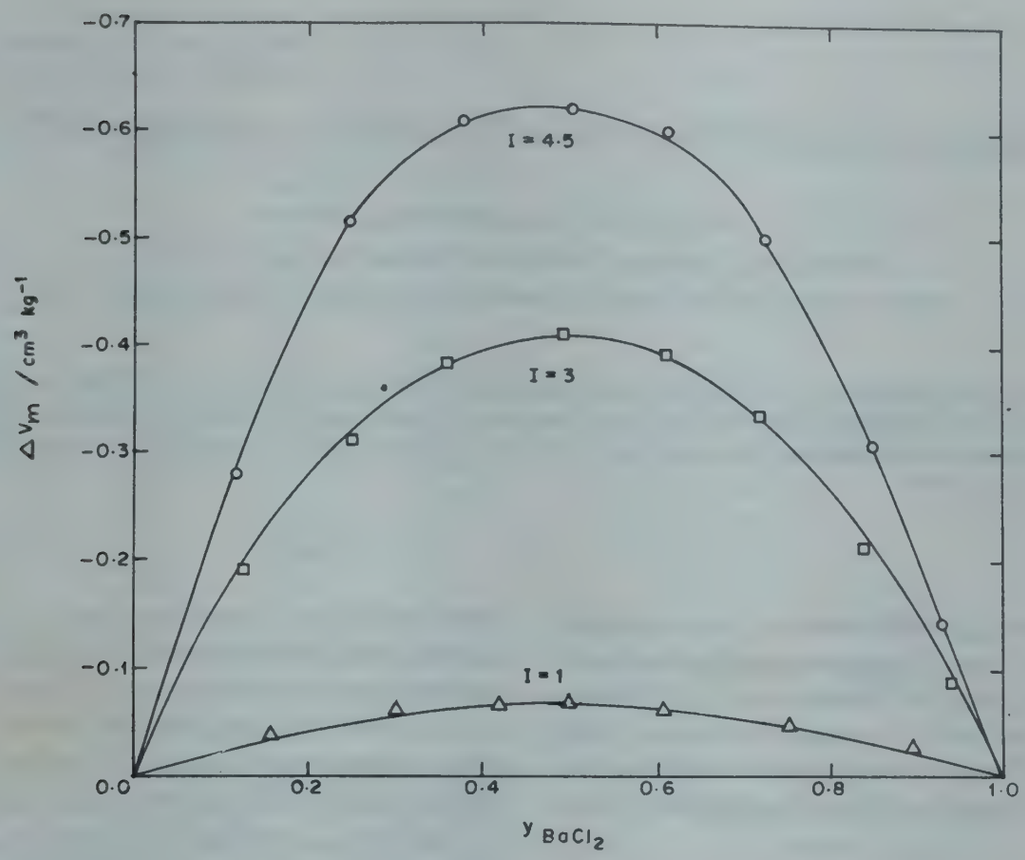

Fig. 2—Excess volumes of mixing ΔV_m as a function of Y_{BaCl_2} at different ionic strengths for aq. KCl-$BaCl_2$

Table 2—Differences (δ, in ppm) between Experimental Densities and Densities Calculated with and without Addition of ΔV_m to Young's Rule for Aqueous KCl-$BaCl_2$ at 298.15K

Ionic strength (mol kg^{-1})	δ (ppm)			
	Without ΔV_m		With ΔV_m	
	Av.	Max.	Av.	Max.
0.5	12	17	6	9
1	44	61	10	14
3	299	411	18	25
4.5	490	672	21	29

densities at $I = 4.5$ mol kg^{-1} can be measured to 15 ppm with the use of ΔV_m values as compared to 490 ppm obtained without its use. As an average, the differences δ are 211 ppm at $I = 0.5$-4.5 mol kg^{-1} without the use of ΔV_m. These differences are reduced to 14 ppm with the use of ΔV_m.

To summarise, the densities of concentrated mixtures of 1-1 and 2-1 electrolytes can be estimated with the Young's rule[12], combined with the correction term or excess volumes. One notes that the average difference δ of 14 ppm remains slightly higher than the experimental accuracy.

Acknowledgement

The author is grateful to the authorities of University of Karlsruhe for permitting him to use the experimental facilities.

References

1 Wirth H E & Mills W L, *J chem engng Data*, **13** (1968) 102.
2 Kumar A, Atkinson G & Howell R D, *J solution Chem*, **11** (1982) 857.
3 Millero F J, Connaughton L M, Vinokurova F & Chetirkin P V, *J solution Chem*, **14** (1985) 837.
4 *DMA instruction manual*, Anton Paar K G, A-8054 Graz, Austria.
5 Kell G S, *J chem engng Data*, **20** (1975) 97.
6 Losurdo A, Alzola E M & Millero F J, *J Chem Thermodyn*, **14** (1982) 649.
7 Millero F J, *Activity coefficients in electrolyte solutions*, Vol II, edited by R M Pytkowicz (CRC Press, Boca Raton) 1979 pp 63.
8 Friedman H L, *Ionic solution theory* (Wiley-Interscience, New York) 1962 pp 265.
9 Wood R H & Gamkhar M, *J phys Chem*, **73** (1969) 3959.
10 Pitzer K S & Kim J J, *J Am chem Soc*, **96** (1974) 5701.
11 Robinson R A & Bower V E, *J Res NBS*, **69A** (1965) 439.
12 Young T F & Smith M B, *J phys Chem*, **58** (1954) 716.

Indian Journal of Chemistry
Vol. 27A, June 1988, pp. 482-486

Electrochemical Behaviour of Bisazo Dye, Acid Red-150

R N GOYAL* & ANOOP KUMAR
Department of Chemistry, University of Roorkee, Roorkee 247 667
Received 30 *July* 1987; *revised* 21 *September* 1987; *accepted* 16 *October* 1987

The electrochemical behaviour of Acid Red-150 has been studied in the *p*H range of 2.2-11.2. Unlike the reduction of bisazobenzene to bishydrazo-benzene, the reduction of azo group attached to napthol moiety in this dye takes place in a ($4e, 4H^+$) reduction step to give amino compound as product of electrode reaction. The products of electrolysis have been separated and identified.

An excellent review is available on the polarographic reduction of azo dyes in aqueous and non-aqueous media[1]. However, most of the studies are confined to the reduction of monoazo compounds and very little is known about the azo compounds containing two azo groups and hence the title investigation was undertaken.

Materials and Methods

Acid Red-150 (I) (Sigma Chemical Co) was used as received. Its stock solution (2 m*M*) was prepared in doubly distilled water. Universal Britton-Robinson[2] buffers (*p*H 2.2-11.2) were used. The *p*H was measured using an ECIL expanded scale *p*H meter (model *p*H 821) after due standardisation with potassium hydrogen phthalate and borax buffers.

Polarograms were recorded on a Cambridge pen recording polarograph. The capillary used had the following characteristics: $m = 1.25$ mgs^{-1}, and $t = 3.90$ at $h = 60$ cm.

For recording polarograms and voltammograms 1 ml of the stock solution of the dye was mixed with 9.0 ml of buffer of appropriate *p*H under total nitrogen blanket. Voltammetric studies were carried out using Micronic cyclic voltammeter and a digigraphic X, Y-t recorder. The details of instruments used for spectral studies have been described elsewhere[3]. Pyrolytic graphite electrode was prepared by the method reported earlier[4]. It had an area ~ 1.8 mm^2. All potentials refer to SCE at 25°C.

Controlled potential electrolysis and product identification

Controlled potential electrolysis of 1 m*M* solution of the dye was carried out in a three-compartment cell at potential more negative to peak Ic or IIc or at the plateau potential of the first or second polarographic wave. The working electrode was pyrolytic graphite plate (area 6 cm^2) or mercury pool, counter electrode was the cylindrical platinum gauze and the reference electrode was a saturated calomel electrode. Nitrogen was bubbled throughout electrolysis and progress of electrolysis was monitored by recording cyclic voltammograms at different intervals of time until the reduction wave completely disappeared.

For the separation and identification of products, the dye (8-10 mg) was electrolysed in a H-type cell. At Hg pool, plateau potential corresponding to first or second wave was applied and at pyrolytic graphite electrode potential more negative to peak Ic or IIc was applied. When electrolysis was complete (~ 99%) the electrolysed solution was made sufficiently acidic and lyopholised. The freeze-dried material was dissolved in water (1-2 ml) and passed through a glass column (70 × 1.6 cm) packed with sephadex G-10 (Sigma Chemical Co) using doubly distilled water as the eluent. Different fractions (10 ml each) were collected. The absorbance of each tube was monitored at 215 nm and was plotted against volume. The first peak (volume 50-200 ml) contained phosphate, borate and acetate, hence was discarded. Other three peaks in the volume ranges 200-270, 280-350, 360-450 ml, respectively were collected separately, freeze-dried and analysed. TLC of electrolysed solution was carried out on silica gel-G plates using methanol-acetic acid-benzene (80:10:10) as developer.

Results and Discussion

Polarographic behaviour

Polarographic reduction of Acid Red-150 occurred in one well-defined diffusion-controlled wave below *p*H 5.5. In the *p*H range of 5.6-8.0, the wave splitted into two waves and the limiting current of the first wave was almost 1/3 of the second wave. At *p*H > 8.0, two waves of equal height were observed. The nature of the waves was found to be diffusion-con-

Table 1—Polarographic Characteristics of Acid Red-150 in B.R. buffers of different *p*H

*p*H	$(-E_{1/2})$ (V)	i_d (μA)	αn	
			log plot method	Oldham's method
2.2	0.22	2.62	1.10	1.12
3.4	0.26	2.62	1.00	1.16
4.4	0.34	2.69	0.90	1.00
5.5	0.45	2.54	1.12	0.98
6.4	0.32	0.825	0.96	0.98
	0.48	1.500	0.98	1.06
7.2	0.37	0.750	1.13	0.98
	0.54	1.650	1.08	1.08
8.6	0.44	1.275	1.12	1.06
	0.65	1.350	0.96	0.96
10.0	0.52	1.350	1.00	1.10
	0.70	1.275	1.10	1.14
11.2	0.58	1.275	1.14	1.12
	0.73	1.275	1.12	1.12

trolled as evidenced by i_d versus $\sqrt{h}$ and low temperature coefficient value (1.2% deg^{-1}). The $E_{1/2}$ was dependent on *p*H and shifted towards more negative value with increase in *p*H. The plots of $E_{1/2}$ versus *p*H were linear for both the waves and can be represented by Eqs (1) and (2),

$$(-E_{1/2})_1 = [0.054\ pH + 0.02] \quad \ldots(1)$$

$$(-E_{1/2})_2 = [0.066\ pH + 0.09] \quad \ldots(2)$$

The limiting current of the wave < 5.5 was practically equal to the sum of the limiting current of the two waves at *p*H > 5.5. This indicates that overall electrode reaction is the same in the entire *p*H range. The effect of dye concentration on $E_{1/2}$ and limiting current was studied in the dye concentration range of 0.05-1.0 m*M*. The i_d versus concentration plot was linear passing through the origin indicating that this dye can be safely estimated in this concentration range by polarographic method. However, $E_{1/2}$ shifted towards more negative value with increase in dye concentration showing irreversible nature (also confirmed by log plot analysis[5]) of the electrode process and possible role of adsorption[5]. The values of αn were determined by log plot analysis as well as the method of Oldham and Perry[6]. The values of αn determined by the two methods at different *p*H values are practically same (Table 1).

Linear and cyclic sweep voltammetry

Linear sweep voltammetry at a sweep rate of 5 mVs^{-1} exhibited one well-defined reduction peak in the *p*H range of 2.2-11.2. The peak potential was dependent on *p*H and shifted towards more negative potential with increase in *p*H. Cyclic sweep voltammetry at a sweep rate of 100 mVs^{-1} exhibited two reduction peaks Ic and IIc, when sweep was initiated in the negative direction. In the reverse sweep, three oxidation peaks were observed. On the second sweep towards positive potential two new cathodic peaks (IIIc and IVc) were noted (Fig. 1). To confirm whether oxidation peaks are due to the oxidation of products formed in Ic/IIc reaction or are due to an independent oxidation of Acid Red-150, cyclic voltammograms were also recorded by initiating the sweep in the positive direction. The absence of oxidation peaks clearly indicated that peaks IIIa-Va are due to oxidation of the product formed in Ic/IIc reaction.

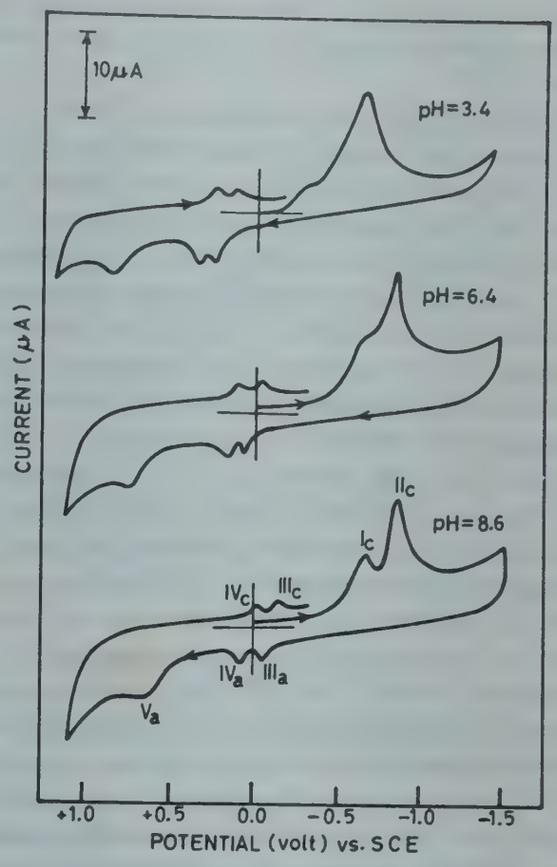

Fig. 1—Cyclic voltammograms observed for 0.2 m*M* Acid Red-150 at PGE. Sweep rate 150 mVs^{-1}

At *p*H 8.6 where two reduction peaks were well-defined, cyclic voltammograms were recorded by changing the direction of the sweep after peak Ic. The peaks IIIa-Va and reduction peaks IVc and Vc were not visible, indicating that these peaks are observed only after complete reduction of the dye. Peaks IIIa/IIIc and IVa/IVc formed an irreversible couple and were observed clearly only at a scan rate > 100 mVs^{-1}. The peak potential of the reduction peaks Ic to IVc was dependent on *p*H and shifted towards more negative potential with increase in *p*H. On the

other hand peak potentials of oxidation peaks IIIa to Va also shifted towards less positive value with increase in *p*H.

Controlled potential coulometry of Acid Red-150 was carried out at mercury pool cathode and at plateau potential of first or second wave. Below *p*H 5.5, where only one wave was observed the value of *n* determined by graphical integration of current-time curve was found to be 8.0 ± 0.2. In the *p*H range 5.6-8.0 the first wave involved 2.0 ± 0.1 electrons whereas second wave involved 6.0 ± 0.2 electrons. This observation was in accordance with the observed limiting currents for the first and second wave. At *p*H > 8.0, the two waves involved 4.0 ± 0.15 electrons as confirmed by practically same equal limiting currents. The values of *n* were also determined using pyrolytic graphite plate. At *p*H < 8.0, the first peak was not very well-defined; hence the value of *n* determined at potentials more negative to peak IIc was found to be 8.0 ± 0.15. At *p*H > 8.0, the value of *n* for the peaks Ic and IIc, was 4.0 ± 0.3 electrons each. The large deviation in *n*-value from the average value at *p*H > 8.0 may be due to the fact that the potential applied for peak Ic also contributed partially to peak IIc, as the potentials of peaks Ic and IIc are very close.

The progress of electrolysis was monitored by recording cyclic voltammograms at different time intervals. On applying potential corresponding to peak IIc, a systematic decrease in peaks Ic and IIc was observed. Whereas the peaks IIIa to Va and IIIc, IVc were clearly visible in exhaustively electrolysed solution. A cyclic voltammogram of exhaustively electrolysed solution at *p*H 3.4 is presented in Fig. 2D. This voltammogram did not change even when the electrolysed solution was left at room temperature for several hours. Thus it is concluded that product or products of electroreduction are electroactive in nature. Similar behaviour was observed at *p*H 7.0 and 10.6.

The progress of electrolysis was also monitored by UV/vis spectra at different interval of times. The UV/VIS spectra of Acid Red-150 in the entire *p*H range, exhibit λ_{max} at 235, 356 and 513 nm, indicating that the dye exists as a neutral species in the entire *p*H range studied. At *p*H 6, upon application of potential more negative to peak IIc, absorbances at 356 and 513 nm systematically decrease whereas the absorbance at 235 nm increases. After about 3 hr of electrolysis the absorbance at 235 nm reaches a maximum while those at 356 and 513 nm reach minimum values. These observations show that no intermediate with sufficient half-life is generated during electrooxidation of the dye.

Product identification

The products of electroreduction at *p*H 3.0, 6.0 and 10.2 at mercury pool or at pyrolytic graphite electrode were characterised as follows: The volumes obtained corresponding to three peaks in liquid chromatography over sephadex G-10 were lyopholised and analysed by TLC, m.ps and IR spectra. The volumes 200-270 (peak 2), 280-350 (peak 3) and 360-450 (peak 4) ml were lyopholised and exhibited R_f values 0.65, 0.47, and 0.19 respectively. Thus it is clear that three products are formed during complete electroreduction of the dye.

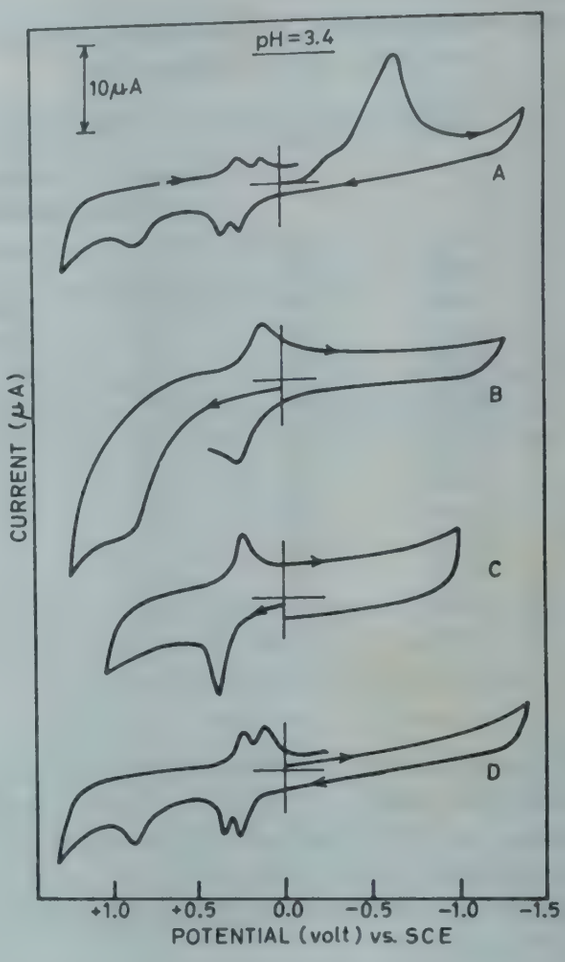

Fig. 2—Cyclic voltammograms observed at *p*H 3.4 for (A) Acid Red-150, (B) aniline, (C) *p*-phenylenediamine, (D) exhaustively electrolysed solution of Acid Red-150 at *p*H 3.4.

The product with R_f 0.65 (peak 2) was identified as aniline by comparison (R_f and IR) with an authentic sample. The product with R_f 0.47 (peak 3) had the m.p. 290°. The IR spectrum of this product exhibited peaks corresponding to SO_3H (1030, 1100 cm^{-1}) and phenolic OH (1250, 1360 cm^{-1}). Based on this the product should have structure similar to 1-amino-2-hydroxynaphthalene-3, 6-disulphonic acid. This product could not be completely identified at this stage due to non-availability of its authentic sample.

The product with R_f 0.19 (peak 4), melted at 140° and exhibited in its IR spectrum bands at 820, 1120, 1260, 1300, 1500 and 1600 cm^{-1}. This product was

identified as *p*-phenylenediamine by direct comparison with an authentic sample.

Hence it is clear that the products of complete electroreduction of Acid Red-150 are aniline, *p*-phenylenediamine and 1-amino-2-hydroxynaphthalene-3, 6-disulphonic acid.

The formation of aniline and *p*-phenylenediamine was further confirmed by recording cyclic voltammograms of authentic samples of aniline and *p*-phenylenediamine, which have been reported electroactive in nature[7,8]. It was interesting to observe that aniline exhibits peaks IIIa, Va and IIIc as reported in literature[9,10] and *p*-pheylenediamine gives peaks IVa and IVc at the same potentials as observed for the dye. Cyclic voltammograms of Acid Red-150, *p*-phenylenediamine and aniline at *p*H 3.4 are presented in Fig. 2, for comparison.

The products corresponding to (4e, $4H^+$) reduction of the dye (I) were also characterised at neutral and alkaline *p*H, where two waves in polarography and two peaks in cyclic voltammetry with equal limiting currents were observed. For this purpose the dye was reduced at peak Ic potential or plateau potential of the first wave. The TLC of this solution gave two spots with $R_f = 0.47$ and 0.56 thus indicating that (4e, $4H^+$) reduction of the dye gives two products. The spot with R_f 0.47 indicates the formation of 1-amino-2-hydroxynaphthelene-3, 6-disulphonic acid as observed earlier. Cyclic voltammogram of this solution was recorded by initiating the sweep in the positive direction. The absence of oxidation peak IIIa-Va and reduction peaks IIIc-IVc clearly indicate that 4e, $4H^+$ reduction of the dye does not give aniline or *p*-phenylenediamine as the product. Thus (4e, $4H^+$) reduction causes cleavage of bulky naphthol moiety to give 1-amino-2-naphthol-3, 6-disulphonic acid (sodium salt) and 4-aminoazobenzene.

Redox mechanism

On the basis of the results obtained, it is clear that the dye undergoes reduction by 8e, $8H^+$ process at d.m.e and pyrolytic graphite electrode in the *p*H range of 2.2-11.2. The (4e, $4H^+$) reduction in neutral and alkaline *p*H ranges does not indicate the formation of aniline and *p*-phenylenediamine. It can be safely concluded that reduction of $-N=N-$ attached to bulkier naphthol moiety takes place easily in comparison to azo group attached to phenyl moiety.

As the final products of electroreduction are aniline, *p*-phenylenediamine and 1-amino-2-naphthol-3, 6-disulphonic acid it is clear that electroreduction of the two azo groups does not stop at hydrazo stage but further reduction of hydrazo group in II takes place to give amino compounds as the ultimate products (Scheme 1). The first (4e, $4H^+$) reduction of the

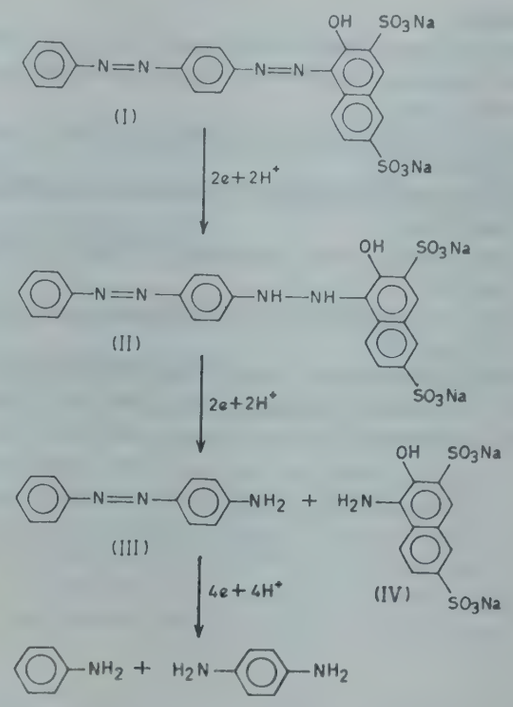

Scheme 1 – Tentative mechanism proposed for the electroreduction of Acid Red-150.

dye causes cleavage of $-N=N-$ to give *p*-aminoazobenzene (III) and aminonaphthol moiety (IV). Further (4e, $4H^+$) reduction causes the cleavage of second $-N=N-$ to give aniline and *p*-phenylenediamine as the products.

Previous results[12] reported in literature indicate that electroreduction of bisazodyes occurs by first taking (4e, $4H^+$) to give bishydrazo derivatives. Bisazobenzene and similar dyes have been reported[13,14] to form bishydrazobenzene at d.m.e. Further (4e, $4H^+$) reduction of bishydrazo derivatives is reported to give amino compounds as the products of reduction. However, in our case bishydrazo derivative is not formed, rather cleavage at $-N=N-$ attached to bulkier naphthol moiety takes place. This difference in behaviour can be due to steric hindrance to coplanarity[15,16] in the molecule, due to the bulkier naphthol group, thereby facilitating cleavage via $-N=N-$. It has also been observed that reduction potentials at pyrolytic graphite are 250 to 500 mV more negative in comparison to that at d.m.e. This behaviour can be explained on the basis of adsorption on the solid electrodes[17]. The solid electrodes also do not permit the free orientation of the species undergoing reduction and hence the potentials observed are always more negative in comparison to those at d.m.e.

Acknowledgement

Thanks are due to M/s Pfizer, USA for the gift of pyrolytic graphite. One of the authors (AK) is thankful to the UGC, New Delhi for the award of a junior research fellowship.

References

1 Eisner U & Eisner E K, in *Encyclopedia of electrochemistry of the elements*, edited by A J Bard (Marcel Dekker, New York) 1979.

2 Britton H T S, *Hydrogen ions* (D Van Nostrand, New York) 1956 P 360.

3 Goyal R N, Bhushan R & Agarwal A, *J electroanal Chem*, **171** (1984) 281.

4 Goyal R N, Srivastava S K & Agarwal R, *Bull Soc Chim Fr*, **4** (1985) 656.

5 Meites L, *Polarographic techniques* (Interscience, New York) 1967 pp 228.

6 Oldham K B & Perry E P, *Analyt Chem*, **40** (1968) 65.

7 Lee H Y & Adams R N, *Analyt Chem*, **34** (1962) 1587.

8 Bacon J & Adams R N, *J Am chem Soc*, **65** (1945) 1938.

9 Wawzonek S & McIntyre T W, *J electrochem Soc*, **114** (1967) 1025.

10 Melchior & Maki A H, *J chem Phys*, **34** (1961) 471.

11 Zeweig A, Lancaster J E, Negalia M T & Jura W H, *J Am chem Soc*, **86** (1964) 4130.

12 Saber T M H, Ali M I & Abed N M, *J electroanal Chem*, **28** (1970) 177.

13 Florence T M, Johnson D A & Batley G E, *J electroanal Chem*, **50** (1974) 411.

14 Florence T M, *J electroanal Chem*, **52** (1974) 115.

15 Zuman P, *Coll n Czech chem Commun*, **27** (1962) 648.

16 Charton M, *J org Chem*, **34** (1969) 278.

17 Adams R N, *Electrochemistry at solid electrodes* (Marcel Dekker, New York) 1969, pp 120.

Indian Journal of Chemistry
Vol. 27A, June 1988, pp. 487-493

Redox Chemistry of Hyponitrous Acid: Part I—Stoichiometry, Kinetics & Mechanism of Its Oxidation by Ethylenediaminetetraacetatothallium (III) in Aqueous Perchloric Acid Medium

MUNI R GOYAL, RAMA K MITTAL & Y K GUPTA*
Department of Chemistry, Rajasthan University, Jaipur 302004

Received 23 *June* 1987; *revised* 21 *September* 1987; *accepted* 16 *November* 1987

One mol of hyponitrous acid ($H_2N_2O_2$) reacts with one mole of thallium (III) in acidic perchlorate solution initially yielding one mol of HNO_2 and 1/2 mol of N_2O gas. The likely subsequent steps are the oxidation of HNO_2 by Tl(III), and the reaction between $H_2N_2O_2$ and HNO_2. In the absence of EDTA, oxidation by Tl(III) occurs and ultimately two mol of Tl(III) are consumed for each mol of $H_2N_2O_2$. In the presence of EDTA the stoichiometry is not definite for solutions in which $[HClO_4]$ is < 1.0 mol dm^{-3}, but in solutions where $[HClO_4]$ is > 1.5 mol dm^{-3}, one mol of Tl(III) consumes two mol of $H_2N_2O_2$. Kinetics studied in the presence of EDTA shows an induction period which is ascribed to the formation of HNO_2.

No mechanistic studies on the oxidation of hyponitrite seem to have been made so far; only its decomposition kinetics[1-6] have been studied. During investigations on the oxidation of hydroxylamine in our laboratory, hyponitrite was found to be one of the intermediate products[7,8]. Also *trans* and *cis* forms of $H_2N_2O_2$ have been reported[2] and it is not known whether the unstable[9,10] *cis*-form has any role in the redox systems. The present paper describes the results of oxidation of $H_2N_2O_2$ with thallium (III). Only one redox reaction in which $H_2N_2O_2$ acts as an oxidizing agents is reported in literature[11].

Our preliminary results revealed that the oxidation of $H_2N_2O_2$ by Tl(III) in acid perchlorate solutions (0.1-0.6 mol dm^{-3}) occurs in two stages. The first reaction is very fast and is over within the time of mixing and corresponds to the stoichiometry of 1:1 ($[Tl(III)]$:$[H_2N_2O_2]$). This fast reaction is followed by a slow reaction characteristic of the oxidation of nitrite[12]. Literature survey reveals that hyponitrous acid is oxidized to oxyhyponitrous acid ($H_2N_2O_3$) which decomposes[13,14] readily yielding HNO_2 and N_2O in aqueous acidic solutions. Our aim is to characterize these two steps separately and to know the product of oxidation of the fast step.

Oxidation of HNO_2 by Tl(III) is slow in the presence of EDTA (0.015 mol dm^{-3}) and yielded HNO_3 as the final product. The reaction[11] of $H_2N_2O_2$ and HNO_2 is also slow in the presence of EDTA. However, the rate of the reaction increases with increase in acidity and is instantaneous in 1.5 mol dm^{-3} $HClO_4$ even in the presence of EDTA. This reaction could not be studied kinetically owing to interference in spectrophotometric measurements by EDTA. Only qualitative tests for HNO_2 could be done.

The main oxidation reaction in the presence of EDTA is attended by an induction period which decreases by the addition of trace amounts of $HNO_2$and disappears completely in the presence of 5×10^{-5} mol dm^{-3} NO_2^-. The magnitude of induction period also decreases with increase in $[H_2N_2O_2]$ and $[HClO_4]$, and no induction period is observed in 1.5 mol dm^{-3} or more $HClO_4$. Hence kinetic runs were made in the presence of 1×10^{-4} mol dm^{-3} NO_2^- so that the induction period is completely eliminated.

Since oxyhypointrous acid (trioxodinitrate or Angeli's salt)[14] is said to be the intermediate oxidation product prior to the formation of HNO_2, this was prepared[9] and a few experiments were also carried out with it to verify whether it could be the intermediate product of fast reaction.

Materials and Methods

Sodium hyponitrite was prepared by the electrolytic method[15] and its purity checked by standard method[16,17]. Solutions of $H_2N_2O_2$ were prepared whenever required in aqueous 0.5 mol dm^{-3} $HClO_4$ to which ethyl alcohol (0.1mol%) was added to prevent its decomposition[4]. For all kinetic experiments *p*H was kept < 3 so that the decomposition of $H_2N_2O_2$ did not occur during the time the kinetics were followed.

Thallic perchlorate solutions were prepared from thallic oxide (BDH, AR) and 70% $HClO_4$ (E. Merck) and were standardized iodometrically. Solutions of $LiClO_4$ were prepared by neutralizing

70% $HClO_4$ with Li_2CO_3 (BDH, AR) to *p*H 6.8. All other chemicals were either AR (BDH) or GR (E. Merck) quality. doubly distilled, conductivity water was used for preparing all solutions.

Oxyhyponitrous acid was prepared by the literataure method[18]. Ethyl nitrate was prepared by mixing calculated amounts of ethyl iodide and solid silver nitrate and distilling under reduced pressure. The solid compound after recrystallisation was stored in ethyl alcohol in the cold. Its analysis corresponded to $Na_2N_2O_3$. Alkaline solutions (0.1 mol dm^{-3}) of the salt absorbed at 248 nm ($\varepsilon = 8.0 \times 10^3$). In aqueous solution it decomposed slowly, but in acidic solutions it decomposed readily[13] and gave no absorption in UV region except that characteristic of HNO_2. Aqueous solutions of the salt were prepared only when needed.

Kinetic procedure

Reaction was initiated by adding the required quantity of $H_2N_2O_2$ to a mixture of Tl(III) and other reactants. Aliquots were added to an equal volume of 6 *N* HCl to quench the reaction [since chloro-complexes of Tl(III) are are not reactive], and analysed iodometrically for unreacted Tl(III). Nitrite was decomposed by the addition of urea before carrying out iodometric determination. Initial rates were detrmined by the plane mirror method. These were reproducible within ± 5%.

Spectrophotometric measurement was carried out on a Perkin-Elmer spectrophotometer fitted with a cell of 1cm path length. *p*H determinations were made on an EC Digital *p*H meter.

Results

Stoichiometry

This was determined in the absence and presence of EDTA. Excess thallium (III) was determined iodometrically and excess hyponitrite determined by the precipitation method[12]. Excess hyponitrite could not be employed in the presence of EDTA since the latter interfered with the precipitation method. UV spectrophotometry also could not be adopted because of the presence of EDTA and possibly other unknown intermediates. Nitrous oxide was collected over water saturated with N_2O. The results are given in Table 1.

The stoichiometry was determined under two conditions: In the absence of EDTA one mol of Tl(III) reacted with one mol of $H_2N_2O_2$ according to Eq. (1).

$$Tl(III) + H_2N_2O_2 + \tfrac{1}{2}H_2O \rightarrow \tfrac{1}{2}N_2O + HNO_2 + Tl(I) + 2H^+ \quad \ldots (1)$$

Table 1—Initial Rates (v_0) at DIfferent [Tl(III)] in Reaction of Tl(III) with $H_2N_2O_2$

[EDTA] = 0.015 mol dm^{-3}; [NO_2^-] = 1.0×10^{-4} mol dm^{-3}; [$HClO_4$] = 0.5 mol dm^{-3}; temp = 35°C

10^3 [$H_2N_2O_2$] (mol dm^{-3})	10^3 [Tl(III)] (mol dm^{-3})	10^7 (v_0) (mol $dm^{-3}s^{-1}$)	
		Obs	Calc[a]
1.0	0.5	2.2	2.2
1.0	0.6	2.5	2.5
1.0	0.8	3.3	3.2
1.0	1.0	4.0	3.7
1.0	2.0	6.0	5.7
1.0	3.0	6.5	6.9
1.0	4.0	7.0	7.7
1.0	6.0	7.0	—
2.0	0.5	4.8	4.4
2.0	1.0	7.8	7.4
2.0	2.0	11.5	11.3
2.0	3.0	13	13.8
2.0	4.0	14.5	15.4
2.0	6.0	14.5	—
3.0	0.5	7.0	6.6
3.0	0.6	7.5	7.6
3.0	0.8	10	9.5
3.0	1.0	12	11.2
3.0	2.0	17.5	17
3.0	3.0	21	20.7
3.0	5.0	21.5	—
3.0	7.0	21.5	—

[a] Calculated from Eq. (14) with $k_1 = 1.2 \times 10^{-3}s^{-1}$ and $k_5/k_4 = 4.5 \times 10^2$.

The reaction mixture containing 5ml of 0.1 mol dm^{-3} $H_2N_2O_2$ and 25ml 0.02 mol dm^{-3} thallium (III) in 0.5 mol dm^{-3} $HClO_4$ yielded an average of 5.4 ml of N_2O at N.T.P. which compared well with the value of 5.6 ml expected from Eq. (1). The mixture responded to tests for HNO_2. One of the forms of oxyhyponitrous acid ($H_2N_2O_3$) reported earlier[13] may be an intermediate in reaction (1), decomposing quickly according to Eq. (2).

$$H_2N_2O_2 \rightarrow \tfrac{1}{2}H_2O + \tfrac{1}{2}N_2O + HNO_2 \quad \ldots (2)$$

The same mixture consumed one more mol of Tl(III), if excess Tl(III) was determied after 2hr. The overall stoichiometry of 2:1 ([(Tl(III)]:[$H_2N_2O_2$]) therefore corresponded to reaction (3)

$$2Tl(III) + H_2N_2O_2 + 1.5H_2O \rightarrow 0.5N_2O + HNO_3 + 2Tl(I) + 4H^+ \quad \ldots (3)$$

This was further supported by the quantitative determination of N_2O and qualitative tests for

HNO_3. Equation (3) is in fact a combination of Eqs (1) and (3a).

$$Tl(III) + HNO_2 + H_2O \rightarrow Tl(I) + HNO_3 + 2H^+ \quad \ldots (3a)$$

The stoichiometry ($[Tl(III)]:[H_2N_2O_2]$) in the presence of EDTA and 0.5 mol dm^{-3} $HClO_4$ was not definite and it always varied between one and two depending on the concentrations of the reactants. The products responded to tests for NO_3^-, N_2 and N_2O. In the presence of EDTA, reaction (1) was slow and subsequent reaction (oxidations of HNO_2 and $H_2N_2O_2$) was still slower.

In (1.5-2.0) mol dm^{-3} $HClO_4$ and in the presence of EDTA, one mol of Tl(III) reacted with two mol of $H_2N_2O_2$. In such a situation reaction (1) seems to be followed by a fast reaction (4)

$$H_2N_2O_2 + HNO_2 \rightarrow N_2 + H_2O + HNO_3 \quad \ldots (4)$$

with an overall stoichiometry given by Eq. (5).

$$2H_2N_2O_2 + Tl(III) \rightarrow N_2 + HNO_3 + Tl(I) + 2H^+ + 0.5N_2O + 0.5H_2O \quad \ldots (5)$$

Nitrogen was estimated after dissolving N_2O in water. In four experiments 10 ml of 0.1 mol dm^{-3} of $H_2N_2O_2$ and 25 ml of 0.02 mol dm^{-3} solution of Tl(III) in 2.0 mol dm^{-3} $HClO_4$ and 0.015 mol dm^{-3} EDTA, yielded an average of 10.8 ml of N_2 at N.T.P. The expected value is 11.2 ml. It is therefore obvious that the intermediate product in all cases is HNO_2 which is oxidized to HNO_3 by Tl(III) in the absence of EDTA, and by $H_2N_2O_2$ in the presence of EDTA both according to definite stoichiometries.

An attempt was made to determine the stoichiometry of the oxidation of oxyhyponitrous acid by Tl(III) and it was found to be between 2:1 and 3:1 ($[Tl(III)]:[H_2N_2O_3]$). Oxyhyponitrous acid partly decomposed in acid solution and stoichiometry was not definite. It we assume that $H_2N_2O_3$ was completely decomposed, then one mol of Tl(III) would be required for one mol of $H_2N_2O_3$ indicating oxidation of decomposition product HNO_2. It was therefore obvious that greater part of $H_2N_2O_3$ was oxidized. The reaction was initiated by the addition of $Na_2N_2O_3$ and excess Tl(III) was determined after about 5 hr. Incidently this also proved that $H_2N_2O_3$ as such was not the intermediate product of the fast reaction between $H_2N_2O_2$ and Tl(III).

Reaction in presence of EDTA and 0.5 *mol* dm^{-3} $HClO_4$*: Thallium (III) dependence*

The results presented in Table 1 show that the rate increases and tends to a limiting value with increase in [Tl(III)] from 6.0×10^{-4} to 7.0×10^{-3} mol dm^{-3} and follows the general rate law (6).

$$-d[Tl(III)]/dt = A[Tl(III)]/(1 + B[Tl(III)]) \quad \ldots (6)$$

where A and B are constants.

The rate was first order in $[H_2N_2O_2]$ (from 7.0×10^{-4} to 1.25×10^{-2} mol dm^{-3}) at different [Tl(III)] and $[H^+]$ as revealed by the results in Table 2. Above 1.0 mol dm^{-3} $HClO_4$ when the stoichiometry was definite, the rate was first order in $[H^+]$ (Table 3).

Reaction in presence of EDTA and 2.0 *mol* dm^{-3} $HClO_4$*: First stage reaction*:

A typical plot under the conditions for decrease in [Tl(III)] with time (Fig. 1) gave the stoichiometry 1:2 ($[Tl(III)]:[H_2N_2O_2]$). The order in [Tl(III)], $[H_2N_2O_2]$ and $[H^+]$ was unity in each case as re-

Table 2—Effect of Varying $[H_2N_2O_2]$ on Initial Rate (v_0) in Oxidation of $H_2N_2O_2$ by Tl(III)

$[EDTA] = 0.015$ mol dm^{-3}; $[NO_2^-] = 1.0 \times 10^{-4}$ mol dm^{-3}; $[HClO_4] = 0.5$ mol dm^{-3}; temp. = 35°C

$10^3[H_2N_2O_2]$ (mol dm^{-3})	$10^7(v0)$ (mol $dm^{-3}s^{-1}$)	$10^3[H_2N_2O_2]$ (mol dm^{-3})	$10^7(v_0)$ (mol $dm^{-3}s^{-1}$)	$10^3[H_2N_2O_2]$ (mol dm^{-3})	$10^7(v_0)$ (mol $dm^{-3}s^{-1}$)
$[Tl(III)] = 3.0 \times 10^{-3}$ mol dm^{-3}		$[Tl(III)] = 2.0$ mol dm^{-3}		$[Tl(III)] = 7.0 \times 10^{-3}$ mol dm^{-3}	
0.7	3.2				
1.0	6.4	1.0	5.0	1.0	7.0
2.0	13	2.0	12	2.0	14
3.0	21	3.0	18	3.0	21
4.0	27				
5.0	31	5.0	27	5.0	38
6.0	36			7.0	52
8.0	50				
10.0	56	10.0	54	10.0	69
12.5	72				

Table 3—Effect of Varying $[H^+]$ on Initial Rates (v_0) in Reaction of Tl(III) with $H_2N_2O_2$

$[Tl(III)] = 2.0 \times 10^{-3}$ mol dm^{-3}; $[H_2N_2O_2] = 1.0 \times 10^{-3}$ mol dm^{-3}; $[NO_2^-] = 1.0 \times 10^{-4}$ mol dm^{-3}; [EDTA] = 0.015 mol dm^{-3}; $I = 2.0$ mol dm^{-3}; temp. = 35°C

$[HClO_4]$ (mol dm^{-3})	$[H^+]$ (mol dm^{-3})	$10^7 (v_0)$ (mol dm^{-3}s^{-1})	$[HClO_4]$ (mol dm^{-3})	$[H^+]$ (mol dm^{-3})	$10^7 (v_0)$ (mol dm^{-3}s^{-1})
0.16	0.08	5.0	0.96	0.68	4.7
0.24	0.15	5.7	1.12	0.76	4.8
0.42	0.22	7.3	1.28	0.86	5.5
0.40	0.30	6.7	1.44	1.04	7.0
0.48	0.37	5.8	1.60	1.04	8.5
0.64	0.50	4.2	1.76	1.43	10
0.80	0.60	4.2	1.92	1.64	11

Table 4—Effect of Varying [Tl(III)], $[H_2N_2O_2]$ and $[HClO_4]$ on Initial Rates (v_0) at 35°

[EDTA] = 0.015 mol dm^{-3}; $[NO_2^-] = 1.0 \times 10^{-4}$ mol dm^{-3}

10^3 [Tl(III)] (mol dm^{-3})	$10^3 [H_2N_2O_2]$ (mol dm^{-3})	$[HClO_4]$ (mol dm^{-3})	$[H^+]$ (mol dm^{-3})	$10^7 (v_0)$ (mol dm^{-3}s^{-1})	v_0/Tl(III)$[H_2N_2O_2][H^+]$ (dm^{6}mol^{-2}s^{-1})
0.6	3.0	2.0	1.7	9.5	0.31
1.0	3.0	2.0	1.7	16	0.31
2.0	3.0	2.0	1.7	33	0.32
3.0	3.0	2.0	1.7	50	0.33
6.0	3.0	2.0	1.7	100	0.32
2.0	2.0	2.0	1.7	22	0.32
3.0	2.0	2.0	1.7	34	0.32
2.0	1.5	2.0	1.7	17	0.33
2.0	1.0	2.0	1.7	11	0.32
2.0	1.0	1.75	1.4	10	0.36
2.0	1.0	1.50	1.1	7.3	0.33
2.0	1.0	1.25	0.84	5.7	0.34
2.0	1.0	1.0	0.70	4.7	0.33

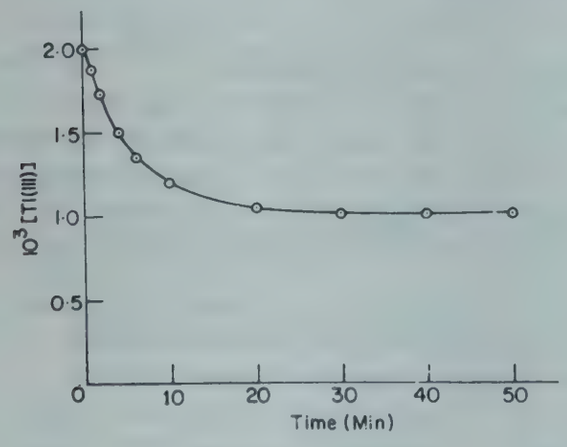

Fig. 1—Plots of Tl(III) versus time at 35°C: Tl(III) = 2.0×10^{-3} mol dm^{-3}; $H_2N_2O_2$ = 2.0×10^{-3} mol dm^{-3}; $HClO_4$ = 2.0×10^{-3} mol dm^{-3}; and EDTA = 0.015 mol dm^{-3}

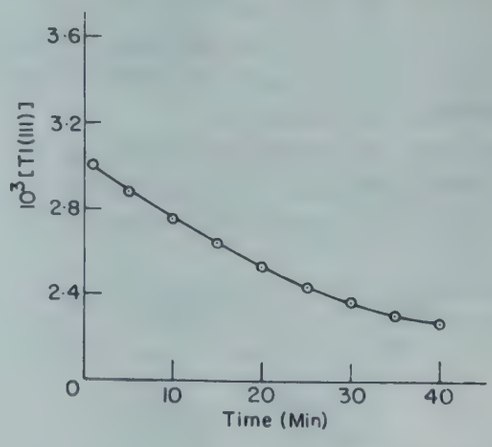

Fig. 2—Plot of Tl(III) versus time at 35°C; Tl(III) initial = 4.0×10^{-3} mol dm^{-3}; Tl(III) after 1 min = 3.0×10^{-3} mol dm^{-3}; $H_2N_2O_2$ = 1.0×10^{-3} mol dm^{-3}; $HClO_4$ = 0.5 mol dm^{-3}

vealed by the result given in Table 4. The otherwise complicated reaction seems to behave in a simple manner in high acid medium, but in order to know more about the products and the mechanism, several reaction mixtures were prepared by mixing Tl(III) and $H_2N_2O_2$ in equivalent amounts corresponding to the stoichiometry of 1:2. After 20 min when the reaction was almost over, more Tl(III) was added to see whether it reacted with the products. These results showed that there was no reducing product in the system and that added Tl(III) reacted only when excess

Table 5—Effect of Oxidation Product of Fast Reaction

$[HClO_4] = 0.5$ mol dm^{-3}; temp. = 35°C

10^3 [Tl(III)]$_i$ (mol dm^{-3})	10^3 [$H_2N_2O_2$]$_i$ (mol dm^{-3})	10^3 [Tl(III)]^a (mol dm^{-3})	10^3 [Product]^a (mol dm^{-3})	10^6 (v_0)^a (mol dm^{-3}s^{-1})
3.0	2.0	1.0	2.0	7.5
4.0	2.0	2.0	2.0	5.0
5.0	2.0	3.0	2.0	3.1
6.0	2.0	4.0	2.0	2.2
7.0	2.0	5.0	2.0	1.8
3.0	1.0	2.0	1.0	1.2
4.0	2.0	2.0	2.0	3.2
5.0	3.0	2.0	3.0	15
6.0	4.0	2.0	4.0	18
8.0	6.0	2.0	6.0	21
10.0	8.0	2.0	8.0	28
12.0	10.0	2.0	10.0	30
22.0	20.0	2.0	20.0	26
32.0	30.0	2.0	30.0	24

a After 1 min

Table 6—Oxidation of Oxyhyponitrous Acid by Tl(III)

[oxyhypointrite] = 0.001 mol dm^{-3}; $[HClO_4] = 0.5$ mol dm^{-3}; temp. = 35°C

Time (min)	Iodometric titre values at different times for 10^3 [Tl(III)](mol dm^{-3})				
	5.0	4.0	2.0[a]	2.0[a,b]	2.0[a,c]
0	10	8.0	8.4	8.4	8.4
1	8.5	6.4	5.5	7.9	8.4
5	8.1	5.8	2.6	6.4	8.4
10	7.8	5.3	1.3	5.0	8.3
20	7.3	4.5	0.3(0)[d]	4.1	8.3
30	6.8	4.1	—	4.1(4.2)[a]	8.2
45	—	3.8	—	8.2	
60	6.3	—	—	—	—
300	5.2(5.1)[d]	—	—	—	8.1
		3.0 (3.1)[d]			

(a) Different solutions of thiosulphate used for titration(b) Reaction initiated by addition of Tl(III)
(c) Reaction in the presence of EDTA
(d) Figures in parentheses give the expected titre values on the arbitrary assumption that 75% $H_2N_2O_3$ undergoes oxidation and 25% of it decomposed.
(e) Figures in parentheses give the expected titre value on the assumption of overall 1:1 stoichiometry.

$H_2N_2O_2$ (>2 molar proportion as required by 1:2 stoichiometry) was initially taken. Further the decrease in [Tl(III)] was characteristic of the plot in Fig. 1.

Reaction with the product of fast reaction: Second stage reaction:

The fast reaction between Tl(III) and $H_2N_2O_2$ which followed 1:1 stoichiometry and slowed down after 1 min was initially studied. A typical plot is shown in Fig. 2. The results at different [product] and unconsumed [Tl(III)] after 1 min, are presented in Table 5. At fixed [product] and different [Tl(III)], the rate decreased. At fixed [Tl(III)] and different [products], the rate increased, passing through a maximum and then decreased. These are characteristics of the oxidation[12] of HNO_2 where 1:2 complex of Tl(III) and HNO_2 was considered to be reactive and 1:1 and 1:3 complexes were considered to be unreactive. The maximum rate at 0.01 mol dm^{-3} HNO_2 is 30×10^{-6} mol dm^{-3}s^{-1} at 35°. In the oxidation[14] of HNO_2, the maximum rate at 0.009 mol dm^{-3} HNO_2 was 8×10^{-6} mol dm^{-3}s^{-1} at 25°. The product of fast reaction therefore appears to be HNO_2.

Reaction of oxyhyponitrous acid with thallium (III)

The reaction conditions for this reaction are shown in Table 6. The reaction was initiated by the addition of a solution of oxyhypointrite. Four facts are obvious from these results: (i) There was a fast reaction between $H_2N_2O_3$ and Tl(III), but Tl(III) consumed was always less than that corresponding to 1:1 stoichiometry, indicating thereby that part of $H_2N_2O_3$ decomposed. Hence oxidation and decomposition of $H_2N_2O_3$ are competitive processes, (ii) After the fast reaction, the magnitude of decrease in [Tl(III)] was less with increase in [Tl(III)]—a characteristic of the oxidation of HNO_2 by Tl(III). Hence the product of fast reaction was HNO_2. (iii) If the reaction was initiated by the addition of Tl(III), $H_2N_2O_3$ already present in the reaction mixture decomposed completely into HNO_2 and there was no initial fast reduction of Tl(III). Total Tl(III) consumed corresponded to 1:1 stoichiometry. (iv) In the presence of EDTA the fast reaction became slow—much slower then the oxidation of $H_2N_2O_2$ under similar conditions.

Immediate product of oxidation of hyponitrous acid

In the absence of EDTA the first step of the oxidation of hyponitrous acid is fast. If oxyhyponitrous acid was the product, its oxidation would be fast and hence the stoichiometry of the fast reaction would require more than one mol of Tl(III) for each mol of $H_2N_2O_2$. Since the stoichiometry of the fast reaction is 1:1 and the reaction mixture immediately after mixing of the reactants does not show absorption at 248 nm the possibility of oxyhyponitrous acid as the reaction product is ruled out. Further the works of Bonner and coworkers[19,20], and Hughes and Wimbledon[21] on the isotopic exchange studies on nitrogen and decomposition of $H_2N_2O_3$, catalyzed by HNO_2 showed that in acid solution NO was formed. We could not detect the presence of NO in the present redox system.

Discussion

The two acid dissociation constants of $H_2N_2O_2$ are reported to be $\sim 10^{-7}$ and $\sim 10^{-11}$ at ordinary temperature and hence hyponitrous acid would exist as $H_2N_2O_2$ under the acid conditions employed in the present investigation. Monoprotonated form $H_3N_2O_2^+$ has also been reported[5] in highly acidic medium. The hydrolysis constant[22] for Tl^{3+} is small and it forms strong complexes[23] with EDTA (H_4L). EDTA can exist in five different forms H_2L^{2-}, H_3L^-, H_5L^+ and H_6L^{2+} and all of them may form complexes with Tl^{3+}.

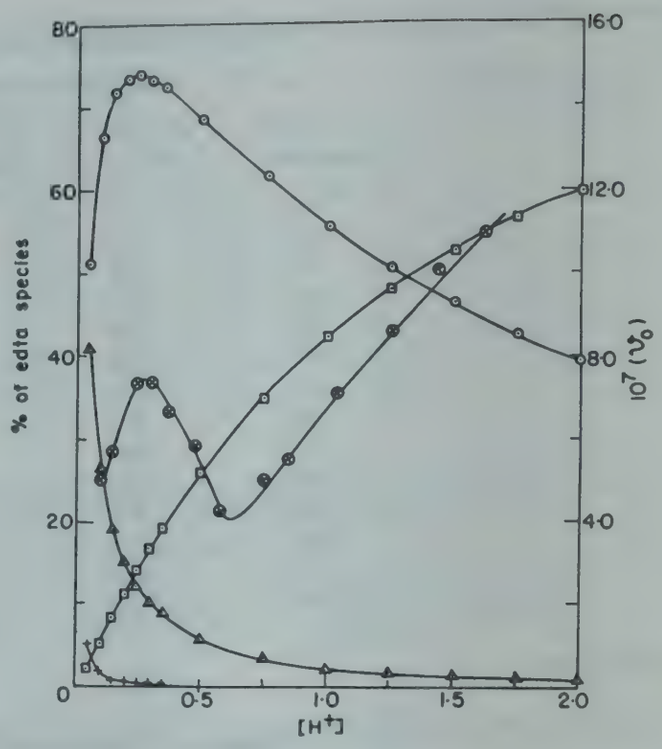

Fig. 3—Plots of percentage of different EDTA species and initial rates at various $[H^+]$ at 35°C (+), H_3L^-; (Δ), H_4L; (○), H_5L^+; (□), H_6L^{2+}; ⊗, initial rate; [EDTA] = 0.015 mol dm^{-3})

A calculation[24] of the population of vairous speciess of EDTA and the rate profile at different $[H^+]$ (Fig. 3) show that perhaps H_5L^+-complex of Tl(III) is the most important reactive species in the lower range of $[H^+]$. Any quantitative interpretation of $[H^+]$ dependence in the lower range of concentration is not reliable in view of the varying stoichiometry at different $[H^+]$.

Induction period

The role of nitrite in eliminating the induction period should be through its reaction with $H_2N_2O_2$ via formation of HNO_2 in the slow step to produce an adduct[11] (HO.N:N.O.NO), which then directly reacts with Tl(III). In highly acidic medium it decomposes to N_2 and HNO_3 without reacting with Tl(III) (see Eqs 7 and 8)

$$H_2N_2O_2 + HNO_2 \rightarrow HO.N:N.O.NO + H_2O \quad \ldots (7)$$

$$HO.N:N.O.NO \rightarrow N_2 + HNO_3 \quad \ldots (8)$$

Hughes and Stedman[11] consider a reaction between $HN_2O_2^-$ and $H_2NO_2^+$ instead of that shown in Eq. (7). It is difficult to distinguish between the two propositions.

Hyponitrous acid is said to exist in, *trans*- and *cis*-forms. The latter form has been indicated only as a transient intermediate in the reaction[9] of HNO_2 with NH_3OH^+ and in the reduction[25] of HNO_2 with europium (II). In the decomposition[2] of $H_2N_2O_2$ also, *cis*-form is proposed to be as

transient intermediate. Since the rate of reaction is independent of large [Tl(III)], hyponitrous acid must be involved in a pre-equilibrium step, with two different forms, active and inactive, or *cis-* and *trans-*. Thus if we ignore $[H^+]$ despendence, mechanism outlined in Eqs (9-12) may be suggested in 0.5 mol dm^{-3} $HClO_4$.

$$H_2N_2O_2\,(\text{trans}) \underset{k_2}{\overset{k_1}{\rightleftharpoons}} H_2N_2O_2\,(\text{cis}) \qquad \ldots(9)$$

$$H_2N_2O_2\,(\text{cis}) + HNO_2 \xrightarrow{k_3} HO.N{:}N.O.NO + H_2O \qquad \ldots(10)$$

$$HO.N{:}N.O.NO \xrightarrow{k_4} N_2 + HNO_3 \qquad \ldots(11)$$

$$HO.N{:}N.O.NO + Tl(III) + 2H_2O \xrightarrow{k_5} H_2N_2O_3 + Tl(I) + HNO_2 + 2H^+ \qquad \ldots(12)$$

The above mechanism leads to the rate law (13).

$$-d[Tl(III)]/dt = \frac{k_1k_3k_5[Tl(III)][H_2N_2O_2][HNO_2]}{(k_4 + k_5[Tl(III)])(k_2 + k_3[HNO_2])} \qquad \ldots(13)$$

where the concentrations refer to total analytical concentrations. In the presence of 1×10^{-4} mol dm^{-3} NO_2^-, $k_3\,[HNO_2]$ appears to be much larger than k_2 and hence rate law (13) reduces to (14).

$$-d[Tl(III)]/dt = k_1k_5[H_2N_2O_2][Tl(III)]/(k_4 + k_5[Tl(III)] \qquad \ldots(14)$$

Again for large [Tl(III)], the rate law (14) is reduced to (15).

$$-d[Tl(III)]/dt = k_1[H_2N_2O_2] \qquad \ldots(15)$$

A plot of $(\text{rate})^{-1}$ versus $[Tl(III)]^{-1}$ is linear with a non-zero intercept and from this k_1 and k_3/k_4 have been calculated as $(1.2 \pm 0.08) \times 10^{-3} s^{-1}$ and $(4.5 \pm 0.6) \times 10^2$ dm^3 mol^{-1} respectively in 0.5 mol dm^{-3} $HClO_4$ and at 35°C.

The reaction at $[H^+] > 0.7$ mol dm^{-3} appears to follow a different mechanism since it has altogether different stoichiometry and Tl(III) dependence, and has no induction period. The reaction is first order in [Tl(III)], $[H_2N_2O_2]$ and $[H^+]$ and these results can be explained by the mechanism represented by Eqs. (16-19).

$$H_2N_2O_2 + H^+ \overset{K_{H^+}}{\rightleftharpoons} H_3N_2O_2^+ \qquad \ldots(16)$$

$$H_3N_2O_2^+ + Tl(III) + H_2O \xrightarrow{k} H_2N_2O_3 + 3H^+ + Tl(I) \qquad \ldots(17)$$

$$H_2N_2O_3 \xrightarrow{\text{fast}} \tfrac{1}{2}N_2O + \tfrac{1}{2}H_2O + HNO_2 \qquad \ldots(18)$$

$$H_2N_2O_2 + HNO_2 \xrightarrow{\text{fast}} N_2 + H_2O + HNO_3 \qquad \ldots(19)$$

Assuming K_{H+} to be small, rate law (17) is obtained.

$$-d[Tl(III)]/dt = kK_{H+}[Tl(III)][H_2N_2O_2][H^+] = k'[H_2N_2O_2][Tl(III)][H^+] \qquad \ldots(20)$$

k' is found to be (0.33 ± 0.01) dm^6 mol^{-2} s^{-1} at 35°.

The rate constant (k_1) *for trans-cis* conversion (Eq. 9) is much larger than the corresponding rate constant for the decomposition[2] of $H_2N_2O_2$. Althogh the actual decomposition step may be preceded by a *trans-cis* conversion, the conditions are entirely different in the two cases. The presence of EDTA, NO_2^- and Tl(III) may greatly influence the rate.

References

1 Buchholz J R & Powell R E, *J Am chem Soc*, **87** (1965) 2350.
2 Hughes M N & Stedman G, *J chem Soc*, (1964) 163.
3 Polydoropoulos C N & Pipinis M, *Z physik chem*, **40** (1964) 322.
4 Buchholz J R & Powell R E, *J Am chem Soc*, **85** (1963) 509.
5 Hughes M N & Stedman G, *J chem Soc*, (1963) 1239.
6 Abel E & Proisl J, *Mh Chem*, **72** (1938).
7 Keshwani P, Goyal M R & Gupta Y K, *J chem Soc Dalton Trans*, (1983) 1831.
8 Thakuria B M & Gupta Y K, *J chem Soc Dalton Trans*, (1975) 77.
9 Hughes M N & Stedman G, *J chem Soc*, (1963) 2824.
10 Hussain M A, Stedman G & Hughes M N, *J chem Soc (A)*, (1968) 597.
11 Hughes M N & Stedman G, *J chem Soc*, (1963) 4230.
12 Thakuria B M & Gupta Y K, Inorg chem, **16** (1977) 1399.
13 Addison C C, Gamlen G A & Thompson R, *J chem Soc*, (1952) 338.
14 Addison C C, Gamlen G A & Thompson R, *J chem Soc*, (1952) 346.
15 Polydoropoulos C N, *Chem & Industry*, (1963) 1686.
16 Polydoropoulos C N & Pipinis M, *Chimica Chromica*, **28A** (1963) 107.
17 Polydoropoulos C N & Voliotis S D, *Anal chim Acta*, **40** (1968) 170.
18 Angeli A, *Gazz*, **30** (1900) 593.
19 Javaid A M, Lutz C A & Bonner F T, *Inorg chem*, **18** (1979) 2369.
20 Bonner F T & Ravid B, *Inorg chem*, **14** (1975) 558.
21 Hughes M N & Wimbledon P R, *J chem Soc Dalton Trans*, (1977) 1650.
22 Biederman G, *Arkiv Kemi*, **6**(5) (1964) 527.
23 Stability Constants, Special Publication No. 17, Chemical Society, London, p 640.
24 Anderegg G, *Helv chem Acta*, **50** (1967) 2333.
25 Fraser R T M, Lee R N & Hayden K, *J chem Soc (A)*, (1967) 741.

Indian Journal of Chemistry
Vol. 27A, June 1988, pp. 494-497

Chromium(VI) Oxidation of Thallium(I) in Aqueous Acetic Acid & Effect of Added Vanadium(V) on the Reaction

G S GOKAVI & J R RAJU*

Department of Chemistry, Karnatak University, Dharwad 580003

Received 10 *June* 1987; *revised* 30 *October* 1987; *accepted* 13 *November* 1987

Chromium(VI) oxidation of thallium(I) in 60% acetic acid containing 1.25 mol dm^{-3} hydrochloric acid is a second order reaction, understood to be between CrO_3Cl^- and TlCl. Increase in $[H^+]$ and $[Cl^-]$ accelerates the reaction. Added V(V) accelerates the reaction till [V(V)] slightly exceeds [Tl(I)] because of a 1:1 interaction between V(V) and Tl(I). At higher [V(V)], the rate constant is lowered due to a specific cation effect. No interaction between added V(V) and Tl(I) is encountered in the case of the reaction in 40% aqueous acetic acid; however, in 80 and 90% aqueous acetic acid, 2:3 and 1:2 interactions between V(V) and Tl(I) are observed.

The oxidation of Tl(I) by Cr(VI) does not occur to any extent in aqueous perchloric and sulphuric acids but the reaction is facile in conc hydrochloric acid medium ($\geqslant 3$ mol dm^{-3}; the reaction is slow at [HCl] lower than 3 mol dm^{-3})[1]. The species in 3.0 mol dm^{-3} HCl solution[1] are reported to be thallium(I) chloride (TlCl) and chlorochromate (CrO_3Cl^-). The formation of chlorochromate is known to be greatly facilitated in aqueous acetic acid solutions as indicated by an equilibrium constant of 14 in water[2] rising to 1×10^5 in 86.5% acetic acid[3]. It was, therefore, worthwhile studying the reaction in 60% (v/v) aqueous acetic acid containing 1.25 mol dm^{-3} HCl. In view of the particular retarding effect of V(V), a product in the Cr(VI)-V(IV) reaction[4], the effect of added V(V) on the title reaction has also been studied.

Materials and Methods

Reagent grade chemicals were used. Doubly distilled water was used throughout this work. Chromium(VI) solution was obtained by dissolving potassium dichromate (BDH, AR) in water and standardised spectrophotometrically. Applicability of Beer's law at 360 nm was tested in the case of the 1.25 mol dm^{-3} HCl in 60% acetic acid solution containing 2.0×10^{-4} to 6.0×10^{-4} mol dm^{-3} Cr(VI) using matched 1 cm cells ($\varepsilon = 1250$). Concentrations of Cr(VI) higher than 6.0×10^{-4} mol dm^{-3} were not required in any of the kinetic runs, because of the limited solubility of Tl(I) in the reaction solution.

The Tl(I) solution was obtained by dissolving thallium(I) chloride (BDH) in water and standardising with bromate. Vanadium(V) solution was obtained by dissolving ammonium vanadate (BDH, AR) in water. Applicability of Beer's law was also tested for the latter solution at 360 nm ($\varepsilon = 75$). Hydrochloric acid (Glaxo, AR) was used throughout this work. Acetic acid was purified by standard procedure.

Kinetic runs

These runs were carried out with solutions of 1.25 mol dm^{-3} HCl in 60% acetic acid at $\mu = 1.26$ mol dm^{-3}. In a typical run, [Cr(VI)] and [Tl(I)] were 2.0×10^{-4} and 3.0×10^{-4} mol dm^{-3} respectively and kinetics were followed spectrophotometrically at 360 nm by mixing the thermally equilibrated reactant solutions and transferring the reaction solution to a 1 cm cell kept in the thermostated cell compartment. The temperature was maintained at 25 ± 0.1°C. Kinetic results could be reproduced to ± 5% and runs were usually followed upto 80% of the reaction.

Results

Since oxidation of HCl by Cr(VI) in the absence of Tl(I) was marginal (0.8% in 50 min), no correction for the oxidation of hydrochloric acid was made.

Stoichiometry

Different reaction mixtures were prepared in 60% acetic acid containing 1.25 mol dm^{-3} HCl at $\mu = 1.26$ mol dm^{-3} and analysed after keeping them for over 3 hr at 25°C. Chromium(VI) was estimated spectrophotometrically at 360 nm while Tl(III) was found as difference of total oxidant titrated by iodometry with 2.0×10^{-3} mol dm^{-3} thiosulphate. The results indicate a 2:3 stoichiometry for Cr(VI) oxidation of Tl(I) in these solutions (see Eq. 1).

$$2Cr(VI) + 3Tl(I) = 2Cr(III) + 3Tl(III) \quad \ldots(1)$$

Order of reaction

The reaction followed second order rate law at [Tl(I)] in the range of 1.0×10^{-4} to 3.0×10^{-4} mol dm^{-3} and [Cr(VI)] in the range of 2.5×10^{-4} to

4.5×10^{-4} mol dm^{-3}. Since [Cr(VI)] was followed by spectrophotometry, its concentration was close to that of Tl(I). The kinetic study was restricted to the narrow range of reactant concentrations because of the low solubility of Tl(I) in 60% acetic acid containing 1.25 mol dm^{-3} HCl.

Effect of added products

The effect of added products, Cr(III) and Tl(III), was studied at $\mu = 1.26$ mol dm^{-3}, [HCl] = 1.25 mol dm^{-3}, [oxidant] = 2.0×10^{-4} mol dm^{-3} and [substrate] = 3.0×10^{-4} mol dm^{-3}. Under these conditions, no variation in second order rate constant was observed. In case of runs involving non-equivalent concentrations of reactants, the rate constant (k) was evaluated using Eq. (2) with a and b representing the initial [Tl(I)] and [Cr(VI)] respectively and x representing the decrease in reactant concentration in time t. Rate constants were determined graphically, the second order plots being linear over 80% of the reaction (Fig. 1).

$$k = \left\{\frac{2.303}{t(a-3b/2)}\right\} \log \left\{\frac{b(a-3x/2)}{a(b-x)}\right\} \qquad \ldots(2)$$

Effect of chloride and hydrogen ions

At fixed [reactant], [H$^+$] and [Cl$^-$] and $\mu = 1.26$ mol dm^{-3}, the second order specific rate constant (k) increased with increase in [Cl$^-$] and/or [H$^+$] (Table 1). The orders of reaction in [Cl$^-$] and [H$^+$] were 1.2 and 2.0 respectively.

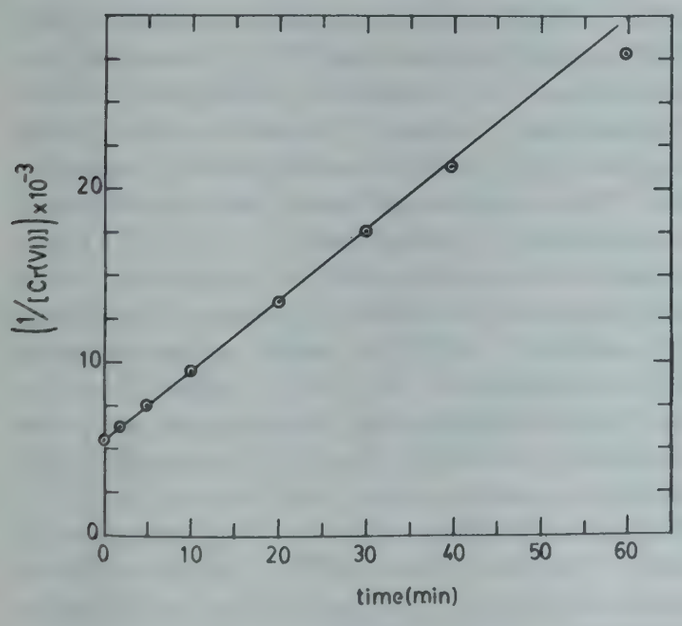

Fig. 1—Second order plot of chromium(VI)-thallium(I) reaction in 60% acetic acid containing 1.25 mol dm^{-3} hydrochloric acid at 25°C ([Cr(VI)] = 2.0×10^{-4} mol dm^{-3}, [Tl(I)] = 3.0×10^{-4} mol dm^{-3}, $\mu = 1.26$ mol dm^{-3})

Table 1—Effect of Varying [H$^+$] and [Cl$^-$] on Chromium(VI)-Thallium(I) reaction

[Cr(VI)] = 2.0×10^{-4} mol dm^{-3}; temp. 25°C; [Tl(I)] = 3.0×10^{-4} mol dm^{-3}; solvent medium: 60% acetic acid.

[Cl$^-$] (mol dm^{-3})	k (dm^{3}mol^{-1}s^{-1})	[H$^+$] (mol dm^{-3})	k (dm^{3}mol^{-1}s^{-1})
[H$^+$] = 1.25 mol dm^{-3}		[Cl$^-$] = 1.25 mol dm^{-3}	
0.25	0.91	0.50	1.0
0.50	1.6	0.75	2.3
0.75	2.9	1.00	3.5
1.00	5.0	1.25	6.3
1.25	6.3		

Effect of added vanadium(V)

The effect of added V(V) on the reaction was studied by taking into account the absorption due to both V(V) and Cr(VI) at 360 nm in runs where [Tl(I)] was greater (1.5 times) than [Cr(VI)]. Under the condition [Cr(VI)] > [Tl(I)], the absorption at 360 nm was regarded as due to the Cr(VI) exclusively, that due to V(V) being neglected in view of the very much higher ε of the former over that of V(V). In the presence of added V(V), the stoichiometry and the effect of added products remained the same as in the absence of V(V). Second order rate constant (k) in 60% acetic acid containing 1.25 mol dm^{-3} HCl in the presence of V(V) first increased till added [V(V)] exceeded that of the [Tl(I)] used; while, with further increase in [V(V)], the k-value progressively decreased. Hence, the order of reaction was determined in the two ranges of increasing and decreasing k in the presence of V(V). In the increasing range of k ([V(V)] < [Tl(I)]), the orders in [Cr(VI)], [Tl(I)] and [V(V)] were 0.85, 1.0 and 0.60 respectively while in the decreasing range of k ([V(V)] > [Tl(I)]), the orders were 0.91, 0.90 and −1.0 respectively. In almost all runs, second order plots were linear practically throughout the 80% reaction range at all [V(V)] used. Such a behaviour of k was not observed in 40% acetic acid solution in the presence of 1.25 mol dm^{-3} HCl and k decreased continuously with increase in [V(V)].

In view of the distinctive effect of added V(V) on the reaction, the spectra of Tl(I) and V(V) were examined in 60% acetic acid containing 1.25 mol dm^{-3} HCl, individually and also together as mixed solution in the range of 250 to 350 nm. In the presence of both Tl(I) and V(V), there was a distinct change in the spectrum and the low intensity absorption bands of Tl(I) and V(V) were replaced by a high intensity band at 252 nm ($\varepsilon \sim 8200$), the latter being presumably due to the interaction between V(V) and Tl(I). Furthermore, a detailed study of the Job's curves[5] in respect of this sys-

tem at 250, 260 and 270 nm each showed the composition of the V(V)-Tl(I) complex as 1:1, 1:1, 2:3 and 1:2 in 60, 70, 80 and 90% acetic acid solutions in the presence of 1.25 mol dm^{-3} HCl in each case.

Effect of Mn(II), Ce(III), Th(IV) and U(VI) on the reaction

Significantly, added Mn(II), Ce(III), Th(IV) and U(VI) in the concentration range of 0.5×10^{-3} to 1.5×10^{-3} mol dm^{-3} did not affect the reaction.

Discussion

The rate data in 60% acetic acid containing 1.25 mol dm^{-3} HCl parallel the results of an earlier study[1b] in 3 mol dm^{-3} HCl solution with respect to reaction order, effect of added products and the influence of Cl^- ions. However, with respect to H^+ ions, the order in the present case is two as against one found in the earlier study[1b]. In the presence of large $[Cl^-]$ and $[H^+]$, Cr(VI) and Tl(I) mainly exist in the form of chlorochromate[2], CrO_3Cl^-, and thallium(I) chloride, TlCl, respectively[1b]. These species may be expected to form in prior equilibria in the present case. The experimental results lead to the mechanism shown in Scheme 1

$$HCrO_4^- + Cl^- + H^+ \rightleftharpoons CrO_3Cl^- + H_2O \qquad \ldots(K_1)$$

$$Tl^+ + Cl^- \rightleftharpoons TlCl \qquad \ldots(K_2)$$

$$CrO_3Cl^- + H^+ + TlCl \rightleftharpoons HCrO_3 + TlCl_2 \qquad (k_1, k_2)$$

$$CrO_3Cl^- + H^+ + TlCl_2 \rightarrow HCrO_3 + TlCl_3 \qquad (k_3)$$

$$2(HCrO_3 + TlCl + 5H^+ \rightarrow Cr^{3+} + TlCl^{2+} + 3H_2O) \qquad (k_4)$$

Scheme 1

Chromium(VI) in acid solutions exists mainly as acid chromate ion[6] ($HCrO_4^-$) and chlorochromate (CrO_3Cl^-) is formed from this species in a preequilibrium. The latter and TlCl, also formed in a preequilibrium, react in a one equivalent reversible step (k_1, k_2) yielding the reactive Cr(V) and Tl(II) species. The Tl(II) interacts (k_3) with a second Cr(VI) ion giving a second Cr(V). The Cr(V) formed oxidises Tl(I) subsequently in a two-equivalent step (k_4). Scheme 1 does not involve any Cr(IV) species but includes Cr(V). However, no direct evidence for Cr(V) could be obtained. While induction experiments[6] with iodide could not be performed to show the intermediacy of Cr(V) as one of the products, Tl(III), also oxidises iodide along with Cr(VI). The Cr(V)-Tl(I) reaction, being a complementary reaction, is also expected to be fast and, as a result, Cr(V) is expected to be present in very low concentrations. In this respect, it is noteworthy that the evidence for the involvement of Cr(IV) in the reaction is negative. Added Mn(II) ions do not influence the reaction to any significant extent. If Cr(IV) was implicated in the mechanism, the presence of Mn(II) ions in the reaction solution would have caused substantial changes[6] in stoichiometry and rate constant.

The application of the steady state approximation to the reactive intermediates, Tl(II) and Cr(V), of Scheme 1 leads to the rate equation (3) which is in agreement with the experimental results and the experimental second order rate constant (k) may be identified with the constant factors in Eq. (3) at fixed $[H^+]$ and $[Cl^-]$. In Eq. (3), K_1 and K_2 are the equilibrium constants of formation of CrO_3Cl^- and TlCl respectively and k_0 is a constant given by Eq. (4), k_1, k_2, k_3 and k_4 in Eq. (4) being the rate constants of the

$$-\frac{d[Cr(VI)]}{dt} = \left\{\frac{k_0 K_1 K_2 [H^+]^2 [Cl^-]^2}{(1 + K_1[H^+][Cl^-])(1 + K_2[Cl^-])}\right\} \times [Cr(VI)][Tl(I)] \qquad \ldots(3)$$

$$k_0 = (k_3 k_4 / k_2)\,[\{1 - (4 k_1 k_2 / k_3 k_4)\}^{1/2} - 1] \qquad \ldots(4)$$

different steps shown in Scheme 1. An alternative pathway, almost identical to that of Scheme 1, except that the reactive intermediates, Cr(V) and Tl(II), are formed in an irreversible step in contrast to the reversible step of Scheme 1, can also be conceived. However, both Cr(V) and Tl(II) are usually formed in reversible steps[7] in noncomplementary electron transfer reactions of Cr(VI) and Tl(I) and Scheme 1 is therefore preferred.

In the presence of added V(V), it is observed that the Cr(VI)-Tl(I) reaction is accelerated till the added [V(V)] is slightly greater than [Tl(I)]. Thereafter, further addition of V(V) lowers the rate constant. In view of the rate law of Scheme 1, the nature of the distinctive effect of V(V) on the reaction needs to be understood. The experimental kinetic and spectroscopic results confirm the formation of a 1:1 V(V)-Tl(I) species and it is this species which is responsible for the initial rate acceleration in 60% acetic acid containing 1.25 mol dm^{-3} HCl. The active reductant under these conditions is a $(VO_2TlCl)^+$ species. Once the latter is completely formed, the rate constant is lowered on the further addition of V(V) because the latter manifests a specific cation effect on the CrO_3Cl^--TlCl reaction. Perhaps the V(V)-V(IV) cycle is now involved. That the influence of V(V) on the reaction is specific and limited to this ion is shown by the fact that the reaction is unaffected by ions of different valences and sizes such as Mn^{2+}, Ce^{3+}, Th^{4+} and UO_2^{2+} in a range of concentrations from one to four times that of the reductant. Because of the specific cation effect,

Table 2—Effect of Added Vanadium(V) on Chromium(VI)-Thallium(I) Reaction at 25°C

$[V(V)] \times 10^4$ (mol dm^{-3})	$k^{a,b}$ ($dm^3 mol^{-1} s^{-1}$)	$k^{a,c}$ ($dm^3 mol^{-1} s^{-1}$)	k^d ($dm^3 mol^{-1} s^{-1}$)
0.0	6.9	5.0	1.9
1.0	8.3	7.7	1.8
2.0	10	8.7	1.7
3.0	12	9.6	1.5
4.0	14	8.8	1.4
5.0	11	8.3	1.3
7.5	8.3		

(a) $[Cr(VI)] = 2.0 \times 10^{-4}$ mol dm^{-3}; $[HCl] = 1.25$ mol dm^{-3}; 60% acetic acid solution.

(b) $[Tl(I)] = 3.0 \times 10^{-4}$ mol dm^{-3}.

(c) $[Tl(I)] = 2.0 \times 10^{-4}$ mol dm^{-3}.

(d) $[Cr(VI)] = 2.0 \times 10^{-4}$ mol dm^{-3}; $[Tl(I)] = 3.0 \times 10^{-4}$ mol dm^{-3}; $[HCl] = 1.25$ mol dm^{-3}; 40% acetic acid solution.

there are two paths now for the reaction: one involving the reductant, $(VO_2TlCl)^+$, and the other, involving TlCl itself. It is noteworthy that the order of reaction in added V(V) is fractional (0.60) in the range of increasing rate constant and 1.0 for the range of decreasing rate constant. While excess V(V) is needed to drive the equilibrium towards complex formation, after the complex is fully formed, all added V(V) contributes to retardation of reaction. It is also possible that the V(V)-V(IV) cycle, marginally involved during catalysis, might be more active during retardation. However, there has been no evidence of any V(IV) during the reaction under a variety of conditions but it is also true that any V(IV) formed will be short-lived in the presence of several powerful oxidants in the reaction.

In 40% acetic acid containing 1.25 mol dm^{-3} HCl, there is no evidence of any V(V)-Tl(I) complex formation and hence the rate decreases with increase in [V(V)] (Table 2), again reinforcing the specificity of V(V) effect. As would be expected, there is no initial acceleration of reaction because no complex is formed in these solutions of higher dielectric constant. It is also apparent from the results of Table 2 that added V(V) decreases the rate much more efficiently in the absence of complex formation in 40% acetic acid solution than in solutions where the complex formation is facilitated.

References

1 (a) Sagi S R, Prakasa Raju G S & Ramana K V, *Talanta*, **22** (1975) 93; (b) Gokavi G S & Raju J R, *Polyhedron*, **6** (1987) 1721.

2 Haight G P Jr, Richardson D C & Coburn N W, *Inorg Chem*, **3** (1964) 1777.

3 Cohen M & Westheimer F H, *J Am chem Soc*, **74** (1952) 4387.

4 Davies K M & Espenson J H, *J Am chem Soc*, **92** (1970) 1889.

5 Job P, *Ann Chim (Paris)*, **9** (1928) 113.

6 Wiberg K B, *Oxidation by chromic acid and chromyl compounds in oxidation in organic chemistry, Part A* (Academic Press, New York) 1965.

7 Basolo F & Pearson R G, *Mechanisms of inorganic reactions*, (Wiley Eastern, New Delhi) 1973, 487-9.

Indian Journal of Chemistry
Vol. 27A, June 1988, pp. 498-503

Kinetics & Mechanism of Oxidation of Glutamine & Serine by Peroxomonosulphate in the Absence & Presence of Acetaldehyde & Propionaldehyde

M S RAMACHANDRAN*, T S VIVEKANANDAM & C NEWMAN PAUL DEVASINGH
School of Chemistry, Madurai Kamaraj University, Madurai 625 021

Received 2 *April* 1987; *revised* 14 *September* 1987; *accepted* 21 *October* 1987

The kinetics of oxidation of three structurally different amino acids, viz. serine, glutamine and alanine by peroxomonosulphate (PMS) in the absence and presence of aldehydes have been investigated in HOAc-NaOAc buffer medium. Analysis of kinetic results in the absence of aldehyde shows that SO_5^{2-} is the reactive species. The kinetic parameters such as rate constant, $\Delta H^{\ddagger}$ and $\Delta S^{\ddagger}$ show a correlation with pK_2 of the amino acid. The results have been analysed on the basis of a mechanism wherein the schiff base is proposed as the reactive intermediate.

In our earlier report[1] on the kinetics and mechanism of oxidation of amino acids (AA) by peroxomonosulphate (PMS)[1], it was observed that the first order plots showed curvature after 5-10% conversion of PMS which we believed was due to the effect of the product formed during the course of reaction. This was confirmed by studying the reactions in the presence of formaldehyde[2]. In order to have some insight in to the mechanism in the presence of aldehyde, presently we have investigated the kinetics of PMS oxidation of three structurally different amino acids namely alanine, serine and glutamine in the presence of acetaldehyde and propionaldehyde. Serine and glutamine have been chosen, in particular, to arrive at any correlation of the rate of oxidation with the structure of amino acids.

Materials and Methods

Potassium peroxomonosulphate (Du Pont) was found to be > 96% pure and its solution was always prepared afresh before use. The solution was standardised by cerimetry using ferroin as an indicator. Amino acids except glutamine were from Loba-Chemie Indo Austranal Co. Glutamine was from Koch-Light, England. Formaldehyde (S. Merck, 30%) was used as such and it was assayed by hypoiodite method[3]. Acetaldehyde and propionaldehyde were purified and assayed by standard procedures.

All the kinetic runs were followed by iodometry at constant $[H^+]$ using HOAc-NaOAc buffer. A high concentration of the buffer (0.2*M*) was maintained in the reaction mixture since the product HSO_4^- is a stronger acid than the oxidant HSO_5^-. No self-decomposition of PMS was observed under our experimental conditions.

Stoichiometry

Reaction mixtures containing large excess of [PMS] over [AA] or [AA + aldehyde] were allowed to stand for several hours (24 to 48 hr) at room temperature and constant $[H^+]$ (*p*H 4.8) and the unconsumed PMS was determined iodometrically. The stoichiometries of the reaction in the absence and presence of aldehyde were:

$$2\text{PMS} + 1\text{AA} \rightarrow \text{products};$$

and

$$3\text{PMS} + 1\text{AA} + 1\text{aldehyde} \rightarrow \text{products}.$$

One of the oxidation products of serine with PMS both in the absence and presence of aldehyde was glycollic acid. An acid product was obtained in the case of glutamine also. However, in this case the product underwent further oxidation on long standing as in the case of glycollic acid (serine-PMS). In the presence of aldehyde the products of oxidation (CH_3COOH etc.) of aldehydes were also detected by spot tests.

Results

(*i*) *Oxidation of serine and glutamine in the absence of aldehyde*

All the experiments were carried out under pseudo-first order conditions: [AA] ≫ [PMS]. Plots of log V_t (V_t = volume of thiosulphate consumed) versus time were linear up to 60% conversion (Fig. 1A). At fixed [AA] and $[H^+]$ the values of pseudo-first order rate constant, (k_{obs}) were independent of the initial (PMS], indicating that rate was proportional to [PMS].

The values of k_{obs} increased linearly with [AA] and the plots of k_{obs} versus [AA] passed through the origin (Fig. 2A). The values of k_{obs} decreased with increase in $[H^+]$ and the plots of k_{obs} versus $1/[H^+]$ were linear and passed through the origin (Fig. 2B).

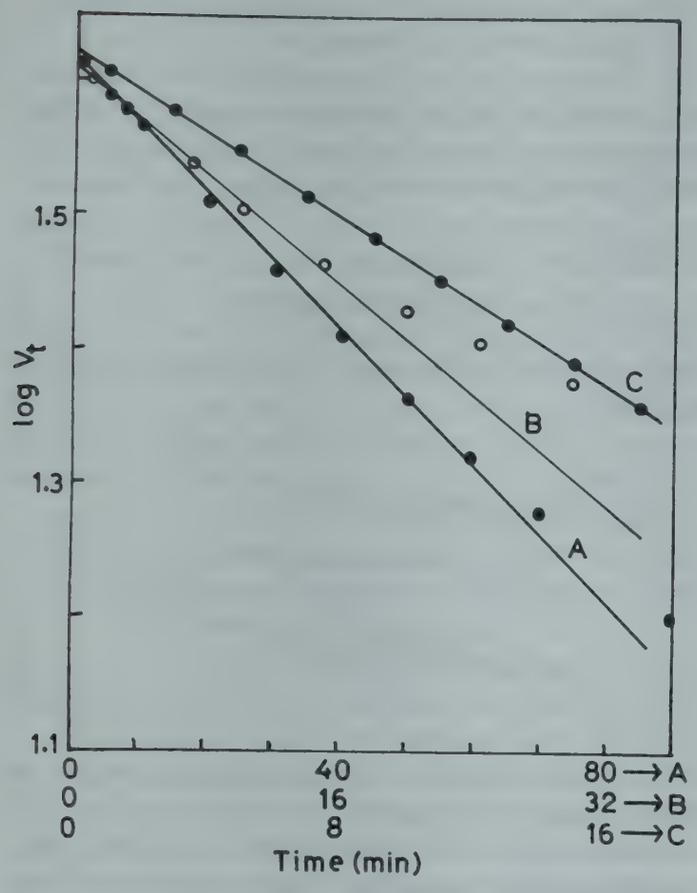

Fig. 1—(A) Plot of log V_t versus time at 31°C. ([glutamine] = 0.05 mol dm^{-3}, [PMS] = 4.19×10^{-3} mol dm^{-3}, pH = 5.2, μ = 0.25 mol dm^{-3}, (B) [alanine] = 0.05 mol dm^{-3}, [PMS] = 4.18×10^{-3} mol dm^{-3}, pH = 4.0; μ = 0.25 mol dm^{-3}, [acetaldehyde] = 2.8×10^{-3} mol dm^{-3}, (C) [serine] = 0.05 mol dm^{-3}, [PMS] = 4.2×10^{-3} mol dm^{-3}, pH = 4.0, μ = 0.25 mol dm^{-3}, [formaldehyde] = 3.03×10^{-3} mol dm^{-3})

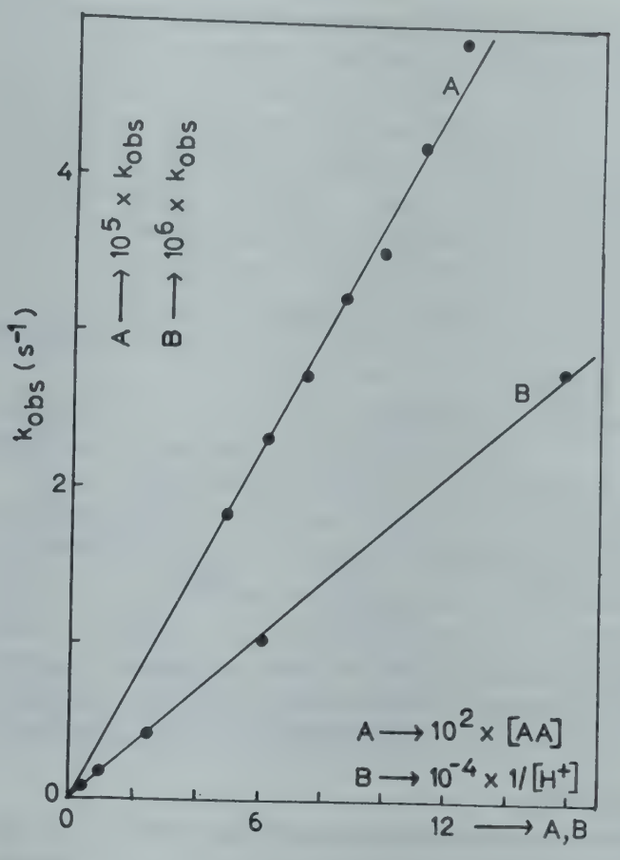

Fig. 2—(A) Plot of k_{obs} versus [amino acid] (AA) at 31°C ([AA] = [serine], [PMS] = 3.93×10^{-3} mol dm^{-3}, pH = 4.0, μ = 0.25 mol dm^{-3}, (B) Plot of k_{obs} versus 1/[H^+] at 31°C [Serine] = 0.05 mol dm^{-3}, [PMS] = 3.93×10^{-3} mol dm^{-3}, μ = 0.25 mol dm^{-3})

The change in ionic strength of the medium from 0.25 to 0.55 by adding potassium sulphate showed almost negligible increase in k_{obs}. The reactions were studied at four different temperatures (30-45°C) and from the temperature dependence of k_{obs} the activation parameters were calculated.

(ii) Oxidation of alanine, serine and glutamine in the presence of aldehyde

In these experiments pseudo-first order conditions were maintained only with respect to [AA]. The [aldehyde] was approximately equal to [PMS] in the oxidation reactions of amino acids in the presence of formaldehyde. But [acetaldehyde] and [propionaldehyde] were slightly less than [PMS]. In the presence of formaldehyde the plots of log V_t versus time were linear (Fig. 1C) even up to 70% conversion of PMS. In the presence of acetaldehyde and propionaldehyde the first order plots were curved (Fig. 1B) and the percentage of [PMS] conversion, corresponding to the point at which the curvature appeared, increased proportionally with increase in [acetaldehyde] and [propionaldehyde]. When the [aldehyde] in the case of acetaldehyde and propionaldehyde was greater than [PMS], the first order plots were linear upto 50% conversion. At fixed [AA], [H^+] and [aldehyde] the values of k_{obs} were independent of the initial [PMS], indicating first order dependence in [PMS].

The values of k_{obs} increased with increase in [AA]. Plots of k_{obs} versus [AA] were linear with a definite positive intercept (Fig. 3). At fixed [H^+] and [AA], the value of k_{obs} increased with increase in [aldehyde] and the plots of k_{obs} versus [aldehyde] were linear passing through the origin.

The values of k_{obs} decreased with increase in [H^+] and the plots of k_{obs} versus 1/[H^+] were linear with a positive intercept, indicating clearly that the reactions proceeded through two independent paths: one was [H^+]$^{-1}$ dependent and the other was [H^+] independent.

The change in ionic strength from 0.25 to 0.55 had negligible effect on k_{obs}. The reactions were studied at four different temperatures in the range 30-45°C and the activation parameters were calculated.

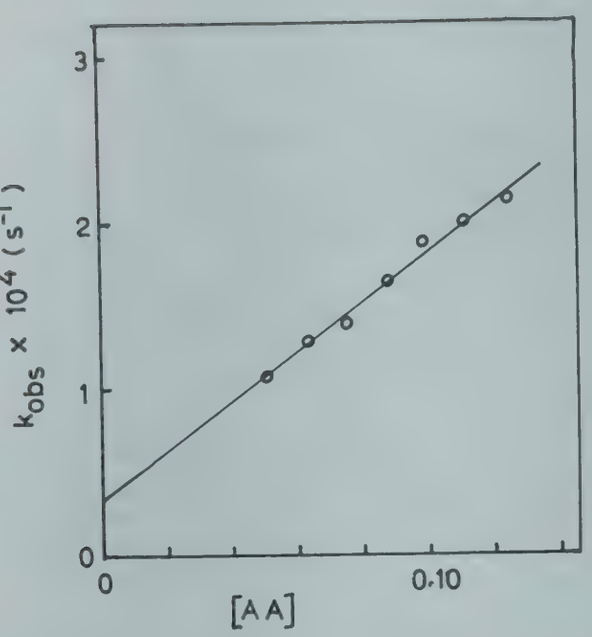

Fig. 3—Plot of k_{obs} versus [amino acid] (AA) at 31°C ([AA]=[glutamine], [PMS]=4.2×10^{-3} mol dm^{-3}, pH=4.0, μ=0.25 mol dm^{-3}, [propionaldehyde]=7.9×10^{-4} mol dm^{-3})

Discussion

Peroxomonosulphuric acid ($HO-OSO_3-H$) has two ionizable protons, viz. sulphuric acid proton and hydrogen peroxide proton. The pK_a value[4] of the sulphuric acid proton lies in a high acidity region and that of hydrogen peroxide proton is 9.4.

For amino acids, the following equilibria (1) exist in acidic/alkaline medium.

$$\underset{\overset{+}{N}H_3}{\overset{|}{R'-CH-COOH}} \overset{K_I}{\rightleftharpoons} \underset{\overset{+}{N}H_3}{\overset{|}{R'-CH-COO^-}} \overset{K_{II}}{\rightleftharpoons} \underset{NH_2}{\overset{|}{R'-CH-COO^-}} \quad \ldots (1)$$

The values of pK_1 and pK_2 for the amino acids[5] studied are 2.2 and 9.1-9.7 respectively and the values are given in Table 1. Under our experimental conditions namely at pH=4.0 all the amino acids would be in the form of zwitter ions. Therefore the amino acid in its zwitterionic form may be the reactive species.

It is well known that amino acids react with aldehyde to give schiff bases. The catalytic effect of pyridoxal phosphate in the amino acid metabolism by enzymes is attributed to the schiff base formed between the amino acid and pyridoxal phosphate[6-8]. We can therefore assume that the following equilibrium (2) exists under the present experimental conditions.

$$\underset{\overset{+}{N}H_3}{\overset{|}{R'-CH-COO^-}} + RCHO \rightleftharpoons \underset{\overset{+}{N}H=CHR}{\overset{|}{R'-CH-COO^-}} \quad \ldots (2)$$

Mechanism of oxidation of serine and glutamine by PMS in the absence of aldehydes

From a knowledge of the possible reactive species that exist under the present experimental conditions oxidation of serine and glutamine in the absence of aldehydes may proceed as shown in Eqs (3) and (4).

$$HOOSO_3^- \overset{K}{\rightleftharpoons} {}^-OOSO_3^- + H^+ \quad \ldots (3)$$

$$\text{Amino acid} + {}^-OOSO_3^- \overset{k_1}{\rightarrow} \text{products} \quad \ldots (4)$$

Rate law corresponding to Eqs (3) and (4) is given by Eq. (5).

$$\frac{-d[PMS]}{dt} = k_1[\text{Amino acid}][SO_5^{2-}] = Kk_1\frac{[\text{Amino acid}][HSO_5^-]}{[H^+]}$$

$$k_{obs} = Kk_1\frac{[\text{Amino acid}]}{[H^+]} \quad \ldots (5)$$

The rate equation (5) explains all the experimental facts. Using the literature[4] value of $K=3.98\times10^{-10}$ the rate constants for the oxidation of SO_5^{2-} (k_1) have been obtained and the values are given in Table 1.

It is interesting to note that though serine is similar to threonine, it reacts only with SO_5^{2-} whereas threonine has been shown to react[9] with both SO_5^{2-} and HSO_5^-. Moreover the reaction of threonine with PMS was studied at pH 3.6, 4.0 and 4.4. In order to

Table 1—Kinetic Parameters for oxidation of Amino Acids at 31 °C in the Absence of Aldehydes[a]

Amino acid[b]	k_1		$\Delta H_{k_1}^{\dagger}$ (K cal mol^{-1})	$\Delta S_{k_1}^{\dagger}$ (cal deg^{-1} mol^{-1})	pK_2
Alanine	24.5	(21.0)	—	—	9.87
Butryne	32.0	(28.0)	—	—	9.83
Valine	10.6	(10.0)	22.6	62.6	9.74
Leucine	7.3	(7.0)	—	—	9.74
Isoleucine	18.4	(17.6)	16.4	46.9	9.76
nor-Leucine	28.0	(28.0)	—	—	9.83
Phenylalanine	47.2	(47.2)	18.0	50.5	9.18
Serine	87.0		17.6	51.4	9.21
Glutamine	60.0		13.4	35.5	9.13
Threonine	88.7	(76.2)	8.6	20.6	9.10

[a] Values given in parentheses are reported values taken from ref (2) and (9).

[b] Since in the oxidation of alanine, butryne and nor-leucine the first-order plots are linear only upto 10% conversion, a large error may be introduced in the calculation of k_{obs}. Therefore the $\Delta H^{\dagger}$ and $\Delta S^{\dagger}$ values are not calculated. We have calculated the $\Delta H^{\dagger}$ and $\Delta S^{\dagger}$ values only for the systems where the first order plot is linear atleast upto 50% conversion.

ascertain the above fact the kinetics were reinvestigated at *p*H 3.6 to 5.2 and from the plot of k_{obs} versus $1/[H^+]$ it was found that only SO_5^{2-} alone reacts with threonine since this plot also passed through origin. This led us to reexamine our earlier report[1] because in the earlier report we have studied the kinetics only upto 5-10% conversion of [PMS] and therefore there may arise some error in the calculation of k_{obs}. The recalculated results are given in Table 1. The values reported in Table 1 are the average of k_1 obtained as a result of $[H^+]$ and [AA] variations. Comparison of k_1 (Table 1) with the earlier reported values for the oxidation by SO_5^{2-} shows only a small difference.

Perusal of the results in Table 1 shows that there exists an approximate correlation between k_1 and pK_2 of the amino acid as expected since the reaction is a nucleophilic attack of SO_5^{2-} on $R'-CH(\overset{+}{N}H_3)COO^-$ at the $-\overset{+}{N}H_3$ group. From Table 1, we can infer that alanine, butryne etc. which are linear amino acids are more reactive than the branched chain amino acids such as leucine, isoleucine, etc. Similarly if we consider the reactivities of phenylalanine, glutamine and threonine, the reactivity order is threonine > glutamine > phenylalanine, as expected on the basis of pK_2 values. Based on this, the k_1 values of serine would be approximately equal to that of phenylalanine. But the observed value is equal to that of threonine. The above three amino acids, in comparison to serine have a different substituent at the β-position. The effect of the different bulkier groups at β-position may be complex and therefore it is difficult to arrive at any correlation in the case of serine.

From the effect of temperature on k_{obs} the activation parameters have been calculated (Table 1).

$$\Delta H^{\ddagger}_{obs} = \Delta H^{\ddagger}_{K} + \Delta H^{\ddagger}_{k_1}$$

$$\Delta S^{\ddagger}_{obs} = \Delta S^{\ddagger}_{K} + \Delta S^{\ddagger}_{k_1}$$

The values of $\Delta S^{\ddagger}_{k_1}$ for all the systems are surprisingly positive and this shows that more than one intermediate/transition state is involved in the reaction pathway.

From the results we can generalize the following facts: (i) The linear α-amino acids (i.e. with no β-substituent) show a curved first order plot after 5-10% conversion of PMS. This is due to the fact that the product aldehyde reacts with the amino acids to give a schiff base which reacts faster than the amino acid. (ii) α-Amino acids having a β-substituent, with the exception of threonine, do not show such a behaviour. This may be due to the fact that the product aldehyde, is not able to form a schiff base due to steric effet. Therefore the first order plots are linear even up to 50% conversion. In the case of threonine a curvature towards X-axis (k_{obs} increases) is noticed in the first order plot after 5-10% conversion and this may be due to further oxidation of product, aldehyde. (iii) All the amino acids are oxidised by SO_5^{2-} and the rate constants (k_1), $\Delta H^{\ddagger}$ and $\Delta S^{\ddagger}$ can approximately be correlated with pK_2. In the case of β-branched α-amino acids the observed rate constant is smaller than the unsubstituted one.

Mechanism of oxidation of alanine, glutamine and serine in the presence of aldehydes

The mechanism of oxidation of amino acids in the presence of HCHO has been discussed earlier in detail[2,9]. The kinetics of oxidation of amino acids in the presence of both acetaldehyde and propionaldehyde are similar to those of formaldehyde. Hence, the mechanism identical to that proposed in the presence of formaldehyde is valid in the case of acetaldehyde and propionaldehyde (see Scheme 1).

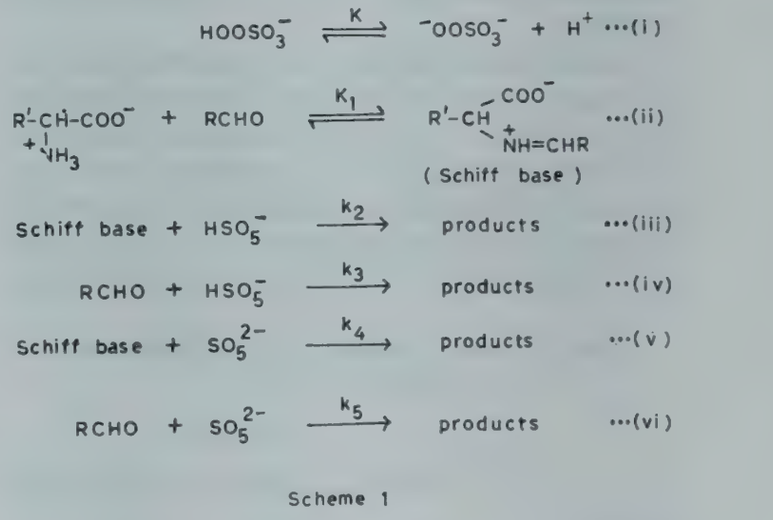
HOOSO3- ⇌ -OOSO3- + H+ ···(i)
R'-CH-COO- + RCHO ⇌ R'-CH(COO-)-NH=CHR ···(ii)
NH3+
(Schiff base)
Schiff base + HSO5- → products ···(iii)
RCHO + HSO5- → products ···(iv)
Schiff base + SO5 2- → products ···(v)
RCHO + SO5 2- → products ···(vi)

Scheme 1

Based on Scheme 1, the rate law at constant *p*H can be expressed by Eq. (6)

$$\frac{-d[PMS]}{dt} = \{k_a[AA][RCHO] + k_b[RCHO]\}[PMS]$$

$$k_{obs} = k_a[AA][RCHO] + k_b[RCHO] \quad \ldots (6)$$

where k_a and k_b represent the rate constants for oxidation of schiff base and aldehydes at constant *p*H. Equation (6) explains the effect of [AA] and [RCHO] variation on the rate. The values of k_b can be calculated from the plots of k_{obs} versus [AA] (Fig. 2) and these values can be compared with the values obtained from the direct oxidation of aldehydes[10]. These two values given in Table 2 agree well and this confirms the validity of the reaction mechanism shown in Scheme 1.

The rate law consistent with Scheme 1 can also be expressed by Eq. (7)

$$\frac{-d[\mathrm{PMS}]}{dt} = (k_4K_1[\mathrm{AA}] + k_5)[\mathrm{RCHO}]_T \frac{K[\mathrm{HSO_5^-}]}{[\mathrm{H^+}]} + (k_2K_1[\mathrm{AA}] + k_3)[\mathrm{RCHO}]_T[\mathrm{HSO_5^-}] \quad \ldots (7)$$

The values obtained for $(k_4K_1[\mathrm{AA}] + k_5)$ and $(k_2K_1[\mathrm{AA}] + k_3)$ from the plots of k_{obs} versus $1/[\mathrm{H^+}]$ are lower than the values of k_5 and k_3 respectively, which are the values from the direct oxidation of the concerned aldehydes[10]. This clearly shows that the rate constants k_5 and k_3 in the presence of amino acids are always smaller than the values obtained by the direct oxidation of aldehydes. This is due to our experimental conditions, viz. [AA] > [PMS] and [RCHO] ≤ [PMS]. Because of this the oxidation of RCHO by PMS may not follow the pseudo-first order kinetics. Therefore, as an approximation k_5 and k_3 can be neglected in Eq. (7) and approximate values of k_4K_1 and k_2K_1 are given in Table 3.

It is well known that the aldehydes in aqueous solution exist as a mixture of free carbonyl form and hydrated form[11]. From the foregoing results we could not say which form of aldehyde reacts with the amino group to form a schiff base. Moreover the values of the equilibrium constant (K_1) for the schiff base formation may be different for different aldehydes. Because of this we could not correlate the rate constants obtained for the oxidation of serine and glutamine in the presence of formaldehyde, acetaldehyde and propionaldehyde.

If the complex between SO_5^{2-} (HSO_5^-) and $-N=CHR$ is assumed as the activated complex, then the formation and decomposition of this activated complex depend on the electron density at the $-N=CHR$ group. According to the +I effect of alkyl group in $-N=CHR$, the electron density at the $-N=CHR$ may be in the order: propionaldehyde > acetaldehyde > formaldehyde. The observed $\Delta H^\dagger$ values for oxidation of glutamine, serine and alanine in the presence of aldehyde show that the order is: propionaldehyde < acetaldehyde < formaldehyde. This clearly indicates that the electronic effect is more pronounced on the decomposition of the activated complex since the reverse order is expected if the complex formation is more pronounced due to increased electron density at $-N=CHR$. Moreoever, in our earlier work[1] the values of $\Delta H^\ddagger$ are almost same for various amino acids in the presence of formaldehyde, showing that $\Delta H^\ddagger$ values do not depend upon the alkyl part of the amino acid but depend only on the $-N=CHR$ group. This is also clearly borne out by the $\Delta H^\ddagger$ values obtained in the presence of acetaldehyde and propionaldehyde (Table 3).

Table 2—Rate Constants (k_b)* for Oxidation of Aldehydes at 31°C

	k_b (from Eq. 6)		
	HCHO	CH_3CHO	CH_3CH_2CHO
Alanine	—	0.08	0.08
Serine	0.06	0.07	0.07
Glutamine	0.09	0.06	0.05
Experimental* [a]	0.11	0.26	0.19

*At pH = 4.0; μ = 0.25; temp. = 31°C.
[a]Obtained from direct oxidation of aldehydes by PMS (see ref. 10).

Acknowledgement

The authors express their deep gratitude to Prof N R Subbaratnam for help and encouragement. One of them (CN) thanks the UGC, New Delhi for the award of a teacher fellowship under Faculty Improvement Programme and the Principal and Management of N.M.S.S.V.N. College for Study leave.

References

1 Ramachandran M S & Vivekanandam T S, *J chem Soc, Perkin Trans*, (1984) 1341.
2 Ramachandran M S, Vivekanandam T S & Malim Mani Raj R P, *J chem Soc, Perkin Trans*, (1984) 1345.
3 Mann F G & Saunders B C, *Practical organic chemistry*, (ELBS and Longman, London) 1974, pp 463.
4 Ball D L & Edwards J O, *J Am chem Soc*, **82** (1960) 1778.

Table 3—Kinetic Parameters for Oxidation of Amino Acids at 31°C in the Presence of Aldehydes

	Serine			Glutamine			Alanine	
	HCHO	CH_3CHO	CH_3CH_2CHO	HCHO	CH_3CHO	CH_3CH_2CHO	CH_3CHO	CH_3CH_2CHO
$10^1 k_2K_1$ ($dm^6\ mol^{-2}\ s^{-1}$)	19.8	13.6	9.0	14.8	9.8	7.2	17.8	12.0
$10^{-5} k_4K^1$ ($dm^6\ mol^{-2}\ s^{-1}$)	8.3	5.8	5.0	8.2	7.4	8.4	3.2	2.8
$\Delta H''$ (k cal mol^{-1})	14.5	9.2	8.2	13.2	8.1	7.4	9.0	7.8

5 *Lange's hand book of chemistry,* edited by J A Dean, Ch 5-15, (McGraw-Hill, New York) 1973.
6 Bruice T C & Benkovic S J, *Bio-organic mechanisms,* Vol. II, (W A Benjamin, New York) 1966, Chapter 8.
7 Martell A E, *Chemical and biological aspects of pyridoxal catalysis,* edited by E E Snell, P M Fasella, A Braunstein & A Rossi Fanelli (Pergamon Press, New York) 1963, pp 13.
8 Braunstein A, *The enzymes,* Vol II, edited by F D Boyer, H Lardy & K Myrbach (Academic Press, New York) 1960, pp 113.
9 Ramachandran M S & Vivekanandam T S, *Tetrahedron,* **40** (1984) 4929.
10 Ramachandran M S, Vivekanandam T S & Arunachalam V, *Bull chem Soc, Japan,* **59** (1986) 1549.
11 Bell R P, *Advan phys org chem,* **4** (1968) 1.

Indian Journal of Chemistry
Vol. 27A, June 1988, pp. 504-506

Synthesis & Characterisation of Potassium, Cesium & Ammonium Oxotetrafluorotitanates(IV)

MIHIR K CHAUDHURI* & BIMAI ENDU DAS
Department of Chemistry, North-Eastern Hill University, Shillong 793 003

Received 7 *July* 1987; *revised and accepted* 24 *August* 1987

A high yield synthetic route to potassium and ammonium oxotetrafluorotitanates(IV) has been developed based on the reaction of freshly precipitated TiO_2 with 4 *M* sulphuric acid to produce TiO_2^{2+} cation which reacts with corresponding alkali fluorides (AF) in the molar ratio 1:7 (Ti:AF) to afford the desired compounds. The corresponding Cs^+ salt is prepared from the ammonium salt by metathesis. The compounds, all of which are white products, have been characterised on the basis of elemental analyses, room temperature magnetic susceptibility measurements, and IR and laser Raman (lR) spectral data. The IR and laser Raman (lR) spectra provide evidence for a distorted octahedral structure of $[TiOF_4]^{2-}$ ion with -Ti-O-Ti- interactions.

Solid oxo-complexes of Ti(IV) are rather fewer as compared to those of V(IV)[1-3]. In the case of Ti(IV), $[TiOF_5]^{3-}$ is the only well characterised[4] fluoro complex, although existence of $[TiOF_3]^-$ is also reported[5]. Of some interest is the complex oxotetrafluorotitanate(IV), $[TiOF_4]^{2-}$. Despite a number of attempts[6,7], synthesis of pure $[TiOF_4]^{2-}$ could not be achieved. In a recent study[8] involving high temperature thermal decomposition of a peroxo complex $K_2[Ti(O_2)F_4]$, $K_2[TiOF_4]$ has been obtained as one of the main products. As a sequel to our efforts on some aspects of titanium chemistry[1,9,10] and also in view of considerable interest on structural assessment of oxotitanates(IV)[11,12], we felt it imperative to synthesise the title compounds in pure forms and characterise them by elemental analyses, and IR and laser Raman (lR) spectral data.

Materials and Methods

Reagent grade chemicals were used throughout. IR spectra were recorded on a Perkin-Elmer model 983 spectrophotometer and laser Raman (lR) spectra on a SPEX Ramalog model 1403 spectrophotometer. The 4880 Å laser line from the Spectra-Physics model 165 argon laser was used as the excitation source. The scattered light at 90° was detected with the help of a cooled RCA 31034 photomultiplier tube followed by photon count processing system. The spectra were recorded at ambient temperature by holding the samples either in a quartz capillary or in the form of a pressed pellet. Magnetic susceptibility measurements were made at room temperature by Gouy's method using Hg $[Co(SCN)_4]$ as the calibrant.

Ammonium oxotetrafluorotitanate(IV), $(NH_4)_2[TiOF_4]$

Freshly prepared TiO_2 (lg, 12.5 mmol) was dissolved in 4 *M* sulphuric acid (36 ml) at room temperature to get a clear solution and to this was added a solution of ammonium fluoride (3.25g, 87.83 mmol) in water (10 ml) followed by addition of ethanol with constant stirring until the white product started appearing. The addition of ethanol was discontinued at this stage, the reaction mixture was cooled in an ice-water bath for 45 min until the preciiptation was complete, filtered, and the precipitate washed twice with ethanol and finally dried *in vacuo* over conc sulphuric acid, yield 1.8g (82%).

Potassium oxotetrafluorotitanate(IV), $K_2[TiOF_4]$

It was prepared as above, except ethanol was not added for precipitation since a white product appeared immediately. The reaction mixture was cooled in an ice-water bath for 15 min and the compound separated by filtration. It was dissolved in warm water (50 ml) which on cooling to room temperature afforded the desired compound which was filtered off, washed twice with ethanol and finally dried *in vacuo* over conc sulphuric acid, yield 1.9g (69.7%).

Cesium oxotetrafluorotitanate(IV), $Cs_2[TiOF_4]$

$Cs_2[TiOF_4]$ precipitated out spontaneously when solid $(NH_4)_2[TiOF_4]$ (2.84 mmol) was added to a clear solution of CsBr (8.52 mmol) dissolved in water (10 ml). The white product obtained was

Table 1 — Analytical Data of Potassium, Cesium and Ammonium Oxotetrafluorotitanates(IV)

Complex	Found (calc), %		
	K or N[a]	Ti[b]	F[c]
$K_2[TiOF_4]$	35.24 (35.77)	21.89 (22.01)	34.50 (34.86)
$Cs_2[TiOF_4]$		11.45 (11.82)	18.24 (18.71)
$(NH_4)_2[TiOF_4]$	15.45 (15.90)	26.80 (27.27)	42.98 (43.18)

(a) Determined as described earlier (see ref. 14)

(b) Determined after precipitation with cupferron (ref. 13a)

(c) Determined as lead chloride fluoride (ref. 13b)

washed with ethanol and finally dried *in vacuo* over conc sulphuric acid, yield 0.9g (78%).

Results and Discussion

The analytical data of the compounds are given in Table 1. Taking into account two important points, (i) that a number of direct methods[6,7] failed to provide pure $[TiOF_4]^{2-}$ and (ii) titanyl cation (TiO^{2+}) certainly exists[11,15,16] in solution, it was thought that an indirect route via the prior formation of an oxotitanates(IV) in solution might be appropriate for the synthesis of pure oxotetrafluorotitanates(IV) reported in this study. Thus freshly prepared TiO_2 (obtained by dissolving commercial titanium dioxide in 40% hydrofluoric acid and then treating with aqueous ammonia) was first dissolved in an excess of dil sulphuric acid to produce titanyl sulphates[17], $TiO(SO_4)$, in solution. The clear solution was then treated with alkali fluoride (AF) to produce the desired compound. The role of alkali fluoride was not only to fluorinate the titanyl (TiO^{2+}) but also to act as a source of counter alkali metal cation. For the preparation of the ammonium compound addition of ethanol was required to just initiate precipitation owing to high solubility of the ammonium salt. Recrystallisation of $K_2[TiOF_4]$ from water was necessary to remove any coprecipitated K_2SO_4. The method is fairly simple and does not involve hydrofluoric acid. The cesium salt $Cs_2[TiOF_4]$ was prepared by metathesis between $(NH_4)_2[TiOF_4]$ and CsBr. It is evident from the above discussion that fluoride is a better ligand for TiO^{2+} than sulphate. Indeed our endeavours to synthesise mixed ligand fluoro(sulphato)titanates(IV) have not been successful so far.

Potassium, cesium and ammonium oxotetrafluorotitanates(IV) are white solids and are stable when out of contact with water. All the compounds are diamagnetic, in conformity with the view that titanium occurs in its +4 oxidation state (d^0) in these compounds. They are also EPR silent. The IR and laser Raman (lR) spectra of all the compounds are identical except for $\nu(NH_4^+)$ mode of the ammonium salt. The occurrence of ν(Ti-F) mode due to coordinated fluoride around 605 cm^{-1} compares favourably with the literature reports[18-20]. The appearance of a medium intensity band at ~720 cm^{-1} may be assigned to ν(Ti-O-Ti)21. The absence of ν(Ti=O) mode at ~980 cm^{-1} indicates that the oxo group does not occur as a terminal one but is present as a bridging group. The band at ~300 cm^{-1} in the compounds may be assigned to a Ti-F deformation mode. The bands at 1400 (s), 3045(s) and 3155(m) cm^{-1} in the IR spectrum of ammonium salt have been attributed to ν_4, ν_1 and ν_3 modes of NH_4^+ (ref. 22), respectively.

The laser Raman (lR) spectra of all the three complexes are similar and exhibit a strong signal at ~610 cm^{-1} assignable to ν(Ti-F)[20]. The spectra also display medium intensity bands at ~650, ~530 and ~435 cm^{-1} originating from -Ti-O-Ti- interactions which, in accord with the literature[12], have been attributed to ν(-Ti-O-Ti-).

Thus, the results of IR and laser Raman (lR) spectral data suggest that the metal centre is hexacoordinated through a -Ti-O-Ti- interaction, and the complexes have polymeric distorted octahedral structures.

Acknowledgement

We thank the Department of Atomic Energy, Bombay for financial support.

References

1 Chaudhuri M K, Ghosh S K & Subramanian J, *Inorg Chem*, **23** (1984) 4439.

2 Ahrland S & Noren B, *Acta Chem Scand*, **12** (1958) 1595.

3 Ortolano T R, Selbin J & McGlynn S P, *J chem Phys*, **41** (1964) 262.

4 Dehnicke K, Pausewang G & Rudorff W, *Z anorg allgem Chem*, **366** (1969) 64.

5 Sengupta A K, Adhikari S K & Dasgupta H S, *J inorg nucl Chem*, **41** (1979) 161.

6 Dmitrevskii G E, Belitskaya A A, Savchenko M I & Kharchenko L P, *Zh Neorg Khim*, **13** (1968) 2663.

7 *Chem Abstr*, **73** (1970) 81105v; **79** (1973) 147791y; **79** (1973) 147794b.

8 Pausewang G & Schmidt R, *Z anorg allgem Chem*, **523** (1985) 213.

9 Chaudhuri M K & Das B, *Polyhedron*, **4** (1985) 1449; *Inorg Chem*, **25** (1986) 168.

10 Chaudhuri M K & Islam N S, *Inorg Chem*, **25** (1986) 3749; Bhattacharjee M & Chaudhuri M K, *J chem Soc, Dalton Trans*, (1987) 477.

11 Gratzel M & Rotzinger F P, *Inorg Chem*, **24** (1985) 2320.
12 Weighardt K, Quilitzch U, Weiss J & Nuber B, *Inorg Chem*, **19** (1980) 2514.
13 Vogel A I, *A text book of quantitative inorganic analysis*, (Longmans Green, London) 1962, (a) pp 544; (b) pp 269.
14 Chaudhuri M K & Ghosh S K, *Inorg Chem*, **21** (1982) 4020.
15 Cagliloti V, Ciavatta L & Liberti A, *J inorg nucl Chem*, **15** (1960) 115.
16 Ellis J D & Sykes A G, *J chem Soc, Dalton Trans*, (1973) 537; Ellis J D, Thompson G A K & Sykes A G, *Inorg Chem*, **15** (1976) 3172.
17 Clark R J H, Bradley D C & Thornton P, *The chemistry of titanium, zirconium and hafnium; Pergamon texts in inorganic chemistry*, vol 19 (Pergamon Press, Oxford) 1975, pp 377.
18 Dean P A W & Evans D F, *J chem Soc (A)*, (1967) 698.
19 Lane A P & Sharp D W A, *J chem Soc (A)*, (1969) 2942.
20 Milicev S & Macek J, *J chem Soc, Dalton Trans*, (1984) 297.
21 Coutts R S P & Wailes P C, *Inorg nucl chem Lett*, **3** (1967) 1.
22 Nakamoto K, *Infrared spectra of inorganic and coordination compounds*, (Wiley-Interscience, New York) 1970, pp 108.

Indian Journal of Chemistry
Vol. 27A, June 1988, pp. 507-509

Synthesis & Infrared, ^{1}H, ^{13}C, ^{119}Sn NMR & ^{119}Sn Mössbauer Studies of Some New Diorganotin Dichloride Adducts

A S KOTHIWAL, A SINGH, A K RAI & R C MEHROTRA*
Department of Chemistry, University of Rajasthan, Jaipur

Received 2 April 1987; revised and accepted 6 October 1987

Adducts of the type $R_2SnCl_2.O(R'')CC_6H_4NR'_2$ (R = Ph, Me; when R′ = H, R″ = CH_3 and R′ = CH_3, R″ = H) have been prepared and characterised by elemental analyses and spectral data (IR, PMR, ^{13}C, ^{119}Sn NMR, and ^{119}Sn Mössbauer).

Though the electrophilic nature of tin in organotin halides is weak, a large number of adducts of organotin halides have been synthesised and characterised. Addition complexes of diorganotin(IV) dihalides with monodentate Lewis bases, in general, depict 1:2 stoichiometry[1], $R_2SnX_2.2L$ (where R = alkyl, aryl; X = halogens; L = monodentate ligand) and octahedral geometry. In contrast, well characterised pentacoordinated complexes are comparatively limited in number[2,3].

In the present paper the mode of complexation of *p*-dimethylaminobenzaldehyde and *p*- or *m*-aminoacetophenone with dialkyl- and diaryl-tin dichlorides has been studied. The *p*- and *m*-aminoacetophenones have been chosen in order to rule out the possibilities of chelate formation. In view of the presence of both nitrogen as well as oxygen donor sites in the ligands, the following interesting possibilities can be envisaged for complexation in these systems: (i) $nNR'_2C_6H_4C(R'')O \rightarrow SnR_2Cl_2$; (ii) $nO(R'')CC_6H_4N(R'_2) \rightarrow SnR_2Cl_2$ and (iii) $R_2(Cl_2)Sn \leftarrow N(R'_2)C_6H_4C(R'')O \rightarrow SnR_2Cl_2$ (where n = 1 or 2).

Materials and Methods

The solvents used were dried before use. The ligands and reactants were purified by usual techniques. Molecular weights were determined in a semi-micro ebulliometer (Gallenkamp) equipped with thermistor sensing. IR spectra were recorded in the region 4000-200 cm^{-1} on a Perkin-Elmer 577 grating spectrophotometer and PMR spectra on Perkin-Elmer R-12B and Varian A-60 spectrometers. Carbon-13 and ^{119}Sn NMR spectra were recorded on a JEOL-PFT-100 FT spectrometer operating at 25.15 and 22.7 MHz respectively. Tin-119 Mössbauer spectra were recorded at 77 K using a conventional constant acceleration spectrometer.

Synthesis of complexes

When a solution of dialkyl/diaryltin dichloride in chloroform was mixed with a chloroform solution containing aminoacetophenone/dimethylaminobenzaldehyde in equimolar amount, heat was evolved and the colour of the reaction mixture changed from colourless to yellow. After stirring for 1 hr at room temperature, dry *n*-hexane was added gradually when a yellow precipitate was obtained leaving the supernatant liquid colourless, which was decanted off. The precipitate was filtered off, dried *in vacuo* at room temperature and recrystallised from benzene to afford a yellow solid. The characterisation data of diorganotin dichloride adducts thus prepared are listed in Table 1.

Results and Discussion

The reaction of dimethyl- and diphenyl-tin dichlorides with *p*-dimethylaminobenzaldehyde and *p*- or *m*-aminoacetophenone in chloroform can be represented by Eqs. (1) and (2), respectively:

$$R_2SnCl_2 + p\text{-}NMe_2C_6H_4CHO \rightarrow R_2SnCl_2.O(H)CC_6H_4NMe_2\text{-}p \quad \ldots (1)$$

$$R_2SnCl_2 + p \text{ or } m\text{-}NR'_2C_6H_4COCH_3 \rightarrow R_2SnCl_2.O(CH_3)CC_6H_4NR'_2\text{-}p \text{ or m} \quad \ldots (2)$$

(R = Ph, Me; R = H or Me)

A noteworthy feature of the above reactions is the formation of addition complexes of 1:1 stoichiometry only even when two-fold excess of the ligand is used (Table 1). All the complexes obtained are coloured solids (organge, yellow, or brown), have sharp melting points and are soluble in common organic solvents. The adducts are monomeric in refluxing benzene.

The infrared spectra of the complexes did not exhibit any shift in νNMe_2 modes of the free ligands

Table 1—Physical and Analytical Data of Some Diorganotin Dichloride Adducts

Sl No.	Complex	m.p. (°C)	Physical state	found (calc.) %		
				N	Cl	Sn
1	p-$NH_2C_6H_4C(Me)O.Ph_2SnCl_2$	121	Orange powder	2.90 (2.94)	14.77 (14.83)	24.78 (24.83)
2	p-$NH_2C_6H_4C(Me)O.Me_2SnCl_2$	101	Yellow powder	3.89 (3.97)	19.87 (20.02)	33.39 (33.52)
3	m-$NH_2C_6H_4C(Me)O.Me_2SnCl_2$	95	Brown solid	3.85 (3.97)	19.85 (20.02)	33.26 (33.52)
4.	p-$NMe_2C_6H_4CHO.Me_2SnCl_2$	95	Yellow powder	3.80 (3.82)	19.17 (19.26)	32.06 (32.25)
5	p-$NMe_2C_6H_4CHO.Ph_2SnCl_2$	103	Lemon Yellow powder	2.80 (2.85)	14.36 (14.41)	24.06 (24.12)

Table 2—Spectral Data of Diorganotin Dichloride Adducts[a]

Sl No.	Complex	IR (cm^{-1})				^1H NMR (δ)		^{119}Sn Mössbauer[b]	
		$\nu C=O$	$\nu Sn-O$	$\nu Sn-Cl$		$=C-H$	$-N(R')_2$	(ΔE) ($mm\ s^{-1}$)	(δ) ($mm\ s^{-1}$)
				asym	sym				
1	p-$NH_2C_6H_4C(CH_3)O.(CH_3)_2SnCl_2$	1675 (1645)	430	320	260	..	..	..	..
2	p-$NH_2C_6H_4C(CH_3)O\,(C_6H_5)_2SnCl_2$	1690 (1645)	440	320	265	..	..	2.81	1.38
3	p-$NMe_2C_6H_4C(H)O.(CH_3)_2SnCl_2$	1680 (1640)	435	330	275	9.55 (9.75)	3.02 (3.01)	3.88	1.48
4	p-$NMe_2C_6H_4C(H)O.(C_6H_5)_2SnCl_2$	1685 (1640)	435	332	278	9.48 (9.75)	3.01 (3.01)	2.89	1.24

(a) The values in parentheses are those of the ligands.
(b) The values are relative to SnO_2

suggesting non-involvement of amino and dimethylamino nitrogens in coordination. Lowering in the $\nu C=O$ by ~40 cm^{-1} may be taken as an evidence for the coordination of the ligand with R_2Sn moiety through the oxygen of CO group. The aromatic $\nu C=C$ modes were observed in the region 1590-1520 cm^{-1}. In the case of dimethyltin adducts, two medium intensity bands at 585 and 530 cm^{-1} could be assigned $\nu_{as}Sn$-C and $\nu_s Sn$-C modes respectively. These modes in diphenyltin adducts appeared at 285 and 250 cm^{-1}, respectively. The appearance of both these modes suggests that C – Sn – C moiety is non-linear as suggested by Tanaka *et al.*[2].

Generally,there are two structural possibilities (A and B) for pentacoordinated dialkyltin dihalide complexes in which the Lewis base(L) occupies the axial[4] or equatorial[5] site depending upon the electronegativity of the donor atom. Further, the positions of νSn-Cl modes are generally taken as diagnostic to distinguish among tetrahedral, trigonal bipyramidal and octahedral geometries. For trigonal bipyramidal geometry, a shift (compared to tetrahedral parent compound) of ~60 cm^{-1} in νSn-Cl is

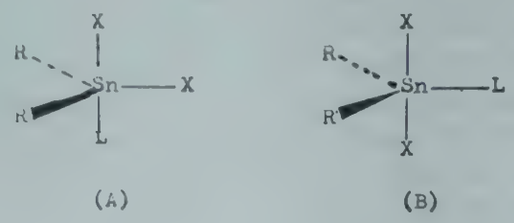

generally observed[6]. In the complexes studied presently, the observed shift (~ 50 cm^{-1}) is consistent with a trigonal bipyramidal geometry. Structure (A) should give rise to two νSn-Cl modes as a split band whereas structure (B) should give rise to only one νSn-Cl. The appearance of both $\nu_{as}Sn$-Cl and $\nu_s Sn$-Cl modes, therefore, indicates that the ligand occupies the axial position, in a structure of the type (A). The appearance of a new band at ~435 cm^{-1} assignable[7] to νSn-O is also confirms the coordination through carbonyl oxygen.

The significant characteristics revealed by the NMR(^1H, ^{13}C and ^{119}Sn) spectra of the complexes as compared with those of the free ligands are:

(i) The aldehydic proton in the adducts appears at higher field, shift being of the order of 0.25 ppm.

This is due to coordination through CO oxygen, which enhances the polarity of C – H bond resulting in greater concentration of electronic charges around the H atom.

(ii) The signals due to dimethylamino/amino protons, of the free ligands remain unaltered in the complexes, thereby providing indirect evidence for coordination through carbonyl oxygen.

(iii) Observed $^2J(^{119}Sn\text{-}^1H)$ values in the range 72-80 Hz provide evidence for pentaccordinated structures[8].

(iv) In the complex $Me_2SnCl_2.O(H)CC_6H_4NMe_2$-*p*, the $^1J(^{119}Sn\text{-}^{13}C)$ value of 597.72 Hz and $^1J(^{117}Sn - ^{13}C)$ value of 610.75 Hz†, confirm that the tin atom has pentacoordinate environment[9].

(v) The ^{119}Sn chemical shift value (+26.8 ppm) observed for the complex $Me_2SnCl_2 \cdot O(H)CC_6H_4$-$NMe_2$-*p* is in excellent agreement with that (δ, + 25.4 ppm) of $Me_3SnCl.NC_5H_5$ which has been shown to be pentacoordinated in a trigonal bipyramidal geometry[10].

The ^{119}Sn Mössbauer parameters (Table 2) obtained for these adducts reveal the following salient features:

(i) The lower isomer shift values for these complexes (1.24-1.48 mm/s) as compared to those reported for Me_2SnCl_2 (1.60 mm/s) and Ph_2SnCl_2(1.5 mm/s) are suggestive of the pentacoordinated geometry[11].

(ii) the higher quadrupole splitting values[12] (ranging between 2.74 and 3.86 mm/s)[13] indicate that the charge distribution around the tin nuclei is highly assymetric and the geometries are considerably distorted.

(iii) Further, the coordination number of the Mössbauer nuclei is also related to the ratio (ρ) of quadrupole splitting (ΔE) and isomer shift (δ). The observed ρ-values which range between 2.00 and 2.60, for the presently studies complexes, reflect a higher (may be pentacoordinated)[14 – 17] coordination number than the four coordination state at the tin atom, as concluded from other physicochemical studies.

On the basis of all the above findings these complexes may be assumed to possess five coordination around tin atom having a distorted trigonal bipyramidal geometry. These conclusions receive further, support from a recent X-ray diffraction authentication[18] of one of the derivatives, i.e. $Ph_2SnCl_2.OCHC_6H_4NMe_2$-*p*.

Acknowledgement

The authors thank the UGC, New Delhi for the award of a senior research fellowship to one of them (ASK). Sincere thanks are due to Prof. C L Khetrapal, Raman Research Institute, Bangalore for ^{13}C NMR and Prof. A G Davies, University College of London, London for the ^{119}Sn NMR and ^{119}Sn Mössbauer spectra.

References

1 Clark H C & Goel R G, *J organomet Chem*, **7** (1967) 263.
2 Tanaka T & Kamitani T, *Inorg Chim Acta*, **2** (1968) 175.
3 Matsubayashi G, Nishii N & Tanaka T, *Bull chem Soc Japan*, **42** (1968) 2369.
4 Cunningham D, Douek I, Frazer M J, Mc Partlin M & Matthews J D, *J Organomet Chem*, **90** (1975) C23.
5 Tzschack A, Weichmann H & Jurkschat K, *J organomet Chem Libry*, **12** (1981) 293.
6 Tzschack A & Jurkschat K, *Comments Inorg Chem*, **3** (1983) 35-50.
7 Saraswat B S, Srivastava G & Mehrotra R C, *J organomet Chem*, **164** (1979) 153; *Inorg Chim Acta*, **36** (1976) 289.
8 Simons P B & Graham W A G, *J organomet Chem*, **8** (1967) 479, and references therein.
9 Domazetis G, Magee R J & James B D, *J inorg nucl Chem*, **41** (1979) 1547.
10 Hunter B K & Reeves L W, *Can J Chem*, **46** (1968) 1399.
11 Parish R V & Platt R H, *J chem Soc (A)* (1969) 2145.
12 Bancroft G M & Platt R H, *Adv Inorg Radiochem*, **15** (1972) 59.
13 Naik D V & Curran C, *J organomet Chem*, **81** (1974) 177.
14 Zuckerman J J, *Adv organomet Chem*, **9** (1970) 21.
15 Lefferts J L, Molloy K C, Zuckerman J J, Haiduc I, Guta G & Ruse D, *Inorg Chem*, **19** (1980) 1662.
16 Lefferts J L, Molloy K C, Zuckerman J J, Haiduc I, Curtui M, Guta G & Ruse D, *Inorg Chem*, **19** (1980) 2861.
17 Mehrotra R C, Srivastava G & Chauhan B P S, *Coord Chem Revs*, **55** (1984) 207.
18 Mahadevan C, Seshasayee M & Kothiwal A S, *Cryst Struct Commun*, **11**(4B) (1982) 1725.

†Due to complexity of the spectra of other derivatives and weak ^{117}Sn and ^{119}Sn signals, the *J* values for all these could not be calculated.

Indian Journal of Chemistry
Vol. 27A, June 1988, pp. 510-513

Synthesis & Characterization of Complexes of Ru(II), Pt(II) & Pd(II) with Substituted Chalcones

T SEETHARAMA RAO, K LAXMA REDDY & P LINGAIAH*
Department of Chemistry, Kakatiya University, Warangal 506 009

Received 24 *February* 1987; *revised* 21 *July* 1987; *accepted* 8 *September* 1987

Complexes of Ru(II), Pd(II) and Pt(II) with 3-(2-furyl)-1-(2-hydroxyphenyl)-2-propen-1-one (FHPO), 3-(2-furyl)-1-(2-hydroxy-5-methylphenyl)-2-propen-1-one (FHMPO), 3-(2-thienyl)-1-(2-hydroxyphenyl)-2-propen-1-one (THPO), 3-(2-pyridyl)-1-(2-hydroxyphenyl)-2-propen-1-one (PHPO), 3-(1-naphthyl)-1-(2-hydroxyphenyl)-2-propen-1-one (NHPO) and 3-(3,4-dimethoxyphenyl)-1-(2-hydroxyphenyl)-2-propen-1-one (DMPHPO) have been synthesized and characterized by analytical, magnetic susceptibility, infrared, electronic and ESR data. Analytical data indicate a 1:2 (metal : ligand) stoichiometry. The IR spectral data of the metal complexes indicate that FHPO, FHMPO, THPO and PHPO act as mononegative tridentate towards Ru(II) and bidentate towards Pd(II) and Pt(II) metal ions, whereas NHPO and DMPHPO act as mononegative towards all the metal ions. The electronic spectral data susggest that all the Ru(II) complexes are octahedral whereas those of Pd(II) and Pt(II) are square planar.

Chalcones derived from *o*-hydroxyacetophenone and 2-furfural, thiophene-2-aldehyde, pyridine-2-aldehyde, naphthalene-1-aldehyde and veratraldehyde possess three coordinating sites for coordination to the metal ions, and therefore, these may act as monodentately, bidentately or tridentately with the different metal ions. In continuation of earlier publication[1], we report herein the synthesis and characterization of Ru(II), Pd(II) and Pt(II) complexes of these chalcones.

Materials and Methods

o-Hydroxyacetophenone, 2-furfural, thiophene-2-aldehyde, pyridine-2-aldehyde, naphthalene-1-aldehyde and veratraldehyde were Aldrich or BDH reagents. All the solvents used were of AR grade. The ligands, viz. 3-(2-furyl)-1-(2-hydroxyphenyl)-2-propen-1-one (FHPO), 3-(2-furyl)-1-(2-hydroxy-5-methylphenyl)-2-propen-1-one (FHMPO), 3-(2-thienyl)-1-(2-hydroxyphenyl)-2-propen-1-one (THPO), 3-(2-pyridyl)-1-(2-hydroxyphenyl)-2-propen-1-one (PHPO), 3-(1-naphthyl)-1-(2-hydroxyphenyl)-2-propen-1-one (NHPO) and 3-(3,4-dimethoxyphenyl)-1-(2-hydroxyphenyl)-2-propen-1-one (DMPHPO) were prepared as reported in literature[2,3] and their purities checked by TLC and melting point determinations. Ruthenium(III) chloride, platinum(II) chloride and palladium(II) chloride (all Johnson Mathew products) were used as such. The complex $RuCl_2(DMSO)_4$ was prepared by the published method[4].

General procedure for the preparation of Ru(II) complexes

The complex $RuCl_2(DMSO)_4$ (1 mol, 0.2 g) was suspended in toluene (30 ml) and refluxed for 1 hr with about four molar proportion of the appropriate ligand in methanol (10 ml). During the period of refluxing the suspension dissolved resulting in a clear solution, which was evaporated under reduced pressure to remove excess of solvent. The residue was treated with diethyl ether when the solid complex precipitated out. This was filtered off, washed several times with diethyl ether and dried *in vacuo* over fused calcium chloride.

General procedure for the preparation of Pt(II) and Pd(II) complexes

Platinum(II) and palladium(II) complexes were prepared by mixing 0.05 *N* HCl solution of metal chloride (0.056 mol) with methanolic solution of the ligands (0.112 mol) and heating the mixture on a hot water-bath for 30 min. The crystalline complexes formed were filtered under suction, washed with hot water followed by methanol and dried *in vacuo* over fused calcium chloride.

Results and Discussion

All the complexes are stable at room temperature, non-hygroscopic, insoluble in water and common organic solvents, but soluble slightly in acetone and freely in DMF and DMSO.

The analytical data presented in Table 1 indicate that the complexes have 1:2 (metal : ligand) stoichiometry. The molar conductances of 1×10^{-3} *M* solutions of the complexes in DMF are in the range of 10-20 $Ohm^{-1}\ cm^2\ mol^{-1}$, indicating their non-ionic nature[5].

The complex, $RuCl_2(DMSO)_4$ is an excellent precursor for the synthesis of many new ruthenium(II)

Table 1—Analytical and Electronic Spectral Data of Complexes of Ru(II), Pt(II) and Pd(II)

Compound	Found (Calc.) %			Electronic spectral bands (cm^{-1})
	C	H	S/N	
FHPO	72.56 (72.90)	4.82 (4.67)	—	—
$[Ru(FHPO)_2]$	59.22 (59.12)	3.68 (3.42)	—	19250, 23900
$[Pd(FHPO)_2]$	58.62 (58.57)	3.42 (3.38)	—	15600, 24600
$[Pt(FHPO)_2]$	50.42 (50.23)	2.92 (2.90)	—	20000, 23950
FHMPO	73.42 (73.68)	5.34 (5.26)	—	—
$[Ru(FHMPO)_2]$	60.42 (60.53)	3.86 (3.96)	—	19000, 24100
$[Pd(FHMPO)_2]$	59.91 (59.93)	3.89 (3.92)	—	15800, 25000
$[Pt(FHMPO)_2]$	51.86 (51.77)	3.42 (3.39)	—	19900, 24000
THPO	67.56 (67.83)	4.52 (4.35)	14.22 (13.91)	—
$[Ru(THPO)_2]$	55.86 (55.80)	3.26 (3.22)	5.86 (5.72)	18900, 24000
$[Pd)THPO)_2]$	56.12 (55.25)	3.76 (3.19)	5.92 (5.67)	15900, 24650
$[Pt(THPO)_2]$	47.92 (47.71)	2.76 (2.82)	4.82 (4.90)	20000, 24250
PHPO	73.26 (73.56)	4.92 (4.72)	6.82 (6.60)	—
$[Ru(PHPO)_2]$	60.26 (59.65)	3.56 (3.44)	5.26 (5.35)	19500, 33000
$[Pd(PHPO)_2]$	59.82 (59.05)	3.56 (3.41)	5.42 (5.30)	15500, 20100
$[Pt(PHPO)_2]$	50.66 (50.56)	2.56 (2.92)	4.72 (4.54)	19500, 23200
NHPO	83.92 (83.21)	5.24 (5,11)	—	—
$[Ru(NHPO)_2DMSO)_2]$	62.82 (62.76)	4.92 (4.73)	8.12 (7.97)	19700, 33300
$[Pd(NHPO)_2]$	69.12 (69.90)	4.12 (3.99)	—	15500, 20250
$[Pt(NHPO)_2]$	61.66 (61.53)	3.62 (3.51)	—	19000, 24000
DMPHPO	72.26 (71.83)	5.12 (5.63)	—	—
$[Ru(DMPHPO)_2DMSO)_2]$	55.62 (55.40)	5.56 (5.10)	7.92 (7.78)	19000, 34000
$[Pd(DMPHPO)_2]$	60.72 (60.68)	4.52 (4.46)	—	15000, 35500
$[Pt(DMPHPO)_2]$	53.96 (53.61)	4.26 (4.94)	—	19100, 24000

complexes (Table 1) and the reactions involving this complex are mainly of the displacement type[6,7]. The reaction of this complex with substituted chalcones at reflux temperature in toluene was rapid and gave good yields of the complexes. Depending on the nature of the chelate this complex undergoes a variety of reactions.

Infrared spectra

The free ligands, FHPO, FHMPO, THPO, PHPO, NHPO and DMPHPO do not exhibit νOH in their IR spectra in KBr or CCl_4 solution, probably due to strong intramolecular H-bonding with oxygen of carbonyl group[8-10]; however, δOH modes appear at 1350, 1360, 1350, 1350, 1370 and 1370 cm^{-1} re-

spectively. The disappearance of these bands in the spectra of the corresponding metal complexes indicates coordination of metal ions via deprotonation of phenolic OH of the ligands.

In the IR spectra of all the ligands, the $\nu C=O$ modes appear as an intense band around 1630 ± 10 cm^{-1} (ref. 12). This band is shifted to lower wavenumbers ($\Delta\nu = 50$ cm^{-1}) in the spectra of the complexes indicating coordination through oxygen of C=O group[13]. The medium intensity band appearing around 1560 ± 10 cm^{-1} in the ligands and the complexes can be assigned to the aromatic $\nu(C=C)$ vibrations, indicating non-participation of π-electron cloud in the M–L bond formation[13].

The O–O–O donor ligands FHPO and FHMPO contain furan ring, O–O–S donor ligand THPO contains thiophene ring and O–O–N donor ligands contain pyridine ring at 3-position. Strong bands at 1280 cm^{-1} in FHPO and FHMPO may be assigned to $\nu(C-O)$ of furan ring[14]; at 1100 cm^{-1} in THPO to $\nu(C-S)$ of thiophene ring[15]; and at 1600 cm^{-1} in PHPO to $\nu(C-N)$ of pyridine ring[16]. All these bands are shifted to lower wavenumbers in the spectra of Ru(II) complexes indicating coordination of oxygen of furan ring, sulphur of thiophene ring and nitrogen of pyridine ring to metal ions. However, all these bands do not undergo any shift in the spectra of Pd(II) and Pt(II) complexes indicating non-involvement of these atoms in coordination.

The ligand DMPHPO contains two methoxy groups in the phenyl ring causing a medium intensity band at 1245 cm^{-1} in its IR spectrum due to $\nu(C-O)$[17]. This band also appears at 1245 cm^{-1} in the IR spectra of complexes of the ligand. This band does not undergo any change.

The absence of DMSO in Ru(II) complexes of FHPO, FHMPO, THPO and PHPO was characterised by the absence of $\nu S=O$ mode of $RuCl_2(DMSO)_4$ in the region 1050-1100 cm^{-1} in the complexes[18]. The $\nu S-O$ modes in the complexes of $RuCl_2(DMSO)_4$ with NHPO and DMPHPO, appear at 1100 cm^{-1} indicating the presence of DMSO groups.

Thus it is clear from the IR data that the ligands FHPO, FHMPO, THPO and PHPO act as uninegative tridentate towards Ru(II), forming minimum possible six and seven-membered rings. However, these ligands also act as uninegative bidentate towards Pt(II) and Pd(II) forming minimum possible six-membered rings. The ligands NHPO and DMPHPO act as mononegative bidentate towards all the metal ions forming six-membered ring.

The participation of oxygen, sulphur and nitrogen is further supported by the appearance of bands at

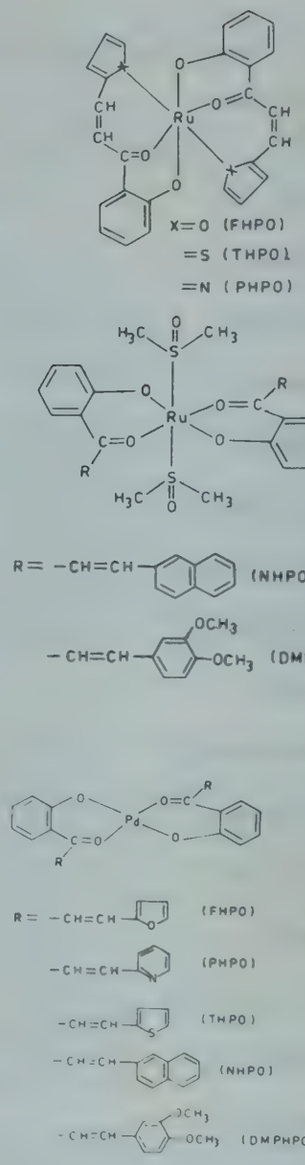

450, 350 and 500 cm^{-1} due to $\nu(M-O)$, $\nu(M-S)$ and $\nu(M-N)$ respectively[19,20].

Electronic, ESR and magnetic data

All the ligands exhibit strong bands around 36000 and 30000 cm^{-1} assignable to $\pi^* \leftarrow \pi$ and $\pi^* \leftarrow n$ transitions, respectively. The two-spin allowed $d-d$ transitions in octahedral complexes are observed around 19000 and 24000 cm^{-1} corresponding to the $^1T_{1g} \leftarrow {}^1A_{1g}$ and $^1T_{2g} \leftarrow {}^1A_{1g}$ transitions, respectively[21]. Absence of splitting of lower energy band (19000 cm^{-1}) in the electronic spectra of Ru(II) complexes, indicates that there is no tetragonal distortion. Electronic spectra of Pd(II) complexes exhibit two bands at 15500 and 25000 cm^{-1} which may be assigned to $^1B_{1g} \leftarrow {}^1A_{1g}$ and $^1E_g \leftarrow {}^1A_{1g}$ transitions, respectively. These are characteristic of square planar geometry[22]. Platinum(II) complexes also exhibit two bands at 21000 and 24000 cm^{-1} characteristic of square planar geometry[23].

The complexes of Ru(II) are found to be diamagnetic, indicating that Ru(II) in the complexes is a low

spin d^6-system. In general, all the octahedral complexes of Ru(II) known till now, are diamagnetic[21] and therefore, an octahedral geometry has been assigned to the complexes. The diamagnetic behaviour of Pd(II) and Pt(II) both belonging to d^8-system indicates the expected preferred square-planar geometry with $^1A_{1g}$ ground state around the metal ions. The diamagnetic behaviour of these complexes is also confirmed by the absence of a peak in their ESR spectra. The structures of Ru(II) and Pd(II) complexes are given in Structures 1 and 2.

References

1 Seetha Rama Rao T, Laxma Reddy K, Swamy S J & Lingaiah P, *Indian J Chem*, **24A** (1985) 942.

2 Ashanina T, *Bull chem Soc Japan*, **9** (1944) 133.

3 Geissman T A & Clinton R O, *J Am chem Soc*, **68** (1946) 697.

4 Evans I P, Spencer A & Wilkinson G, *J chem Soc, Dalton Trans*, (1973) 204.

5 Geary M J, *Coord chem Rev*, 7 (1971) 81.

6 Laxma Reddy K, Veera Reddy K & Lingaiah P, *Polyhedron*, **5(10)** (1986) 1519.

7 Ravinder V, Veera Reddy K & Lingaiah P, *Inorg chim Acta*, **87** (1984) 35.

8 Ingraham, Corsel Bailey & Stilt, *J Am chem Soc*, **71** (1952) 2297.

9 Rasmussen, Tunncliff & Brattain, *J Am chem Soc*, **21** (1949) 1068.

10 Koji Nakanshi, *Infrared absorption spectroscopy* (Practical Nankolo Company, London) (1964) 167.

11 Ramaswamy K K, Jose C I & Sen D N, *Indian J Chem*, **5** (1967) 156.

12 Dhar D N & Gupta V P, *Indian J Chem*, **9** (1971) 818.

13 Laxma Reddy K, Sri Hari S & Lingaiah P, *Indian J Chem*, **24A** (1985) 318.

14 Mahmoud M R, Hamide R & Haty M T, *Indian J Chem*, **19A** (1980) 345.

15 Centreras G & Cortes H, *J inorg nucl Chem*, **33** (1971) 1337.

16 Laxma Reddy K, Sri Hari S & Lingaiah P, *Indian J Chem*, **23A** (1984) 172.

17 Daniel J Pasto & Carl R Johnson, *Organic structure determination* (Prentice Hall Inc.) (1969) 172.

18 Reynolds M L, *Progr Inorg Chem*, **12** (1970) 1.

19 Laxma Reddy K, Sri Hari S & Lingaiah P, *Indian J Chem*, **24A** (1984) 318.

20 Shaw R N & Shaw J R, *Indian J Chem*, **22A** (1982) 372.

21 Pretic Tosi G & Zannini P, *J inorg nucl Chem*, (1979) 485.

22 Living Stones E, *The chemistry of ruthenium, rhodium, palladium, osmanium, iridium and platinum*, Vol. 25 (Pergmann Press Monograph) 1973, 1286.

23 Singh P P, Srivastava A K & Khan Sushil A, *Aust J Chem*, **28** (1975) 267.

Indian Journal of Chemistry
Vol. 27A, June 1988, pp. 514-518

Metal Complexes of Some Peptide Derivatives: Part V—Complex Formation of Copper(II) with N-Salicyloyl Derivatives of Some Amino Acids

G N MUKHERJEE* & (Miss) S SARKAR

Department of Chemistry, Calcutta University, University College of Science, 92 Acharya Prafulla Chandra Road, Calcutta 700 009

Received 30 *March* 1987; *revised* 27 *July* 1987; *accepted* 24 *August* 1987

Complex formation of Cu(II) with N-salicyloyl derivatives of some amino acids has been studied by equilibrium method at 25, 30, 35 and 45°C in 50% v/v aq. ethanol and at $\mu = 0.2$ *M* ($NaNO_3$). Thermodynamic parameters associated with complexation equilibria have been correlated with the structure and bonding of the complexes.

Interactions of transition metal ions with amino acids and small peptide derivatives offer simple models for metal-protein interactions and enzymes[1-5]. In neutral solution protonation and metallation with the amide ($-CONH-$) bond occur at the amide carbonyl oxygen atom. Metallation at the amide nitrogen occurs only through substitution of the amide proton provided there is a possibility of chelation of the metal ions[2,5,6]. With a view to understanding the effect of an adjacent phenolic OH group on the coordinating properties of the amide bond we had earlier studied the complexation equilibria of Cu(II) with N-salicyloylglycine (SG)[7], and N-salicyloyl *dl*-α-alanine (SA)[8] at 30°C in 50% v/v aq. ethanol medium at a constant ionic strength ($\mu = 0.2$ *M* $NaNO_3$). Complexation equilibria of Cu(II) with N-salicyloyl-β-alanine (SB) and N-salicyloyl-*dl*-methionine (SM), in the same solvent medium have been studied. Complexation equilibria of the Cu(II)-SG and Cu(II)-SA system have also been studied at 25°, 35° and 45°C; the data for these systems at 30°C were obtained from literature[7,8]. Some solid complexes of Cu(II) have also been isolated and characterised on the basis of IR and UV-VIS spectral data.

Materials and Methods

All the ligands were prepared as described earlier[7,8] and their purities were checked by elemental analyses, m.ps, UV and IR spectra. All the other reagents used were of AR quality.

Bright green crystalline Cu(II) complexes, $Cu(HL\text{-}H).2H_2O$, (where H_2L = SB and SM) were obtained by treating the monosodium salts (NaHL) of the respective ligands with Cu(II) sulphate in aqueous solution as described earlier[7,8]. These complexes on acetylation furnished the monoacetyl derivatives, $Cu(CH_3COL\text{-}H).2H_2O$.

The procedure for the *p*H-metric study was the same as described earlier[7,8]. Preliminary values of the equilibrium constants were evaluated by the procedure of Irving and Rossotti[9] and the values were finally refined employing the computer programme[10] SCOGS.

Results and Discussion

Characterisation of solid complexes $Cu(HL\text{-}H).2H_2O$ *and* $Cu(CH_3COL\text{-}H).2H_2O$ (H_2L = *SB, SM*)

The IR spectra of ligands in KBr exhibited νCOOH modes in the region 1740-1720 cm^{-1}. These modes were absent in the spectra of $Cu(HL\text{-}H).2H_2O$ or $Cu(CH_3COL\text{-}H).2H_2O$. However, the spectra of the complexes displayed two new bands at 1540-1530 and 1370-1330 cm^{-1} assigned to $\nu_{as}COO^-$ and ν_sCOO^- respectively, suggesting $Cu^{2+} - {}^-OOC$ bonding in the complexes[11]. The amide I and II bands in these complexes were observed at 1600-1590 and 1450-1440 cm^{-1} in comparison to those at 1660-1600 (br), 1550-1540 and 1300-1280 cm^{-1} respectively due to amide I, II and III bands for the free ligands. Such shifts of the amide bands indicated bonding of deprotonated amide nitrogen[3,4,12] to Cu(II) in these complexes. Both the series of complexes exhibited ν(O-H) mode in the region 3400-3300 cm^{-1} which, however, could not be considered as a diagnostic for the free phenolic OH group, as similar bands were expected to appear due to H_2O molecules. Formation of $Cu(CH_3COL\text{-}H).2H_2O$ through acetylation of $Cu(HL\text{-}H).2H_2O$ by the procedure usually applied for acetylation of phenols indicated the presence of free phenolic OH group in the parent $Cu(HL\text{-}H).2H_2O$ complexes. Analytical data of $Cu(CH_3COL\text{-}H).2H_2O$ also supported substitution

Table 1—Proton-Ligand Constants at Different Temperatures and Associated Thermodynamic Parameters at 25°C

[Solvent = 50% (v/v) aq. ethanol; $\mu = 0.2\ M(NaNO_3)$]

Ligand	Constant[c]	25°	30°	35°	45 ± 0.1°C	ΔG^a	ΔH^a	ΔS^b
SG	$pK^H_{H_2L}$	4.00	3.98[7]	3.96	3.91	−23.0	−8.4	49
	pK^H_{HL}	8.86	8.83[7]	8.79	8.74	−50.8	−12.8	128
SA	$pK^H_{H_2L}$	4.22	4.18[8]	4.15	4.10	−24.2	−9.6	49
	pK^H_{HL}	9.36	9.30[8]	9.25	9.16	−53.7	−12.8	137
SB	$pK^H_{H_2L}$	4.82	4.80	4.77	4.73	−27.6	−8.5	64
	pK^H_{HL}	9.02	8.98	8.96	8.90	−51.7	−13.0	130
SM	$pK^H_{H_2L}$	4.05	4.04	4.02	3.98	−23.2	−8.7	49
	pK^H_{HL}	8.78	8.75	8.72	8.66	−50.4	−19.2	105

(*a*): $kJmol^{-1}$ (*b*): $JK^{-1}mol^{-1}$; (*c*): error limits for constants, ± 0.05 in log scale; for ΔG, ΔH, ± 0.5 $kJmol^{-1}$ and for ΔS, ± 3 $JK^{-1}mol^{-1}$.

of one hydrogen atom in $Cu(HL\text{-}H).2H_2O$, preferably phenolic proton by an acetyl group. This was supported by the fact that while $Cu(HL\text{-}H).2H_2O$ gave intense violet colour with neutralised $FeCl_3$ solution, the corresponding acetyl derivatives did not give any colour with this reagent.

Electronic spectra of both $Cu(HL\text{-}H).2H_2O$ and $Cu(CH_3COL\text{-}H).2H_2O$ were almost superimposable and maximum absorption in the region 610-600 nm were indicative of coordination of Cu(II) by deprotonated amide nitrogen and carboxylate oxygen atoms in a square planar $Cu(N,O)(H_2O)_2$ geometry without having any apical coordination[5,13] as might be provided by the phenolic oxygen atom. As the ligand ion, $(CH_3COL\text{-}H)^{2-}$ could provide only bidentate (N,O) chelation via the deprotonated amide nitrogen and the carboxylate oxygen atoms, it may, therefore, be inferred that in $Cu(HL\text{-}H).2H_2O$ the ligand $(HL\text{-}H)^{2-}$ is (N,O) bidentate leaving the phenolic OH intact. The possibilty of coordination of SCH_3 moiety of SM ligand was also ruled out because the electronic spectra of Cu(II) complexes of SM were superimposable with those of SG, SA and SB. Room temperature magnetic moment values of all the Cu(II) complexes were in the range 1.76-1.84 B.M. as expected for one unpaired electron and indicated the absence of any Cu...Cu interaction in these complexes.

Proton-ligand and Cu(II)-ligand equilibria

The ligands SB and SM like SG and SA could also be titrated as biprotic acids (H_2L), deprotonation occurring from −COOH and phenolic −OH groups in successive steps giving two well separated buffer regions in the *p*H ranges 2.5-6.5 and 8-12. That the phenolic OH and not the amide (−CONH−) group was deprotonated in the second step, was confirmed by the monoprotic nature of benzoylglycine ($C_6H_5CONHCH_2COOH$), which gave a single buffer region (*p*H 2.5-6.5) in the entire *p*H range (2-12) studied. Increase of K^H_{COOH} and K^H_{OH} values (Table 1) with increase in temperature indicated that COOH and OH are involved in H-bonding in the ligands. The H-bonding breaks down at higher temperature thus accounting for enhanced acidity. Positive entropy changes (ΔS) associated with proton-ligand equilibria indicate increased flexibility of the deprotonated forms of the ligands due to the absence of H-bonding. Enthalpy changes (ΔH) accompanying deprotonation of phenolic OH are found to be roughly 1.5 times higher than the corresponding values for the deprotonation of −COOH, probably due to the labilizing influence of C=O moiety of −COOH function on O−H bond. Higher acidities (K^H_{OH}) of phenolic OH of the ligands over that of salicylic acid may be due to stabilization of the L^{2-} anion by H-bonding involving amide proton.

Buffer regions (*p*H 2.5-6.5) are observed[7] at lower *p*H values in the presence of Cu(II) while the regions *p*H 8-12 do not show any change. Complexation with Cu(II), in solution, therefore, occurs only via deprotonation of −COOH. Four protons per Cu(II) are released in the *p*H range 2.5-6.5, where hydrolysis of the Cu^{2+} (*aq.*) ion does not occur. Mole ratio study of Cu(II)-H_2L mixtures at *p*H values corresponding to $\bar{n}\dagger \geqslant 4$, by spectrophotometric method

†$\bar{n}$: Average number of protons released due to the reaction of Cu(II) with the ligands, H_2L.

Table 2—Formation Constants[a] of Cu(II) Complexes at Different Temperatures

[Solvent = 50% (v/v) aq. ethanol; $\mu = 0.2\ M(NaNO_3)$]

System	Temp. (±0.1°C)	$pK^{2H}_{Cu+H_2L}$	$pK^{2H}_{Cu(HL\text{-}H)+H_2L}$	$pK^{H}_{Cu(HL\text{-}H)_2}$	$pK^{H}_{Cu(L\text{-}H)(HL\text{-}H)}$
Cu(II)+SG	25	6.15	6.40	8.54	10.02
	30 (ref. 7)	6.06	6.32	8.43	9.98
	35	5.97	6.24	8.32	9.94
	45	5.81	6.10	8.14	9.82
Cu(II)+SA	25	6.52	6.90	8.77	10.53
	30 (ref. 8)	6.42	6.79	8.66	10.49
	35	6.33	6.68	8.55	10.45
	45	6.18	6.51	8.39	10.34
Cu(II)+SB	25	7.96	9.14	*b*	*b*
	30	7.87	9.03	*b*	*b*
	35	7.80	8.92	*b*	*b*
	45	7.66	8.73	*b*	*b*
Cu(II)+SM	25	6.39	6.59	8.40	10.35
	30	6.34	6.54	8.35	10.32
	35	6.29	6.49	8.31	10.29
	45	6.18	6.38	8.23	10.23

(*a*) Error limits for constants, ±0.05 in log scale; (*b*) constants could not be determined due to precipitation.

Table 3—Thermodynamic Parameters[a] Associated with Formation of Cu(II) Complexes at 25 ± 0.1°C

[Solvent = 50% (v/v) aq. ethanol, $\mu = 0.2\ M(NaNO_3)$]

Parameter	Cu(II)-SG	Cu(II)-SA	Cu(II)-SB	Cu(II)-SM
		$Cu^{2+} + L^{2-} \rightleftharpoons Cu(HL\text{-}H)$		
$\log K^{Cu}_{Cu(HL\text{-}H)}$	6.71	7.05	5.88	6.44
ΔG (kJmol^{-1})	−38.5	−37.0	−33.7	−36.9
ΔH (kJmol^{-1})	12.8	3.0	9.6	2.0
ΔS (JK^{-1}mol^{-1})	172	146	145	131
		$Cu(HL\text{-}H) + L^{2-} \rightleftharpoons Cu(HL\text{-}H)_2^{2-}$		
$\log K^{Cu(HL\text{-}H)}_{Cu(HL\text{-}H)_2}$	6.46	6.67	4.70	6.24
ΔG (kJmol^{-1})	−37.0	−40.4	−27.0	−35.8
ΔH (kJmol^{-1})	8.0	8.8	9.5	2.0
ΔS (JK^{-1}mol^{-1})	151	158	123	127
		$Cu(HL\text{-}H)_2^{2-} \rightleftharpoons Cu(L\text{-}H)(HL\text{-}H)^{3-} + H^+$		
$pK^{H}_{Cu(HL\text{-}H)_2}$	8.54	8.77	*b*	8.40
ΔG (kJmol^{-1})	−49.0	−50.3	*b*	−48.2
ΔH (kJmol^{-1})	−38.5	−36.6	*b*	−16.5
ΔS (JK^{-1}mol^{-1})	35(40)	46(49)	*b*	106(49)
		$Cu(L\text{-}H)(HL\text{-}H)^{3-} \rightleftharpoons Cu(L\text{-}H)_2^{4-} + H^+$		
$pK^{H}_{Cu(L\text{-}H)(HL\text{-}H)}$	10.02	10.53	*b*	10.35
ΔG (kJmol^{-1})	−57.4	−60.4	*b*	−59.3
ΔH (kJmol^{-1})	−19.2	−18.3	*b*	−11.5
ΔS (JK^{-1}mol^{-1})	128(128)	141(137)	*b*	160(105)

(*a*) Error limits: for the constants ±0.05 in the log scale; for ΔG and ΔH, ±0.5 kJmol^{-1}; and for ΔS, ±3 JK^{-1}mol^{-1}. (*b*) Could not be determined due to precipitation. Values in the parentheses are for the deprotonation equilibria of the free ligand.

at 610-600 nm established the 1:2 (Cu:ligand)stoichiometry. Therefore, hydroxo complexes and complexes higher than 1:2 were omitted in calculating the Cu(II)-ligand constants. Formation of Cu(II)-$2H_2L$ complexes can, therefore, be accounted for by asuming the substitution of −COOH and amide (−CONH−) protons of the ligands by Cu(II) (Eqs 1 and 2):

$$Cu^{2+} + H_2L \rightleftharpoons Cu(HL-H) + 2H^+$$

$$K^{2H}_{Cu+H_2L} = ([H]^2\,[Cu(HL-H)])/([Cu]\,[H_2L]) \quad \ldots\ldots(1)$$

$$Cu(HL-H) + H_2L \rightleftharpoons Cu(HL-H)_2^{2-} + 2H^+$$

$$K^{2H}_{Cu(HL-H)+H_2L} = ([H]^2\,[Cu(HL-H)_2])/([Cu(HL-H)]\,[H_2L]) \quad \ldots\ldots(2)$$

The higher *p*H buffer region (*p*H 8-12) arose because of the deprotonation of phenolic OH of the free ligand, HL^- ions, together with the deprotonation of uncoordinated phenolic OH in $Cu(HL\text{-}H)_2^{2-}$ complexes (Eqs 3 and 4):

$$Cu(HL-H)_2^{2-} \rightleftharpoons Cu(L-H)(HL-H)^{3-} + H^+$$

$$K^{H}_{Cu(HL-H)_2} = ([H]\,[Cu(L-H)(HL-H)])/[Cu(HL-H)_2] \quad \ldots\ldots(3)$$

$$Cu(L-H)(HL-H)^{3-} \rightleftharpoons Cu(L-H)_2^{4-} + H^+$$

$$K^{H}_{Cu(L-H)(HL-H)} = ([H]\,[Cu(L-H)_2])/[Cu(L-H)(HL-H)] \quad \ldots\ldots(4)$$

Charges were dropped from these expressions for clarity. The $(HL\text{-}H)^{2-}$ ions in the complexes stand for the ligand species which have lost their carboxylic ($-COOH$) and amide ($-CONH-$) protons while still retaining the phenolic OH protons and the $(L\text{-}H)^{3-}$ ions stand for the fully deprotonated ligand species[5,13]. Equilibria (3) and (4) could not be followed for Cu(II)-SB system due to precipitation at *p*H ≥ 9.5. Equilibrium constants for equilibria (1-4) are presented in Table 2.

Stability constants $K^{Cu}_{Cu(HL-H)}$ and $K^{Cu(HL-H)}_{Cu(HL-H)_2}$ (Table 3) were calculated with the help of the relations (5) and (6) respectively.

$$\log K^{Cu}_{Cu(HL-H)} = \log K^{2H}_{Cu+H_2L} + pK^{H}_{COOH} + pK^{H}_{OH} \quad \ldots\ldots(5)$$

$$\log K^{Cu(HL-H)}_{Cu(HL-H)_2} = \log K^{2H}_{Cu(HL-H)+H_2L} + pK^{H}_{COOH} + pK^{H}_{OH} \quad \ldots\ldots(6)$$

Formation of Cu(HL-H) and $Cu(HL\text{-}H)_2^{2-}$ complexes through metal-promoted deprotonation of the amide bond was accompanied by positive enthalpy change (Table 3). Positive entropy changes accompanying the formation of Cu(HL-H) and $Cu(HL\text{-}H)_2^{2-}$ complexes suggested their chelated structures. The $\bar{n}$(*p*H) plot corresponding to the two series of equilibria, (1), (2) and(3), (4) showed a sharp increase from $\bar{n}=0$ to $\bar{n}=4$ (*p*H 2.5-6.5) and a flat rise in the region from $\bar{n}=4$ to $\bar{n}=6$ (*p*H 8-12). Absorption maxima λ_{max} of 1:5 Cu(II):H_2L mixtures at *p*H values corresponding to $\bar{n}=0$, 2, 4 and 6 were 730, 650, 620-610 and 620-610 nm respectively for all the systems. This blue shift of 90 nm in the absorption maxima indicated a change from an octahedral $Cu(O)_6$ system in Cu^{2+} (*aq.*) ion to a square planar $Cu(N,O)_2$ system in $Cu(HL\text{-}H)_2^{2-}$ complexes. The constancy of λ_{max} in going from $\bar{n}=4$ to $\bar{n}=6$ indicates the retention of square planar $Cu(N,O)_2$ geometry even in the fully deprotonated $Cu(L\text{-}H)_2^{4-}$ complexes. The observed λ_{max} values 620-610 nm for the $Cu(HL\text{-}H)_2^{2-}$ and $Cu(L\text{-}H)_2^{4-}$ complexes are quite close within experimental errors, to the calculated values[5] (605 nm) for square planar $Cu(N,O)_2$ systems, where Cu(II) is coordinated to two deprotonated amide nitrogen and two carboxylate oxygen atoms. This observation further rules out the possibility of apical coordination of Cu(II) by phenolic oxygen in the $Cu(L\text{-}H)(HL\text{-}H)^{3-}$ and $Cu(L\text{-}H)_2^{4-}$ complexes. However, the possibility of chelation *via* hydrogen bonding of the phenolic proton with the amide carbonyl oxygen in the $Cu(HL\text{-}H)_2^{2-}$ complexes cannot be ruled out. Comparable magnitudes of $pK^{H}_{Cu(HL-H)}$ and pK^{H}_{HL} values for all these systems indicate deprotonation equilibria (3) and (4) of $Cu(HL\text{-}H)_2^{2-}$ complexes to be analogous to deprotonation of the phenolic moieties of the free ligands (HL^-) species. With the exception of Cu(II)-SM system, even the entropy changes (ΔS) corresponding to deprotonation of $Cu(HL\text{-}H)_2^{2-}$ complexes (Eqs 3 and 4) are comparable (Tables 1 and 3) with those of the free phenolic OH of the free ligand ion (HL^-). Positive ΔS values for these equilibria are the result of breakdown of H-bonding in uncoordinated phenolic OH with C=O of the amide group.

Comparable magnitudes of formation constants (Tables 2 and 3) and identical λ_{max} values of Cu(II) complexes derived from SG, SA and SB with those derived from SM which has an extra binding site, viz. the SCH_3 moiety, suggest similar type of coordination, viz. (N,O) bidentate chelation by all the four ligands. The SCH_3 moiety of SM was not probably associated to Cu(II) in the complexes. Compratively higher entropy change associated with deprotonation equilibria (3) and (4) of Cu(II)-SM system may be due to release of some sort of a hydrophopic strain involving $-CH_2CH_2SCH_3$ moiety. Stabilities of Cu(II) complexes follow the ligand order: SA > SG > SM > SB. The lowest stabilities of Cu(II)-SB complexes are probably the result of angle strain in the six-membered chelate rings without having a double bond[14] as against five-membered chelate rings in the complexes derived from the other three ligands. Electron releasing effect of CH_3 group at α-position to amide and COOH moieties in SA ligand provides additional basicity to the donor atoms and consequently Cu(II) complexes with SA ligands are more stable than those with SG. Similar trends in stability have also been observed for Cu(II)

complexes with glycylglycinate[15] ad glycyl-*dl*-α-alaninate[16]. The bidentate (N,O) chelated square planar $Cu(HL\text{-}H)_2^{2-}$ complexes are predominant ($\approx 95\%$) in Cu(II) containing species in the region of biological *p*H.

References

1 Dobbie H & Karmack W O, *Biochem J*, **59** (1955) 246.
2 Dutta S P & Rabin B R, *Trans Faraday Soc*, **52** (1956) 1123; *Biochem Soc Symp*, **15** (1958) 21.
3 Kim M K & Martell A E, *J Am chem Soc*, **84** (1963) 3080; *Biochemistry*, **3** (1964) 1169.
4 Nakon R & Angelici R J, *Inorg Chem*, **12** (1973) 1269.
5 Siegel H & Martin R B, *Chem Rev*, **82** (1982) 385.
6 Scheller-Krattiger V, Schellar K H, Sinn E & Martin R B, *Inorg chim Acta*, **60** (1982) 45.
7 Mukherjee G N, Sarkar (Miss) S & Chatterjee S K, *J Indian chem Soc*, **59** (1982) 1117.
8 Mukherjee G N & Sarkar (Miss) S, *Indian J Chem*, **22A** (1983) 539.
9 Irving H M & Rossotti H S, *J chem Soc*, (1954) 2904; (1953) 3397.
10 Sayce I G, *Talanta*, **15** (1968) 1397.
11 Bellamy L J, *The infrared spectra of complex molecules*, Vol 1, 3rd Ed (Chapman & Hall, London), 1975, Pp. 183-202.
12 Kabanos T A & Tangarish J M, *J coord Chem*, **13** (1984) 89.
13 Gamp H, Siegel H & Zuberbuhler A D, *Inorg Chem*, **21** (1982) 1190.
14 Siegel H, *Angew Chem* (Int Edn), **14** (1975) 394.
15 Martin R P, Mosoni L & Sarkar B, *J biol Chem*, **246** (1971) 5944.
16 Brunetti A, Burke E J, Lim M C & Nancollas G H, *J soln Chem*, **1** (1972) 153.

Indian Journal of Chemistry
Vol. 27A, June 1988, pp. 519-522

Coordination Compounds of Organometallic Bases of Group(IV) Elements: Part XI—Reactions of N,N′-(Phenyl/*o*-chlorophenyl/*p*-methylphenyl/benzyl/diethyl)-1,1-di-*n*-propoxy/*n*-butoxy-silanediamines† with Tin(IV) & Titanium(IV) Chlorides at −10°C

SURAJ P NARULA*, NEETA KAPUR, RAVI SHANKAR, ARUN CHODHA & RAJESH MALHOTRA
Department of Chemistry, Panjab University, Chandigarh 160 014

Received 5 *June* 1987; *revised and accepted* 1 *October* 1987

The title reactions in 1:1 molar ratio in petroleum ether (40-60°) afford adducts having rearranged bases with composition $[(RO)_nSi(NHR')_{4-n}.xMCl_4]$ where R = C_3H_7 or *n*-C_4H_9; R′ = $C_6H_5CH_2$, *o*-ClC_6H_4 or *p*-$CH_3C_6H_4$; *n* = 0 or 1; and x = 2 or 3 as evidenced by elemental analyses, IR and PMR spectral data as well as base exchange reactions. Filtrates of these reactions after keeping at room temperature for 48-72 hr, give solid complexes of the type $[(RO)_2Si(NHR')_2.2MCl_4]$ in each case. The reaction with the tertiary amines such as N,N′-diethyl-1,1-di-*n*-propoxy di-*n*-butoxysilanediamine form normal 1:1 adducts $[(n\text{-}C_3H_7O/n\text{-}C_4H_9O)_2\ Si[N(CH_2CH_3)_2]_2.MCl_4$ and no base rearrangement is observed. A tentative mechanism of the disproportionation reactions is proposed.

The conversion of triorganoxy/organo-organoxy-silanamines into organoxy/organo-silanetriamines and even into silanetetramines in the presence of titanium(IV) and tin(IV) chlorides and antimony (III) halides, has been demonstrated by us[1-6]. It has further been shown that the electronic and steric effects of substituents on silicon and nitrogen atoms significantly influence the conversion into silane polyamines[4-7]. For example N-(2-fluorophenyl)-1,1,1-trialkoxy silanamine is converted into N,N′-(2-fluorophenyl)-1,1-dialkoxy silanediamine while N-*n*-butyl/*p*-methylphenyl-1-chloro-1,1-dialkoxy silanamines are converted into N,N′, N″,N‴-(*p*-methylphenyl/*n*-butyl)silanetetramines[6]. However, these studies have so far been confined to secondary silanamines $[(RO)_3SiNHR']$ containing single Si−N bond. With a view to checking the general validity of such reactions, it was thought appropriate to extend these investigations to other Si−N compounds. One such strategy is to attempt these reactions with secondary silanediamines $[(RO)_2Si\text{-}(NHR')_2]$ and tertiary silanediamines $[(RO)_2Si\text{-}(NR'_2)_2]$. The results of these studies are being reported here.

Materials and Methods

All experiments were carried out at −10°C under dry nitrogen atmosphere. The solvents used were dried by conventional methods. Tin(IV) and titanium(IV) chlorides (Reidel, pure) were distilled before use.

Infrared spectra were recorded in nujol on a Perkin-Elmer model 621, double beam grating spectrophotometer having NaCl/KBr optics and PMR spectra in $CDCl_3$ + DMSO-d_6 on a Varian 390, 90 MHz instrument; chemical shifts are in δ-scale downfield from TMS internal reference.

The constant reaction temperature (−10°) of the bath was maintained using "cryo cool" model CC-100 II Neslab, Italy.

The ligands, N,N′-(phenyl/*o*-chlorophenyl/*p*-methylphenyl/benzyl/diethyl)-1,1-di-*n*-propoxy/di-*n*-butoxysilanediamines were prepared by the reaction of corresponding dichlorosilanes with amines in 1:4 molar ratio in dry diethyl ether at 0°C. The filtrates obained after removal of the amine hydrochlorides were fractionally distilled under reduced pressure. All these silanediamines were characterised and their purity checked by IR and PMR spectral data.

Reactions of ligands with tin(IV) and titanium(IV) chlorides

Addition of a solution of tin(IV) or titanium(IV) chloride in petroleum ether to a solution of a silanediamine in the same solvent at −10°C in equimolar ratios resulted in the precipitation of a solid compound in each case. The compounds were filtered in the cold, washed and dried under reduced pressure. The filtrates on standing at room temperature for 48-72 hr afforded another solid in each case which was isolated as above and characterised.

Base exchange reactions

The above complexes (10 mmol) were added to

*Nomenclature in accordance with IUPAC rules

Table 1—Analytical Data of Complexes of N,N′-Organo-1,1-(diorganoxy)silanediamines

Sl No.	Compound	Found (Reqd) (%)			
		Cl	Ti/Sn	Si	N
1.	$(PrO)Si(NHC_6H_5)_3.2TiCl_4$	38.0 (38.22)	12.8 (12.92)	3.4 (3.77)	5.54 (5.65)
2.	$(PrO)Si(NHC_6H_5)_3.2SnCl_4$	32.21 (32.09)	26.70 (26.89)	2.91 (3.16)	4.65 (4.74)
3.	$(BuO)Si(NHC_6H_5)_3.2TiCl_4$	37.41 (37.52)	12.43 (12.68)	3.6 (3.7)	5.35 (5.55)
4.	$(BuO)Si(NHC_6H_5)_3.2SnCl_4$	31.41 (31.59)	26.35 (26.47)	2.99 (3.11)	4.53 (4.67)
5.	$Si(NHC_6H_4CH_3-p)_4.3TiCl_4$	41.75 (41.68)	14.29 (14.09)	2.4 (2.74)	5.38 (5.48)
6.	$Si(NHC_6H_4CH_3-p)_4.3SnCl_4$	34.2 (34.49)	28.4 (28.9)	2.15 (2.27)	4.40 (4.53)
7.	$(PrO)Si(NHC_6H_4Cl-o)_3.2TiCl_4$	33.43 (33.55)	11.2 (11.34)	3.2 (3.31)	4.8 (4.96)
8.	$(PrO)Si(NHC_6H_4Cl-o)_3.2SnCl_4$	28.4 (28.73)	23.79 (24.07)	2.57 (2.83)	4.12 (4.25)
9.	$(BuO)Si(NHC_6H_4Cl-o)_3.2TiCl_4$	32.72 (33.0)	10.9 (11.16)	3.0 (3.25)	4.75 (4.88)
10.	$(BuO)Si(NHC_6H_4Cl-o)_3.2SnCl_4$	28.19 (28.32)	23.59 (23.74)	2.60 (2.79)	4.10 (4.19)
11.	$(PrO)Si(NHCH_2C_6H_5)_3.2TiCl_4$	36.0 (36.18)	12.10 (12.23)	3.45 (3.51)	5.25 (5.35)
12.	$(PrO)Si(NHCH_2C_6H_5)_3.2SnCl_4$	30.57 (30.64)	26.35 (25.67)	2.94 (3.02)	4.44 (4.53)
13.	$(PrO)_2Si[N(C_2H_5)_2]_2.TiCl_4$	29.72 (29.58)	10.14 (10.00)	5.62 (5.83)	5.79 (5.83)
14.	$(BuO)_2Si[N(C_2H_5)_2]_2.TiCl_4$	27.72 (27.95)	9.52 (9.45)	5.39 (5.51)	5.47 (5.51)
15.	$(PrO)_2Si[N(C_2H_5)_2]_2.SnCl_4$	25.57 (25.77)	21.51 (21.60)	4.98 (5.08)	5.01 (5.08)
16.	$(BuO)_2Si[N(C_2H_5)_2]_2.SnCl_4$	24.69 (24.52)	20.42 (20.55)	4.67 (4.84)	4.87 (4.84)

ethylenediamine (25 mmol), molten 2,2′-bipyridyl (25 mmol) or pyridine-d_5 (25 mmol) under dry nitrogen atmosphere and kept at 35-40°C for 5-6 hr. Thereafter dry carbon tetrachloride was added, filtered, and the solids obtained identified by the chemical shifts and proton counts.

Results and Discussion

Analytical data (Table 1) of the adducts conform to the composition $[(RO)Si(NHR')_3.2MCl_4]$ except in the case of the ligands N,N′-*p*-methylphenyl-1,1-di-*n*-propoxy/*n*-butoxysilanediamines and N,N′-diethyl-1,1-di-*n*-propoxy/*n*-butoxysilanediamines. Whereas the former affords adducts of the type $Si(NHC_6H_4CH_3-p)_4.3MCl_4$, the latter forms normal 1:1 adducts and no rearrangement is observed in the ligands. All the adducts are extremely hygroscopic and insoluble in common organic solvents except DMSO.

Infrared spectra

Infrared spectra of adducts $[(RO)_2Si(NR')_2.2MCl_4]$, $[(RO)Si(NHR')_3.2MCl_4]$ and $[Si(NHR')_4.3MCl_4]$ are similar to those already reported[6]. However, the IR spectra of 1:1 adducts $[n\text{-}C_3H_7O/n\text{-}C_4H_9O]_2Si(NCH_2CH_3)_2].MCl_4$ display νCO and νSiO(C) modes at 1080 and 1020-30 cm^{-1} respectively. The νCN (aliphatic) modes at 1290 cm^{-1} in these ligands undergo shift to lower wavenumbers ($\Delta\nu = 15\text{-}20$ cm^{-1}) indicating coordination through nitrogen atom. The bands at 300 and 375 cm^{-1} have been assigned to coordinated νSnCl and νTiCl modes of the Lewis acids used.

PMR spectra

The chemical shift (δ) values along with the number of protons for each group are recorded in Table 2. From a comparison of proton counts of the parent ligand with those of the ligands in the

Table 2—PMR Spectral Data of Complexes of N,N′-(Phenyl/*o*-chlorophenyl/*p*-methylphenyl/benzyl/diethyl)-1,1-diorganoxy-silanediamines with Tin(IV) and Titanium(IV) Chlorides

Complexes*	CH_3	CH_2	CH_2O	CH_2N	NH	C_6H_5/C_6H_4	ring CH_3
1,2	0.85 (t, 3H)	1.2 (m, 2H)	3.6 (t, 2H)	—	4.2 (s, 3H)	7.4 (m, 15H)	—
3,4	0.90 (t, 3H)	1.2 (m,4H)	3.5 (t, 2H)	—	4.1 (s, 3H)	7.45 (m, 15H)	—
7,8	0.85 (t, 3H)	1.15 (m, 2H)	3.5 (t, 2H)	—	4.3 (s, 3H)	7.4 (m, 12H)	—
9,10	0.8 (t, 3H)	1.2 (m, 4H)	3.55 (t, 2H)	—	4.2 (s, 3H)	7.35 (m, 12H)	—
5,6	—	—	—	—	4.35 (s, 4H)	7.5 (m, 16H)	2.25 (s, 12H)
11,12	0.8 (t, 3H)	1.4 (q, 2H)	3.55 (t, 2H)	4.05 (s, 6H)	1.5 (s, 3H)	7.35 (s, 15H)	—
13,15	0.8 (t,6H)	1.4 (m, 12H)	3.6 (t, 4H)	2.85 (q, 8H)	—	—	—
14,16	0.85 (t, 6H)	1.4 (m, 14H)	3.6 (t, 4H)	2.90 (q, 8H)	—	—	—

*Sl nos refer to complexes listed in Table 1

adducts, it is apparent that the proton count due to alkylamino/anilino moieties in the ligands of the adducts have undergone three to four fold increase. On the other hand the proton count due to alkoxy groups in the adducts have suffered corresponding decrease. This shows that on reaction the ligands are disproportionated to alkoxysilanetriamines or silanetetramines, which are precipitated as the adducts. However, no such change is observed in the adducts of the tertiary amines such as $(n\text{-}C_3H_7O/n\text{-}C_4H_9O)_2Si\ [N(CH_2CH_3)_2]_2$. This observation indicates that no base rearrangement occurs for the ligand in tertiary silanamine which is contrary to the observations in secondary silanamine reactions.

Base exchange reaction

Further evidence in support of the compositions of the adducts is provided by the results of the base exchange reactions. Using the stronger electron donors such as 2,2′-bipyridyl, pyridine-d_5 and ethylenediamine in carbon tetrachloride separately, the silanamines could be regenerated and their identity confirmed through IR and PMR spectra.

From the foregoing data, it is apparent that under the same experimental conditions, the silanediamines like, silanamines[1-6] are converted into silanetriamines. N,N′-(*p*-Methylphenyl)-1,1-dialkoxysilanediamines are rearranged to silanetetramines[7]. The liberated silanamine from $(n\text{-}C_3H_7O/n\text{-}C_4H_9O)_2Si[N(CH_2CH_3)_2]_2.MCl_4$ is the original base molecule, which supports the view that tertiary silanamines do not undergo disproportionation in these donor-acceptor reactions.

Complexes isolated from filtrates

The filtrates of the above reactions at room temperature after 48-72 hr, afford another solid (15-20%), in each case. The composition of these compounds as evidenced by elemental analyses (Table 3), IR spectra [νNH 3200; νCO 1100-1080; νSiO(C) 1060 cm^{-1}], PMR spectra [CH_3, CH_2, CH_2O, C_6H_5, C_6H_5Cl and $CH_3(Ph)$ proton signals at 0.8 to 0.9, 1.3 to 1.4, 3.6 to 3.8, 6.8 to 7.5 and 2.4 ppm respectively along with proton integration] corresponds to $(OR)_2Si(NHR')_2.2MCl_4$. These adducts have also been isolated from the filtrates of the similar reactions of N-organo-1-chloro-1,1 dialkoxysilanamines[6]. In the case of N,N′-diethyl-1,1-dialkoxysilanediamines, only the residual normal 1:1 adducts were obtained.

The donor-acceptor reactions of organoxysilanamines studied so far[1-7], give adducts I-IV as the major reaction products.

$(RO)_2Si(NHR')_2.MCl_4$ (I) $\qquad$ $(RO)_2Si(NHR')_2.2MCl_4$ (II)

$(RO)Si(NHR')_3.2MCl_4$ (III) $\qquad$ $Si(NHR')_4.3MCl_4$ (IV)

Adducts (I) are obtained[4] from the ligands $[(RO)_3SiNHR']$ ($R = ClC_2H_4$; $R' = C_6H_5/C_6H_5CH_2$ and $R = CF_3CH_2$; $R' = C_6H_4F/C_6H_3F_2$). Adducts (II) are formed[4] from the ligand having mixed 2-chloroethoxy and *n*-propoxy/*n*-butoxy groups on silicon atom and $R' = C_6H_5/C_6H_5CH_2$. Adducts (III) are most common of the complexes isolated and are obtained from ligands having different R and

Table 3—Analytical Data of Complexes Isolated from Filtrates

Compound	Found (Reqd) %			
	Cl	Ti/Sn	Si	N
$(PrO)_2Si(NHC_6H_5)_2.2TiCl_4$	39.72 (40.0)	13.4 (13.52)	3.7 (3.94)	3.8 (3.94)
$(PrO)_2Si(NHC_6H_5)_2.2SnCl_4$	33.16 (33.33)	27.7 (27.93)	3.0 (3.29)	3.2 (3.29)
$(BuO)_2Si(NHC_6H_5)_2.2TiCl_4$	38.3 (38.48)	12.85 (13.01)	3.7 (3.79)	3.65 (3.79)
$(BuO)_2Si(NHC_6H_5)_2.2SnCl_4$	32.02 (32.27)	27.16 (27.04)	2.9 (3.18)	3.22 (3.18)
$(PrO)_2Si(NHC_6H_4Cl-o)_2.2TiCl_4$	36.29 (36.45)	12.24 (12.34)	3.7 (3.59)	3.65 (3.59)
$(PrO)_2Si(NHC_6H_4Cl-o)_2.2SnCl_4$	30.95 (30.84)	25.7 (25.84)	2.8 (3.04)	3.16 (3.04)
$(BuO)_2Si(NHC_6H_4Cl-o)_2.2TiCl_4$	35.05 (35.19)	11.7 (11.89)	3.27 (3.47)	3.42 (3.47)
$(BuO)_2Si(NHC_6H_4Cl-o)_2.2SnCl_4$	29.85 (29.93)	25.12 (25.08)	2.9 (2.95)	3.01 (2.95)
$(PrO)_2Si(NHC_6H_4CH_3-p)_2.2TiCl_4$	38.35 (38.48)	12.90 (13.01)	3.68 (3.79)	3.12 (3.79)
$(PrO)_2Si(NHC_6H_4CH_3-p)_2.2SnCl_4$	32.14 (32.27)	27.15 (27.04)	3.02 (3.18)	3.12 (3.18)
$(BuO)_2Si(NHC_6H_4CH_3-p)_2.2TiCl_4$	36.91 (37.07)	12.40 (12.53)	3.39 (3.65)	3.59 (3.65)
$(BuO)_2Si(NHC_6H_4CH_3-p)_2.2SnCl_4$	31.15 (31.27)	26.07 (26.21)	3.21 (3.08)	3.01 (3.08)
$(PrO)_2Si(NHCH_2C_6H_5)_2.2TiCl_4$	38.39 (38.48)	12.89 (13.01)	3.58 (3.79)	3.65 (3.79)
$(PrO)_2Si(NHCH_2C_6H_5)_2.2SnCl_4$	32.35 (32.27)	26.92 (27.04)	3.0 (3.18)	3.11 (3.18)

R′ groups[1-6]. Adducts (IV) are rare and are obtained as in the present case as well as when $R = CF_3CH_2$; $R' = C_6H_4F$. However, the present report and the literature observations also record the precipitation of adducts (II) as the minor products from the filtrates during the formation of III and IV. Even adduct III has been found in small amounts in the reaction giving IV as the main product[8].

Thus adducts (II) and (III) may be presumed to be the unconsumed intermediate products leading to the formation of the appropriate silane polyamines. The tentative mechanism may therefore, be written as shown in the Scheme 1.

(i) $(RO)_3SiNHR' + MCl_4 \rightarrow (RO)_3SiNHR'.MCl_4$

(ii) $(RO)_3SiNHR'.MCl_4 + (RO)_3SiNHR' \rightarrow (RO)_2Si(NHR')_2.MCl_4 + (RO)_4Si$

(iii) $(RO)_2Si(NHR')_2.MCl_4 + MCl_4 \rightarrow (RO)_2Si(NHR')_2.2MCl_4$

(iv) $(RO)_2Si(NHR')_2.2MCl_4 + (RO)_3SiNHR' \rightarrow (RO)Si(NHR')_3.2MCl_4 + (RO)_4Si$

(v) $(RO)Si(NHR')_3.2MCl_4 + MCl_4 \rightarrow (RO)Si(NHR')_3.3MCl_4$

(vi) $(RO)Si(NHR')_3.3MCl_4 + (RO)_3SiNHR' \rightarrow Si(NHR')_4.3MCl_4 + (RO)_4Si$

Scheme (1)

As mentioned above, adducts I-IV are stable and isolable under appropriate experimental conditions. However, the adducts $(RO)_3SiNHR'.MCl_4$ and $(RO)Si(NHR')_3.3MCl_4$ have not yet been isolated and/or identified. In the case of tertiary silanamines the reaction stops after the first reaction and affords only 1:1 adducts.

References

1 Narula S P & Kapur N, *Indian J Chem*, **22A** (1983) 557.

2 Narula S P & Kapur N, *Inorg chim Acta*, **73** (1983) 183.

3 Narula S P & Kapur N, *Inorg chim Acta*, **86** (1984) 37.

4 Narula S P, Shankar R & Kumar S, *Indian J Chem*, **23A** (1984) 661.

5 Narula S P, Shankar R & Kapur N, *J Indian chem Soc*, **62** (1985) 925.

6 Narula S P, Kapur N, Chodha A, Shankar R & Malhotra R, *Indian J Chem*, **26A** (1987) 135.

7 Narula S P, Kapur N, Shankar R & Kumar S, *Proc Indian natn Sci Acad*, **52A** (1986) 1049.

8 Shankar R, *Reactions of organoxy/organo-organoxy silicon compounds containing Si–N bond with Lewis acids*, Ph.D. Thesis, Panjab University, Chandigarh, 1985.

Indian Journal of Chemistry
Vol. 27A, June 1988, pp. 523-526

Solvent Extraction Studies of Mixed Chelates of Europium

P R SANGURDEKAR† & M SUDERSANAN*
Analytical Chemistry Division, Bhabha Atomic Research Centre, Trombay, Bombay 400 085

Received 27 *July* 1987; *revised and accepted* 5 *October* 1987

Mixed chelates of europium with β-diketones and oxine have been studied by solvent extraction using carbon tetrachloride as the medium. Extraction of europium by mixtures of HBFA–HFTA, HBFA–HTFA as well as oxine-HBFA/HFTA/HTFA have been studied (where HBFA = benzoyltrifluoroacetone, HTFA = trifluoroacetylacetone and HFTA = furoyltrifluoroacetone). Mixed complexes are formed in all the cases and the nature of the extracted species and their equilibrium constants have been evaluated by graphical methods.

Mixed chelate formation in solution has been studied by various methods[1,2]. Mixed chelates of metals like copper, zinc, indium and europium with ligands like HTTA and isopropyltropolone have been reported[3]. Mixed chelates of lutetium[4] and uranium[5] have been reported. In our laboratories, a systematic study of indium[6], hafnium[7] and uranium[8] systems have been carried out. In continuation of this work, solvent extraction studies on the formation of mixed chelates of europium with two β-diketones or a mixture of a β-diketone and oxine are presented here. The studies using oxine have been made with a view to assessing the possibility of formation of adducts besides mixed chelates.

Materials and Methods

Europium, in the form of $^{152+154}$Eu, was obtained from Isotope Group, BARC. Benzoyltrifluoroacetone (HBFA), furoyltrifluoroacetone (HFTA) and trifluoroacetylacetone (HTFA) (all from K&K Labs, USA) and oxine (BDH, AR) were used as a solution in carbon tetrachloride (E. Merck, GR).

Extraction experiments were carried out by equilibrating for 6 hr at 30 ± 2°C the aqueous phase (10 ml) containing europium ($\sim 10^{-5}$ *M*), sodium chloride to maintain the ionic strength at 0.5 and acetic acid + sodium hydroxide (~ 0.02 *M*) to adjust the *p*H with an equal volume of the organic phase containing the extractants. The two phases were separated and the *p*H of the aqueous phase was measured using a Beckman Expandomatic SS-2 *p*H meter (M/s Beckman Instruments Inc, USA). Europium in the two phases was assayed by gamma counting using a thallium-activated sodium iodide crystal with a single channel analyser (M/s ECIL, Hyderabad). Background corrections were applied in all the cases. The mass balance for europium was good.

Results and Discussion

The mixed chelate formation of europium with two ligands, HA and HB, can be described by Eq. (1)

$$Eu^{3+} + n[HA]_0 + (3-n)[HB]_0 \rightleftharpoons [EuA_nB_{3-n}]_0 + 3H^+ \quad \ldots (1)$$

and the equilibrium constant is given by Eq. (2)

$$K_{BA} = K_{(3-n),n} = \{[EuA_nB_{3-n}]_0[H]^3[Eu]^{-1}[HA]_0^{-n}[HB]_0^{-(3-n)}\} \quad \ldots (2)$$

where the charges have been omitted for convenience. The distribution ratio(D) is given by Eq. (3).

$$D = \frac{[EuA_3]_0 + [EuA_2B]_0 + [EuAB_2]_0 + [EuB_3]_0}{[Eu]} \quad \ldots (3)$$

Substituting in terms of equilibrium constants and on rearranging, we get

$$F_0 = D[H]^3/[HA]_0^3 = K_{03} + K_{12}[L] + K_{21}[L]^2 + K_{30}[L]^3 \quad \ldots (4)$$

where [L] represents $[HB]_0/[HA]_0$ and can be solved for various equilibrium constants by graphical methods.

Extraction of europium was studied using a mixture of β-diketones or a β-diketone and oxine. Various β-diketones were selected in order to study the influence of the terminal groups of the β-diketones on the stability of mixed chelates.

Europium-HBFA-HFTA system

Extraction of europium was studied in the presence of a mixture of HBFA (HA) and HFTA (HB). The distribution ratio (D) was measured as a function of *p*H at fixed [HBFA] and [HFTA]. Studies were also made at varying [HBFA] or [HFTA]

†Health Physics Division, BARC, Bombay 400 085

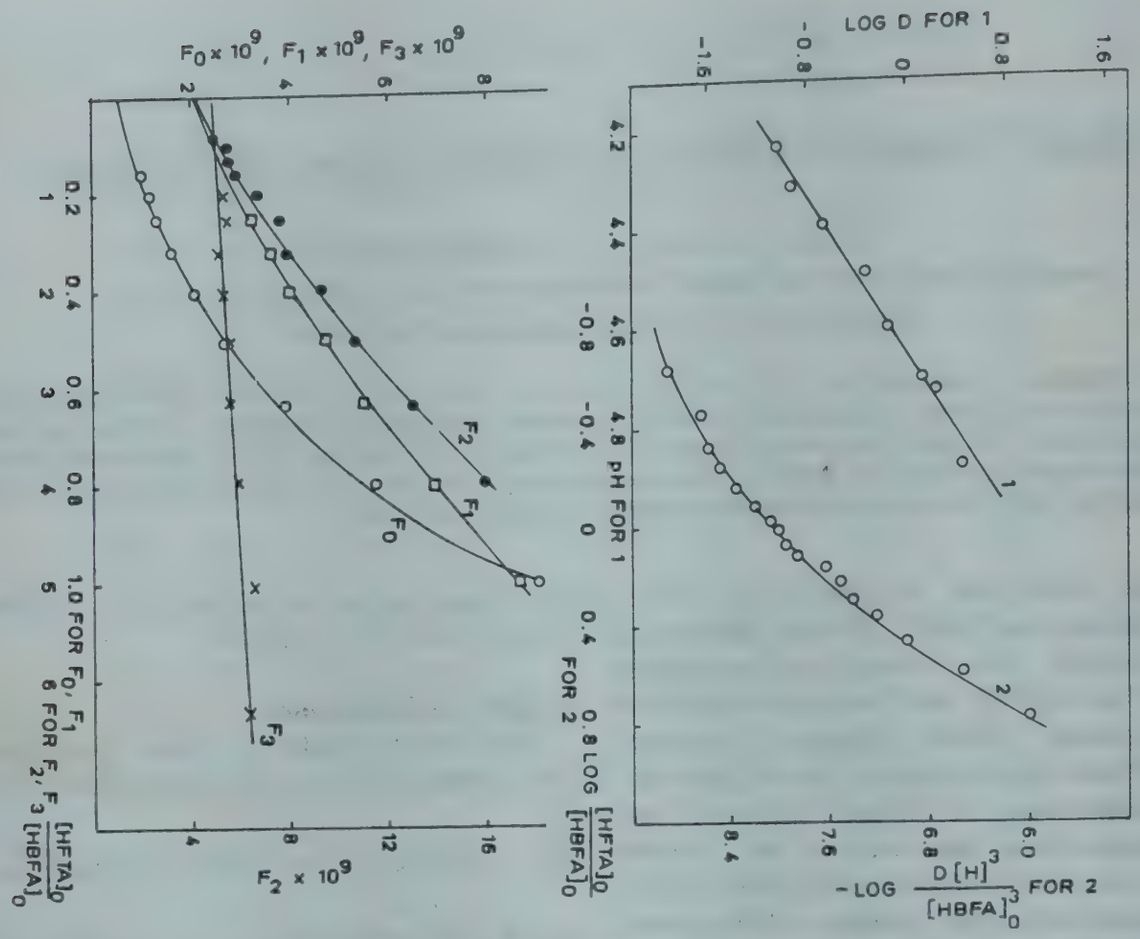

Fig. 1—Europium-HBFA-HFTA system (Plots 1 and 2 represent the plot of log D versus pH and log $D\,[H]^3/[HBFA]_0^3$ versus $[HFTA]_0/[HBFA]_0$ respectively. Other plots represent the various F_j functions)

while maintaining the pH and concentration of the either β-diketone constant. The concentrations of the β-diketones were calculated taking into account the partition coefficients of the two β-diketones[9,10]. Values of partition coefficients were obtained from literature as log $P_{HA} = 2.47$ for HBFA and 0.82 for HFTA. The dissociation constants (pK) for HBFA and HFTA are 6.01 and 6.18 respectively[9].

The plot of function F_0, calculated using Eq. (4) resulted in a curve (Fig. 1) indicating the formation of mixed chelates. The plot of F_0 versus [L], when extrapolated to [L]→0, gives the value of K_{03} as the intercept. Another function F_1 can be written as

$$F_1 = \frac{F_0 - K_{03}}{[L]} = K_{12} + K_{21}[L] + K_{30}[L]^2 \qquad \ldots (5)$$

A plot of F_1 versus [L] gives the value of K_{12} as the intercept when [L]→0. Other functions can be written in a similar manner and solved to obtain the various equilibrium constants. Typical plots are given in Fig. 1 and the equilibrium constants are presented in Table 1.

Table 1—Values of Equilibrium Constants

System (HA−HB)	K_{BA}	$-\log K_{BA}$
HBFA−HFTA	K_{03}	9.30
	K_{12}	8.70
	K_{21}	8.40
	K_{30}	8.60
HBFA−HTFA	K_{12}/K_1	7.66
	K_{21}/K_1	6.90
HFTA-oxine	K_{03}	7.92
	K_{12}	7.00
HBFA-oxine	K_{03}	8.36
	K_{12}	9.30
	K_{21}	8.32
HTFA-oxine	K_{12}/K_1	6.12

Europium-HBFA-HTFA system

Extraction of europium using a mixture of HBFA (HA) and HTFA (HB) was also studied in a similar manner. The concentration of HTFA in the organic phase was calculated taking into account the dissociation constant[9] (K_a) and partition coefficient (P) using the relation (6)

$$[HTFA]_0 = \frac{P_{HTFA}[HTFA]_{tot}}{1 + P_{HTFA} + K_a[H]^{-1}} \qquad \ldots (6)$$

where $P_{HTFA} = 0.646$ and $pK_a = 6.09$. Extraction of europium was studied around *p*H 5.6 by varying the concentration of HBFA (0.001 to 0.01 *M*) at a fixed concentration of HTFA (0.0165 *M*) and also at varying concentrations of HTFA and a fixed concentration of HBFA (0.01 *M*). Extraction of europium occurred at a higher *p*H of 5 to 6 and hence the aqueous phase complexes of Eu-TFA were to be considered for the analysis of data. The formation of $(Eu\ TFA)^{2+}$ can be described by the reaction (7)

$$Eu^{3+} + [HTFA]_0 \rightleftharpoons (Eu\ TFA)^{2+} + H^+ \quad \ldots (7)$$

with the equilibrium constant K_1 given by Eq. (8)

$$K_1 = [Eu\ TFA][H]/[Eu][HTFA]_0 \quad \ldots (8)$$

Assuming Eu-TFA to be the predominant species in the aqueous phase, Eq. (5) can be rearranged to get

$$F_0 = \frac{D[H]^3[HTFA]_0}{[HBFA]_0^3[H]} = \frac{1}{K_1}\{K_{03} + K_{12}[L] + K_{21}[L]^2 + K_{30}[L]^3\} \quad \ldots (9)$$

where [L] represents $[HTFA]_0/[HBFA]_0$. Various functions were calculated from the data and were analysed to obtain the various constants by the graphical method. The values of K_{12}/K_1 and K_{21}/K_1 were calculated as 2.2×10^{-8} and 1.27×10^{-7} respectively, indicating the formation of mixed chelates. However, the higher *p*H of extraction and the presence of $(Eu-TFA)^{2+}$ complex in the aqueous phase complicates further analysis of the data.

Europium-HBFA- oxine system

Mixed complex formation of europium using mixtures of HBFA (HA) and oxine (HB) was also studied in a similar manner. Studies were made at fixed concentrations of HBFA and oxine of 0.01 *M* each and varying *p*H in the range of 4.2 to 4.6. Studies were also made at a nearly constant *p*H of about 4.5 and varying concentrations of one ligand at a fixed concentration (0.01 *M*) of the other ligand. The concentration of oxine in the organic phase was calculated taking into account the influence of protonation and partition coefficient of oxine[10], ($P_{Hox} = 10^{2.06}$) using Eq. (10),

$$[Hox]_0 = P_{Hox}[Hox]_{tot} / \left\{1 + P_{Hox} + \frac{[H]^2 + K_1K_2}{K_1[H]}\right\} \quad \ldots (10)$$

where K_1 and K_2 represent the dissociation constants of oxine[11], being equal to 5.09 for pK_1 and 9.02 for pK_2.

Extraction of europium in the presence of varying concentrations of HBFA and oxine was found to be higher than that due to the reagents alone. The data were analysed on the basis of formation of mixed chelates in order to obtain the values of equilibrium constants. The function F_0 or $D[H]^3[HBFA]_0^{-3}$, plotted as a function of $\log\{[Hox]_0/[HBFA]_0\}$ resulted in a smooth curve indicating the presence of mixed chelates. The various constants were calculated as described earlier (Table 1). The value of K_{30} could not be evaluated because of relatively small changes in the values of F_j functions at higher concentrations of oxine indicating the contribution of $Eu(ox)_3$ to the extraction to be small compared to those of mixed chelates. Details of analysis and the plots are not presented for the sake of brevity.

Europium-HFTA- oxine system

Extraction of europium in the presence of HFTA was studied in a similar manner around *p*H 4.3 and the data were analysed in a similar manner. The values of K_{03} and K_{12} were calculated as 1.2×10^{-8} and 1.0×10^{-7}, respectively while those for the higher complexes could not be evaluated from the data.

Europium-HTFA- oxine system

Studies were also extended to the extraction of europium by a mixture of HTFA and oxine around *p*H 4.9. The concentrations of oxine and HTFA in the organic phase were calculated using Eqs. (6) and (10), respectively. The data were analysed considering the presence of $(Eu-TFA)^{2+}$ in the aqueous phase as discussed in an earlier section. The plot of log F_0 versus log [L] where [L] represents $[Hox]_0/[HTFA]_0$ indicated the absence of extraction by HTFA alone under the present experimental conditions and the predominance of the first mixed chelate, $Eu(TFA)_2ox$. The values of constants are summarised in Table 1.

The results obtained in the case of β-diketones can be attributed to the formation of mixed chelates. The values of stabilisation constants (K_s) were calculated for Eu-HBFA-HFTA system. The values of K_s given by Eq. (11)[1]

$$K_s = K_{obs}/K_{stat} \quad \ldots (11)$$

were found to be 0.78 for $Eu(BFA)_2FTA$ and 0.91 for $Eu(BFA)(FTA)_2$, indicating that the complexes were stabilised as expected on the basis of statistical factors. However, in the case of Eu-β-diketone-oxine systems, the values of K_{03} obtained from the data on mixed chelates were somewhat higher than those obtained on binary systems.

This indicated the probable formation of adducts with oxine in addition to mixed chelates. Sekine and Dyrssen[3] also found evidence for the formation of self-adducts or adducts with one of the ligand (isopropyltropolone, IPT) in their studies on the formation of mixed chelates of europium with HTTA and IPT. An increase in the values of K_{03} by a factor of 5 to 10 can probably be attributed to this effect.

Acknowledgement

The authors wish to thank Dr A K Sundaram for his valuable guidance throughout the course of this work and Shri S Somasundaram, Head, R & H C Section for keen interest in the studies.

References

1 Marcus Y & Eliezer I, *Coord chem Rev*, **4** (1969) 273.
2 Fridman Ya D, *Proceeding third symposium on coordination chemistry*, Vol 2, edited by M T Beck (Akademiai Kiado, Budapest) 1970, pp. 77.
3 Sekine T & Dyrssen D, *J inorg nucl Chem*, **26** (1964) 1727, 2013; **29** (1967) 1489.
4 Shigematsu T & Honjyo T, *Bull chem Soc Japan*, **43** (1970) 796.
5 Newman L & Klotz P, *Solvent extraction chemistry*, edited by D Dyrssen, J O Liljenzin & J Rydberg (North Holland, Amsterdam) 1967, pp. 128.
6 Sudersanan M & Sundaram A K, *Proc Indian Acad Sci*, **82A** (1975) 77.
7 Pushparaja & Sudersanan M, *J inorg nucl Chem*, **43** (1981) 1371.
8 Malhotra R K & Sudersanan M, *Indian J Chem*, **25A** (1986) 744.
9 Sekine T, Hasegawa Y & Ihara N, *J inorg nucl Chem*, **35** (1973) 3968.
10 Leo A, Hansch C & Elkins D, *Chem Rev*, **71** (1971) 525.
11 Smith R M & Martell A E, *Critical stability constants*, Vol 2 (Plenum, New York) 1975.

Indian Journal of Chemistry
Vol. 27A, June 1988, pp. 527-528

Notes

Application of Mean Spherical Approximation in Estimating Activity Coefficients of Aqueous Mixed Electrolyte Solutions

ANIL KUMAR

Department of Sugar Chemistry, Deccan Sugar Institute, Manjari (Bk), Pune 412 307

Received 30 *July* 1987; *revised and accepted* 12 *October* 1987

The mean spherical approximation theory is applied to estimate the activity coefficients in aqueous mixed electrolyte solutions. The contribution due to hard-sphere term in the excess free energy is considered. The only adjustable parameter is the ionic diameter. The equations tested for aq. $HCl-CoCl_2$ at 25°C and aq. $HBr-CaBr_2$ from 5 to 45°C show excellent agreement with experimental data.

Recently there has been growing interest in developing methods for predicting thermodynamic properties of aqueous mixed electrolyte solutions. Of various methods, the mean spherical approximation (MSA) has frequently been employed[1-4] to predict thermodynamic properties of single electrolyte solutions. Humffray[5] included hard-sphere (non-electrostatic) terms into the MSA treatment of mixtures reported by Vericat and Grigera[6] and predicted the activity coefficients in aq. $NaCl-CaCl_2$ differing from the experimental values by 13%. Corti[7] applied the MSA theory to simple electrolyte mixtures like $NaCl-HCl$ upto the ionic strength of 1 mol kg^{-1} of water.

In this note, an attempt is made to explore the possibility of using MSA theory to relatively complicated systems like $HCl-CoCl_2-H_2O$[8] at 25°C and $HBr-CaBr_2-H_2O$[9,10] from 5 to 45°C in the region of moderately concentrated electrolyte solutions. Temperature dependence of the adjustable parameter is also discussed.

Theoretical equation for estimating the free energy in a mixture of hard-spheres as applied to the systems undertaken here may be written as[11,12]

$$\ln \gamma_i^{hs} = \ln\Delta\left(\gamma_i - 1 - \frac{2\eta_i}{\eta} y_3\right) + \frac{\eta}{\Delta^2}\left\{3(1-\alpha_i) + \gamma_i + \frac{3\eta}{2}(\alpha_i - \beta_i - \gamma_i - 1)\right\} + \frac{\eta}{\Delta^3}\left\{\eta\left[5y_3 - \frac{9}{2}y_1 - 2 + \eta\left(\frac{3}{2}y_1 - 3y_2 - 4y_3 + 1\right)\right] - 2y_3 + 4\right\} \quad \ldots(1)$$

Equation (1) is consistent with Baxter equation[13], which is applicable for the calculation of activity coefficient in low concentration range.

According to unrestricted MSA model[14,15], the electrostatic contribution towards excess free energy of an electrolyte mixture, as applicable to present systems containing ionic species with charge Z_i and diameter σ_i, is given by Eq. (2)

$$\ln \gamma_i^e = \frac{\beta e^2 Z_i M_i}{\varepsilon_0} - \frac{P_n}{4\Delta}\left(\Gamma a_i + \frac{\pi}{12\Delta}\alpha^2 P_n \sigma_i^2\right) \quad \ldots(2)$$

The physical significance of various terms involved in Eqs (1) and (2) is discussed elsewhere[11,12,14,15].

The total exces free energy for an electrolyte mixture is given by Eq. (3), which is a combination of Eqs (1) and (2)

$$\ln \gamma_i = \ln \gamma_i^e + \ln \gamma_i^{hs} \quad \ldots(3)$$

The values of σ for H^+, Co^{2+}, Ca^{2+}, Cl^- and Br^- were obtained by fitting the experimental activity coefficient data taken from literature[16]. Table 1 lists the σ-values at different temperatures. In this study, it is assumed that σ-values remain constant over the full range of concentration and composition. The ionic activity coefficients in a mixture obtained using σ-values given in Table 1 were converted into practical molal activity coefficients using densities of the mixtures. These densities were obtained from the viral coefficient approach of Pitzer[17]. The compressibility effects at atmospheric pressure were neglected.

In Fig. 1 are plotted the calculated results along with the experimental points as a function of Y_{CoCl_2}, the ionic strength fraction of $CoCl_2$ for aq. $HCl-CoCl_2$ at different ionic strengths. The results for aq. $HBr-CaBr_2$ at $Y_{CaBr_2}=0.5$ at various temperatures are also shown in Fig. 1. The experimental mixture data fit the MSA theory with ex-

Table 1—Estimated Ionic Diameters (σ, Å) in MSA Theory at Different Temperatures

Ions	σ (Å) at temp				
	5°	15°	25°	35°	45°
H^+	5.20	4.70	4.45	4.21	4.10
Ca^{2+}	5.80	5.62	5.52	5.30	5.19
Co^{2+}	—	—	5.10	—	—
Cl^-	—	—	3.60	—	—
Br^-	4.00	4.00	3.90	3.82	3.78

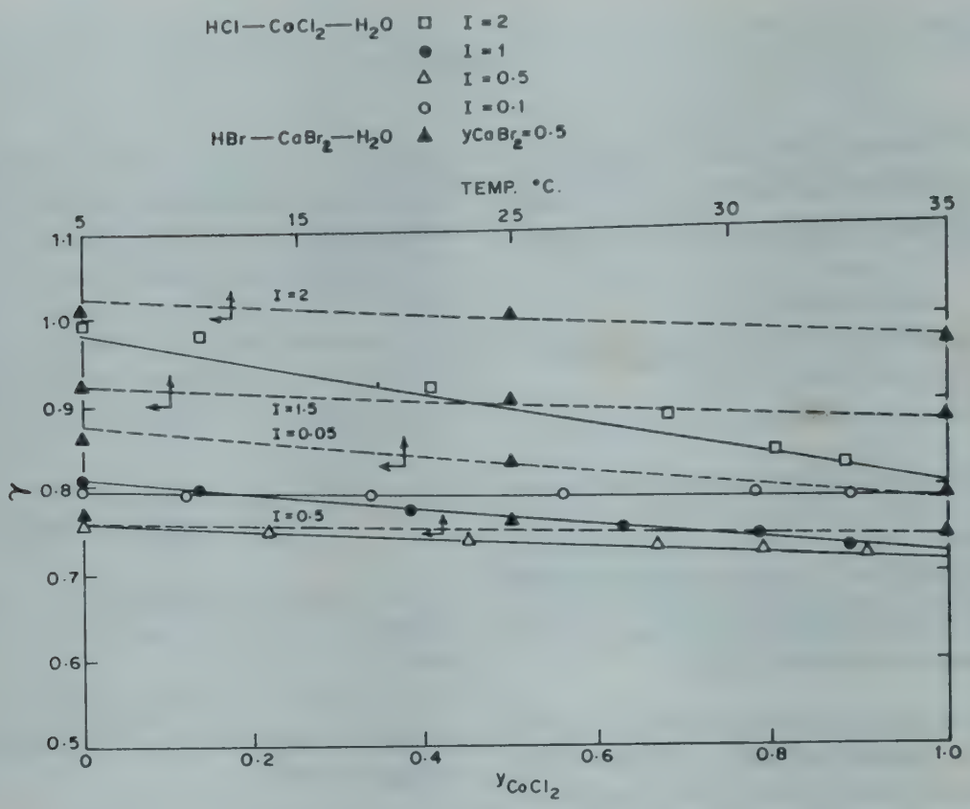

Fig. 1—Comparison of experimental and calculated activity coefficients for aq. $HCl-CoCl_2$ (_____) and aq. $HBr-CaBr_2$ (– – ▲ – –) systems (Temperature dependence is at $y=0.5$)

cellent accuracy upto ionic strength of 1 mol kg^{-1}, but a systematic deviation starts to occur beyond ionic strength of 2 mol kg^{-1}. The estimation for aq. $HBr-CaBr_2$ are fairly good even at ionic strength of 1.5. The poor fit in the range of high concentrations is due to the fact that the hydration around ions changes and thus the ionic diameters might be varying in the high concentration region. A consideration of concentration-dependent σ, however, will further complicate the system of equations. It was noted that σ_{H^+} values for both aq. $HCl-CoCl_2$ and aq. $HBr-CaBr_2$ at 25°C were approximately the same and thus an average value at this temperature is given in Table 1. The values of σ decrease with increase in temperature; however, the temperature dependence of for H^+ is very strong.

In summary, the MSA theory with an adjustable parameter, acts as a powerful tool for predicting the activity coefficients.

The author is thankful to the referee for suggestions.

References

1 Triolo R, Grigera J R & Blum L, *J phys Chem*, **80** (1976) 1858.
2 Triolo R, Blum L & Floriano M A, *J phys Chem*, **82** (1977) 1368.
3 Corti H R & Fernandez Prini R, *J chem Soc Faraday Trans-I*, (1986) 921.
4 Ebling W & Grigo M, *Ann Phys* (Leipzig), **37** (1980) 21.
5 Humffray A A, *J phys Chem*, **87** (1983) 5521.
6 Vericat F & Grigera J R, *J phys Chem*, **86** (1982) 1030.
7 Corti H R, *J phys Chem*, **91** (1987) 686.
8 Khoo K H, Lim T K & Chan C Y, *J chem Soc Faraday Trans*-1, (1978) 2037.
9 Khoo K H, Lim T K & Chan C Y, *J chem Soc Faraday Trans-I*, (1979) 1067.
10 Roy R N, Wood M D, Johnson D & Roy L N, *J chem Thermodyn*, **19** (1987) 307.
11 Mansoori G A, Carnahan N F, Starling K E & Leland T W, *J chem Phys*, **54** (1971) 1523.
12 Ebling W & Scherwinski K, *Z phys Chem* (*Leipzig*), **264** (1983) 1.
13 Baxter R J, *J chem Phys*, **52** (1970) 4559.
14 Hoye J S & Blum L, *Mol Phys*, **35** (1978) 299.
15 Blum L & Hoye J S, *J phys Chem*, **81** (1977) 1311.
16 Robinson R A & Stokes R H, *Electrolyte solutions* (Butterworths, New York) 1959.
17 Kumar A, *J chem engng Data*, **32** (1987) 106.

Indian Journal of Chemistry
Vol. 27A, June 1988, pp. 529-531

Excess Properties of Binary Liquid Mixtures at 293.15 K†

T M AMINABHAVI*, L S MANJESHWAR,
S B HALLIGUDI‡ & R H BALUNDGI

Department of Chemistry,
Karnataka University Dharwad 580 003

Received 28 *July* 1987;
revised and accepted 16 *November* 1987

Reported values of density, viscosity and refractive index at 293.15 K for six binary mixtures, viz. benzene + cyclohexane, benzene + ethyl acetate, benzene + carbon tetrachloride, cyclohexane + ethyl acetate, cyclohexane + carbon tetrachloride, and ethyl acetate + carbon tetrachloride have been used to predict a number of thermodynamic, hydrodynamic and optical excess quantities. Results are discussed in terms of deviations from ideal behaviour.

In continuation of our earlier work on excess properties of binary solvent mixtures[1-3], we now report additional data on excess molar volume (V^E), excess Gibb's free energy of flow (G^E), excess viscosity (η^E), excess refractive index (n^E) and excess molar refraction (R^E) at 293.15 K for six binary mixtures, viz. (i) benzene + cyclohexane, (ii) benzene + ethyl acetate, (iii) benzene + carbon tetrachloride, (iv) cyclohexane + ethyl acetate, (v) cyclohexane + carbon tetrachloride and (vi) ethyl acetate + carbon tetrachloride. The properties are studied over the entire range of composition of the mixtures and the results are interpreted in terms of interaction forces and the nature of mixing components.

In view of the availability of the data[4-6] further experimentation appeared unnecessary. Solvents used were of the highest purity and their purities were checked by gas chromatography. Details of the measurements of density, viscosity and refractive index (at 589, 546 and 436 nm) have been outlined in previous papers[4,5]. All mixtutres were made on volume fraction (ϕ) basis and measurements at 293.15 ± 0.01 K were made on the same day on which mixtures were prepared.

Various excess quantities were calculated employing Eqs. (1-5)

$$V^E(cm^3/mol) = V_m - V_1\phi_1 - V_2\phi_2 \quad \ldots (1)$$

$$R^E(cm^3/mol) = R_m - R_1\phi_1 - R_2\phi_2 \quad \ldots (2)$$

$$n^E = n_m - n_1\phi_1 - n_2\phi_2 \quad \ldots (3)$$

$$\eta^E(cP) = \eta_m - \eta_1\phi_1 - \eta_2\phi_2 \quad \ldots (4)$$

$$G^E(cal/mol) = RT\,[\ln \eta_m V_m - \phi_1 \ln \eta_1 V_1 - \phi_2 \ln \eta_2 V_2] \quad \ldots (5)$$

In the above equations $V_m[\equiv(M_1\phi_1 + M_2\phi_2)/\rho_m]$ is the molar volume of the mixture (M_1, M_2 and ρ_m represent the molecular weights of components 1, 2 and density of the mixture respectively); V_1 ($\equiv M_1/\rho_1$) and $V_2(\equiv M_2/\rho_2)$ represent the molar volumes of components 1 and 2, respectively (ρ_1 and ρ_2 are their densities); R_1, R_2 and R_m are respectively the molar refractivities of components 1, 2 and their mixtures, respectively. The refractivity of the mixture (R_m) was calculated using Lorentz-Lorenz[7] mixing rule, i.e. $R_m \equiv [(n_m^2 - 1)/(n_m^2 + 2)]\ (V_m)$, where n_m represents the refractive index of the mixture and n_1, n_2 are the refractive indices of components 1 and 2. η_1, η_2 and η_m are the viscosities of components 1, 2 and of the mixture respectively. The term RT has its usual meaning.

The excess quantities were fitted to a polynomial relation (Eq 6) to evaluate the coefficients (a_i)

$$X^E = \sum_{i=1}^{2} a_i(\phi_2 - \phi_1)^{i-1} \quad \ldots (6)$$

where X^E represents the appropriate excess quantity. The fitted values were used to draw smooth curves in all the plots wherein the experimental data are given as points. The percentage error in the calculation of all the excess quantities seldom exceeded 5×10^{-4} units. All computations were done at CSMCRI, Bhavnagar, using HP 1000 computer.

Excess molar volumes are plotted against ϕ_1 in Fig. 1. A large negative V^E observed for cyclohexane + carbon tetrachloride mixture is due to the more flexible cyclohexane molecule, which seems to be oscillating rapidly between *cis*- and *trans*-configurations in the presence of a spherical molecule such as carbon tetrachloride leading to high levels of specific interactions between unlike species. Small negative V^E is observed for ethyl acetate + carbon tetrachloride mixture, again suggesting specific interactions between the components. Positive V^E values over the whole composition scale for the mixtures of benzene with cyclohexane, ethyl acetate and CCl_4 suggest that dis-

† Based on the Ph D thesis of LSM submitted to Karnatak University (1987)

‡ Central Salt & Marine Chemicals Research Institute, Bhavnagar 364 002

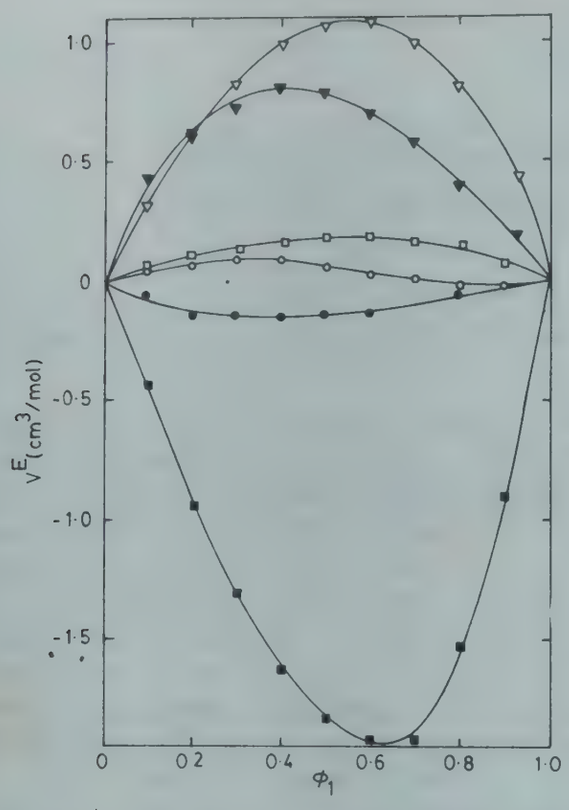

Fig. 1 – Excess molar volume (V^E) versus volume fraction (ϕ_1) of first component [○, benzene + cyclohexane; ▽, benzene + carbon tetrachloride; □, benzene + ethyl acetate; ■, cyclohexane + carbon tetrachloride; ●, ethyl acetate + carbon tetrachloride and ▼, ethyl acetate + cyclohexane]

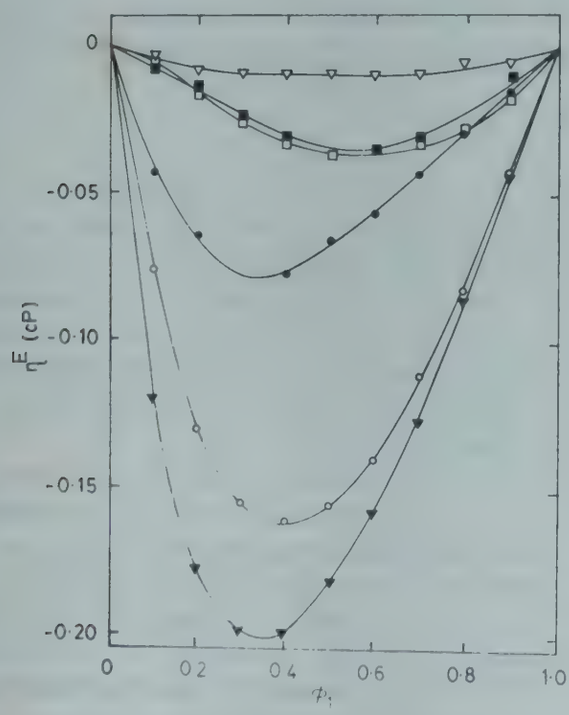

Fig. 2 – Excess viscosity (η^E) versus volume fraction (ϕ_1) of first component [symbols represent the mixtures given in Fig. 1]

persion forces are operative in these mixtures. When ethyl acetate (polar molecule) is mixed with cyclohexane (nonpolar molecule) again V^E is positive suggesting the existence of weak physical forces in the mixture.

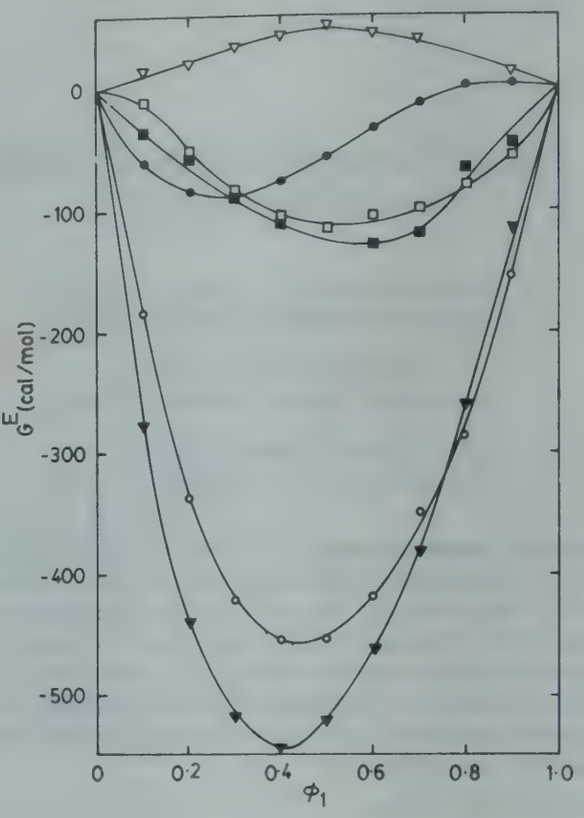

Fig. 3 – Excess Gibbs free energy (G^E) of flow versus volume fraction (ϕ_1) of first component [symbols have the same significance as in Fig. 1]

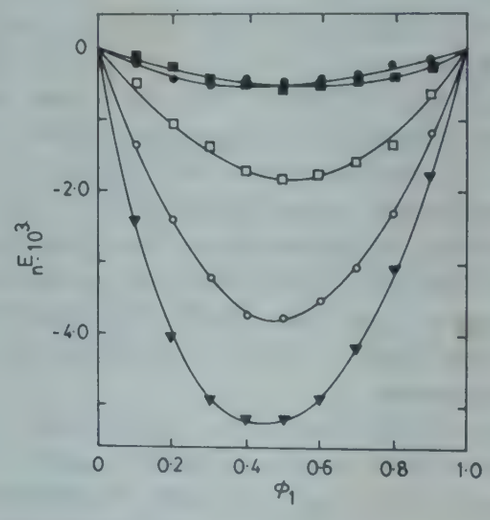

Fig. 4 – Excess refractive index (n^E) versus volume fraction (ϕ_1) of first component [symbols are the same as in Fig. 1]

The trend in the behaviour of η^E and G^E is similar for ethyl acetate + cyclohexane and benzene + cyclohexane mixtures as both of these exhibit large negative values with the minima occurring around $\phi_1 = 0.35$-0.5 on the composition scale (Figs 2 and 3). However, mixtures such as ethyl acetate + carbon tetrachloride and cyclohexane + carbon tetrachloride exhibit negative quantities but with different trend in their variations over the composition scale. A flattened U-shaped

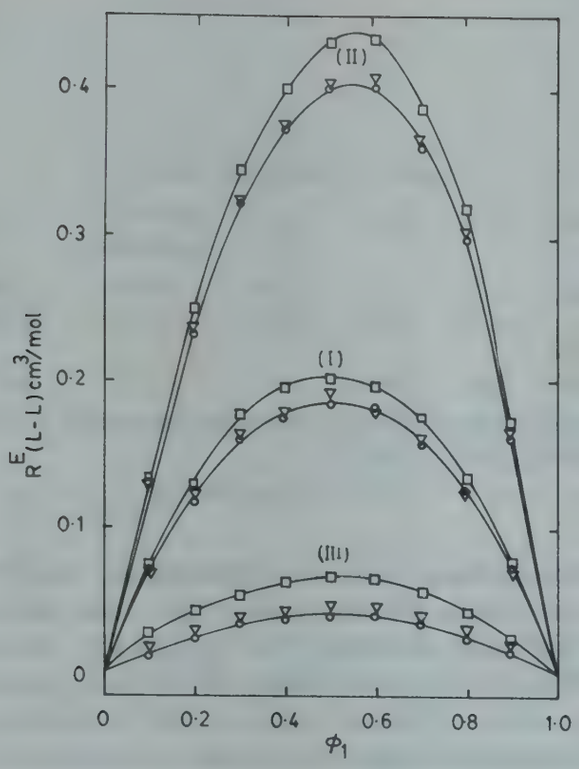

Fig. 5 – Excess molar refraction (R^E) versus volume fraction (ϕ_1) of benzene in mixtures with (I)-ethyl acetate, (II)-carbon tetrachloride and (III)-cyclohexane at wavelengths (○) 589 nm; (▽) 546 nm and (□) 436 nm.

behaviour is seen for G^E and η^E of benzene + carbon tetrachloride mixture whereas ethyl acetate + carbon tetrachloride shows a sigmoid behaviour for G^E. For benzene + ethyl acetate mixture, both G^E and η^E are negative.

Large negative n^E is observed for benzene + cyclohexane and ethyl acetate + cyclohexane mixtures at 589 nm (Fig. 4). However, benzene + ethyl acetate, cyclohexane + carbon tetrachloride and ethyl acetate + carbon tetrachloride mixtures at 589 nm show small negative n^E. The only system which exhibits positive n^E is benzene + carbon tetrachloride. It may be pointed out that for this system even values of V^E, G^E and R^E are also positive. The data at other wavelengths namely, 546 and 436 nm are not presented but the trend in their behaviour at these wavelengths is more or less the same. It should be noted that Eq. (3) used to compute n^E is identical to Heric and Posey relation[8]. The binary interaction term A_{12} as suggested by Heric and Posey[8] is the same as n^E of Eq. (3).

Dependence of ϕ_1 on excess molar refraction (R^E) as calculated from Lorentz-Lorenz mixing rule[7] is shown in Fig. 5 for only a few representative mixtures at three selected wavelengths. The curves are symmetric showing maxima around the middle of the composition scale. Larger positive values are seen for benzene + carbon tetrachloride mixture as compared to the mixture of benzene with either ethyl acetate or cyclohexane. However, for other mixtures namely, ethyl acetate + cyclohexane, ethyl acetate + carbon tetrachloride and cyclohexane + carbon tetrachloride negative values of R^E are observed (graphs not displayed). Very small negative values for ethyl acetate + carbon tetrachloride and large negative values for cyclohexane + carbon tetrachloride have been observed.

T M Aminabhavi wishes to thank Prof. P E Cassidy of Southwest Texas State University for facilities provided during the preparation of this manuscript.

References

1 Aminabhavi T M, Manjeshwar L S & Balundgi R H, *Indian J Chem*, **25A** (1986) 465.
2 Aminabhavi T M, Manjeshwar L S & Balundgi R H, *Indian J Chem*, **25A** (1986) 820.
3 Aminabhavi T M, Manjeshwar L S, Balundgi R H & Muddapur M V, *Indian J Chem*, **26A** (1987) 106.
4 Aminabhavi T M, *J chem Engng Data*, **32** (1987) 406.
5 Aminabhavi T M & Munk P, *Macromolecules*, **12** (1979) 607.
6 Aminabhavi T M & Munk P, *Macromolecules*, **12** (1979) 1186.
7 Lorentz H A, *Theory of electrons* (Teabner & Leipzig) 1909.
8 Heric E L & Posey C D, *J chem Engng Data*, **10** (1965) 340.

Indian Journal of Chemistry
Vol. 27A, June 1988, pp. 532-535

Studies of New Zeolite Derivatives of Stilbite

NEELU SINGHAI & SATI PRASAD BANERJEE*
Department of Chemistry, Dr H.S. Gour Vishwavidyalaya
Sagar 470 003

Received 15 *May* 1987; *revised and accepted* 16 *November* 1987

Natural zeolite stilbite and its Ag(I)-exchanged derivative have been studied by IR spectral, XRD and TG analyses and the results obtained have been reported. Both physical and chemical adsorptions have been indicated in the interactions of CO_2, NH_3 and H_2S adsorbates with adsorbents stilbite and its Ag(I)-exchanged form.

Naturally occurring mineral stilbite has been used to prepare cation-exchanged derivative with Ag(I) and both the zeolites have been used for adsorbing CO_2, NH_3 and H_2S. The aim of the present study is to test their suitability as cation exchangers and adsorbents for CO_2, H_2S and NH_3. Ag(I)-exchanged zeolites have found applications in radio-iodine monitoring[1] and isomerization of 1-butene[2]. Similarly, adsorbates like H_2S and NH_3 pose hazards both in the atmosphere and water and need to be controlled[3].

The stilbite specimen, from the region around Deccan trap, was obtained from GSI, Pune. It was finely powdered in a mechanical grinder and sieved to obtain uniform particle size. Its Ag(I)-exchanged derivative was prepared by treating a portion repeatedly with aqueous silver sulphate solution followed by filtration, washing and air-drying. The adsorbed derivatives were prepared by the procedures described in an earlier communication[4]. Both stilbite and Ag(I)-exchanged form were analyzed for Na(I), Ca(II) and Al(III) using a Varian Techtron AA-6 Atomic Absorption Spectrometer. TG analysis of the samples was carried out upto 800°C at a heating rate of 10°C min^{-1} on a thermobalance supplied by FCIL, Sindri IR spectra of the samples and their residues, after TG analysis, were recorded between 4000 and 200 cm^{-1} in KBr on a Perkin-Elmer IR spectrophotometer. The X-ray diffractograms, obtained between 2θ angles of 5° and 70° using a Philips PW1140 XRD unit and copper target, are reproduced in Figs 1 and 2.

The analytical data of stilbite sample are given in Table 1. TG analysis gave a mass loss of 17.66% which can be attributed to its dehydration. The analytical data for Ag(I)-exchanged stilbite are also given in Table 1. It showed a mass loss of 20.99% on TG analysis. The change in the composition is the direct result

Table 1—Analytical Data

Sample	Na%	Ca%	Al%	Si% + O% (by difference)	H_2O%
1. Stilbite	0.62 (0.79)†	4.76 (5.50)	8.15 (9.28)	68.81 (64.63)	17.66 (19.80)
2. Ag(I)—stilbite	0.46	0.80	6.57	71.18	20.99

† Figures in parentheses are for the ideal composition of stilbite: $NaCa_4Al_{10}Si_{26}O_{72}.32H_2O$[14]

of cation exchange and can be interpreted as follows. Whereas stilbite showed Ca(II)/Na(I) ratio as 4.4:1, Ag(I)-exchange altered it to 1:1 thereby showing more than four times exchange of Ca(II) compared to that of Na(I). The reduction in the percentage of Al(III) is an indication of the extent of dealumination and increase in the Si/Al ratio. IR spectral data between 4000 and 200 cm^{-1} and XRD data using CuK_α radiation of both stilbite and the Ag(I)-exchanged form have been used to characterize them[5-7]. The results of IR spectral studies (Table 2) of the adsorbed derivatives exhibit the presence of the adsorbate species. Additional bands for free CO_3^{2-}(II) ions (1440 cm^{-1}), physically adsorbed H_2S (1390 cm^{-1}) and NH_4(I) ions (1450 cm^{-1}) are seen in the IR spectra of the CO_2, H_2S and NH_3 interacted derivatives of stilbite. On the other hand, IR band for physically adsorbed CO_2 (2300 cm^{-1} appears in the case of CO_2-interacted Ag(I)-exchanged stilbite. There is also definite indication of complex formation with NH_3, giving rise to $[Ag(NH_3)_2]^+$ species in the IR spectrum of ammonia interacted Ag(I)-exchanged stilbite which shows IR bands at 1500 and 250 cm^{-1}. The H_2S interaction results in the formation of a black sample, and the presence of Ag_2S species is indicated by the IR band at 2380 cm^{-1}. The IR spectra of the residues obtained after TG analysis show no bands for physically adsorbed water molecules and the adsorbed species indicating thereby dehydration, desorption and dehydroxylation as the major thermal events on heating the samples at a constant rate. Most of the TG plots exhibit loss of physically adsorbed water and the adsorbates at temperature upto 573K and dehydroxylation and decomposition above it. All the eight samples studied show distinct features in their TG plots and different values for total mass loss upto 1073K. Thus, H_2S interacted stilbite shows a fast rate of mass loss starting around 673 K over a 80 K stretch in its TG plot. Ammonia-interacted stilbite, on the other hand, shows an abrupt and very fast mass loss step around

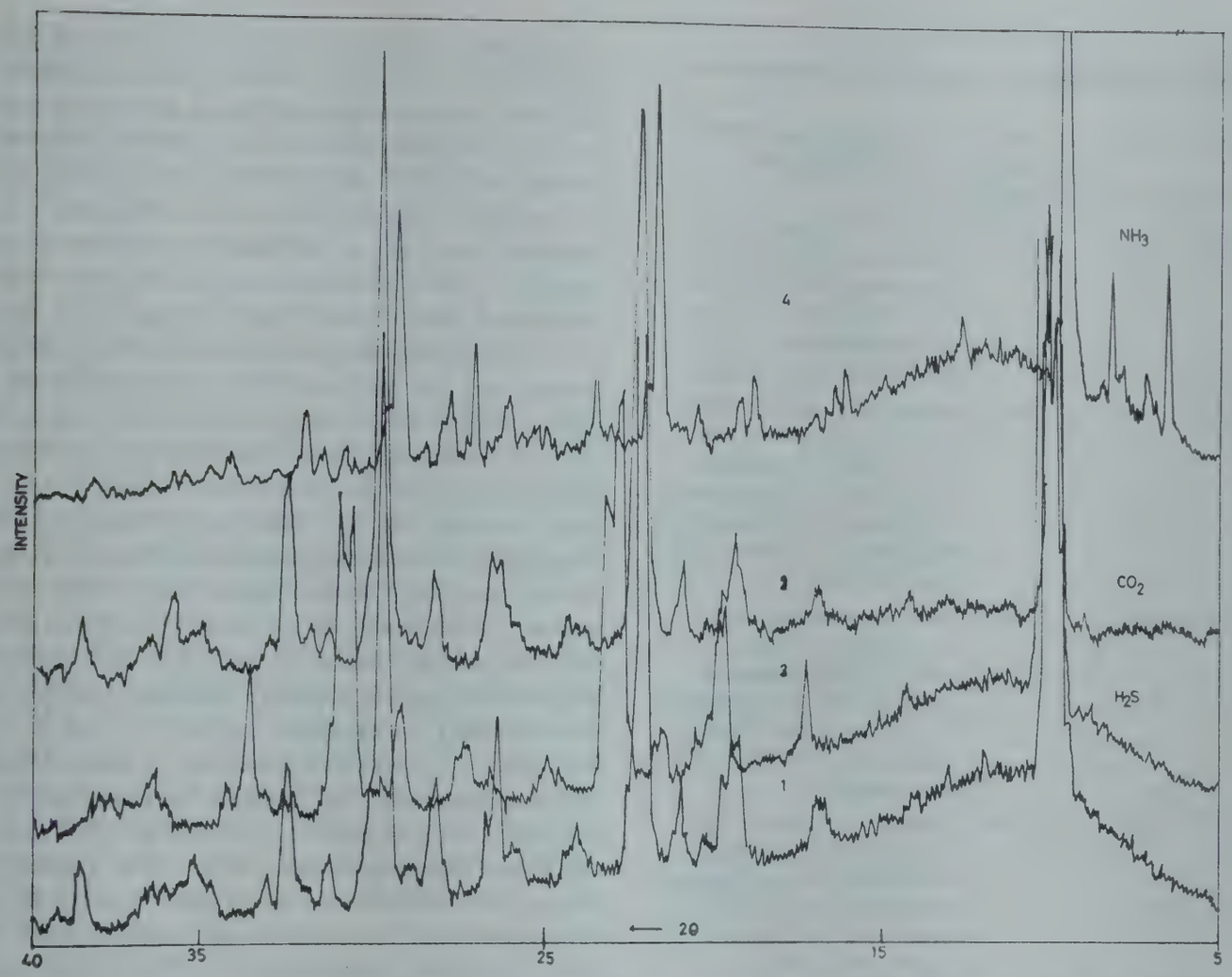

Fig. 1—X-ray diffractogram between 2θ-values of 5° & 40° of 1. stilbite, 2. stilbite + CO_2, 3. stilbite + H_2S. 4. stilbite + NH_3

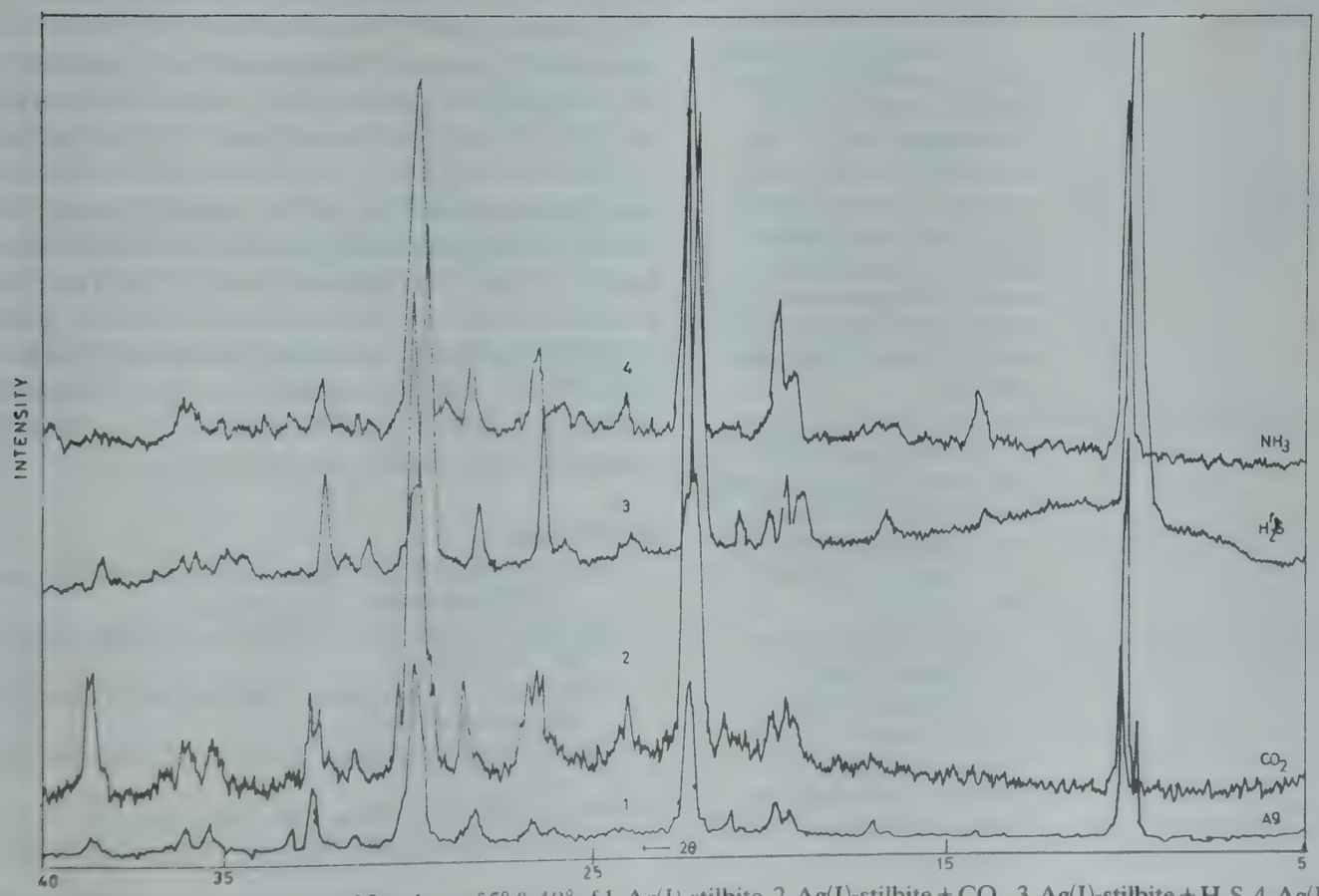

Fig. 2—X-ray diffractogram between 2θ-values of 5° & 40° of 1. Ag(I)-stilbite, 2. Ag(I)-stilbite + CO_2, 3. Ag(I)-stilbite + H_2S, 4. Ag(I)-stilbite + NH_3

Table 2—Summary of Thermal & IR Spectral Data

Sample	Total mass loss(%)	IR peaks (cm^{-1}) with assignments
1. Stilbite	17.66	3620 (O—H stretch), 1675 (O—H bend), 975-1095 (asymmetric T—O stretch), 710 (symmetric T—O stretch), 570 (double rings), 450 (T—O bend), 330 (pore opening).
2. Stilbite + CO_2	16.45	3600 (O—H stretch), 1670 (O—H bend), 1440, 1430 (CO_3^{2-}), 1050 (asymmetric T—O stretch), 715 (symmetric T—O stretch), 580 (double rings), 460 (T—O bend), 310 (pore opening).
3. Stilbite + H_2S	20.18	3630 (O—H stretch), 1680 (O—H bend), 1390 (H_2S phys.), 1030 (asymmetric T—O stretch), 710 (symmetric T—O stretch), 560 (double rings), 445 (T—O bend), 280 (pore opening).
4. Stilbite + NH_3	29.69	3590 (O—H stretch), 3470 (NH_4^+), 1695 (O—H bend), 1460 (NH_4^+), 960-1100 (asymmetric T—O stretch), 725 (symmetric T—O stretch), 580 (double rings), 450 (T—O bend), 360 (pore opening).
5. Ag(I)-Stilbite	20.99	3610 (O—H stretch), 1665 (O—H bend), 1030 (asymmetric T—O stretch), 710 (symmetric T—O stretch), 560 (double rings), 440 (T—O bend), 315 (pore opening).
6. Ag(I)-Stilbite + CO_2	16.55	3420, (O—H stretch), 2320 (CO_2 phys.), 1630 (O—H bend), 1020 (asymmetric T—O stretch), 690 (symmetric T—O stretch), 550 (double rings), 440 (T—O bend), 310 (pore opening).
7. Ag(I)-Stilbite + H_2S	25.10	3600 (O—H stretch), 2380 (H—S bend), 1665 (O—H bend), 1430 (H_2S phys.), 1080 (asymmetric T—O stretch), 565 (double rings), 430-460 (T—O bend, Ag—S bend), 345 (pore opening).
8. Ag(I)-Stilbite + NH_3	13.53	3600 (O—H stretch), 3480 (N—H stretch), 1690 (O—H bend), 1530 (N—H bend), 1040 (asymmetric T—O stretch), 720 (symmetric T—O stretch), 570 (double rings), 440 (T—O bend), 250 (Ag—N linkage).

T = $(Al, Si)O_4$ tetrahedron

733K due to the loss of adsorbed H_2S and NH_3 respectively. Loss of water and CO_2 from stilbite and the CO_2-interacted sample occurs in more gradual steps and above 673K mass loss in both these cases becomes negligible. Among the four zeolite samples prepared by Ag(I)-exchange and subsequent interaction with the three adsorbates the high temperature mass loss is most prominent only in the case of the H_2S interacted derivatives. From around 873K the TG plot of this derivative indicates a fast mass loss step, comprising almost one-third of the total mass loss, due primarily to the decomposition of Ag_2S. Influence of dehydration and repetitive oxidation and reduction steps on the structures of Ag(I)-Y type zeolites[8] and Ag(I)-stilbite[9] has been investigated earlier. During the reduction Ag metal was found to precipitate as cluster within the void of the zeolite network and as crystallites on the surface. XRD plots are reproduced in Figs 1 and 2. Crystal structure of stilbite is known from earlier studies[10]. Evidence of site selectivity of Ag(I) in synthetic zeolites A and Y is also available[11-13] and the knowledge of these structural orientations forms the basis in the interpretation of the XRD data of stilbite derivatives obtained with Ag(I) and the various adsorbates. The intensities of the peaks of stilbite are decreased as a result of exchange with Ag(I) ions showing loss of crystal structure. The (230) reflection at 3.98Å becomes very strong from the adsorption of carbon dioxide on Ag(I)-stilbite, while the intensity of (001) reflection is increased to a considerable extent as a result of adsorption of hydrogen sulphide. Ammonia adsorption on Ag(I)-stilbite produces a new (030) reflection at 6.23Å while the (600) reflection becomes diffused. It has been suggested by earlier workers that interference by the high scattering power of silver may be misleading. Some differences exist in the X-ray diffractograms of stilbite and its adsorbed derivatives. Intensity of (001) reflection is reduced as a result of adsorption of CO_2. The H_2S adsorbed derivative exhibits doublets at 8.95Å, 3.90Å and at 2.97Å. Ammonia adsorption produces some new reflections.

References

1 SooHoo G Y, Lin Chien-Chang, Norris R M & Wilkinson C D, *IEEE Trans Nucl Sci*, **22** (1975) 657.

2 Sugihara H, Chen L Y & Yasumori Iwao, *Bull chem Soc Japan*, **47** (1974) 2089.

3 Manahan S E, *Environmental chemistry* (Willard Grant Press, Massachusetts) 1975.

4 Bhattacharya S & Banerjee S P, *Indian J Chem*, **25A** (1986) 104.

5 Pechar F & Rykl D, *Chem Zvesti*, **35** (1981) 189.

6 Joshi M S & Bhaskar B T, *Indian J pure appl Phys*, **19** (1981) 560.

7 Breck D W, *Zeolite molecular sieves, structure, chemistry & use* (John Wiley, New York) 1974.

8 Gellens L R, Mortier W J & Uytterhoeven J B, *Zeolites*, **1** (1981) 85.
9 Herman K, Bica I & Jacob P A, *Magy Kim Foly*, **83** (1977) 34.
10 Slaughter M, *American Mineralogist*, **55** (1970) 387.
11 Nitta M, Matsumoto S & Aomura K, *JCS Chem Commun*, (1974) 552.
12 Nitta M, Ogawa K & Aomura K, *JCS Chem Commun*, (1974) 1015.
13 Matsumoto S, Nitta M, Ogawa K & Aomura K, *Bull chem Soc Japan*, **48** (1975) 1169.
14 Deer W A, Houri R A & Zussman J, *Rockforming minerals*, **Vol. 4** (Longman, London) 1975.

Indian Journal of Chemistry
Vol. 27A, June 1988, pp. 536-537

Studies on New Mesogens: Part II-*p*-(*p'*-*n*-Alkoxycinnamoyloxy)benzylidene-*p''*-*n*-butoxyanilines

J M LOHAR & D N DHABHAI*

P G Chemistry Department, M L V Govt. College, Bhilwara 311 001

Received 8 *April* 1987; *revised* 28 *July* 1987; *accepted* 6 *October* 1987

The title series (I) is a very high melting series and exhibits rich mesomorphism. The polymesomorphism prevails at about 85°C. The nematic-isotropic transitions show odd-even effect. The smectic-nematic transition curve rises smoothly enhancing the smectic mesophase range at the cost of nematic mesophase length. The nematic mesophase shows a threaded texture while the smectic mesophase exhibits a focal conic fan-shaped smectic A texture.

A new homologous series of mesogens, *p*-(*p'*-*n*-alkoxycinnamoyloxy) benzylidene-*p''*-*n*-butyoxyanilines (I) has been synthesised and the behaviour of the compounds as liquid crystals has been studied.

Compounds (I) were synthesised as follows: A mixture of equimolar amounts (0.01 mol) of *p*-(*p'*-*n*-alkoxycinnamoyloxy)benzaldehyde[1] and *p*-*n*-butoxyaniline[2] in ethanol (20 ml) containing a few drops of acetic acid was refluxed for 1-3 hr depending upon the starting aldehyde. The solid products obtained were crystallized from benzene-ethylalcohol (20:80) mixture. The analytical data and transition temperatures of schiff base obtained are compiled in Table 1. Purity of the compounds was checked by TLC.

p-(*p'*-*n*-Alkoxycinnamoyloxy)benzylidene-*p''*-*n*-butoxyanilines (I) are high melting solids. The solid mesomorphic curve follows a zig-zag rising and falling pattern. The nematic-isotropic transition curves show a continuous falling tendency simultaneously displaying odd-even effect upto the eighth homologue, while the nematic property is exhibited upto the octadecyl homologue. Polymesomorphism is exhibited by the series from the sixth member and persists till the last octadecyloxy member. The sixth homologue shows monotropic smectic mesophase. The range of smectic mesophase gets enhanced as the series is ascended.

Extrapolation of the smectic-nematic transition curve to the left is rendered difficult on account of its extremely steep nature at the left tailing end.

The nematic mesophase, as observed under polarising microscope, shows a threaded texture while the smectic mesophase shows a focal conic fan-shaped smectic 'A' texture.

The thermal stabilities and other characteristics of the compounds(I) have been compared with other homologous series, viz. *p*-(*p'*-*n*-alkoxycinnamoyloxy)benzylidene-*p''*-anisidenes[3] (II), *p*-(*p'*-*n*-alkoxycinnamoyloxy)benzylidene-*p''*-phenetidenes[4] (III) and *p*-(*p'*-*n*-alkoxycinnamoyloxy)benzylidene-*p''*-*n*-propoxyanilines[5] (IV).

$$p\text{-}R-O-C_6H_4-CH=CH-COO-C_6H_4-CH=N-C_6H_4-R'(p)$$

Series I: R' = *n*-butoxy; II, R' = methoxy; III, R' = ethoxy and IV, R' = *n*-propoxy.

Table 1—Analytical Data & Transition Temperatures of *p*-(*p'*-*n*-Alkoxycinnamoyloxy)benzylidene-*p''*-*n*-butoxyanilines (I)

n-Alkyl group (R)	Mol. formula	Transition temperatures °C			Found (Calc) %			% Required		
		Smectic	Nematic	Isotropic	C	H	N	C	H	N
Methyl	$C_{27}H_{27}O_4N$	—	134	292	75.5	6.21	3.22	75.52	6.29	3.26
Ethyl	$C_{28}H_{29}O_4N$	—	150	295	75.8	6.52	3.13	75.7	6.6	3.2
Propyl	$C_{29}H_{31}O_4N$	—	145	278	76.1	6.7	3.02	76.15	6.78	3.06
Butyl	$C_{30}H_{33}O_4N$	—	145	283	76.41	6.9	2.95	76.43	7.00	2.97
Pentyl	$C_{31}H_{35}O_4N$	—	131	263	76.69	7.20	2.85	76.70	7.22	2.89
Hexyl	$C_{32}H_{37}O_4N$	(105)	120	270	76.90	7.40	2.80	76.95	7.41	2.81
Heptyl	$C_{33}H_{39}O_4N$	116	142	248	77.12	7.5	2.71	77.19	7.60	2.73
Octyl	$C_{34}H_{41}O_4N$	115	160	258	77.40	7.74	2.65	77.42	7.78	2.66
Decyl	$C_{36}H_{45}O_4N$	105	175	246	77.83	8.10	2.51	77.84	8.11	2.52
Dodecyl	$C_{38}H_{49}O_4N$	117	185	235	78.21	8.38	2.39	78.22	8.40	2.40
Tetradecyl	$C_{40}H_{53}O_4N$	105	188	223	78.55	8.65	2.28	78.56	8.67	2.29
Octaldecyl	$C_{44}H_{61}O_4N$	115	185	200	79.15	9.12	2.08	79.16	9.14	2.09

Value in parenthesis indicates monotropy

Table 2—Average Thermal Stabilities (°C) of Series I-IV

Phase	II	III	IV	I
Nematic-Isotropic	270 (C_6-C_8)	281.3 (C_6-C_8)	254.6 (C_6-C_8)	258.6 (C_6-C_8)
Smectic-nematic or Smectic-isotropic	167.2 (C_{12}-C_{18})	178.6 (C_{12}-C_{18})	182.6 (C_{12}-C_{18})	186 (C_{12}-C_{18})
Commencement of smectic phase	C_8	C_8	C_7 (C_6)*	C_6 (C_5)*

*Monotropy

It is observed that compounds belonging to series II-IV exhibit wider nematic mesomorphic range than those of series (I). These series (II-IV) have lesser smectic mesophase ranges. In terms of the substituent (R′) in the aniline moiety the series I-IV, show the nematic order: II ≥ III > IV > I while the smectic order is: I ≥ IV > III > II. This is also the sequence for the odd-even effect.

Thermal stabilities of the compounds of the present homologous series (I) have also been compared with those of the series II-IV. The calculated values of average thermal stabilities are given (Table 2).

The nematic-isotropic thermal stabilities of these series are quite high, the highest being for series (III). It is observed that as the $-CH_2$ units are added at the right terminal alkyl chain, the nematic-isotropic thermal stability decreases. The $-OC_2H_5$ group in series (III) is highly polar and hence gives rise to high end-to-end adhesion.

The more significant thing is the alternation of the nematic-isotropic stabilities of these series. The series (II and IV) having odd number of carbons at their right terminal alkyl chain show lower thermal stability as compared to that of series I and III having even number of carbons at their right terminal alkyl chain.

References

1 Lohar J M & Patel G H, Paper presented at International Liquid Crystal Conference, Bangalore, 1979.

2 Woodmansee W E, *Mater Evaluation*, **24** (1966) 504.

3 Lohar J M & Dave J, *Mol Cryst Liq Cryst*, **70** (1981) 279-287.

4 Lohar J M & Patel G H, Paper presented at the eleventh National Conference on Crystallography held in Calcutta, 1980.

5 Lohar J M & Dhabhai D N, *J Indian chem Soc*, **64** (1987) 600.

Indian Journal of Chemistry
Vol. 27A, June 1988, pp. 538-539

Charge Density—Activation Energy Correlations in Bromination of Thiophenes by N-Bromosuccinimide in Solution

LALITHA RAJARAMAN & M J NANJAN
Physical Chemistry Department, University of Madras, Madras 600 025
and
V KANNAPPAN*
Chemistry Department, Presidency College, Madras 600 005

Received 5 *August* 1986; *revised and accepted* 4 *August* 1987

The activation energies for N-bromosuccinimide bromination of several thiophene derivatives in 80% (v/v) aqueous acetic acid have been determined and discussed in the light of electron densities at the reaction site. The effect of substituents at different positions of thiophene ring has been investigated quantitatively by the actual calculation of total ($\pi + \sigma$) charge densities at various positions of the substituted thiophenes.

Earlier work from this laboratory reported on the charge-density distributions in several benzene and thiophene derivatives using Hückel LCAO MO and Del Re methods and their correlation with the experimental activation energy (E_a) values in the bromination of these compounds by molecular bromine in 100% acetic acid and acetic acid-water mixtures[1-3]. As an extension, charge densities of eleven thiophene derivatives have now been correlated with activation energies of their bromination by N-bromosuccinimide (NBS) in order to generalise the effect of substituents in thiophene ring towards electrophiles from quantum mechanical data.

Fluka (purum) samples of thiophene, 2-chlorothiophene and ethyl thiophene-2 carboxylate were used as such. 2-Bromothiophene (Fluka), 3-bromothiophene and 2-acetylthiophene were distilled before use. 2-Iodothiophene (b.p. 90°/30 mm) was prepared by iodination of thiophene[4]. 2-Fluorothiophene (b.p. 83°) was prepared by *ipso* fluorination of 2-iodothiophene[5]. Acetic acid (LR, BDH) was purified before use[6]. N-Bromosuccinimide (Riedel, m.p. 176°) was recrystallised and used. The procedure for the rate measurements has been described earlier[6].

The method of separation of bromination products under kinetic conditions has been described elsewhere[7]. The analysis of bromination product of thiophene was done at 220°C using a Varian GC dual column chromatograph model 3700 fitted with a 10%. OV-101 stainless steel column-chrom WHP 80/100 (2m × 1/8 inch) with nitrogen as the carrier gas. The GLC results showed the formation of only 2-bromothiophene. NBS bromination of 2-bromothiophene in 80% (v/v) aqueous acetic acid led to 2,5-dibromothiophene as confirmed by its PMR spectra. 3-Bromothiophene was bromination at position-2. Ethyl thiophene 2-carboxylate, 2-acetylthiophene and 3-acetylthiophene underwent bromination exclusively at 5-position[8-10]. Benzothiophene on bromination gave 3-bromobenzothiophene.

Charge-density calculations

The calculation of σ- and π-charges for 2-acetyl- and 3-acetyl-thiophenes was programmed in FORTRAN for the computer IBM 1130. The π-charges were calculated by the Hückel LCAO MO method. Del Re method was used for σ-charge calculations. Veillard and Pullman[11] have shown that with the correct choice of parameters, this method gives satisfactory charge density distributions comparable with those obtained by SCF calculations, even in large molecules of biological importance. Berthod-Pullman atom and bond parameters were used in these calculations. The π- and σ-systems have been treated separately and the total ($\pi + \sigma$) charge density (Table 1) on an atom was obtained as usual by adding the π- and σ-charge densities on that atom. The data used for other molecules have already been reported by us[2].

The kinetic data obtained for the bromination of thiophenes in aqueous acetic acid using NBS as the brominating agent are given in Table 2. On simple electrostatic considerations, the strong electrophile,

Table 1—π-Charges, σ-Charges and Total ($\pi + \sigma$) Charge Densities at Various Ring Positions in 2-Acetyl- and 3-Acetyl-thiophenes

Position	Charge Densities × 10^3		
	ΔQ_π	ΔQ_σ	ΔQ_t
	2-Acetylthiophene		
S_1	+799	+040	+839
C_2	−177	+003	−174
C_3	−134	−051	−185
C_4	−148	−042	−190
C_5	−151	−081	−232
	3-Acetylthiophene		
S_1	+785	+048	+833
C_2	−141	−089	−230
C_3	−169	+043	−126
C_4	−138	−045	−183
C_5	−156	−086	−242

Table 2—Rate Constants and E_a Values for NBS Bromination of Thiophenes and Charge Densities at Reaction Sites

([Substrate] = [NBS] = 2×10^{-3} mol dm^{-3}; solvent: 80% (v/v) aq. acetic acid)

Compound	$k_1 \times 10^3$ s^{-1} (20°C)	E_a (kJ mol^{-1})	$\Delta Q_t \times 10^3$
Thiophene	17.77	52.3	−256
2-Fluorothiophene	11.51	48.5	−258
2-Chlorothiophene	4.08	58.6	−249
2-Bromothiophene	4.08	51.5	−249
2-Iodothiophene	6.67	43.9	−254
3-Bromothiophene	27.29	55.2	−242
2,5-Dibromothiophene	5.33	63.2	−189
3-Acetylthiophene	1.92	55.2	−242
Benzothiophene	40.30	57.3	−254
Ethylthiophene-2 carboxylate	1.25†	55.2	−216
2-Acetylthiophene	1.38†	59.4	−232

†$k_2 \times 10^5$ (dm^3 mol^{-1} s^{-1}) values at 20°C.

Br^+ is expected to undergo electrophilic attack more easily than the dipolar bromine molecule. This should lead to smaller E_a values in NBS bromination. Contrary to expectations NBS bromination of thiophenes involves higher E_a value as compared to that by molecular bromine. This may be due to the fact that in NBS bromination the approaching electrophile Br^+ is not a bare cation but it is highly solvated in aqueous acetic acid and the extent of solvation should be more than that in the case of bromine molecule.

The experimental activation energy (E_a) value decreases as the total ($\pi + \sigma$) charge density at the reaction centre increases. There is a satisfactory linear correlation between the calculated charge densities and the experimental activation energies. This supports our earlier proposal that Arrhenius activation energy values can be explained on the basis of electron density at the reaction site for bromination of aromatic compounds[12,13]. The linear equations (1) and (2) can be obtained for the E_a values of bromination by molecular bromine and NBS respectively in terms of total charge density (ΔQ_t) at the reaction centre.

$$38.6 - 120 \times \Delta Q_t \quad (n = 10; r = 0.99) \quad \ldots (1)$$

$$33.6 - 82 \times \Delta Q_t \quad (n = 11; r = 0.98) \quad \ldots (2)$$

It is clear from the slopes that in the case of bromination by NBS the effect of total charge density in the E_a values is less than that in bromination by molecular bromine. Thus, the susceptibility of Br^+ to approach reaction centres of different total charge densities is less than that of molecular bromine, which is anticipated on the basis of their relative electrophilicities. Similar observation has also been made in the case of homocyclic aromatic compounds[6].

References

1 Nanjan M J, Kannappan V & Ganesan R, *Mh Chem*, **112** (1981) 581.
2 Nanjan M J, Kannappan V & Ganesan R, *Z Physik Chem, Frankfurt*, **127** (1981) 13.
3 Kannappan V, *Ph.D Thesis, University of Madras*, 1980.
4 Lew H Y & Noller C R, *Org Synth*, **30** (1950) 53.
5 Van Vleck R T, *J Am Chem Soc*, **71** (1949) 3256.
6 Sivakamasundari A S & Ganesan R, *Int J Chem Kinet*, **XII** (1980) 837.
7 Kannappan V, Nanjan M J & Ganesan R, *Indian J Chem*, **19A** (1980) 1183.
8 Marino G, *Prac Nauk Inst Chem Tech Naft Wegla Polit Wrocla*, **15** (1973) 89; *Chem Abstr*, **79**, 77565a.
9 Marino G, *Acad Naz Lineei Rend, Series VIII*, **38** (1965) 700.
10 Hartough H D, *The chemistry of heterocyclic compounds* (Interscience, New York) 1952.
11 Veillard A & Pullman B, *J theor Biol*, **4** (1963) 37.
12 Ganesan R, *Z physik Chem, Frankfurt*, **90** (1974) 82.
13 Nanjan M J & Ganesan R, *Mh Chem*, **110** (1979) 647.

Indian Journal of Chemistry
Vol. 27A, June 1988, pp. 540-541

Mechanism of Ligand Substitution Reaction of Monobipyridyl Complex of Manganese(II)

H M ABU EL-NADER* & M N H MOUSSA

Chemistry Department, Faculty of Science, Mansoura University, Egypt

Received 26 *February, revised* 27 *July* 1987; *accepted* 29 *October* 1987

The kinetics of ligand substitution reaction of $Mnbipy^{2+}$ complex with the trisoxalatocobalt(III) has been investigated spectrophotometrically at 600 nm. The reaction follows a first order kinetics. The rate of reaction increases with increase in [bipyridyl] in the reaction mixtures. Activation parameters have been evaluated. A mechanism consistent with the results has been suggested.

Complexes of Mn(II) are important due to their role in enzyme reactions[1]. The kinetics of complex formation of Mn(II) with bipyridyl was recently studied in different acidic solutions[2]. The relatively low value of the stability constant[3,4] of the complex, $Mnbipy^{2+}$ (4×10^{-4}), which is in accord with the low complexation reactivity of Mn^{2+} aqua ion led us to undertake the title investigation. The results of such studies using the trisoxalatocobalt(III) are reported in this note.

The substitution reaction was studied in the temperature range of 20-40°C, since in this temperature range the rate constant for the thermal decomposition of $K_3[Co(C_2O_4)_3]$ is extremely low[2].

$Mnbipy^{2+}$ complex was prepared in doubly distilled water using Merck grade $MnCl_2.4H_2O$ and 2,2′-bipyridyl. The complex $K_3[Co(C_2O_4)_3].3H_2O$ was prepared according to the method described before[5]. The reaction was followed at 600 nm, the λ_{max} of trisoxalatocobalt(III) using a Unicam SP 1800 UV spectrophotometer. All solutions were allowed to equilibrate at the desired temperature for 1 hr before mixing.

In a series of runs the [trisoxalate complex] was kept constant at 5×10^{-4} mol dm^{-3} while varying $[Mnbipy^{2+}]$. Under these conditions, the reaction followed first order kinetics as revealed by the linear plot of $2+\log(A_t-A_\infty)$ versus time. It is seen that the rate constant decreased with increase in the concentration of $MnCl_2$ and bipyridyl mixtures (Table 1). To attain maximum degree of complexation ($\alpha=0.997$) large excess of $MnCl_2$ solution was used (0.86 mol dm^{-3}).

Table 1—Rate Constants at Different Concentrations of $MnCl_2$ and Bipy

$[(K_3[Co(C_2O_4)_3]=5\times10^{-4}$ mol dm^3 at 28°C)]

$[MnCl_2]_0$ (mol dm^{-3})	[bipy] (mol dm^{-3})	Degree of complexation	$10^4[Mnbipy^{2+}]$ (mol dm^{-3})	$10^3\,k_1$ (s^{-1})
5×10^{-4}	5×10^{-4}	0.15	0.73	9.3
1×10^{-3}	1×10^{-3}	0.25	2.34	3.6
2×10^{-3}	2×10^{-3}	0.35	6.88	2.4

The kinetic measurements were performed at three different temperatures. The rate constants at 20°, 28°, and 35.5°C and $[Mnbipy^{2+}]=[K_3Co(C_2O_4)_3]=10^{-3}$ mol dm^{-3} came out to be 5.35×10^{-4}, 7.4×10^{-4} and 1.07×10^{-3} s^{-1} respectively. The system obeyed the Arrhenius equation. The values of E_a, A, $\Delta H^{\ddagger}$, $\Delta G^{\ddagger}$ and $\Delta S^{\ddagger}$ were evaluated as 34.02 kJ mol^{-1}, 1.2×10^{-3} s^{-1}, 31.51 kJ mol^{-1}, 92.42 kJ mol^{-1} and -202.86 JK^{-1} mol^{-1} respectively. Within the experimental errors, similar values of the activation parameters were obtained at $[K_3Co(C_2O_4)_3]=10^{-3}$ mol dm^{-3} and $[Mnbipy^{2+}]=3\times10^{-3}$ mol dm^{-3}.

The composition of the complex formed between $Mnbipy^{2+}$ and $[Co(C_2O_4)_3]^{3-}$ applying Mauser's method[6,7] (Fig. 1) and Yoe-Jones[8] method was found to be 1:1 irrespective of $[Mnbipy^{2+}]$.

Finally using different concentration ratios of the reactants it was observed that the rate constant increased with increase in $[Mnbipy^{2+}]$ in the pres-

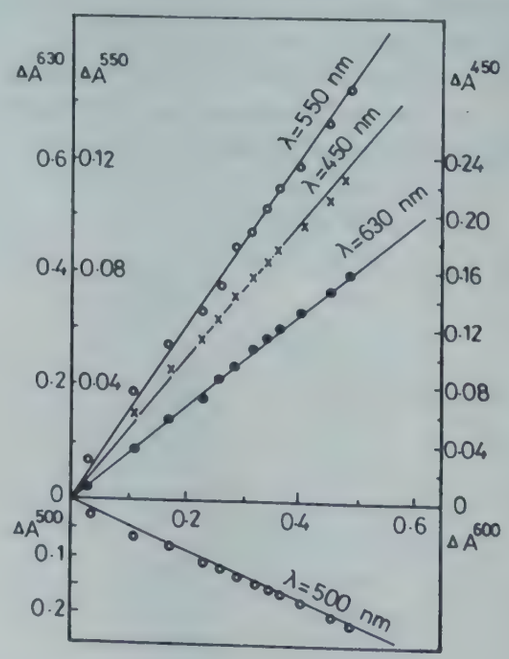

Fig. 1—ΔA diagram for $K_3[Co(C_2O_4)_3]$ and $[Mn\ bipy]^{2+}$ reaction

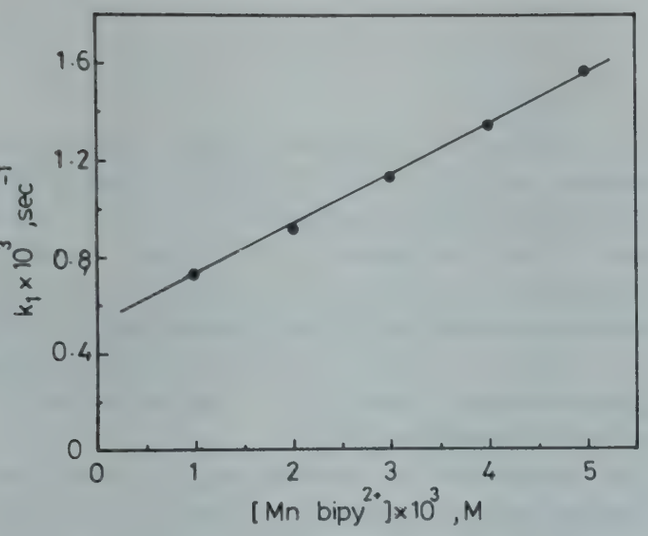

Fig. 2—Variation of k_1 with increasing [Mn bipy^{2+}] at 28°C

ence of large excess of $MnCl_2$ used to diminish the presence of free bipyridyl (Fig. 2). This behaviour is opposite to that observed on adding bipyridyl only to the $K_3[Co(C_2O_4)_3]$ complex[4].

On the basis of observation recorded above, a mechanism shown in Scheme 1 can be suggested for the ligand substitution reaction[9].

$$\text{Mnbipy2} + \underset{k_{-1}}{\overset{k_1}{\rightleftharpoons}} Mn^{2+} + \text{bipy} \qquad \ldots (1)$$

$$\text{bipy} + [Co(C_2O_4)_3]^{3-} \underset{k_{-2}}{\overset{k_2}{\rightleftharpoons}} Co(C_2O_4)_2\text{bipy}^{-1} + C_2O_4^{2-} \qquad \ldots (2)$$

$$C_2O_4^{2-} + \text{Mnbipy}^{2+} \xrightarrow{k_3} MnC_2O_4 + \text{bipy} \qquad \ldots (3)$$

$$C_2O_4^{2+} + Mn^{2+} \xrightarrow{k_4} MnC_2O_4 \qquad \ldots (4)$$

Scheme 1

Based on Scheme 1 the rate-law (5) can be derived:

$$v = k_2[\text{bipy}][Co(C_2O_4)_3]^{3-} = k_3[C_2O_4^{2-}][\text{Mnbipy}^{2+}] \qquad \ldots (5)$$

The above mechanism is supported by the following observations:

(i) First order kinetics in [trisoxalate] at 600 nm. The formation of mixed ligand complex $[Co(C_2O_4)_2$ bipy] is an accepted fact since it has been synthesized and characterized spectrophotometrically[10]. (ii) Reaction rate increases with increase in [Mnbipy^{2+}]. (iii) Similar values of activation parameters obtained irrespective of reactant concentration ratios suggest the formation of only one activated complex. Also, Mouser's method sustains only one linear independent reaction (Fig. 1). (iv) High negative $\Delta S^{\dagger}(= -202.86$ JK^{-1} mol$^{-1})$ confirms that the activated complex $[Co(C_2O_4)_3\text{bipy}]^{1-}$ results from $Co(C_2O_4)_3^{3-}$ in accordance with the extended Hückel theory[11].

References

1 Cohn M & Reuben J, *Account chem Res*, **4** (1971) 214.
2 Murgulescu I G & Oncescu T, *Z phys Chem*, (Leipzig) **214** (1960) 238.
3 Hague D N & Martin S R, *J chem Soc Dalton Trans*, (1974) 254.
4 Abu El Nader H M & Oncescu T, under publication.
5 Werner A, *Ann des Phys*, **59** (1919) 635.
6 Mauser H, *Z Naturforsch*, **23b** (1968) 1021.
7 Mauser H, *Z Naturforsch*, **23b** (1968) 1025.
8 Yoe J H & Jones A L, *Ind Eng Chem Anal Edition*, **16** (1944) 111.
9 Olson D C & Margerum D W, *J Am chem Soc*, **85** (1963) 297.
10 Broombhead J A, Dwyer M & Kane Maguire N, *Inorg Chem*, **7** (1968) 1388.
11 Benedix R, Reinhold J & Henning H, *Inorg chim Acta*, **40** (1980) 47.

Indian Journal of Chemistry
Vol. 27A, June 1988, pp. 542-544

Complexes of Oxovanadium(IV), Chromium(III), Manganese(II), Iron(II), Cobalt(II), Nickel(II) & Copper(II) with 6-Chloro-4-hydroxy-3-acetylcoumarin (Cl – HAC)

(Miss) L NALANDA SHARADA & M C GANORKAR*

Department of Chemistry, Osmania University, Hyderabad 500 007

Received 18 *May* 1987; *revised* 16 *July* 1987; *rerevised and accepted* 7 *September* 1987

Complexes of 6-chloro-4-hydroxycoumarin (Cl – HAC) with oxovanadium(IV), chromium(III), manganese(II), iron(II), cobalt(II), nickel(II) and copper(II) have been prepared and characterised on the basis of analytical, conductance, magnetic moment and spectral data. Magnetic measurements, IR and electronic spectral studies suggest octahedral geometry for Cr(III), Mn(II), Fe(II), Co(II), Ni(II) and Cu(II) complexes and square-pyrimidal geometry for oxovanadium(IV) complex. Infrared spectral studies show monobasic bidentate behaviour of Cl – HAC with oxygen donor system.

Although solution chemistry of transition metal complexes of 4-hydroxy-3-acetylcoumarin is reported[1], no work is done on the synthesis and structural aspects of solid complexes. This note deals with the preparation and characterisation of oxovanadium(IV), Cr(III), Mn(II), Fe(II), Co(II), Ni(II) and Cu(II) complexes of 6-chloro-4-hydroxy-3-acetylcoumarin (Cl – HAC).

All the metal chlorides used were of AR grade. Malonic acid (Riedel), *p*-chlorophenol (Riedel), anhydrous aluminium chloride (Ranbaxy) and acetic anhydride (E. Merck) were used for the preparation of the ligand. The ligand (Cl – HAC) was prepared by reported procedure[2] and its purity was checked by TLC and melting point determination (m.p. 180°C).

The metal complexes were prepared by mixing the hot ethanolic solution of the metal chloride (0.01 mol) and the ethanolic solution of the ligand Cl – HAC (0.02 mol) in 1:2 molar ratio. Vanadyl sulphate and ferrous ammonium sulphate were used for the preparation of oxovanadium(IV) and Fe(II) complexes, respectively. The reaction mixture was refluxed for 2 hr and then cooled. The respective metal chelates separated from the solution at *p*H 6-7. The products thus obtained were filtered, washed successively with ethanol and petroleum ether (60-80°) and dried *in vacuo*. All the complexes are coloured and stable towards air and moisture. They decompose at 300°C. They are insoluble in common organic solvents and sparingly soluble in DMF, dioxane and DMSO. The molar conductance values of 1×10^{-3} *M* solutions of the complexes in DMF show their non-electrolytic behaviour (2-10 mhos cm^2 mol^{-1}). Electrical conductances were measured on a digital conductivity meter model D_1-909 (Digism Electronics) and digital direct reading conductivity meter 304 (Systronics).

The complexes were analysed for their metal contents employing standard procedures after destroying the organic matter with nitric acid. Chloride was estimated as AgCl. Nitrogen was determined by microanalysis.

The magnetic susceptibilities of the complexes were determined by the Gouy method using $Hg[Co(NCS)_4]$ as the calibrant, and experimental magnetic susceptibilities were corrected for diamagnetism[3]. Analytical data of the complexes are given in Table 1.

The electronic spectra of the complexes were recorded on a Carey-14 spectrophotometer in nujol. The infrared spectra of the ligand and the complexes were recorded on a Perkin-Elmer instrument in KBr. ESR spectra were recorded as powder at room temperature on a JEOL-JES-F3X spectrometer.

4-Hydroxycoumarins are known to exhibit tautomerism and the present ligand Cl – HAC can exist in the tautomeric lactone (a) and chromone (b)

Table 1—Analytical Data of the Complexes of Cl – HAC

Complex (molecular formula)	Found (Calc.) %			
	Metal	Carbon	Hydrogen	Chlorine
Cl – HAC	—	55.35	2.93	14.88
($C_{11}H_8O_4Cl$)		(55.34)	(2.99)	(14.90)
Oxovanadium (IV)				
$(Cl – HAC)_2$	9.50	48.82	2.22	12.90
($VC_{22}H_{12}O_9Cl_2$)	(9.40)	(48.83)	(2.210)	(12.93)
$Cr(III)(Cl – HAC)_2Cl.H_2O$	8.961	45.50	2.50	18.40
($CrC_{22}H_{14}O_9Cl_3$)	(8.959)	(45.48)	(2.41)	(18.26)
$Mn(II)(Cl – HAC)_2.2H_2O$	9.80	46.80	2.85	12.60
($MnC_{22}H_{16}O_{10}Cl_2$)	(9.707)	(46.65)	(2.82)	(12.52)
$Fe(II)(Cl – HAC)_2.2H_2O$	(9.90)	46.65	2.75	12.12
($FeC_{22}H_{16}O_{10}Cl_2$)	(9.85)	(46.57)	(2.82)	(12.09)
$Co(II)(Cl – HAC)_n$	10.37	46.45	2.81	12.45
$Co(C_{11}H_6O_4Cl)_n$	(10.34)	(46.327)	(2.80)	(12.44)
$Ni(II)(Cl – HAC)_n$	10.33	46.40	2.90	12.45
$Ni(C_{11}H_6O_4Cl)_n$	(10.30)	(46.34)	(2.808)	(12.44)
$Cu(II)(Cl – HAC)_n$	11.90	49.10	2.99	13.20
$(CuC_{11}H_6O_4Cl)_n$	(11.80)	(49.02)	(2.97)	(13.16)

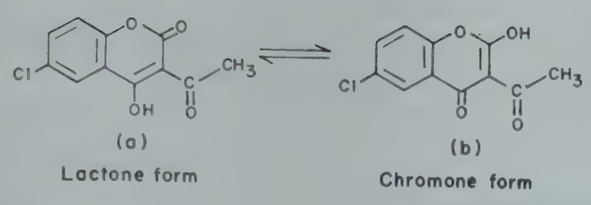

forms. The lactone and chromone forms are expected to show νC=O at 1710 and 1665 cm^{-1}, respectively.

The IR spectrum of Cl−HAC shows a strong band at 1720 cm^{-1}, which confirms that the ligand is in the lactone form. The bands at 1610 and 1440 cm^{-1} are assignable to νC=O (acetyl) and νC−O (phenolic) respectively. The band due to νOH is observed at 3010 cm^{-1} in the ligand spectrum; its low position is attributed to the strong intramolecular hydrogen bonding between the hydroxyl group and acetyl group.

In the IR spectra of all the complexes of Cl−HAC, the band assigned to νOH in the free ligand is absent, suggesting the cleavage of intramolecular hydrogen bonded νOH[5] with subsequent deprotonation of the phenolic OH group and coordintion of oxygen to the metal ion. The positive shift of νC−O (phenolic) by 10 cm^{-1} in all the complexes further confirms coordination through the oxygen of the phenolic group[6]. A new broad absorption in the region 3150-3500 cm^{-1} is observed in case of Cr(III), Mn(II), and Fe(II) complexes which is attributed to the presence of coordinated water[7]. Its presence is further confirmed by the appearance of a non-ligand band at 820 cm^{-1} in Cr(III) and Fe(II) complexes, and at 840 cm^{-1} in Mn(II) complex. The presence of coordinated water was also confirmed by TG and DT analyses[8]. A negative shift of νC=O (acetyl) in all the complexes by 10 cm^{-1} shows the participation of oxygen of the acetyl carbonyl group in complexation. An interesting phenomenon that has been observed is the downward shift by 20-45 cm^{-1} of νC=O (lactone) in Ni(II), Co(II) and Cu(II) complexes indicating the participation of oxygen of the lactone carbonyl in coordination.

Coordination through the oxygen of lactone carbonyl was suggested by some earlier workers for the transition metal complexes of 4-hydroxycoumarins and coumarin-3-carboxylic acid[9]. In other complexes, i.e., complexes of oxovanadium (IV), Cr(III), Mn(II) and Fe(II), no change is observed in νC=O (lactone). New peaks of medium intensity are observed in the range 600-400 which are ascribed to νM−O vibrations[8,10]. For oxovanadium(IV) complex, a strong non-ligand band is observed at 900 cm^{-1} which is assigned to νV=O vibrations[11]. On the basis of IR spectral data, it is concluded that the ligand Cl−HAC utilizes the deprotonated phenolic oxygen and acetyl oxygen as coordinating centres in all the complexes. In addition to these centres, the oxygen of lactone carbonyl is coordinating in Co(II), Ni(II) and Cu(II) complexes.

The oxovanadium(IV) complex is paramagnetic and shows $\mu_{eff.}$ value of 1.75 B.M. which is in good agreement with the expected spin-only value for one unpaired electron at room temperature[12]. Its electronic spectrum displays two absorption bands at 15625 and 20408 cm^{-1} which are assigned to $b_2 \rightarrow e$ and $b_2 \rightarrow a$ transitions respectively[12-14] suggesting square-pyramidal geometry. The room temperature magnetic moment value of Cr(III) complex is 3.9 B.M. which is in agreement with the presence of three unpaired electrons. Irrespective of the strength of the ligand field, there will be three unpaired electrons in mononuclear Cr(III) complexes. The electronic spectrum of Cr(III) complex exhibits three bands at 17400, 24600 and 37060 cm^{-1}. They are assigned to $^4A_{2g} \rightarrow {}^4T_{2g}$, $^4A_{2g} \rightarrow {}^4T_{1g}(F)$ and charge-transfer respectively. From the electronic spectrum it is concluded that Cr(III) complex may have an octahedral geometry[14,15]. The observed magnetic moment value of Mn(II) complex of Cl−HAC is found to be 5.36 B.M. which is low compared to the spin-only value for high-spin Mn(II) complexes. The low value can be attributed to the presence of Mn(III) species[16]. The weak spectral bands in Mn(II) complex observed at 17241, 21276 and 24290 cm^{-1} are attributed to $^6A_{1g} \rightarrow {}^4T_{1g}$ (G), $^6A_{1g} \rightarrow {}^4T_{2g}$ (G) and $^6A_{2g} \rightarrow {}^4E_g$ transitions, respectively. They are in accordance with octahedral stereochemistry[17-19]. The room temperature magnetic measurements of Fe(II) complex show magnetic moment of 5.12 B.M. indicating the presence of four unpaired electrons[20]. The electronic spectrum of Fe(II) complex displays only one band at 12120 cm^{-1} which is assignable to $^5T_{2g} \rightarrow {}^5E_g$ transition. This is consistent with its high-spin octahedral geometry[21]. The magnetic moment of Co(II) complex is 4.46 B.M. suggesting a high-spin octahedral configuration[22]. The high value may be due to the orbital contribution. The Co(II) complex exhibits three bands at 11765, 18180 and 26660 cm^{-1} in the electronic spectrum. The bands can be assigned to $^4T_{1g} \rightarrow {}^4T_{2g}(F)$, $^4T_{1g} \rightarrow {}^4A_{2g}$ and $^4T_{1g}(F) \rightarrow {}^4T_{1g}(P)$ transitions respectively, which are in accordance with its high-spin octahedral geometry[19]. The Ni(II) complex is paramagnetic and shows an effective magnetic moment of 2.8 B.M. which is within the range expected for two

Table 2—Magnetic and Electronic Spectral Data of the Complexes of Cl – HAC

Complex	$\mu_{eff.}$ (B.M.)	λ_{max} (cm^{-1})
Oxovanadium(IV)$(Cl-HAC)_2$	1.75	15625
		20408
Cr(III)$(Cl-HAC)_2Cl.H_2O$	3.9	17400
		24600
		37060
Mn(II)$(Cl-HAC)_2.2H_2O$	5.36	17241
		21276
		24290
Fe(II)$(Cl-HAC)_2.2H_2O$	5.12	12120
Co(II)$(Cl-HAC)_n$	4.46	11765
		18180
		26660
Ni(II)$(Cl-HAC)_n$	2.8	10525
		20000
		25000
Cu(II)$(Cl-HAC)_n$	1.85	15385

unpaired electrons[23]. Its electronic spectrum shows three bands at 10525, 20000 and 25000 cm^{-1} which are attributed respectively to $^3A_{2g} \rightarrow {}^3T_{2g}(F)$, $^3A_{2g}(F) \rightarrow {}^3T_{1g}(F)$ and $^3A_{2g}(F) \rightarrow {}^3T_{1g}(P)$ transitions[19,24]. The observed magnetic moment of Cu(II) complex of Cl – HAC is 1.85 B.M. This value is in good agreement with the presence of one unpaired electron[22]. The Cu(II) complex exhibits an intense broad band in the range 15385 cm^{-1}, which is attributed to $^2T_{2g} \rightarrow {}^2E_g$ transition, suggesting distorted octahedral geometry[19]. The electronic spectral data and magnetic moment data are given in Table 2.

The ESR spectrum of Cu(II) complex is in agreement with the presence of one unpaired electron. The '*g*' value is calculated and found to be 2.545 which is characteristic of the octahedral Cu(II) complexes[25,26] and indicates strong interaction between the ligand and the metal ion.

On the basis of the analytical and conductivity data, magnetic susceptibility measurements, IR, electronic and ESR spectral data, it is concluded that the ligand Cl – HAC behaves as a monobasic bidentate oxygen donor system forming octahedral complexes in the case of Cr(III), Mn(II), Fe(II), Co(II), Ni(II) and Cu(II) and square-pyramidal complex with oxovanadium(IV) ion.

One of the authors (L N S) is thankful to the CSIR, New Delhi, for the award of a Junior as well as a Senior Research Fellowship.

References

1 Manku G S, *Aust J Chem*, **24** (1971) 925.
2 Venkateswara Rao K & Sundera Murthy, *Proc Indian Acad Sci*, **81A** (1975) 118.
3 Figgis B N & Lewis J, *Modern coordination chemistry*, edited by J Lewis & R G Wilkins (Interscience, New York) (1960) 403.
4 Hay R W & Williams P P, *J chem Soc*, (1964) 2270.
5 Rana A K & Shah J R, *J Indian chem Soc*, **58** (1981) 1100.
6 John R Dyer, *Applications of absorption spectroscopy of organic compounds* (Prentice-Hall, New Delhi) 1984.
7 Dutta R L & Ray R K, *J Indian chem Soc*, **60** (1983) 185.
8 Nakamoto K, *Infrared spectra of inorganic and coordination compounds* (Wiley Interscience, New York) 214.
9 Manku G S & Gurucharan S, *Fresenius Z Anal Chem*, **258** (1972) 365.
10 Narang K K & Agarwal A, *Inorg chim Acta*, **9** (1974) 137.
11 Selbin J, *Coord Chem Rev*, **1** (1966) 293.
12 Selbin J & Ortolano T R, *J inorg nucl Chem*, **26** (1964) 37.
13 Donini J C, Hollebone B R & Lever A B P, *Progr inorg nucl Chem*, **22** (1977) 225.
14 Thotia M P, Gurtu J N & Rana V B, *Indian J Chem*, **19A** (1980) 133.
15 Fatta A M & Lintredi R L, *Inorg Chem*, **10** (1971) 478.
16 Holm R H, Everett (Jr) G W & Chakravorty A, *Progr inorg Chem*, **7** (1966) 120.
17 Sengupta S K, Sahni S K & Kapoor R N, *Indian J Chem*, **20A** (1981) 692.
18 Preti C & Tosi G, *Aust J Chem*, **20A** (1976) 543.
19 Lever A B P, *Inorganic electronic spectroscopy* (Elsevier, Amsterdam) 1968, 294.
20 Cotton F A & Wilkinson G, *Advanced inorganic Chemistry*, 3rd Edn. (Wiley Eastern, New Delhi) 1976, 862.
21 Srivastava R S, Yadav L D S, Khare R K & Srivastava A K, *Indian J Chem*, **20A** (1981) 516.
22 Figgis B N & Lewis J, *Progr inorg Chem*, **6** (1964) 37, 67, 157, 185, 210.
23 Drago R S, *Physical methods in inorganic chemistry*, (East-West Press, New Delhi) 1971, 395, 328.
24 Singh N K, Agarwal Seema & Agarwal R C, *Indian J Chem*, **21A** (1982) 973.
25 Toy A D, Cheston S H A, Pilbrow I R & Smith T D, *Inorg Chem*, **10** (1971) 2219.
26 Hathway B J & Billing D E, *Coord Chem Rev*, **5** (1970) 143.

Indian Journal of Chemistry
Vol. 27A, June 1988, pp. 545-546

Lanthanide Nitrate Complexes of Schiff Base Derived from 1-Isonicotinyl-Hydrazide & 2-Hydroxy-1-Naphthaldehyde

H JAYASANKAR & P INDRASENAN*
Department of Chemistry,
University of Kerala, Trivandrum 695034

Received 31 *August* 1987;
revised and accepted 12 *October* 1987

New complexes of lanthanide nitrate with 1-isonicotinyl-2-(2-hydroxy-1-naphthylidene)hydrazine (INHNH) having the general formula $[Ln(INHNH)_2NO_3]$ (where Ln = La, Pr, Nd, Sm, Gd, Dy and Y), have been synthesised and characterised by elemental analyses, and magnetic, conductance, IR and electronic spectral data. The ligand is shown to act as a monovalent terdentate ligand and the nitrate ion is coordinated monodentately offering a coordination number of seven to the lanthanide ion.

Recently, some interesting lanthanide complexes with schiff bases derived from salicylaldehyde, *o*-hydroxyacetophenone and 2-hydroxynaphthaldehyde and benzoyl- and 2-picolyl-hydrazides have been reported[1]. As a part of our programme on the synthesis and characteristion of solid lanthanide complexes[2-5], we report herein the synthesis and characterisation of lanthanide nitrate complexes with a schiff base derived from isonicotinylhydrazide and 2-hydroxy-1-naphthaldehyde. The ligand, 1-isonicotinyl-2-(2-hydroxy-1-naphthylidene) hydrazine (INHNH) is of special interest as it contains four potential donor sites.

The nitrates of lanthanum, praseodymium, neodymium, samarium, gadolinium, dysprosium and yttrium were prepared in the laboratory[5]. The ligand (INHNH) was prepared by a method similar to that given in literature[6,7]. The purity of the ligand was checked by its melting point, elemental analyses and IR spectrum.

Lanthanide nitrate (2 mmol) was dissolved in acetone (15 ml). The ligand, INHNH (4.1 mmol) was suspended in acetone (150 ml) and refluxed on a water-bath until it was completely dissolved. The lanthanide nitrate solution was slowly added to it. The resulting solution was further refluxed for 2 hr. The precipitated complex was filtered, washed several times with hot acetone and dried *in vacuo* over P_4O_{10}. The metal contents of the complexes were determined by conventional method[8].

The room temperature ($28 \pm 2°C$) magnetic susceptibilities of the complexes were measured by Gouy's method and appropriate diamagnetic corrections were applied[9]. The molar conductances of 10^{-3} *M* solutions of the complexes in methanol were determined at $28 \pm 2°C$ using an ELICO CM 82T conductivity bridge with a dip-type cell with platinum electrodes (cell constant = 1.32

Table 1 – Elemental Analysis, Magnetic Moment and Molar Conductivity Data of Lanthanide Nitrate Complexes of 1-Isonicotinyl-2-(2-hydroxy-1-naphthylidene)hydrazine (INHNH)

Complex	Elemental analysis*				Magnetic moment μ_{eff} BM	Molar conductivity in methanol $Ohm^{-1}cm^2mole^{-1}$
	Metal %	Carbon %	Hydrogen %	Nitrogen %		
$[La(INHNH)_2NO_3]$	17.54 (17.78)	52.10 (52.25)	3.12 (3.32)	12.32 (12.54)	0.0 (0.0)	58.08
$[Pr(INHNH)_2NO_3]$	17.47 (17.99)	52.04 (52.11)	3.20 (3.32)	12.28 (12.52)	3.4 (3.6)	31.68
$[Nd(INHNH)_2NO_3]$	18.00 (18.34)	51.75 (51.89)	3.18 (3.30)	12.16 (12.46)	3.5 (3.6)	32.47
$[Sm(INHNH)_2NO_3]$	19.32 (18.97)	51.32 (51.49)	3.14 (3.28)	12.15 (12.37)	1.5 (1.5-1.6)	36.83
$[Gd(INHNH)_2NO_3]$	20.07 (19.77)	50.92 (51.04)	3.08 (3.25)	12.02 (12.26)	7.6 (7.9)	32.52
$[Dy(INHNH)_2NO_3]$	20.04 (20.10)	50.52 (50.71)	3.02 (3.23)	11.96 (12.18)	10.6 (10.6)	48.31
$[Y(INHNH)_2NO_3]$	12.21 (12.16)	55.46 (55.82)	3.20 (3.56)	12.98 (13.40)	0.0 (0.0)	36.23

*Calculated values are in parentheses.

cm^{-1}). The IR spectra were recorded in KBr on a Perkin-Elmer 397 IR spectrophotometer. The electronic spectra were recorded in methanol ($\sim 10^{-4}$ *M*) on a Hitachi 220 A UV-visible spectrophotometer in the range 185-900 nm.

The analytical, magnetic moment and molar conductivity data are presented in Table 1. These complexes are reddish-violet, non-hygroscopic solids soluble in methanol and ethanol and insoluble in acetone, acetonitrile, nitrobenzene, benzene, petroleum ether and diethyl ether. These complexes have the general formula $Ln(INHNH)_2NO_3$ (where Ln = La, Pr, Nd, Sm, Gd, Dy and Y). Molar conductances of the complexes in methanol (Table 1) indicate their nonelectrolytic nature. This shows that the nitrate ion present in each complex is coordinated to the metal ion. The magnetic moments measured at room temperature show that La and Y complexes are diamagnetic and the other five complexes are paramagnetic as expected. The observed moments are generally found to agree well with the theoretical values calculated by the Van Vleck formula[10].

The ligand exhibits bands in its IR spectrum at 3200, 1670, 1600 and 1275 cm^{-1} assignable to νOH (H-bonded), νC=O, νC=N and νC−O (phenolic), respectively. However, in the spectra of the complexes, the νOH (phenolic) mode disappears indicating deprotonation followed by coordination to the metal ion. This agrees with the elimination of two of the three nitrate ions originally present in the metal salt used. The νC=O, νC=N and νC−O bands were found to shift and appeared at 1610, 1550 and 1300 cm^{-1}, respectively. These shifts indicate that the ligand acts as a monovalent terdentate ligand coordinating through the oxygen atoms of the phenolic −OH and >C−O groups and nitrogen atom of the >C=N group. The higher shift of phenolic νC−O (from 1275 to 1300 cm^{-1}) suggests the chelate formation on complexation.

The two medium bands at ~1455 and 1330 cm^{-1}, which are present only in the IR spectra of the complexes are assigned to ν_4 and ν_1 vibrations, respectively of the coordinated nitrate ion. The magnitude of $\nu_4 - \nu_1$ is ~125 cm^{-1} in these complexes, which indicates that the nitrate group is coordinated to the lanthanide ion in a monodentate fashion[11].

The electronic spectrum of the free ligand exhibits two $n \rightarrow \pi^*$ transitions at 27.02 and 30.30 kK, and a $\pi \rightarrow \pi^*$ transition at 42.55 kK. For the complexes, the higher freqency $n \rightarrow \pi^*$ transition is unchanged in energy, the lower energy $n \rightarrow \pi^*$ transition is not observed and the $\pi \rightarrow \pi^*$ band is split and appears at ~45.45 and ~39.21 kK. These complexes show a very broad band at 23.81 kK in the visible region, which is assigned to L→M charge-transfer transition. This band is so strong that the *f-f* bands of the lanthanide ions are obscured. No band due to hypersensitive transition is observed for the Nd^{3+} complex.

On the basis of the above discussion, in these complexes the ligand, INHNH forms two six-membered rings with the metal ion, which is a very stable arrangement. The ideal geometries for the complexes with a coordination number of seven are monocapped trigonal prism, monocapped octahedron and pentagonal bipyramid. The exact geometries of the present complexes can be ascertained only by X-ray diffraction studies on single crystals.

We are thankful to Prof C G R Nair for his keen interest and helpful suggestions and the University of Kerala for the award of a research fellowship to one of us (HJ).

References

1 Dutta R L & Das B R, *Indian J Chem*, **22A** (1983) 207.
2 Giri V & Indrasenan P, *Polyhedron*, **2** (1983) 573.
3 Radhakrishnan P K, Indrasenan P & Nair C G R, *Polyhedron*, **3** (1984) 67.
4 Jayasankar H & Indrasenan P, *Indian J Chem*, **26A** (1987) 964.
5 Jayasankar H & Indrasenan P, *J Less-Comm Metals*, **132** (1987) 43.
6 Woodman A G & Seymour D E, *Brit*, **727** (1955) 486; *Chem Abstr*, **50** (1956) 5038f.
7 Vogel A I, *A text-book of practical organic chemistry* (Longmans, London), 1956; p. 653.
8 Kolthoff I M & Elving P J, *Treatise on analytical chemistry*, Vol 8, Part 2 (Wiley-Interscience, New York), 1960, p. 29.
9 Lewis J & Wilkins R G (Eds), *Modern coordination chemistry*, (Interscience, New York), 1960, p. 409.
10 Van Vleck J H & Frank N, *Phys Rev*, **34** (1929) 1494.
11 Curtis N F & Curtis Y M, *Inorg Chem*, **4** (1965) 804.

Indian Journal of Chemistry
Vol. 27A, June 1988, pp. 547-549

Mixed Valence Paramagnetic Trinuclear Complexes of Rhodium with N-alkylphenothiazines

B KESHAVAN* & R JANARDHAN

Department of Post-graduate Studies and Research in Chemistry, University of Mysore, Mysore 570 006

Received 24 *July* 1987; *revised and accepted* 7 *December* 1987

Eight mixed valence paramagnetic trinuclear complexes of rhodium, $Rh_3L_2Cl_8$ (L=N-alkylphenothiazine), have been synthesised. The complexes have been characterized on the basis of analytical, conductometric, magnetic, thermal, electronic, IR and EPR spectral data.

Rhodium complexes are receiving increasing attention in recent years owing to their potential as anticancer agents[1]. Paramagnetic complexes of rhodium(II)[2–7] and mixed valence complexes of Rh are rare. N-Alkylphenothiazines are extensively used as tranquilizers[8]. These are excellent electron donors[9]. Complex formation between Rh(III) and phenothiazines in aqueous medium has provided a basis for the spectrophotometric determination[10–12] of Rh(III). Lack of information on mixed valence complexes of Rh has prompted us to undertake the present study on the complexes of Rh with N-alkylphenothiazines.

Rhodium(III) chloride trihydrate and N-alkylphenothiazines (NAP) were used as received. Absolute ethanol and reagent grade ether (dried over sodium) were used.

The complexes were prepared as follows: An ethanolic solution of NAP was added slowly to a constantly stirred ethanolic solution of rhodium(III) chloride trihydrate at room temperature. The rhodium-NAP complexes precipitated immediately; these were filtered, washed several times with ethanol, ether and dried *in vacuo* over fused $CaCl_2$.

Analysis for carbon, hydrogen and nitrogen were performed at the Micro-analytical section of the Central Drug Research Institute, Lucknow. The electrical conductances of the complexes were measured in acetonitrile. The IR spectra were recorded on a Perkin-Elmer IR spectrophotometer Model 257 in KBr discs, far IR spectra on Fourier Transform far IR spectrophotometer Model PE 983 in polythene discs, electronic spectra on a Beckman Model DB spectrophotometer in methanol and EPR spectra on X-Band Varian E4 spectrometer at liquid nitrogen temperature (LNT). Magnetic susceptibilities were determined at room temperature using a Guoy balance. Thermograms were recorded using an Ulvac Sniku-Riko Thermal Analyser TA 1500.

Complexes reported in the present investigation are coloured, non-hygroscopic and are stable at room temperature for long periods. These do not possess sharp melting points. These are slightly soluble in acetonitrile and methanol, freely soluble in DMF and DMSO but insoluble in other common organic solvents and water. Analytical data (Table 1) suggest the formula $Rh_3L_2Cl_8$ {L= propionyl proma-

Table 1—Analytical and Magnetic Data of Rhodium Complexes

Compound	Colour	Found (Calc.), %				$\mu_{eff.}$ (B.M.)
		Rh	C	H	N	
$Rh_3(PP)_2Cl_8$	Violet	24.40 (24.32)	36.78 (37.70)	3.58 (3.76)	4.21 (4.38)	1.52
$Rh_3(MTM)_2Cl_8$	Red	24.62 (24.71)	36.21 (36.50)	3.72 (3.84)	4.71 (4.48)	1.22
$Rh_3(PPC)_2Cl_8$	Red	23.02 (23.45)	36.82 (38.11)	3.26 (3.18)	6.35 (6.35)	1.78
$Rh_3(P)_2Cl_8$	Dark brown	24.20 (24.36)	35.62 (35.79)	3.21 (3.15)	6.49 (6.61)	1.44
$Rh_3(CP)_2Cl_8$	Brown	22.55 (22.72)	34.92 (33.58)	3.46 (3.39)	4.02 (4.12)	1.20
$Rh_3(IP)_2Cl_8$	Brown	26.48 (26.64)	37.21 (37.14)	3.72 (3.44)	4.69 (4.82)	1.63
$Rh_3(AP)_2Cl_8$	Brown	24.82 (24.88)	36.42 (36.56)	3.88 (4.00)	6.48 (6.73)	1.80
$Rh_3(EI)_2Cl_8$	Brown	24.64 (24.84)	37.22 (38.54)	3.62 (3.21)	4.61 (4.50)	1.45

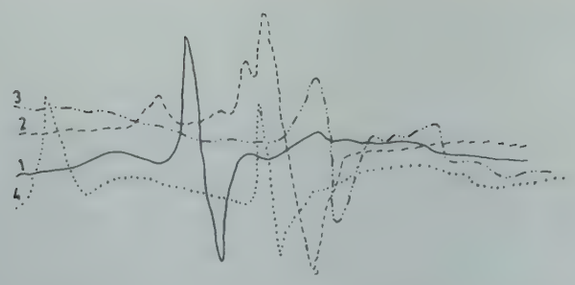

Fig. 1—Powder EPR spectra (LNT) of rhodium complexes of 1. PPC; 2, P; 3, IP; 4, PP

zine (PP), methotrimeprazine (MTM), propericiazine (PPC), perazine (P), chlorproethazine (CP), isopromethazine (IP), aminopromazine (AP) or ethylisobutrazine (EI)} for the complexes. The molar conductances of the complexes in acetonitrile are in the range 15-20 $Ohm^{-1}cm^2mol^{-1}$ indicating the non-electrolytic nature of the complexes.

The $\mu_{eff.}$ values, assuming a trimeric structure for the complexes, are in the range 1.2 to 1.8 B.M per trimer. The paramagnetism of the complexes indicates the presence of Rh(II) in the complexes[2]. N-Alkylphenothiazines, being good reducing agents[9], bring about the reduction of Rh(III) to Rh(II). The EPR spectra of the complexes at LNT (field set: 3200, scan range: 4000, modulation frequency: 100 Hz, microwave frequency: 9.132 GHz, gain: 1.25×10^2g, M.A: $4 \times 10°$ g) exhibit three anisotropic signals[2] (Fig. 1) confirming the presence of Rh(II). A trimeric structure is tentatively proposed for the complexes (Structure I). In this structure, two

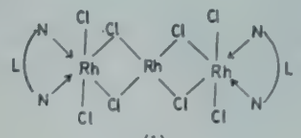

(I)

six-coordinated Rh(III) ions occupy the extreme positions while a four-coordinated Rh(II) ion occupies the middle position. The three metal ions are connected by dichlorobridges. Absence of hyperfine splitting indicates the absence of interacting atoms in the vicinity of Rh(II). Further, the anisotropic signals indicate a planar geometry around Rh(II). The four chlorine atoms surrounding the Rh(II) are probably responsible for the lower magnetic moments shown by the complexes. The insolubility of the complexes in water and common organic solvents and lack of sharp melting points support the polymeric nature of the complexes. The g values obtained for the complexes are in good agreement with those reported for the rhodium maleonitriledithiolate complex[2] (Table 2).

Table 2—EPR Spectra of Rhodium Complexes at LNT

Complex	g_x	g_y	g_z
$Rh_3(PP)_2Cl_8$	2.092	2.014	1.982
$Rh_3(MTM)_2Cl_8$	2.106	2.016	1.952
$Rh_3(PPC)_2Cl_8$	2.102	2.012	1.948
$Rh_3(P)_2Cl_8$	2.108	2.010	1.966
$Rh_3(CP)_2Cl_8$	2.102	2.018	1.958
$Rh_3(IP)_2Cl_8$	2.102	2.016	1.984
$Rh_3(AP)_2Cl_8$	2.096	2.016	1.972
$Rh_3(EI)_2Cl_8$	2.098	2.012	1.964

Sharp bands in the 240-270 nm region found in the UV spectra of both the ligands and their rhodium complexes are assigned to $\pi \rightarrow \pi^*$ transitions. Weak bands in the 300-320 nm region present in the spectra of ligands are shifted towards higher energy region in the spectra of their complexes. This band may be assigned to $n \rightarrow \pi$ transitions[8] and the shift may be due to coordination. Bands observed in the 405-420 nm region in the spectra of the complexes may be due to $^1A_{1g}$ - $^1T_{2g}$ transitions[13] of Rh(III).

In the N-alkylphenothiazine drugs $-R_3NH^+$ interaction with Cl^- ion gives rise to a broad band in the 2500-2300 cm^{-1} region[14]. A broad band observed in the 2600-2350 cm^{-1} region in the infrared spectra of the free ligands corresponds to the $-CH_2NR_2H^+$ (R = Me, Et or Bu) moiety together with X^- (X = Cl, PO_4, malonate or fumarate). In the infrared spectra of the corresponding rhodium complexes, this band either disappears or is reduced to a small hump showing that the tertiary nitrogen atom of the side chain of N-alkylphenothiazines is a site of coordination for the metal. Bands observed in the 2860-2825 cm^{-1} region in the infrared spectra of N-alkylphenothiazines may be assigned to the heterocyclic nitrogen atom attached to alkyl groups[15]. In the infrared spectra of the corresponding rhodium complexes, this band suffers a significant positive shift suggesting the participation of the heterocyclic nitrogen atom in coordination[15]. Thus, infrared spectra has shown that N-alkylphenothiazines act as bidentate chelating agents.

Bands in the 480-460 cm^{-1} region may be assigned to ν(Rh-N) modes and bands around 350 and 280 cm^{-1} are assigned to the terminal and bridging ν(Rh-Cl) modes[16]. Thus, far infrared spectra confirmed the presence of chlorine bridging in the complexes.

The thermal data of the rhodium complexes indicate that the complexes decompose at 190-240°C and attain constant weight at 500-580°C. The final product of decomposition has been characterised as metallic rhodium by X-ray diffraction. The final mass loss suffered by the complexes was in good

agreement with the calculated mass loss in each case.

References

1 Cleare M J, *Coord Chem Rev*, **12** (1974) 349.

2 Billing E, Shupack S I, Waters J H, Williams R & Gray H B, *J Am chem Soc*, **86** (1964) 926.

3 Fischer E O & Wawersik H, *J organomet Chem*, **5** (1966) 557.

4 Masters C, Modonald W S, Raper G & Shaw B L, *J chem Soc Chem Commun*, (1971) 210.

5 James B R & Snynes D V, *J Am chem Soc*, **94** (1972) 6225.

6 Moers F G, Dejong J A M & Beanmont P M H, *J inorg nucl Chem*, **35** (1973) 1915.

7 Van Gaal H L M & Verlaak J M J, *Inorg chim Acta*, **23** (1977) 43.

8 Satoskar R S & Bhandarkar S D, *Pharmacology and pharmacotherapentics* (Popular Press, Bombay) 1976.

9 Dwivedi P C, Rao K G, Bhat S N & Rao C N R, *Spectrochim Acta*, **31A** (1975) 129.

10 Keshavan B & Nagaraja P, *Analyst*, **109** (1984) 835.

11 Keshavan B & Nagaraja P, *Mikrochim Acta*, **III** (1984) 283.

12 Keshavan B & Nagaraja P, *Ann Quim (Rome)*, **75** (1985) 179.

13 Ball Hausen C J, *Introduction to ligand field theory* (McGraw Hill, New York) 1962, 276.

14 Katritzky A R & Boulton A J, *Advances in heterocyclic chemistry*, Vol 9 (Academic Press, New York) 1968, 336-338.

15 Garg S P, Srivastava N M & Sharma V N, *J Indian chem Soc*, **52** (1975) 1160.

16 Finch A, Gates P N, Radcliffe K, Dickson F N & Bentley F F, *Chemical applications of far infrared spectroscopy* (Academic Press, London) 1970, 148.

Indian Journal of Chemistry
Vol. 27A, June 1988, pp. 550-551

Molecular Adducts of Tellurocyclopentane Diperchlorate with Neutral Donors

T N SRIVASTAVA*, M A SIDDIQUI & S K SRIVASTAVA
Chemistry Department, University of Lucknow,
Lucknow 226 007

Received 11 *May* 1987; *revised and accepted* 23 *November* 1987

A freshly prepared solution of tellurocyclopentane diperchlorate reacts with Lewis bases to yield cationic complexes of the type $[C_4H_8Te(L)_2][ClO_4]_2$. These adducts have been characterised and a trigonal bipyramidal structure with one lone pair of electrons occupying one of the positions is proposed for the complex cations.

Triorganotellurium salts containing $[R_3Te]^+$ are known[1], but those containing $[R_2Te]^{2+}$ have been little studied. The first attempt was made by Lowry and Gilbert[2] who prepared dimethyltellurium(IV) diperchlorate, and on the basis of conductivity data formulated it as $[Me_2Te(ClO_4)]^+[ClO_4]^-$. In continuation of our work[3] on the synthesis and reactivity of diorganotellurium(IV) diperchlorates $[R_2Te(ClO_4)_2$, where R = Ph, *p*-$CH_3OC_6H_4$], we report herein the preparation and characterisation of some molecular adducts of tellurocyclopentane diperchlorate with a few Lewis bases.

All operations were carried out under dry N_2 blanket. 1-Tellurocyclopentane diiodide[4] ($C_4H_8TeI_2$) and silver perchlorate[5] were prepared by reported methods. The Lewis bases, viz. pyridine N-oxide (PyO), lutidine N-oxide(Lnt-O), β-picoline N-oxide (β-Pico), quinoline (Q), ν-picoline (ν-pic), 2,2′-bipyridyl (Bipy), phenanthroline (Phen), tetramethylethylenediammine (TMEN) and propylenediamine (pn) (all from BDH) were purified by distillation/recrystallisation.

In a typical preparation, a solution of the $C_4H_8TeI_2$ (0.87 g, 2 mmol) in dichloromethane (~ 30 ml) was stirred with $AgClO_4$ (0.83 g, 4 mmol) for 1 hr at room temperature. The precipitated silver iodide (0.93 g, 98%) was filtered off and the filtrate was treated with a solution of PyO (0.38 g, 4 mmol) in dichloromethane (~ 10 ml). The mixture was refluxed for 5 hr, excess of solvent distilled off, the product precipitated by the addition of excess pet ether (60-80°), filtered, washed repeatedly with the same solvent and dried *in vacuo*.

The analytical data of the molecular adducts are summarised in Table 1. The compounds which are light brown crystalline solids are stable in air and soluble in common organic solvents. These explode on heating. Molecular weights of the adducts were determined in freezing nitrobenzene and are found to be approximately one third of the calculated values indicating these to be 1:2 elecrolytes[6]. This is supported by their molar conductances in acetonitrile and ace-

Table 1—Analytical Data, Melting Points and IR Data of the Adducts

L	m.p.*	Found (Calc) %				ν N=O or ν C=N	
		Te	C	H	N	Free Ligand	Complex
Pyo	210	22.2 (22.2)	29.2 (29.3)	3.0 (3.1)	4.8 (4.8)	1265	1235
LutO	185	20.2 (20.2)	34.3 (34.3)	4.1 (4.1)	4.4 (4.4)	1246	1230
β-PicO	182	21.2 (21.2)	32.1 (31.9)	3.7 (3.6)	4.5 (4.6)	1275	1240
Quo	170	18.8 (18.9)	39.3 (39.2)	3.2 (3.2)	4.1 (4.1)	1230	1210
ν-Pic	120	23.3 (23.4)	30.7 (30.8)	4.0 (4.0)	5.0 (5.1)	1578	1605
Bipy	130	23.2 (23.6)	31.1 (31.1)	3.1 (3.2)	5.1 (5.1)	1560	1575
TMEN	135	25.6 (25.5)	24.0 (24.0)	4.7 (4.8)	5.5 (5.6)	1253 1150 1130 1020	1270 1170 1150 1025
Phen	210	22.6 (22.6)	34.1 (34.1)	3.0 (2.8)	5.0 (4.9)	1578 1485	1585 1530
Pn	142	28.0 (27.9)	18.3 (18.3)	3.8 (3.9)	6.0 (6.1)	1370	1150

*Explode

tone ($10^{-3}M$ solutions) which fall in the range 258.5-278.5 and 185-193 mho mol^{-1} cm^2, respectively.

Infrared spectra of the complexes exhibit strong bands due to $\nu OClO_3$ around 1100 (ν_3) and 625 cm^{-1} (ν_4) indicating that both the perchlorate groups are ionic[7] in confirmity with their molecular weights and molar conductances. Their coordination with oxygen donor ligands occuring via the oxygen atom is revealed by the shift of the free ligand $\nu N=O$ to lower wavenumbers[8]. The ν C=N modes in free bipy[9], phen[10], ν-pic[11] and TMEN[12] undergo shifts to higher wavemembers in the spectra of the complexes suggesting coordination of the bases through nitrogen atoms. The $\nu C=N$ in pn shifts on to lower wavenumbers again indicating coordination through the nitrogen atom[13]. The complexes may be represented as $[C_4H_8Te(L)_2][ClO_4]_2$.

The PMR spectra of $[C_4H_8Te(Bipy)]$ $[ClO_4]_2$ and $[C_4H_8Te(PyO)_2][ClO_4]_2$ were recorded in $CDCl_3$ at room temperature. In the PMR spectra of the complexes, two multiplets of equal intensity appearing at δ 3.30(4H) and 2.38(4H) are attributed to CH_2-Te-CH_2 and $-CH_2$-C protons of the respective ring. In the spectrum of bipy in deuterated chloform, peaks appearing at δ 8.675, 8.490, 7.798 and 7.282 undergo significant shift and appear at δ 8.550(2H), 8.333(2H), 7.830(2H), and 7.349(2H) respectively on complexation. In the spectrum of $[C_4H_8Te(PyO)_2][ClO_4]_2$ phenyl protons of the ligand appear at δ 7.89. The spectra and their integration correspond to the proposed stoichiometry of the complexes. A trigonal bipyramidal structure with one lone pair of electrons occupying one of the positions is tentatively assigned for the complex cations.

Financial assistance from the UGC, New Delhi is gratefully acknowledged.

References

1 McWhinnie W R & Mallaki J, *Polyhedron*, **1** (1982) 13.
2 Lowry T M & Gilbert F L, *J chem Soc*, (1929) 2076.
3 Srivastava T N, Srivastava V K & Srivastava R C, *Polyhedron*, **4** (1985) 1223.
4 Morgon G T & Burstall F H, *J chem Soc*, (1931) 180.
5 Macy R, *J Am chem Soc*, **47** (1925) 1031.
6 Geary W J, *Coord chem Rev*, **7** (1971) 110.
7 Mathaway B J & Underhill A E, *J chem Soc*, (1961) 3091.
8 Sharp D W A, Brown D H & Amasa S, *J chem Soc* **A** (1969) 2892.
9 Carty A J & Tuck D G, *J chem Soc*, (1966) 1081.
10 Schilt A A & Taylor R C, *J inorg nucl Chem*, **9** (1959) 211.
11 Cook D, *Can J Chem*, **42** (1964) 2523.
12 Srivastava T N & Kemboj P C, *Indian J Chem*, **19A** (1980) 167.
13 Srivastava T N, Singh Mala & Singh H B, *Indian J Chem*, **21A** (1982) 307.

Indian Journal of Chemistry
Vol. 27A, June 1988, pp. 552-554

Mixed Ligand Complexes of Uranium

S G DESHPANDE & S C JAIN*
Chemistry Division, Bhabha Atomic Research Centre,
Bombay 400 085

Received 27 *July* 1987; *revised and accepted*
13 *November* 1987

Mixed ligand complexes of U(IV) and dioxouranium(VI) such as UCl_4.2DPC.EA, $2UCl_4$.DPC.2EA, UO_2Cl_2.2DPC.EA, $2UO_2Cl_2$.DPC.2EA, UO_2Cl_2.2DPTC.EA, $UO_2(NO_3)_2$.2DPC.EA, and $UO_2(NO_3)_2$.2DPTC.EA have been prepared by the interaction of UCl_4, UO_2Cl_2 or $UO_2(NO_3)_2$ with 1,5-diphenylcarbazide (DPC) or 1,5-diphenylthiocarbazide (DPTC) as primary ligand and ethyl acetate (EA) as secondary ligand. The compounds have been characterised by elemental analysis, infrared spectral data, molar conductance and thermogravimetric analysis.

1,5-Diphenylcarbazide (DPC) and 1,5-diphenylthiocarbazide (DPTC) are multidentate ligands having five donor atoms each. While in *trans* form these molecules can coordinate to two metal atoms forming two independent 5-membered chelates, in the *cis* form the molecules can form only one 5-membered chelate. The present work was taken up to study whether the ligand molecules could be stabilised in a particular isomeric form by varying the experimental conditions. It was also thought of interest to use ethyl acetate as secondary ligand to utilise other available coordination sites on the metal atoms to obtain mixed ligand complexes.

Uranium salts were prepared and purified by suitable methods[1]. The ligands (Aldrich) were used as such without further purification. The complex compounds were prepared in dry box flushed continuously with dry nitrogen by mixing the reactants in different stoichiometries using tetrahyrofugan (THF) as the solvent. typical examples for the two types of compounds synthesized are given below.

$[UO_2Cl_2.2DPC.EA]$: This class of compounds were prepared in two steps. In the first step, the uranium salt {UCl_4, $UO_2Cl_2.2H_2O$ or $UO_2(NO_3)_2.5H_2O$} and the primary ligand (DPC or DPTC in THF) were mixed in 1:2 molar ratio. The resulting mixture gave an oily product when *n*-.hexane or pentane was added to it. The oily product gave a solid product on reacting with EA (secondary ligand). The product was filtered, washed with 50% (v/v) THF-pentane and dried *in vacuo* at room temperature for several hours.

$[UO_2Cl_2)_2DPC(EA)_2]$: In this case the uranium salt and the primary ligand were reacted in 2:1 molar ratio respectively followed by the addition of EA (secondary ligand) to obtain free flowing solid. The compound was filtered, washed and dried *in vacuo*. The analytical results are reported in Table 1.

The IR spectroscopic measurements in nujol mull (4000-200 cm^{-1}) were carried out on a Perkin-Elmer grating spectrophotometer, Model 577. Molar conductances of the complexes in acetonitrile (10^{-3} *M* solutions) were measured with an Industrial Instrument Inc. conductivity bridge model RC-216-Bl at room temperature. Thermogravimetric measurements of some of the compounds were carried out (300 mg) in air (2.5 lit. h^{-1}) at a heating rate of 4 K min^{-1} using a Stanton thermobalance.

The IR spectra of the 1:2:1 complexes show that in

Table 1—Analytical Results

Compound	Colour (m.p., °C)	Found (Calc.), %					Molar conductance ($Ohm^{-1}cm^2mol^{-1}$)	Mass loss started at °C (TG Data)
		U%	Cl%	C	H	N		
$UCl_4(DPC)_2EA$	Pink (85(d))	24.96 (25.00)	14.54 (14.90)	38.13 (37.79)	4.09 (3.78)	9.43 (11.76)	250	
$2UCl_4DPC\ 2EA$	Brick red (100(d))	41.26 (40.4)	12.13 (12.05)	20.57 (21.40)	3.63 (3.6)	5.25 (4.8)	—	—
$UO_2Cl_2(DPC)_2EA$	Pink (140(d))	26.0 (26.1)	7.07 (7.78)	38.1 (39.4)	2.74 (3.9)	10.4 (12.27)	255	160
$UO_2Cl_2(DPTC)_2EA$	Brown (160(d))	25.41 (25.21)	7.13 (7.52)	39.09 (38.1)	2.81 (3.8)	9.19 (11.85)	260	145
$2UO_2Cl_2DPC_2EA$	Black (170(d))	40.79 (39.47)	13.06 (11.76)	21.14 (20.89)	2.11 (2.48)	3.84 (4.64)	—	170
$UO_2(NO_3)_2(DPC)_2EA$	Blue (145(d))	24.14 (24.62)	— —	38.09 (37.24)	4.1 (3.72)	9.86 (11.58)	255	165
$UO_2(NO_3)_2(DPTC)_2EA$	Black (126(d))	23.16 (23.8)	— —	36.52 (36.05)	3.9 (3.6)	9.92 (11.2)	265	—

this class of compounds the ligand (DPC or DPTC) behaves as a bidentate molecule. The $\nu(C=O)$ and $\nu(C=S)$ bands for the free ligands at 1685 and 825 cm^{-1} shift to ~1616 and ~760 cm^{-1} respectively for the complexes. The N – H stretching frequencies for free DTC consist of several bands in the region 3480-3280 cm^{-1}. These bands in the complexes shift to 3500-3240 cm^{-1} indicating that all the nitrogen atoms are not involved in the coordination. Only the $\nu(N-H)$ bands associated with the coordinating nitrogen and the neighbouring nitrogen are expected to show a negative shift and the others are expected to show a positive shift. The $\nu(C=O)$ band for free ethyl acetate at 1740 cm^{-1} is shifted to 1680 cm^{-1} in the complexes. A bathocromic shift of 60 cm^{-1} suggests bonding of EA through CO group. Since the $\nu(C-O)$ band at 1250 cm^{-1} and $\nu(C'-O)$ band at 1050 cm^{-1} for the free EA $[CH_3C=O-C']$ are also lowered by about 50 cm^{-1}, it is reasonable to propose that EA forms a four-membered ring chelate in the complexes[2].

In the case of 2:1:2 adducts the IR spectra in the $\nu(N-H)$ region show a general lowering of the bands from 3480-3280 cm^{-1} (free ligand) to 3240-3110 cm^{-1} (complex). The $\nu(C=O)$ band of DPC is again lowered from 1685 to 1615 cm^{-1} due to coordination[3]. The $\nu(C=O)$ and $\nu(O-C)$ bands of the secondary ligand EA also appear in the lower wave number region for the adducts. From this, it would seem that DPC molecule coordinates to two uranium atoms forming 5-membered chelate with each uranium atom and EA coordinates forming 4-membered chelate.

Molar conductance measurements of the compounds provide interesting results. While the 2:1:2 adducts in acetonitrile solutions are non-conducting, the 1:2:1 adducts appear to be 1:2 electrolytes[4,5] (Λ_M = 250-60 ohm^{-1} cm^2 mol^{-1}). From the available experimental results it would seem that the 1:2:1 adducts can be formulated as:

$$[UCl_4.(DPC)_2.EA] \rightarrow [UCl_2.(DPC)_2.EA]^{2+} + 2Cl^-$$

$$[UO_2Cl_2.(DPC)_2.EA] \rightarrow [UO_2.(DPC)_2.EA]^{2+} + 2Cl^-$$

$$[UO_2(NO_3)_2.(DPC)_2.EA] \rightarrow [UO_2.(DPC)_2.EA]^{2+} + 2NO_3^-$$

In such a formulation uranium would exhibit a coordination number of eight, the axial oxygens in UO_2 being also considered as ligands. Appearance of IR bands at 1310, 750 and 700 cm^{-1} for ionic nitrate further confirm the ionisation of NO_3^- in the compound[6]. In view of the above observations the 1:2:1 adducts can tentatively be assigned structure(I).

In the case of the 2:1:2 adducts, the DPC molecule can be assumed as a tetradentate bridging ligand, co-

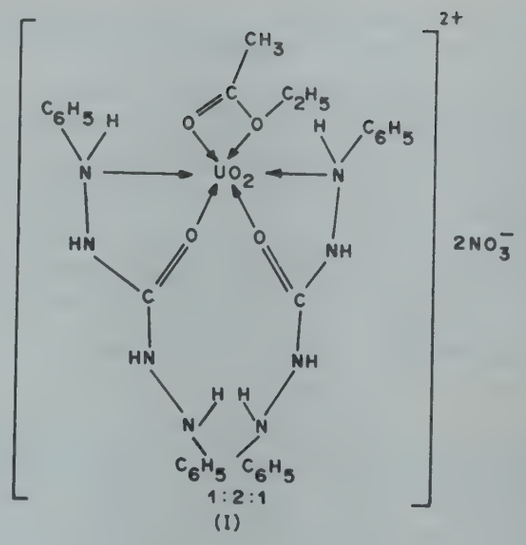

(I)

ordinating to two uranium atoms. The EA molecules occupy two coordinating sites each as shown in structure II.

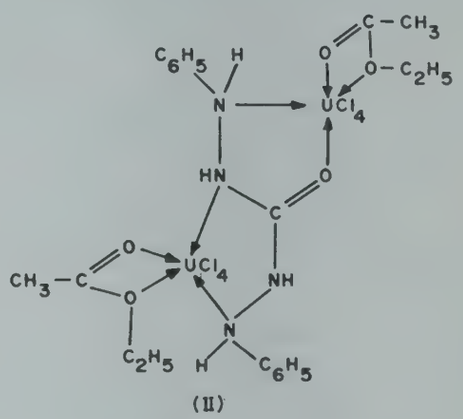

(II)

Thus, a coordination number of eight is attained by uranium atom in both the cases. In the case of $2UO_2Cl_2.DPC.2EA$ adduct, a similar structure would provide equatorial coordination number 6 and axial coordination number 2 to uranium. As expected, the $\nu(N-N)$ band at 985 cm^{-1} (ref. 7) for free DPC is lowered by about 60 cm^{-1} for the 2:1:2 adducts. For the 1:2:1 adducts, however, both shifted and unshifted bands of $\nu(N-N)$ are observed. This further indicates that in the former group of compounds the ligand is acting as tetradentate and in the latter group of compounds as bidentate.

In the case of DPTC adducts the involvement of the C = S group in bonding is supported by the lowering of the $\nu(C=S)$ band from 965 to 930 cm^{-1} as a result of complex formation[8]. The $\nu_{as}(UO_2)$ band for free uranyl ion appears[9] at 965 cm^{-1}. A ligand which forms strong bonding with the uranium atom of UO_2 moiety can effectively decrease the U = O bond order. As a result, $\nu_{as}UO_2$ lowered in the complexes[10]. Using the magnitude of this shift as a criterion of the relative bonding ability of DPC and DPTC towards

UO_2Cl_2 and $UO_2(NO_3)_2$, one can conclude that DPC forms stronger complexes than DPTC.

In the far infrared region, the new bands in the region 450-500 cm^{-1} can be assigned to ν(U-O)[11] where oxygen is of EA and/or DPC. The nitrogen is expected to form a weaker bond with uranium; therefore, the bands in the region 380-400 cm^{-1} are assigned to $\nu(U-N)$[12] and the bands at 265 and 270 cm^{-1} to $\nu(U-S)$. For UCl_4.2DPC.EA and $2UCl_4$.DPC.2EA complexes the bands at 270 and 255 cm^{-1} are assigned to $\nu(U-Cl)$ modes[6].

Thermogravimetric analysis data of these complexes (Table 1) indicate that most of these compounds show major mass loss in the region 250°-400°C. There seems to be a simultaneous decomposition of organic moieties leading to the formation of U_3O_8 as the final residue in each case.

The authors sincerely thank Dr R M Iyer, Director, Chemical Group, Dr J.P. Mittal, Head, Chemistry Division and Dr A.J. Singh, Head, Inorganic Chemistry and Pure Materials Section for their interest in the work.

References

1 Brauer G, *Handbook of preparative inorganic chemistry*, 2nd edn, Vol. 2 (Academic Press, London) 1965.
2 Jain S C & Rivest R, *Can J Chem*, **40** (1962) 2243.
3 Jain S C & Rivest R, *Can J Chem*, **45** (1967) 139.
4 Geary W J, *Coord Chem Rev*, **7** (1971) 81.
5 Giesprecht E & Osorio V K L, *J inorg nucl Chem*, **37** (1975) 1409.
6 Jain S C, Gill M S & Rao G S, *J Indian chem Soc*, **58** (1981) 210.
7 Asmy A A H, Bekheit M, Ibrahim K M & Mostafa M M, *Acta chim hung*, **121** (1986) 391.
8 Beecroft B, Campbell J M & Grzeskowiak R, *J inorg nucl Chem*, **36** (1974) 55.
9 Balakrishnan P V, Patil S K, Sharma H D & Venkatasetty H V, *Can J Chem*, **43** (1965) 2052.
10 Rao G S, Jain S C & Gill M S, *Indian J Chem*, **21A** (1982) 526.
11 Sagoria V S, Gill M S, Jain S C, Ahuja H S & Rao G S, *Inorg chim Acta*, **121** (1986) 233.
12 Jain S C, Gill M S & Rao G S, *J Indian chem Soc*, **63** (1986) 195.

Indian Journal of Chemistry
Vol. 27A, June 1988, pp. 555-557

Studies on the Formation Equilibria of Binary & Ternary Complexes of Copper(II) with Acetylacetone & Some Amino Acids

Y ANJANEYULU*,
N KAMESWARA RAO & R PRABHAKARA RAO
Department of Chemistry,
Nagarjuna University, Nagarjuna Nagar 522 510

Received 5 *May* 1987; *revised* 7 *September* 1987;
accepted 3 *November* 1987

The formation equilibria of [CuAB] type of complexes in six ternary systems where HA = acetylacetone and H_2B = glycine, DL-α-alanine, DL-2-aminobutyric acid, DL-valine, DL-leucine and DL-β-phenylalanine have been studied *p*H metrically at 30°C and $\mu = 0.05$ *M* KNO_3 in 60% (v/v) water-ethanol medium. The acid dissociation constants of these ligands and the stability constants of their binary chelates with Cu(II) have also been determined under identical conditions by Irving-Rossotti method. The stability constants data are discussed in terms of the effect of basicity of the ligand, statistical factors and ring size upon chelation.

Though mixed ligand complexes of Cu(II) with various amino acids have been extensively investigated[1,2], no work has been reported so far on the formation constants of ternary complexes of Cu(II) with acetylacetone and amino acids. In this note a systematic *p*H-metric investigation has been carried out on the formation equilibria of ternary complexes of Cu(II) with acetylacetone and various amino acids viz. glycine (gly), DL-α-alanine (ala), DL-2-aminobutyric acid (2-aba), DL-valine (val), DL-leucine (leu), and DL-β-phenylalanine (pala).

All the chemicals used were of AR grade. Amino acids and cupric nitrate were BDH (India) reagents and acetylacetone Veb Chemie (Germany) reagent. All the amino acids were recrystallised from water-ethanol mixture and their purities were checked before use. Doubly distilled water was used in the preparation of the solutions.

A systronics digital *p*H-meter model No 335 with a combined glass electrode was used. The accuracy of the *p*H-meter was ±0.01 *p*H unit. It was calibrated by buffers of *p*H 4.00 and 9.20 at 30°C.

*p*H-metric titrations were carried out at 30 ± 0.1°C and at an ionic strength of 0.05 *M* (KNO_3) under nitrogen gas free of O_2 and CO_2 atmosphere using a standard experimental set up described elsewhere[3]

The electrode system was calibrated by the method described by Uitert *et al*[4]. The metal to ligand ratio was maintained at 1:5 in the case of binary complexes and 1:1:1 in the case of ternary systems. Due to the low solubility of these complexes in water, the systems were studied in 60% (v/v) water-ethanol medium.

Stabilities of binary complexes

Although the *pK* values of the ligands and the stability constants of binary complexes of Cu(II) with these ligands have already been reported[1,2], we have redetermined these values for the sake of uniformity in experimental conditions, by Irving-Rossotti technique[5] in 60% (v/v) water-ethanol medium at 30°C and $\mu = 0.05$ *M* (KNO_3) and the results are presented in Table 1. The pK_1 and pK_2 values of amino acids agree well with reported values in 50-60% (v/v) isoproponol-water medium[6]. It can be seen from Table 1, that the log K^{Cu}_{CuB} and log $K^{CuB}_{CuB_2}$ metal-ligand formation constants of Cu(II) with amino acids follow the order, gly ≈ ala > 2-aba > val ≈ leu > pala. The values of proton-ligand stabilities of all these ligands are nearly same (except for β-phenylalanine which has low *pK* value) and it can be reasonably expected that their tendencies to form complexes would be similar. However, it can be seen that the complexes with glycine, α-alanine and 2-aminobutyric acid have almost the same log K^{Cu}_{CuB} and log $K^{CuB}_{CuB_2}$ values while valine and leucine, though having basicity closer to that of glycine, have lower values of metal-ligand formation constants. In case of valine and leucine the bulky methyl groups at α-carbon atom cause steric hindrance and make the chelate less stable (Structures A and B). It is also reported that an increase in

Table 1 – Stability Constants of Binary Complexes of Copper(II)

Ligand	pK_1	pK_2	log K^{Cu}_{CuB}	log $K^{CuB}_{CuB_2}$
Acetylacetone (A)	9.80		*9.50	**8.12
DL-Glycine	3.15	9.80	9.50	7.12
DL-α-Alanine	3.25	9.85	9.51	7.04
DL-2-Aminobutyric acid	3.23	9.90	9.47	6.99
DL-Valine	3.22	9.73	9.10	6.60
DL-Leucine	3.30	9.72	9.10	6.60
DL-β-Phenylalanine	3.30	9.25	8.90	5.90

*log K^{Cu}_{CuA}; **log $K^{CuA}_{CuA_2}$

chain length of amino acid results in the decrease in stability of the corresponding complex, which has been explained on the basis of restricted rotation of methyl group around C–C bond in solvent as the chain length is increased[7].

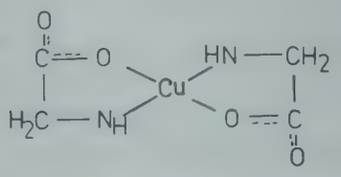

A

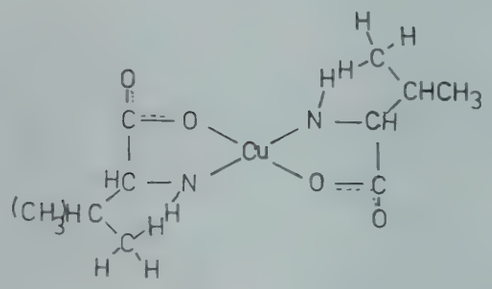

B

The metal-ligand formation constant in the case of β-phenylalanine which can form siz membered metal cheiate rings, is found to be lower than those of complexes with all other α-amino acids which can form only five-membered metal chelate rings.

Stabilities of ternary complexes

The stability constants for the ternary systems were computed from the titrations in which the concentrations of Cu(II)(0.001 *M*):ligand A:ligand B were kept in the ratio 1:1:1. The acid dissociation constants of the ligands A and B, and the stability constant data for the parent binary complexes of Cu(II) with A and B, which were obtained by the Irving-Rossotti method were held constant in the computer calculations for the ternary systems.

The formation constants of ternary complexes ($\beta_{MAB}=[MAB]/[M][A][B]$) with HA and H_2B were calculated using appropriate mass balance equations and solving the corresponding cubic equations[8]. A computer programme written in Fortran IV was used to calculate the formation constants of ternary complexes and to calculate the concentrations of various species present in solution at each point on the titration. The calculations were restricted to *p*H value below 8, in order to avoid complications due to the hydrolysis of various complex species at higher *p*H. The results obtained are listed in Table 2. The charges for all the complex species reported in this paper are omitted for the sake of clarity.

Table 2 – Stability Constants of Ternary Complexes of Copper (II)

[$\mu = 0.05$ *M* KNO_3; temp. = 30 ± 0.1°C]

Ligand	log K^{CuA}_{CuAB}	log β_{CuAB}	*Δ log *K*	log *X*	Δ log *β*
Glycine	8.54	18.04	−0.96	1.86	0.51
DL-α-Alanine	8.46	17.96	−1.05	1.75	0.56
DL-2-Aminobutyric acid	8.36	17.86	−1.11	1.64	0.53
DL-Valine	8.25	17.75	−0.85	2.18	0.56
DL-Leucine	7.91	17.41	−1.19	1.49	0.43
DL-β-Phenylalanine	6.94	16.44	−1.96	0.46	0.14

*$\Delta \log K = \log K^{CuA}_{CuAB} - \log K^{Cu}_{CuB} = \log K^{CuB}_{CuBA} - \log K^{Cu}_{CuA}$.

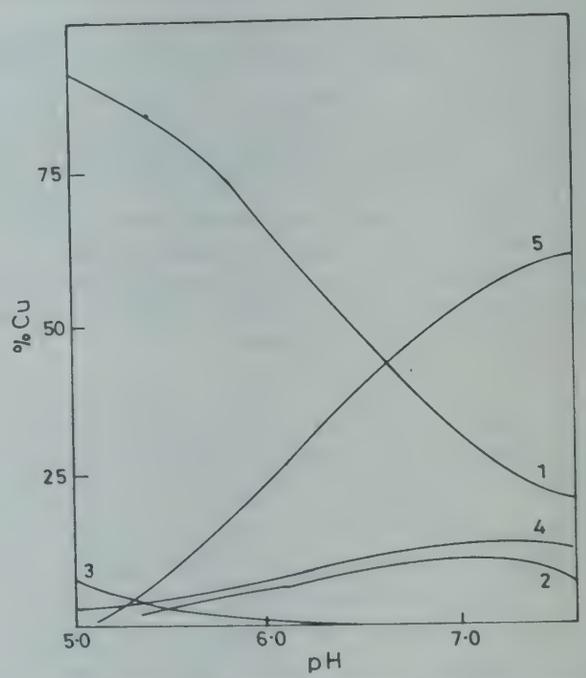

Fig. 1 – Distribution of complex species for Cu(II)-acetylacetone. (A) – glycine (B) system 1. CuA, 2. CuA_2, 3. CuB, 4. CuB_2, 5. CuAB.

The species distribution curve for copper(II)-acetylacetone-glycine system is shown in Fig. 1. It can be seen that under experimental conditions, nearly 90% of the total metal ion is present as CuA at *p*H 5 and the concentration of the complex decreases with increasing *p*H, at the same time the concentration of the ternary complex which is negligible at *p*H 5, gradually increases with increasing *p*H to a value of 60% at *p*H 7.5. The complexes CuA_2 and CuB_2 are formed to an extent of 10% and 12% respectively at *p*H 7. The CuB complex is formed in low concentration in the *p*H range 5 to 7. The species distribution diagrams for other systems exhibited similar qualitative features.

In order to compare the stabilities of the ternary complex species with those of the parent binary complexes, the values of Δlog *K*, the differ-

ence between the stabilities of the binary and the ternary complexes, log X, the disproportionation constant, were determined for all the ternary systems. From statistical considerations, it has been shown that considerably less negative values of $\Delta\log K$ and more positive values of log X indicate greater stabilities of the ternary complexes relative to those of the binary analogues.

The parameters $\Delta\log K$ and log X for the Cu-AB complexes are determined by Eqns 1 to 8,

$$Cu + B \rightleftharpoons CuB \quad \ldots (1)$$

$$CuA + B \rightleftharpoons CuAB \quad \ldots (2)$$

$$\Delta\log K = \log K^{CuA}_{CuAB} - \log K^{Cu}_{CuB} \quad \ldots (3)$$

$$Cu + A \rightleftharpoons CuA \quad \ldots (4)$$

$$CuB + A \rightleftharpoons CuBA \quad \ldots (5)$$

$$\Delta\log K = \log K^{CuB}_{CuBA} - \log K^{Cu}_{CuA} \quad \ldots (6)$$

$$CuA_2 + CuB_2 \rightleftharpoons 2CuAB$$

$$X_{CuAB} = [CuAB]^2/[CuA_2][CuB_2] \quad \ldots (7)$$

$$\log X_{CuAB} = 2\log\beta_{CuAB} - (\log\beta_{CuA_2} + \log\beta_{CuB_2}) \quad \ldots (8)$$

A critical examination of the values of $\Delta\log K$, log X and $\Delta\log\beta$ (Table 2) reveal that all the ternary complexes of Cu(II) with acetylacetone and amino acids, except that with β-phenylalanine, have $\Delta\log K$ values in the range -0.85 to 1.19. This range is close to -0.9, the value given by Sigel[1] as an indicator of strong ternary complex formation. These $\Delta\log K$ values are further supported by positive $\Delta\log X$ values occurring in the range 1.40-1.76, which are greater than 0.6, a value for the existence of 50% ternary complex species when the binary species are present to the extent of 25% each. Similarly, all the ternary complexes possess positive $\Delta\log\beta$ values.

The formation constant values of these ternary complexes (Table 2) show that in all these cases except with β-phenylalanine, the Cu(II)-acetylacetone-amino acid ternary complexes are more stable than the 1:2 Cu(II)-acetylacetone or Cu(II)-amino acid binary complexes. Further, the log K^{CuA}_{CuAB} are in the order, gly > ala > 2-aba > val > leu > pala.

Thus the 1:1 copper(II)-acetylacetone complex has a greater tendency towards combination with any amino acid molecule (except with β-phenylalanine) rather than that with another acetylacetone molecule. It is well known that acetylacetone forms a six-membered metal chelate ring, while the α-amino acids can form only five-membered metal chelate rings. Thus the high stability of the ternary complexes may be due to the preference of Cu(II) ion to possess one five-membered ring and one six-membered ring over two five- or two six-membered rings. Similar observations were also made by several earlier workers[9-11]. This is further confirmed by the fact that the formation constant of ternary complex with β-phenylalanine, which can form only six-membered chelate ring with copper(II) has lower values of all the ternary complexes with other amino acids in the present investigations. It is also interesting to note that the 1:1 Cu(II)-acetylacetone complex has lesser tendency to combine with another molecule of β-phenylalanine than with acetylacetone.

Two of us (N K Rao & R P Rao) gratefully acknowledge the financial assistance from UGC, New Delhi for carrying out this work.

References

1 *Metal ions in biological systems*, Vol 2, edited by H Sigel (Marcel Dekker, New York) 1973.

2 Sivasankaram Nair M & Santappa M, *Indian J Chem*, **20A** (1981) 990.

3 Bond A M & Hefter G, *J electroanal Chem*, **68** (1976) 203.

4 Van Uitert L G & Haas C C, *J Am chem Soc*, **75** (1953) 451.

5 Irving H M & Rossotti H S, *J chem Soc*, (1954) 2904.

6 Dey B P, Dutta S & Lahiri S C, *Indian J Chem*, **21A** (1982) 886.

7 Irving H & Williams R J R, *J chem Soc*, (1953) 3192.

8 Beck M T, *Chemistry of complex equilibria* (Van Nostrand Reinhold Company, London) 1970, 70-73.

9 El Ezaby M S, Marafie H M & Fareed S, *J Inorg Bio Chem*, **11** (1979) 317.

10 Brookes G & Pettit L D, *J chem Soc (Dalton)*, (1977) 1918.

11 Sigel H, Caraw R & Prijs B, *Inorg Chem*, **13** (1974) 462.

Indian Journal of Chemistry
Vol. 27A, June 1988, pp. 558-560

Atomic Absorption Spectrophotometric Determination of Copper after Adsorption of Its Rubeanate onto Microcrystalline Naphthalene

B K PURI

Department of Chemistry, Indian Institute of Technology, Hauz Khas, New Delhi 110 016

M KATYAL

St. Stephen's College, Delhi 110 007
and

M SATAKE* & L F CHANG

Faculty of Engineering, Fukui University, Fukui 910, Japan

Received 20 *July* 1987; *revised* 24 *September* 1987; *accepted* 23 *October* 1987

A highly sensitive and fairly selective atomic absorption spectrophotometric method has been developed for the determination of copper after adsorption of its rubeanate onto microcrystalline naphthalene in the *p*H range of 2.0-8.3. Beer's law is obeyed in the concentration range of 2.0-90.0 μg of copper at 324.7 nm in 10 ml of the final solution. Eight replicate analysis on a sample solution containing 45 μg of copper gave a mean absorbance of 0.250 with a relative standard deviation of ± 1.77%. The sensitivity for 1 % absorption is 0.079 μg/ml (0.133 μg/ml for the direct atomic absorption spectrophotometric method from the aqueous phase). The interference of various ions has been studied and the method has been employed for the determination of copper in various standard alloys and human hair etc.

Rubeanic acid(dithiooxamide) has been employed in the detection and determination of some metal ions[1-5]. The colorimetric method for the copper determination involves rigid conditions[6], e.g. absorbance has to be measured within 2-3 min. Preliminary observations reveal that copper reacts with rubeanic acid to form a coloured, water insoluble, thermally stable complex which cannot be extracted into any of the organic solvent but can be adsorbed onto microcrystalline naphthalene simply by shaking for a few seconds even from a large volume of the aqueous phase (~ 1.6 litres). In the present communication an atomic absorption spectrophotometric method has been developed for the trace determination of copper after adsorption of its rubeanate complex onto microcrystalline naphthalene. The interference of various ions has been studied and the method has been utilized for the determination of copper in various standard reference samples and complex materials like human hair etc.

Stock solution of copper sulphate was prepared in deionised, distilled water and standardized. A working solution(10 ppm) was prepared by appropriate dilution. A 0.1% solution of rubeanic acid was prepared in ethanol. Buffer solutions of *p*H 3-6 and 8-11 were prepared by mixing 1*M* acetic acid/1*M* ammonium acetate and 1*M* aqeous ammonia/1*M* ammonium acetate respectively. A 20% solution of naphthalene was prepared in acetone. For dissolving the metal complex and naphthalene, dimethylformamide (DMF, 100 ml), thiourea (300 mg) and 7.3*N* nitric acid(1ml) were mixed. These amounts were established by trial experiments. All other reagents used were of AR grade.

A Perkin-Elmer model 403 atomic absorption spectrophotometr and a Toa-Dempa model HM-5A *p*H meter were used. All absorbances were measured using an air-acetylene flame and a copper cathode lamp at 324.7 nm.

General procedure

To an aliquout of copper solution containing 2-90 μg of copper were added rubeanic acid(0.1%, 1 ml) and the buffer (*p*H 3.8, 2 ml). It was diluted to 50 ml with water, mixed well and allowed to stand for about 5 min at room temperature for complete formation of the complex. To this 20% naphthalene solution(1.2 ml) in acetone was added and shaken vigourously for 30 sec. The solid mass consisting of naphthalene and the metal complex was separated by filtration, dissolved in DMF-thiourea-nitric acid mixture and diluted to 10 ml in a standard flask. This solution was aspirated into air-acetylene flame at 324.7 nm using a copper hollow cathode lamp.

Reaction conditions were established by taking 45 μg of copper. The adsorption of copper rubeanate was maximum and constant in the *p*H range 2.0-8.3; below and above this *p*H range adsorption was incomplete. Addition of 0.5-5.0 ml of buffer (*p*H 3.8) virtually caused no variation in adsorbance and 2.0 ml were recommended in the all experiments.

A minimum of 0.05 ml of rubeanic acid(0.1%) was needed for the complete reaction. However, 1.0 ml of 0.1% rubeanic acid has been recommended to be on safe side. Absorbance increased with the increase in volume of naphthalene upto 0.25 ml of 20% naphthalene solution, then remained constant between 0.25 and 3.0 ml. Therefore, 1.2 ml of naphthalene were used. The formation of the copper rubeanate is fairly rapid at room temperature, however, a 5-min digestion time is maintained in all the cases. The adsorption is very rapid, being practically complete in less than 10 sec, and a shaking time of 30 sec gives an ample safety margin. Adsorption is quantitative when the volume of the aqueous phase does not exceed 1.6 litres and is best kept to 50 ml for convenience.

Table 1—Effect of Diverse Ions in Determination of Copper as Copper Rubeanate

Salt	Tolerance limit	Ion	Tolerance limit
$NaClO_4.H_2O$, NaCl, KNO_3, $CH_3COONa.3H_2O$, NH_4Cl, Na_2SO_4, Sodium tartrate, Sodium citrate	2 g	Mg^{2+}, Ca^{2+}	500 mg
KH_2PO_4	1 g	Cr^{3+}, Cr^{6+}	100 mg
KI, KSCN, NH_4F	500 mg	Mn^{2+}	50 mg
Malonic acid, Ethylenediamine	50 mg	Cd^{2+}	20 mg
DTCS, $Na_2S_2O_3$, $Na_2C_2O_4$, thiourea	100 μg	Pb^{2+}, Zn^{2+}	10 mg
Na_2-EDTA	10 μg	Al^{3+}, Fe^{3+}	10 mg
KCN	5 μg	Bi^{3+}	2 mg
		Co^{2+}, Ni^{2+}	1 mg
		V^{5+}	200 μg
		Rh^{3+}	100 μg
		Os^{8+}, Ir^{3+}	50 μg
		Hg^{2+}	30 μg
		Pd^{2+}, Mo^{6+}	20 μg
		W^{6+}	10 μg
		Ru^{3+}, Ag^{+}, Pt^{4+}, Au^{3+}	5 μg

Table 2—Analysis of Copper in Standard Reference Samples

Sample	Copper certified value (%)	Copper content^{+} (%)	
		Present method	DDTC-MIBK method
N.B.S., SRM-94c Die Casting alloy	1.01	1.017 ± 0.009	1.041 ± 0.007
N.B.S., SRM-629 Zinc-base alloy	1.50	1.671 ± 0.009	1.504 ± 0.008
JSS 611-7 High speed steel	0.036	0.0359 ± 0.0004*	0.0364 ± 0.0003
JSS 508-4 Ni-Cr steel	0.12	0.108 ± 0.003*	0.115 ± 0.002
JSS 513-4 Cr steel	0.074	0.0728 ± 0.0006*	0.0745 ± 0.0008
Nippon Aluminium Co., No. 3A-30 Al alloy	0.059	0.0601 ± 0.0017	0.0583 ± 0.0013

*Malonic acid (80 mg) was added as a masking reagent for Fe^{3+}.
$^{+}$Mean of 5 individual determinations.

The composition of copper rubeanate was established by Job's method of continuous variation. A break at 0.50 mol fraction confirmed the formation of $Cu(C_2H_2N_2S_2)$ under these conditions which is the same as reported in the literature[1,2].

Copper rubeanate is insoluble in a large number of organic solvents, like benzene, toluene, xylene, *o*-chlorobenzene, *o*-dichlorobenzene, nitrobenzene, chloroform, carbon tetrachloride, 1,2-dichloroethane, isoamyl acetate, diethyl ether, *n*-amylalcohol, isoamylalcohol, ethanol, methyl isobutyl ketone, dioxane, DMF, dimethyl sulphoxide, propylene carbonate, acetonitrile, etc. It was also found to be insoluble in mixed solvents like DMF-HNO_3, DMF-$HClO_4$, DMF-HCl, *n*-butylamine-DMF, propylamine-DMF and isobutylamine-DMF. However, it is found to be soluble in DMF-thiourea-HNO_3 or DMF-*n*-butylamine-KCN. The results of preliminary observations reveal that a ternary mixture consisting of DMF(100 ml), thiourea(300 mg) and 7.3*N* HNO_3 (1 ml) is the most suitable solvent for dissolving the metal complex. The calibration curve at 324.7 nm is found to be linear over copper concentration range of 2.0-90.0 μg in 10 ml in the ternary mixture solvent.

Table 3—Determination of Copper in Water Samples and Human Hair

Sample (vol taken)	Copper found (ppb)*	
	Present method	DDTC-MIBK method+
Hot spring water (Awara) (500 ml)	6.3 ± 0.2	5.5 ± 0.3
Lake water (Kitagata) (500 ml)	0.8 ± 0.1	0.8 ± 0.1
River water (Oyabe) (500 ml)	0.4 ± 0.1	0.4 ± 0.1
Human hair (male)	0.00153 ± 0.00007(%)	0.00159 ± 0.00004(%)

*Mean of 5 individual determinations.
+DDTC-MIBK method: Japanese Industrial Standard, JIS K0102, p.154 (1981)

Eight determinations of a sample solution containing 45 μg of copper gave a mean absorbance of 0.250 with a relative standard deviation of 1.77%. The sensitivity for 1% absorption is found to be 0.079 μg/ml (0.133 μg/ml for the direct atomic absorption spectrophotometric determination from the aqueous solution). The sensitivity of this method may be further improved by carrying out the adsorption from a larger volume of the aqueous phase(1.6 litres) instead of 50 ml as suggested in the general procedure.

Sample solutions containing 45 μg of copper and various amounts of different alkali metal salts or metal ions were prepared and the determination of copper was carried out by the general procedure. The tolerance limit(error ± 3%) of diverse ions is given in Table 1. Many ions can be tolerated upto mg level except oxalate, cyanate, EDTA, thiourea, thiosulphate, DTCS[N-(dithiocarboxy) sarcosine], *o*-phenanthroline, Mo^{6+}, W^{6+}, Hg^{2+}, V^{5+}, Ru^{3+}, Rh^{3+}, Os^{8+}, Ag^{+}, Au^{3+}, Ir^{3+}, Pt^{4+} and Pd^{2+}. The interference of the anions is probably due to the formation of more stable complexes with copper than copper rubeanate, while that of the metal ions it may be due to their reaction with the reagent under these conditions.

Determination of copper in standard reference materials

Sample (0.05-1 g) of the alloy was completely dissolved in 1:1 HCl (20-40 ml) by heating on a water-bath. To this 30% H_2O_2 (2-3 ml) was added. The excess of H_2O_2 was decomposed by heating the solution on a water-bath. The solution was cooled, filtered and diluted to 500 ml in a standard flask. An aliquot of this solution was taken and copper was determined by the general procedure (Table 2).

Determination of copper in water samples

The water samples from different sources were collected. Each of the water sample was adjusted to *p*H 1.0 with HNO_3, filtered through a filter paper No. 5C and copper was determined in the filtrate by the general procedure (Table 3).

Determination of copper in human hair

A sample(10 g) of human hair was taken and dissolved by heating it in a Kjeldahl flask containing conc HNO_3 (30 ml) and conc HCl (3 ml). The solution was cooled, filtered, diluted to 200 ml with distilled water and copper was determined in an aliquot of this solution by the general procedure (Table 3).

In all the cases the results were compared with the standard DDTC-MIBK method.

References

1 Welcher F J, *Organic analytical reagents*, Vol 4 (D Van Nostrand Company, London) 1948, p 148.
2 Kodama K, *Methods of quantitative inorganic analysis* (Interscience Publishers, London) 1963.
3 Chawla R S, Singh R P & Trikha K C, *Talanta*, **18** (1971) 1245.
4 Brajker K & Kozika U K, *Talanta*, **26** (1979) 417.
5 Saha M B & Chakraburtty A K, *J Indian chem Soc*, **60** (1983) 176.
6 West P W & Compare M, *Analyt Chem*, **21** (1949) 628.
7 Perrin D D, *Masking and demasking of chemical reactions* (Wiley-Interscience, London) 1970.

CSIR SCIENTIFIC PERIODICALS

JOURNAL OF SCIENTIFIC & INDUSTRIAL RESEARCH (Monthly)

With a fine record of over 45 years' service to the scientific community, this journal has grown into India's leading general science periodical. Intended to fulfil the responsibility of helping the research workers to keep themselves abreast of current developments in various fields of science and technology the journal carries editorial features highlighting important scientific events in India and abroad, articles on science policy and management of science review articles on topics of current research interest, technical reports on international and national conferences, reviews of scientific and technical publications, and notes on major advances in various fields.

Annual Subscription	Rs 200.00	$ 70.00	£ 45.00
Single copy	20.00	7.00	4.50

INDIAN JOURNAL OF CHEMISTRY (Monthly)

Section A: Started in the year 1963, the journal is devoted to papers in Inorganic, Physical, Theoretical and Analytical Chemistry.

Annual Subscription	Rs 300.00	$100.00	£ 70.00
Single copy	30.00	10.00	7.00

Section B: This journal is devoted to papers in Organic Chemistry, including Medicinal Chemistry.

Annual Subscription	Rs 300.00	$100.00	£ 70.00
Single copy	30.00	10.00	7.00

INDIAN JOURNAL OF PURE & APPLIED PHYSICS (Monthly)

Started in the year 1963, this journal is devoted to original research communications (full papers and short communications) in all conventional branches of physics (except radio and space physics).

Annual Subscription	Rs 250.00	$ 85.00	£ 55.00
Single copy	25.00	8.50	5.50

INDIAN JOURNAL OF RADIO & SPACE PHYSICS (Bimonthly)

The journal, which is being published beginning from March 1972, is intended to serve as a medium for the publication of the growing research output in various areas of radio and space physics, such as ionospheric propagation, magnetosphere, radio and radar astronomy, physics and chemistry of the ionosphere; neutral atmosphere; airglow, winds and motion in the upper atmosphere; stratosphere-mesosphere coupling, ionosphere-magnetosphere coupling; solar-terrestrial relationship, etc.

Annual Subscription	Rs 125.00	$ 42.00	£ 28.00
Single copy	25.00	8.50	5.50

INDIAN JOURNAL OF TECHNOLOGY (INCLUDING ENGINEERING) (Monthly)

This journal publishes papers reporting results of original research of applied nature pertaining to unit operations, heat and mass transfer, products, processes, instruments and appliances, etc. The journal is of special interest to research workers in departments of applied sciences in universities, institutes of higher technology, commodity research laboratories, industrial cooperative research institutes, and industrial research laboratories.

Annual Subscription	Rs 250.00	$ 85.00	£ 55.00
Single copy	25.00	8.50	5.50

INDIAN JOURNAL OF EXPERIMENTAL BIOLOGY (Monthly)

This journal, devoted to the publication of research communications in the fields of experimental botany, zoology, microbiology, pharmacology, endocrinology, nutrition, etc., is the only one in India with such a wide coverage and scope.

Annual Subscription	Rs 250.00	$ 85.00	£ 55.00
Single copy	25.00	8.50	5.50

INDIAN JOURNAL OF BIOCHEMISTRY & BIOPHYSICS (Bimonthly)

This journal, published in association with the Society of Biological Chemists (India), Bangalore, is the only research journal in India devoted exclusively to original research communications in biochemistry and biophysics.

Annual Subscription	Rs 125.00	$ 42.00	£ 28.00
Single copy	25.00	8.50	5.50

INDIAN JOURNAL OF MARINE SCIENCES (Quarterly)

Commencing publication from June 1972, this journal is devoted to research communications (full papers and short communications) pertaining to various facets of marine research, viz. biological, physical, geological and chemical oceanography.

Annual Subscription	Rs 125.00	$ 42.00	£ 28.00
Single copy	35.00	12.00	8.00

RESEARCH AND INDUSTRY (Quarterly)

Intended to serve as a link between science and industry, this journal is addressed primarily to technologists, engineers, executives and others in industry and trade. It publishes informative original articles containing practical details of processes and products devoted in India, which show promise of ready utilization, and technical digests on new processes, products, instruments and testing methods which are of interest to industry Developments in Indian industry are regularly reported.

Annual Subscription	Rs 125.00	$ 42.00	£ 28.00
Single copy	35.00	12.00	8.00

INDIAN JOURNAL OF TEXTILE RESEARCH (Quarterly)

Commencing publication from March 1976, this journal is devoted to the publication of papers reporting results of fundamental and applied researches in the field of textiles.

Annual Subscription	Rs 125.00	$ 42.00	£ 28.00
Single copy	35.00	12.00	8.00

MEDICINAL & AROMATIC PLANTS ABSTRACTS (Bimonthly)

Carries informative abstracts of scientific papers published in important Indian and foreign journals relating to different aspects of medicinal and aromatic plants. Each issue contains about 350 abstracts with a subject index.

Annual Subscription	Rs 225.00	$ 75.00	£ 50.00
Single copy	45.00	15.00	10.00

CURRENT LITERATURE ON SCIENCE OF SCIENCE (Monthly)

Carries abstracts, digests, book reviews, news & notes and R&D statistics with emphasis on problems of S&T in developing countries, it also covers the areas of science policy, R&D planning and management, technology transfer, technology assessment and science and society.

Annual Subscription	Rs 100.00	$ 30.00	£ 12.00
Single copy	10.00	3.00	1.20

Please contact

SENIOR SALES AND DISTRIBUTION OFFICER
PUBLICATIONS & INFORMATION DIRECTORATE, CSIR
Hillside Road, New Delhi 110012

RN 7090/63

CSIR PUBLICATIONS

WEALTH OF INDIA

An encyclopaedia of the economic products and Industrial resources of India issued in two series

RAW MATERIALS SERIES – Contains articles on plant, animal and mineral resources.

	Rs.	$	£
Vol. I(A) (Revised)	300.00	94.00	74.00
Vol. I (A-B)	120.00	60.00	26.00
Vol. II (C)	143.00	66.00	34.00
Vol. III (D-E)	158.00	64.00	40.00
Vol. IV (F-G)	98.00	54.00	24.00
Supplement (Fish & Fisheries)	84.00	32.00	21.00
Vol. V (H-K)	171.00	68.00	42.00
Vol. VI (L-M)	135.00	68.00	30.00
Supplement (Livestock including Poultry)	153.00	68.00	39.00
Vol. VII (N-Pe)	150.00	60.00	38.00
Vol. VIII (Ph-Re)	129.00	64.00	28.00
Vol. IX (Rh-Se)	156.00	70.00	38.00
Vol. X (Sp-W)	338.00	150.00	85.00
Vol. XI (X-Z)	223.00	77.00	44.00

INDUSTRIAL PRODUCTS SERIES – Deals with major, Small-Scale and Cottage Industries

Part I (A-B)	87.00	40.00	22.00
Part II (C)	111.00	48.00	28.00
Part III (D-E)	150.00	67.00	39.00
Part IV (F-H)	189.00	84.00	48.00
Part V (I-L)	135.00	46.00	34.00
Part VI (M-Pi)	42.00	16.00	5.60
Part VII (Pl-Sh)	90.00	36.00	12.00
Part VIII (Si-Ti)	99.00	54.00	20.00
Part IX (To-Z)	120.00	68.00	24.00

BHARAT KI SAMPADA (Hindi Edition of Wealth of India, Raw Materials):

Vol. I (अ-औ)	57.00	32.00	13.00
Vol. II (क)	54.00	30.00	12.00
Vol. III (ख-न)	54.00	30.00	12.00
Vol. IV (प)	125.00	68.00	32.00
Vol. V (फ-मेरे)	90.00	44.00	20.00
Vol. VI (मेल-रू)	120.00	54.00	26.00
Vol. VII (रे-वाटा)	203.00	80.00	50.00
Vol. VIII (वाय-सीसे)	300.00	80.00	50.00
Livestock (Kukkut Palan)	51.00	30.00	12.00
Fish & Fisheries (Matsya aur Matsyaki)	74.00	42.00	10.00
A Dictionary of Generic & Specific Names of Plants & Animals Useful to Man	45.00	22.00	10.00

Please Contact :

SENIOR SALES & DISTRIBUTION OFFICER
PUBLICATIONS & INFORMATION DIRECTORATE, CSIR
HILLSIDE ROAD, NEW DELHI - 110012

OTHER PUBLICATIONS

	Rs.	$	£
The Useful Plants of India	192.00	64.00	48.00
A Dictionary of the Flowering Plants in India by H. Santapau & A.N. Henry	63.00	28.00	16.00
Glossary of Indian Medicinal plants by R.N. Chopra, S.L. Nayar & I.C. Chopra	93.00	32.00	20.00
Supplement to Glossary of Indian Medicinal Plants by R.N. Chopra, I.C. Chopra & B.S. Verma	51.00	18.00	12.00
The Flora of Delhi by J.K. Maheshwari	42.00	16.00	5.50
Illustrations to the Flora of Delhi by J.K. Maheshwari	105.00	44.00	26.00
Herbaceous Flora of Dehra Dun by C.R. Babu	216.00	120.00	44.00
Gnetum by P. Maheshwari & Vimla Vasil	30.00	12.00	4.00
Marsilea by K.M. Gupta	62.00	27.00	16.00
Aquatic Angiosperms	30.00	12.00	4.00
Indian Fossil Pteridophytes by K.R. Surange	99.00	44.00	25.00
Cedrus by P. Maheshwari & Chhaya Biswas	63.00	28.00	16.00
Proteaceae by C. Venkata Rao	108.00	48.00	27.00
Pinus by P. Maheshwari & R.N. Konar	45.00	22.00	16.00
Loranthaceae by B.M. Johri & S.P. Bhatnagar	83.00	37.00	21.00
Abies & Picea by K.A. Chowdhury	21.00	12.00	4.20
Indian Thysanoptera by T.N. Ananthakrishnan	39.00	16.00	5.20
The Millipede Thyropygus by G. Krishnan	18.00	7.00	2.40
Indian Sardines by R.V. Nair	33.00	14.00	4.40
Drug Addiction with special Reference to India by R.N. Chopra & I.C. Chopra	19.00	7.00	2.40
Diosgenin & other Steroid Drug Precursors by L.V. Asolkar & Y.R. Chandha	54.00	26.00	12.00
Cholera Bacteriophages by Dr. Sachimohan Mukerjee	45.00	20.00	12.00
Cottonseed Chemistry & Technology by K.S. Murti & K.T. Achaya	116.00	64.00	26.00
Corrosion Map of India	27.00		3.60
Rural Development and Technology: A Status Report-cum-Bibliography by PR Bose and V.N. Vashist	150.00	76.00	34.00
Termite Problems in India	14.00	6.00	1.80
Research & Development Management	38.00	20.00	
Proceedings of the Seminar on Primary Communications in Science & Technology in India by R.N. Sharma & S. Seetharama	78.00	35.00	68.00

Packing and Postage Extra

Printed & Published by Shri S.S. Saksena, Editor, Publications & Information Directorate (PID) Hillside Road, New Delhi 110012, at PID Photocomposition-cum-Printing Unit

Regd No. D(C)-1018